



UNIVERSITY OF CYPRUS

DEPARTMENT OF CIVIL AND ENVIRONMENTAL ENGINEERING

**Investigation of the response and behaviour of ancient columns
and colonnades under seismic excitations using the discrete
element method**

by

Loizos Papaloizou

Diploma of Civil Engineering, Aristotle University of Thessaloniki, Greece

M.Sc. in Earthquake Resistant Design of Structures, Aristotle University of Thessaloniki, Greece

*Submitted to the Department of Civil and Environmental Engineering of the University of
Cyprus in partial fulfilment of the requirements for the degree of*

Doctor of Philosophy

Nicosia, June 2009

© Loizos Papaloizou

Loizos Papaloizou

**Investigation of the response and behaviour of ancient columns and
colonnades under seismic excitations using the discrete element method**

*Διερεύνηση της απόκρισης και συμπεριφορά αρχαίων κίονων και κιονοστοιχιών υπό
σεισμικές διεγέρσεις χρησιμοποιώντας τη μέθοδο διακριτών στοιχείων*

by

Loizos Papaloizou

Examination Committee

Marios C. Phocas, Assistant Professor (Chairman)

Department of Civil and Environmental Engineering, University of Cyprus

Stavroula J. Pantazopoulou, Professor

Department of Civil Engineering, Democritus University of Thrace

Ioannis N. Doudoumis, Professor

Department of Civil Engineering, Aristotle University of Thessaloniki

Dimos Charmpis, Lecturer

Department of Civil and Environmental Engineering, University of Cyprus

Petros Komodromos, Lecturer

Department of Civil and Environmental Engineering, University of Cyprus

Thesis Advisory Committee

Marios C. Phocas, Assistant Professor

Department of Civil and Environmental Engineering, University of Cyprus

Dimos Charmpis, Lecturer

Department of Civil and Environmental Engineering, University of Cyprus

Petros Komodromos, Lecturer

Department of Civil and Environmental Engineering, University of Cyprus

Thesis Supervisor

Petros Komodromos, Lecturer

Department of Civil and Environmental Engineering, University of Cyprus



APPROVAL PAGE

Doctor of Philosophy Dissertation

**Investigation of the response and behaviour of ancient columns and colonnades
during earthquake excitations using the discrete element method**

by

Loizos Papaloizou

Research Supervisor

Petros Komodromos

Committee Member (Chairman)

Marios C. Phocas (Chairman)

Committee Member

Ioannis N. Doudoumis

Committee Member

Dimos Charmpis

Committee Member

Stavroula J. Pantazopoulou

Loizos Papaloizou

ABSTRACT

“Investigation of the response and behaviour of ancient columns and colonnades under seismic excitations using the discrete element method”

Strong earthquakes are common causes of destruction of ancient monuments, such as classical columns and colonnades. Ancient columns of great archaeological significance can be found in high seismicity areas in the Eastern Mediterranean. Understanding of the behaviour and response of these historic structures during strong earthquakes is useful for the assessment of conservation and rehabilitation proposals for such structures. The seismic behaviour of ancient columns and colonnades involves complicated rocking and sliding phenomena that very rarely appear in modern structures. Analytical study of such multi-block structures under strong earthquake excitations is extremely complicated if not impossible. Computational methods can be used to simulate the dynamic behaviour and seismic response of these structures.

The discrete element method (DEM) is utilized to investigate the response of ancient multi-drum columns and colonnades during harmonic and earthquake excitations by simulating the individual rock blocks as distinct rigid bodies. A specialized software application has been designed and developed, using modern object-oriented technologies and computer graphics to perform efficient seismic simulations of multi-block structures. The developed software is thoroughly validated by comparing the computed responses of various fundamental problems, such as sliding, rocking and free vibration dynamics of rigid bodies, with corresponding analytical solutions as well as results obtained from experiments that are available in the literature.

A large number of parametric simulations of multi-drum columns and colonnades, as well as colonnade systems with two rows of columns, one on top of the other, have been conducted in order to investigate and understand the influence of different characteristics of earthquake excitations as well as various mechanical and geometrical characteristics of these structures on their seismic response. Parametric studies have been performed by varying the excitation frequency and acceleration, as well as the frictional coefficient and the geometric characteristics of the simulated columns and colonnades in order to assess the influence of these parameters in their seismic response and behaviour.

The analysis results indicate that the frequency and peak ground acceleration of an excitation, significantly affect the dynamic response of monolithic and multi-drum standalone columns and colonnades. In particular, for low frequency harmonic ground excitations, the exhibited response is dominated by rocking, while sliding prevails in cases of harmonic excitations with very high frequencies. In between the two extremes, the response contains both rocking and sliding phenomena. Furthermore, according to the conducted simulations the required acceleration to initiate rocking or sliding of a multi-drum column decreases as the excitation frequency increases. The acceleration that is needed to overturn a multi-drum column also increases as the frequency increases.

By examining the stability of multi-drum columns and colonnades under earthquake excitations that were selected from regions where these monuments are often found, such as the Eastern Mediterranean region, the simulations reveal that the columns have the capacity to withstand strong earthquakes without collapse. The mode of failure under harmonic excitations is similar to the mode of failure under earthquake excitations with similar predominant frequencies. The required acceleration to overturn a column or a colonnade decreases as the predominant frequency of the earthquake decreases.

In addition, colonnade systems with two rows of columns, one over the other, have been examined with ground motions of various excitation frequencies. Specifically, earthquake ground motions as well as harmonic excitations have been used. The computed results show that the frequency content of the ground motion affects mostly the response. The displacements of the upper level columns in respect to the displacements of the lower level columns are affected more by the frequency content of the excitation.

Περίληψη

“Διερεύνηση της απόκρισης και συμπεριφορά αρχαίων κίωνων και κιονοστοιχιών υπό σεισμικές διεγέρσεις χρησιμοποιώντας τη μέθοδο διακριτών στοιχείων”

Η διερεύνηση της σεισμικής συμπεριφοράς αρχαίων μνημειακών κατασκευών με σπονδυλωτούς κίονες παρουσιάζει μεγάλο επιστημονικό ενδιαφέρον αφού η απόκρισή τους περιέχει εξαιρετικά σύνθετα φαινόμενα λικνισμού και ολισθήσεων. Επειδή ο υπολογισμός με αναλυτικές λύσεις τέτοιων συστημάτων υπό σεισμικές διεγέρσεις είναι πρακτικά αδύνατος, χρησιμοποιούνται κατάλληλες αριθμητικές μέθοδοι για την προσομοίωση τους.

Για το σκοπό αυτό έχει αναπτυχθεί εξειδικευμένο λογισμικό, υλοποιώντας τη Μέθοδο των Διακριτών Στοιχείων (ΜΔΣ), το οποίο παρέχει τη δυνατότητα προσομοίωσης διακριτών στερεών σωμάτων υπό αρμονικές και σεισμικές διεγέρσεις, καθώς και εκτέλεσης σχετικών παραμετρικών αναλύσεων. Για την ανάπτυξη του λογισμικού χρησιμοποιήθηκε μία σύγχρονη γλώσσα αντικειμενοστραφούς προγραμματισμού, βελτιστοποιώντας αλγόριθμους επαφής και διάφορα σχεδιαστικά πρότυπα ανάπτυξης λογισμικού για το συγκεκριμένο πρόβλημα. Για την επαλήθευση της ορθότητας του λογισμικού που αναπτύχθηκε γίνεται σύγκριση των αποτελεσμάτων του, με αντίστοιχα αποτελέσματα αναλυτικών λύσεων απλοποιημένων προβλημάτων καθώς και με πειραματικές μετρήσεις.

Με αυτό το λογισμικό έχει πραγματοποιηθεί σημαντικός αριθμός παραμετρικών αναλύσεων για να διερευνηθεί η επίδραση των χαρακτηριστικών της διέγερσης, καθώς και των γεωμετρικών και μηχανικών χαρακτηριστικών σπονδυλωτών κίωνων και κιονοστοιχιών στη συμπεριφορά και απόκρισή τους υπό αρμονικές και σεισμικές διεγέρσεις. Εξετάζονται διάφορες παράμετροι της επιβαλλόμενης κίνησης της βάσης καθώς και παράμετροι που αφορούν τα μηχανικά και γεωμετρικά χαρακτηριστικά των προσομοιούμενων κατασκευών.

Οι αναλύσεις έδειξαν πως οι τιμές παραμέτρων όπως η μέγιστη επιτάχυνση του εδάφους καθώς και η συχνότητα διέγερσης είναι καθοριστικές στην απόκριση σπονδυλωτών κίωνων και κιονοστοιχιών. Συγκεκριμένα, παρατηρήθηκε πως για χαμηλές συχνότητες διέγερσης, είτε αυτή είναι αρμονική διέγερση είτε αναφέρεται σε προέχουσα συχνότητα σεισμικής διέγερσης, η απόκριση κυριαρχείται από φαινόμενα λικνισμού. Αντίθετα, όσο η συχνότητα διέγερσης αυξάνεται, τόσο περιπλέκεται και η ολίσθηση στην απόκριση αυτών των κατασκευών. Σε εξαιρετικά υψηλές συχνότητες αρμονικών διεγέρσεων, η απόκριση

φαίνεται να κυριαρχείται αποκλειστικά από φαινόμενα ολίσθησης. Επίσης παρατηρήθηκε ότι η απαιτούμενη επιτάχυνση εδάφους που χρειάζεται για να αρχίσει ένας κίονας να ολισθαίνει ή να λικνίζεται μειώνεται όσο αυξάνεται η συχνότητα της επιβαλλόμενης διέγερσης. Αντίθετα, η επιτάχυνση εδάφους που χρειάζεται ένας κίονας για να ανατραπεί, αυξάνεται με την αύξηση της συχνότητας διέγερσης.

Επιπλέον, εξετάστηκε η ευστάθεια κίωνων και κionoστοιχιών σε σεισμικές διεγέρσεις, με σχετικά ψηλές προέχουσες συχνότητες, όπως αυτές που συναντώνται στο μεσογειακό χώρο, όπου και βρίσκονται πολλά μνημεία τέτοιου είδους. Οι πραγματοποιηθείσες αναλύσεις έδειξαν ότι οι κίονες και οι κionoστοιχίες έχουν σημαντική ικανότητα να υποστούν, χωρίς να καταρρεύσουν, σεισμικές διεγέρσεις με τέτοιο συχνοτικό περιεχόμενο. Επίσης, παρατηρήθηκε πως η μορφή ανατροπής υπό σεισμικές διεγέρσεις μοιάζει με αυτήν των αρμονικών διεγέρσεων. Η επιτάχυνση του εδάφους που χρειάζονται οι εξεταζόμενοι κίονες και κionoστοιχίες για να ανατραπούν, αυξάνεται με την αύξηση της προέχουσας συχνότητας του σεισμού.

Επιπρόσθετα, ο συντελεστής τριβής μεταξύ των σπονδύλων, η μορφή και αριθμός των σπονδύλων, η απόσταση μεταξύ των κίωνων, ο τύπος και η μάζα του επιστυλίου είναι σημαντικοί παράγοντες που επηρεάζουν την απόκριση τέτοιων συστημάτων.

Τέλος, η εργασία αυτή μελετά την απόκριση συστημάτων σπονδυλωτών κionoστοιχιών με δύο σειρές κίωνων, τοποθετημένες η μία πάνω στην άλλη, υπό σεισμικές και αρμονικές διεγέρσεις. Οι αναλύσεις έδειξαν ότι η απόκριση μετακινήσεων της άνω σειράς κίωνων σε σχέση με τις μετακινήσεις της κάτω σειράς, επηρεάζεται σημαντικά από το συχνοτικό περιεχόμενο της διέγερσης της βάσης.

Acknowledgments

First and foremost, I would like to express my sincere gratitude to my academic and research advisor, Prof. Petros Komodromos for his guidance, encouragement and unfailing support during my studies at the University of Cyprus. This research work would not have been in any way possible without his zealous devotion and determination towards the success of his students.

My warmest thanks to my doctoral committee members, Prof. Marios C. Phocas, Prof. Dimos Charmpis, Prof. Ioannis N. Doudoumis and Prof. Stavroula J. Pantazopoulou for the valuable advice and their excellent comments on my thesis.

I am particularly grateful to my professors during my studies at the Aristotle University of Thessaloniki, Prof. Efi Mitsopoulou, Prof. Ioannis N. Doudoumis, Prof. Asimina Athanatopoulou and Prof. Panikos Papadopoulos for the valuable knowledge and education they have offered me in the areas of structural and computer-aided engineering.

I would also like to thank my friends and co-workers in the “Archimedes” Laboratory Panagiotis Polycarpou, Ernestos Sarris, Eftychia Mavronicola and George Pamboris who kept me going and supported me during my studies in many different ways.

I would like to specifically thank my parents, Sophia and Zenon, as well as my sister Maria for their love, encouragement and for helping me in fulfilling my goals. Without their endless support this achievement would not have been possible.

Last but not least, I cannot find words to express my love and gratitude to Georgia whose love, encouragement, and understanding have been a constant source of motivation and strength for me.

Loizos Papaloizou

Dedicated to Georgia

TABLE OF CONTENTS

APPROVAL PAGE	5
ABSTRACT	7
ΠΕΡΙΛΗΨΗ	9
ACKNOWLEDGMENTS.....	11
TABLE OF CONTENTS	13
LIST OF FIGURES	16
LIST OF TABLES	23
1. INTRODUCTION.....	24
1.1. MOTIVATION.....	24
1.2. ANCIENT GREEK ARCHITECTURE	26
1.3. OBJECTIVES.....	28
1.4. OUTLINE.....	30
2. LITERATURE REVIEW	33
2.1. RIGID BODY MOTION.....	33
2.2. DYNAMIC RESPONSE OF MULTI-DRUM COLUMNS	37
3. FORMULATION OF THE PHYSICAL PROBLEM	43
3.1. DISCRETE ELEMENT METHODS (DEM).....	43
3.2. CONTACT MODELLING	43
3.3. BLOCK DEFORMABILITY.....	44
3.4. CONTACT INTERACTIONS.....	46
3.5. SIMULATING DISCONTINUOUS SYSTEMS	47
3.6. CONTACT DETECTION	49
3.7. CONTACT PLANE.....	53
3.8. CONTACT FORCES.....	56
3.9. EQUATIONS OF MOTION	57
3.10. ANALYSIS PROCEDURE	61

4.	SOFTWARE DEVELOPMENT	64
4.1.	SOFTWARE DESIGN	65
4.2.	DESIGN PATTERNS (DPs).....	68
4.2.1.	<i>Creational design patterns</i>	70
4.2.2.	<i>Structural design patterns</i>	72
4.2.3.	<i>Behavioural design patterns</i>	73
4.3.	SOFTWARE DEVELOPMENT	74
4.4.	GRAPHICAL USER INTERFACE (GUI)	75
4.5.	INPUT FILES	77
4.6.	LIMITATIONS OF THE TWO DIMENSIONAL ANALYSIS.....	79
4.7.	OTHER USES OF THE DEVELOPED SOFTWARE	80
4.7.1.	<i>Masonry structures</i>	80
4.7.2.	<i>Rock masses – Land slides</i>	82
4.7.3.	<i>Realistic multi-body animations</i>	83
4.7.4.	<i>Multi-body dynamic and mechanical systems</i>	84
5.	VERIFICATION OF THE DEVELOPED SOFTWARE	85
5.1.	ANALYTICAL VALIDATION.....	85
5.1.1.	<i>Free vibration rocking period</i>	85
5.1.2.	<i>Energy loss during impact</i>	87
5.1.3.	<i>Sliding response to acceleration pulses</i>	90
5.1.4.	<i>Sliding response to earthquake motions</i>	93
5.1.5.	<i>Rocking response to earthquake motions</i>	97
5.1.6.	<i>Rocking response during free vibration of two rigid bodies</i>	100
5.2.	EXPERIMENTAL VALIDATION	103
5.2.1.	<i>Rigid body free vibration</i>	103
5.2.2.	<i>Small-scale standalone multi-drum columns</i>	106
5.2.3.	<i>Small-scale colonnades with epistyles</i>	108
6.	NUMERICAL SIMULATIONS OF STANDALONE COLUMNS	110
6.1.	INFLUENCE OF THE EXCITATION’S PGA AND FREQUENCY	111
6.2.	INFLUENCE OF THE COEFFICIENT OF FRICTION	114
6.3.	INFLUENCE OF THE OF DRUMS	115
6.3.1.	<i>Number of drums</i>	115
6.3.2.	<i>Shape of drums</i>	118
6.4.	RESPONSE TO STRONG MOTION EXCITATIONS.....	120
6.5.	DIFFERENT FRICTIONAL LEVELS BETWEEN DIFFERENT BLOCKS OF THE ASSEMBLY	126

7.	NUMERICAL SIMULATION OF COLONNADES WITH AN EPISTYLE.....	132
7.1.	COMPARISON WITH STANDALONE COLUMNS.....	142
7.2.	ACCELERATION REQUIRED TO OVERTURN A SYSTEM	142
7.3.	NUMBER OF DRUMS OF COLUMNS	144
7.4.	NUMBER OF COLUMNS OF COLONNADES.....	146
7.5.	DISTANCE BETWEEN COLUMNS OF COLONNADES	148
7.6.	TYPES OF EPISTYLES.....	150
7.7.	EPISTYLE MASS.....	152
7.8.	TAPERED SHAPE COLONNADES WITH AN EPISTYLE.....	155
7.9.	COLONNADES WITH TWO ROWS OF COLUMNS.....	161
8.	CONCLUDING REMARKS.....	171
8.1.	SUMMARY	171
8.2.	CONTRIBUTIONS AND CONCLUSIONS	172
8.3.	FUTURE WORK.....	175
	REFERENCES.....	177
	INDEX.....	187

LIST OF FIGURES

Figure 1.1. Ancient columns with an epistyle (Sanctuary of Apollo, Cyprus) and free standalone multi-drum columns (Amathus, Cyprus).....	24
Figure 1.2: Ancient columns located at the “Sanctuary of Amathus”, Limassol, Cyprus.....	25
Figure 1.3. Architecture of a typical classical monument.....	26
Figure 1.4. Greek orders: (a) Doric (b) Ionic (c) Corinthian.....	27
Figure 1.5. (a) Elevation and (b) section illustration of a typical ancient Greek temple.....	28
Figure 2.1. Motion of a rigid body left to oscillate freely from an initial inclination angle.....	33
Figure 3.1. Contact between two bodies: (a) contact region and (b) contact plane.....	46
Figure 3.2. Contact springs and dashpots: (a) in the normal and (b) tangential directions.....	47
Figure 3.3. Calculation of the normal and tangential contact plane.....	49
Figure 3.4. Contact checks for each body using only adjacent bodies.....	50
Figure 3.5. Spatial reasoning based on the body’s position and boundary diameter.....	52
Figure 3.6. Spatial reasoning based on the projection of each body’s bounds on the X and Y axes.....	52
Figure 3.7. Normal (red) and tangential (blue) plane.....	53
Figure 3.8. (a) quadrilateral and (b) triangular overlapping contact area.....	54
Figure 3.9. Calculation of the contact area of a (a) quadrilateral and (b) triangular contact region.....	54
Figure 3.10. Contact springs and dashpots: (a) in the normal direction and (b) in the tangential direction.(c) Contact Forces.....	57
Figure 3.11. Transformation of the contact forces to the centre of mass of each rigid body.....	57
Figure 3.12. Variation of the relative impact velocity in the normal direction during impact.....	61
Figure 3.13. Build-up of the contact force in the normal direction during impact.....	61
Figure 3.14. Flow of control of the developed algorithms.....	62
Figure 4.1. Graphical-user interface of the developed software.....	64
Figure 4.2. Utilization of the Abstract Factory DP.....	71
Figure 4.3. Example of using the Composite DP to represent earthquakes.....	73
Figure 4.4. Use of the Strategy DP to define various contact detection algorithms.....	73
Figure 4.5. Graphical-user interface of the developed software.....	76
Figure 4.6. Typical input file.....	79
Figure 4.7. Masonry building under dynamic loading using FEM [53].....	81
Figure 4.8. Sliding of multiple bodies of various sizes sliding on an inclined surface.....	83

Figure 4.9. Multi-body animations of colliding bodies.....	84
Figure 4.10. Objects getting stucked while moving down a cone.....	84
Figure 5.1. Rocking block.....	86
Figure 5.2. Period T of a block rocking with amplitude θ_o	87
Figure 5.3. Time-history response of a rigid block left to freely vibrate from an initial angle, with energy loss during impacts.	88
Figure 5.4. Computed time-history response of a rigid block left to freely vibrate from an initial angle, with energy loss during impacts.	89
Figure 5.5. Reduction of the maximum rotation angle of each cycle due to impact.....	90
Figure 5.6. Rigid body on a horizontal plane subjected to a rectangular pulse acceleration.....	90
Figure 5.7. Normalized maximum relative displacements of a rigid body, resting on a surface with coefficient of friction μ , subjected to rectangular acceleration pulses.....	92
Figure 5.8 Time-history relative displacements of a sliding block under rectangular pulse accelerations.	93
Figure 5.9. Rigid body on a horizontal plane subjected to earthquake excitations.....	93
Figure 5.10. Sliding response of a rigid body under an earthquake excitation.	95
Figure 5.11. Sliding response of a rigid body under an earthquake excitation.	96
Figure 5.12. Model of a rigid block used for the validation under earthquake motions.	97
Figure 5.13. Rocking response of a rigid body under earthquake excitations.	99
Figure 5.14. Free oscillation of two rigid bodies released from an initial inclination angle of 0.1 rad	100
Figure 5.15. Rotation of the two bodies obtained analytically and numerically.....	101
Figure 5.16. Rotation of Block 1 from an initial rotation angle of 0.15 rad as computed by a nonlinear analytical formulation provided by Spanos [79].....	102
Figure 5.17. Rotation of Block 1 from an initial rotation angle of 0.15 rad as computed using simulation with the developed software.	102
Figure 5.18. Experimental Setup [62].....	103
Figure 5.19. Rotation of a rigid body obtained experimentally by Pena et. al. [62].	104
Figure 5.20. Rotation of the rigid body obtained numerically with the developed software.	104
Figure 5.21. The effect of the contact damping coefficient on the free vibration of a rigid body.	105
Figure 5.22. (a) Experimental column dynamic response (b) Computed response from numerical simulations.	107
Figure 5.23. Specimen acceleration for sliding or rocking effect.	107

Figure 5.24. Required base acceleration so that either sliding or rocking occurs.	109
Figure 6.1. Total sliding and rocking computed in numerical simulations for (a) different coefficients of friction and (b) different peak ground accelerations.	111
Figure 6.2. Response of a multi-drum column under a harmonic excitation with 0.5 Hz frequency and 0.25 m amplitude.	112
Figure 6.3. Response of a multi-drum column under a harmonic excitation with 2 Hz frequency and 0.25 m amplitude.	113
Figure 6.4. Response of a multi-drum column under a harmonic excitation with 20 Hz frequency and 0.25 m amplitude.	113
Figure 6.5. Ratio of total sliding to total base movement response under harmonic excitations with an amplitude of 0.5 m for full-scale columns (6 m height and 1 m width) constructed with eight drums.	114
Figure 6.6. Rocking response under harmonic excitations with an amplitude of 0.5 m for full-scale columns (6 m height and 1 m width) constructed with eight drums.	115
Figure 6.7. Response of a multi-drum (drum height = 1.5 m) column under harmonic excitation with 0.5 Hz frequency and 0.25 m amplitude.	116
Figure 6.8. Response of a multi-drum (drum height = 3 m) column under harmonic excitation with 0.5 Hz frequency and 0.25 m amplitude.	116
Figure 6.9. Mean rotation of the column with various number of drums under monotonically increasing base acceleration.	118
Figure 6.10. Required acceleration to initiate rocking and overturning, in terms of the number of drums of the column.	118
Figure 6.11. Models of the examined tapered columns.	119
Figure 6.12. Mean rotation of the column with various shapes of the drums under monotonically increasing base acceleration.	119
Figure 6.13. Required acceleration to initiate rocking and overturning of the column with various shapes of tapered drums.	120
Figure 6.14. Pseudo-acceleration response spectra ($\xi=10\%$) of the scaled earthquake records.	121
Figure 6.15. Time-history response of a multi-drum column under the Athens Earthquake scaled appropriately to cause collapse.	122
Figure 6.16. Time-history response of a multi-drum column under the Kalamata Earthquake scaled appropriately to cause collapse.	122
Figure 6.17. Time-history response of a multi-drum column under the Mexico City Earthquake scaled appropriately to cause collapse.	122

Figure 6.18. Time-history response of a two-drum standalone column under the record from the Athens Earthquake scaled to a PGA of 26.43 m/sec^2	123
Figure 6.19. Time-history response of a three-drum standalone column under the record from the Athens Earthquake scaled to a PGA of 26.43 m/sec^2	124
Figure 6.20. Time-history response of a two-drum standalone column under the record from the Kalamata Earthquake scaled to a PGA of 9.35 m/sec^2	124
Figure 6.21. Time-history response of a three-drum standalone column under the record from the Kalamata Earthquake scaled to a PGA of 9.35 m/sec^2	124
Figure 6.22. Time-history response of a two-drum standalone column under the record from the Mexico City Earthquake scaled to a PGA of 1.47 m/sec^2	125
Figure 6.23. Time-history response of a three-drum standalone column under the record from the Mexico City Earthquake scaled to a PGA of 1.47 m/sec^2	125
Figure 6.24. Different frictional levels between different blocks for a four block assembly ($n=0.05$).	127
Figure 6.25. Different frictional levels between different blocks for a four block assembly ($n=0.2$).	128
Figure 6.26. Different frictional levels between different blocks for a four block assembly ($n=0.25$).	128
Figure 6.27. Different frictional levels between different blocks for a four block assembly ($n=0.35$).	129
Figure 6.28. Different frictional levels between different blocks for an eight block assembly.	130
Figure 6.29. Different frictional levels between different blocks for an eight block assembly.	130
Figure 6.30. Different frictional levels between different blocks for an eight block assembly.	131
Figure 6.31. Different frictional levels between different blocks for an eight block assembly.	131
Figure 7.1. Time-history response of a colonnade with two drums under an accelerogram from the Athens Earthquake scaled to a PGA of 32.21 m/sec^2	132
Figure 7.2. Time-history response of a colonnade with three drums under an accelerogram from the Athens Earthquake scaled to a PGA of 32.21 m/sec^2	132
Figure 7.3. Time-history response of a colonnade with two drums under an accelerogram from the Kalamata Earthquake scaled to a PGA of 17.35 m/sec^2	133
Figure 7.4. Time-history response of a colonnade with three drums under an accelerogram from the Kalamata Earthquake scaled to a PGA of 17.35 m/sec^2	133
Figure 7.5. Time-history response of a colonnade with two drums under an accelerogram from the Mexico City Earthquake scaled to a PGA of 2.45 m/sec^2	133
Figure 7.6. Time-history response of a colonnade with three drums under an accelerogram from the Mexico City Earthquake scaled to a PGA of 2.45 m/sec^2	134
Figure 7.7. Time-history response of a colonnade with each column having one drum and a capital under the Athens Earthquake scaled to a PGA of 32.21 m/sec^2	135

Figure 7.8. Time-history response of a colonnade with each column having two drums and a capital under the Athens Earthquake scaled to a PGA of 32.21 m/sec^2	135
Figure 7.9. Time-history response of a colonnade with each column having three drums and a capital under the Athens Earthquake scaled to a PGA of 32.21 m/sec^2	135
Figure 7.10. Time-history response of a colonnade with each column having seven drums and a capital under the Athens Earthquake scaled to a PGA of 32.21 m/sec^2	135
Figure 7.11. Time-history response of a colonnade with each column having one drum and a capital under the Kalamata Earthquake scaled to a PGA of 17.35 m/sec^2	136
Figure 7.12. Time-history response of a colonnade with each column having two drums and a capital under the Kalamata Earthquake scaled to a PGA of 17.35 m/sec^2	136
Figure 7.13. Time-history response of a colonnade with each column having three drums and a capital under the Kalamata Earthquake scaled to a PGA of 17.35 m/sec^2	136
Figure 7.14. Time-history response of a colonnade with each column having seven drums and a capital under the Kalamata Earthquake scaled to a PGA of 17.35 m/sec^2	136
Figure 7.15. Time-history response of a colonnade with each column having one drum and a capital under the Mexico City Earthquake scaled to a PGA of 2.45 m/sec^2	137
Figure 7.16. Time-history response of a colonnade with each column having two drums and a capital under the Mexico City Earthquake scaled to a PGA of 2.45 m/sec^2	137
Figure 7.17. Time-history response of a colonnade with each column having three drums and a capital under the Mexico City Earthquake scaled to a PGA of 2.45 m/sec^2	137
Figure 7.18. Time-history response of a colonnade with each column having seven drums and a capital under the Mexico City Earthquake scaled to a PGA of 2.45 m/sec^2	137
Figure 7.19. Horizontal displacements of the epistyle for different arrangements of multi-drum colonnades under the Athens Earthquake scaled 9.0 times.....	139
Figure 7.20. Horizontal displacements of the epistyle for different arrangements of multi-drum colonnades under the Kalamata Earthquake 3.5 times.	140
Figure 7.21. Horizontal displacements of the epistyle for different arrangements of multi-drum colonnades under the Mexico City Earthquake scaled 1.4 times.....	141
Figure 7.22. Rotation of a standalone column compared to the rotation of a colonnade with an epistyle.....	142
Figure 7.23. Arrangements of the simulated systems.	143
Figure 7.24. Horizontal displacements of the epistyle for an arrangement of three colonnades with a single epistyle with different numbers of drums.	144
Figure 7.25. Horizontal displacements of an epistyle for an arrangement of four colonnades with a single epistyle with different numbers of drums.	145

Figure 7.26. Horizontal displacements of an epistyle for an arrangement of five colonnades with a single epistyle with different numbers of drums.	145
Figure 7.27. Horizontal displacements of the epistyle for different arrangements of monolithic colonnades considering multiple epistyles, under the Athens Earthquake scaled to a PGA of 29.09 m/sec^2	146
Figure 7.28. Horizontal displacements of the epistyle for different arrangements of monolithic colonnades considering single body epistyles, under the Athens Earthquake scaled to a PGA of 29.09 m/sec^2	147
Figure 7.29. Horizontal displacements of the epistyle for different arrangements of two-drum colonnades with monolithic epistyle, under the Athens Earthquake scaled to a PGA of 29.09 m/sec^2	147
Figure 7.30. Horizontal displacements of the epistyle for different arrangements of four-drum colonnades with monolithic epistyle, under the Athens Earthquake scaled to a PGA of 29.09 m/sec^2	148
Figure 7.31. Variation of the distance between monolithic columns of colonnades with an epistyle.	149
Figure 7.32. Variation of the distance between monolithic columns of colonnades and the load of the epistyle, under the Athens Earthquake scaled to a PGA of 29.09 m/sec^2	149
Figure 7.33. The effect of different types of epistyles considering three monolithic columns with various types of epistyles, under the Athens Earthquake scaled to a PGA of 29.09 m/sec^2	151
Figure 7.34. The effect of different types of epistyles considering four monolithic columns with various types of epistyles, under the Athens Earthquake scaled to a PGA of 29.09 m/sec^2	151
Figure 7.35. Effect of the epistyle mass for a colonnade system with three monolithic columns and a single epistyle, under the Athens Earthquake scaled to a PGA of 29.09 m/sec^2	152
Figure 7.36. Effect of the epistyle mass for a colonnade system with three (two drum) columns and a single epistyle, under the Athens Earthquake scaled to a PGA of 29.09 m/sec^2	153
Figure 7.37. Effect of the epistyle mass for a colonnade system with four monolithic columns and a single epistyle, under the Athens Earthquake scaled to a PGA of 29.09 m/sec^2	153
Figure 7.38. Effect of the epistyle mass for a colonnade system with four (two drum) columns and a single epistyle, under the Athens Earthquake scaled to a PGA of 29.09 m/sec^2	154
Figure 7.39. Effect of the epistyle mass for a colonnade system with five monolithic columns and a single epistyle, under the Athens Earthquake scaled to a PGA of 29.09 m/sec^2	154
Figure 7.40. Effect of the epistyle mass for a colonnade system with five (two drum) columns and a single epistyle, under the Athens Earthquake scaled to a PGA of 29.09 m/sec^2	155
Figure 7.41. The effect of monolithic tapered colonnades, under the Athens Earthquake scaled to a PGA of 29.09 m/sec^2	156
Figure 7.42. Displacements of monolithic tapered and non-tapered columns with various epistyle masses, under the Athens Earthquake scaled to a PGA of 29.09 m/sec^2	157
Figure 7.43. Displacements of (two-drum) tapered and non-tapered columns with various epistyle masses, under the Athens Earthquake scaled to a PGA of 29.09 m/sec^2	157

Figure 7.44. Displacements of monolithic, as well as, two and four drum tapered columns, under the Athens Earthquake scaled to a PGA of 29.09 m/sec^2	158
Figure 7.45. Displacements of monolithic, as well as, two and four drum tapered columns for increased epistyle mass, under the Athens Earthquake scaled to a PGA of 29.09 m/sec^2	158
Figure 7.46. Comparison of tapered colonnades with a non-tapered monolithic colonnades, under the Athens Earthquake scaled to a PGA of 29.09 m/sec^2	159
Figure 7.47. Comparison of tapered multidrum (two drum) colonnades with a non-tapered ones, under the Athens Earthquake scaled to a PGA of 29.09 m/sec^2	159
Figure 7.48. Comparison of tapered multidrum (three drum) colonnades with a non-tapered ones, under the Athens Earthquake scaled to a PGA of 29.09 m/sec^2	160
Figure 7.49. Comparison of tapered (four-drum) colonnade with a non-tapered one, under the Athens Earthquake scaled to a PGA of 29.09 m/sec^2	160
Figure 7.50. Athens Earthquake (scaled acceleration by 9.0).....	162
Figure 7.51. Mexico City Earthquake (scaled acceleration by 1.5).....	163
Figure 7.52. Response of a two level column system under a harmonic excitation with 2 Hz frequency and 0.25 m amplitude.	164
Figure 7.53. Response of a two level column system under a harmonic excitation with 1.33 Hz frequency and 0.25 m amplitude.	165
Figure 7.54. Response of a two level column system under a harmonic excitation with 1.00 Hz frequency and 0.25 m amplitude.	166
Figure 7.55. Response of a two level column system under a harmonic excitation with 0.5 Hz frequency and 0.1 m amplitude.	167
Figure 7.56. Response of a two series (2 drum) column system colonnade, under a harmonic excitation with 1.33 Hz frequency and 0.25 m amplitude.....	168
Figure 7.57. Response of a two series (2 drum) column system colonnade, under a harmonic excitation with 1 Hz frequency and 0.1 m amplitude.	169
Figure 7.58. Response of a two series (2 drum) column system colonnade, under a harmonic excitation with 0.5 Hz frequency and 0.25 m amplitude.....	170

LIST OF TABLES

Table 6.1. List of earthquake records that have been used in the analyses.....	121
Table 7.1. Acceleration that is required to cause failure.....	143
Table 7.2. Types of epistyles that have been analyzed.....	150

Loizos Papaloizou

1. Introduction

1.1. Motivation

Ancient classical columns and colonnades of great archaeological significance can be abundantly found in the Eastern Mediterranean region. Such columns were once part of entire monuments, usually carrying the load of an entablature (Figure 1.1 and Figure 1.3), which is the section of a classical structure that lies between the columns and the roof. Different types of columns can be found in different sizes and with numerous variations of their geometric characteristics. The columns are typically constructed of stone or marble blocks that are placed on top of each other, usually without connecting material between them. Today's remains of such ancient monuments are usually monolithic or multi-drum standalone columns, or series of remaining columns (colonnades), sometimes with epistyles laying on their tops (Figure 1.1 and Figure 1.2).



Figure 1.1. Ancient columns with an epistyle (Sanctuary of Apollo, Cyprus) and free standalone multi-drum columns (Amathus, Cyprus).

Unfortunately, most of these monuments are built in high seismicity areas, where the seismic risk is considerable. Therefore, it is very important to understand the seismic behaviour of these structures so that correct assessments of potential proposals for their structural rehabilitation and strengthening can be made. Moreover, it is very intriguing to understand why and how classical columns and colonnades, which have been exposed to

large numbers of very strong earthquakes, throughout the many centuries of their lifetimes, are still standing today. It may also be useful to identify the mechanisms that allow those structural systems to evade structural collapse and destruction after experiencing several strong earthquakes. Furthermore, the investigation of the dynamic response of such monumental structures may reveal certain information from past strong earthquakes that have struck the respective regions.



Figure 1.2: Ancient columns located at the “Sanctuary of Amathus”, Limassol, Cyprus.

Multi-drum structures display a very different dynamic response compared to modern structures as they exhibit complex rocking and sliding phenomena among the individual blocks of the structures. The drums can undergo rocking, either individually, or in groups, resulting in several different and alternating shapes of oscillations. This response can be characterized as highly non-linear due to the continuously changing geometry and boundary conditions of the structural system. Considering that analytical study of such multi-block structures under strong ground motions is extremely complicated, if not impossible, for more than a couple of distinct blocks, whereas laboratory experiments are very difficult and costly to perform, therefore, numerical methods are employed to simulate their dynamic responses and assess their seismic behaviours.

1.2. Ancient Greek architecture

In ancient Greece the temples formed the most important class of buildings erected during that era. These monuments can be classified into three "Orders of Architecture", the Doric, Ionic and Corinthian order (Figure 1.3). An "order" in Greek architecture consists of the column, including the base and the capital, and the entablature (Figure 1.4). The entablature is divided into the epistyle or architrave (lower part), the frieze (middle part) and the cornice (upper part). The differences among these three orders are reflected to the dimensions, proportions, mouldings and decorations of the various parts.

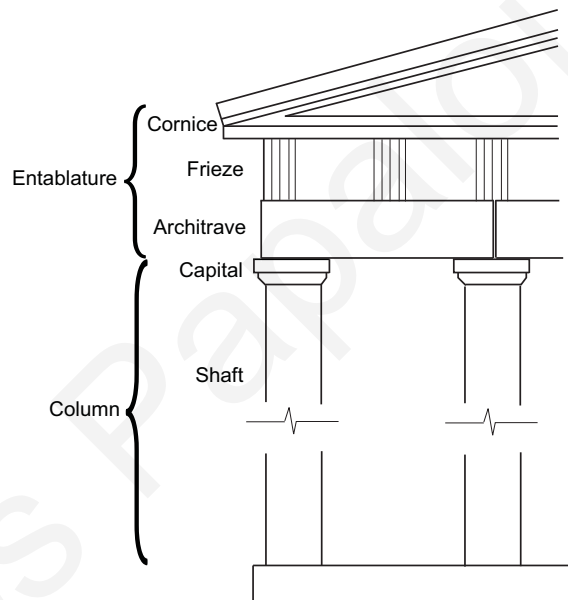


Figure 1.3. Architecture of a typical classical monument.

The Doric order, which is the oldest and plainest order, is traced by many to an Egyptian prototype. The column has no base, and stands directly on a stylobate usually of three steps. The stylobate is a flat pavement on which the columns are placed. Including the capital, the column's height is from 4 to 6.5 times the diameter at the base. The entablature was usually about 25% of the total height of the column and the entablature.

The Ionic order is characteristic for its scroll (volute) capital. The earlier findings of Ionic capitals were at Lesbos, Neandra and Cyprus [24]. The columns have shafts usually about nine times the lower diameter in height, including the capital and the base. The entablature varies in height, but is usually about one-fifth of the whole order.

Finally, the Corinthian order, which is more complex than the Ionic, was modestly used by the Greeks. The column, the base and shaft of which resemble those of the Ionic order, is generally about ten times the diameter in height, including the capital, and is placed on a stylobate. The distinctive capital is much higher than the Ionic, being about 100 to 115 % of the diameter in height.

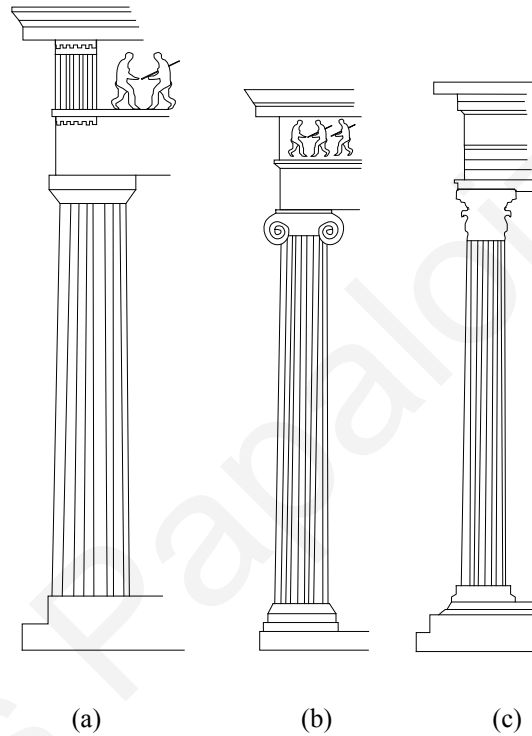


Figure 1.4. Greek orders: (a) Doric (b) Ionic (c) Corinthian.

The roof of a temple was constructed of timber and was usually covered with marble slabs. The outer columns of the monument supported the load of the entablature, while the load of the wooden roof was supported by walls, the cella walls. In some large temples there were internal colonnades of columns, placed over each other, to support the roof (Figure 1.5).

The main construction material used in such monuments was stone or marble. Columns could be either monolithic (solid) or multi-drum, consisting of a number of drums (blocks). The columns had to be placed comparatively close to each other, since large epistyles were difficult to be constructed in a single monolithic piece. Mortar, was

not used as the blocks (drums) of each column were shaped to have very fine surfaces. In some cases iron or wooden cramps were used.

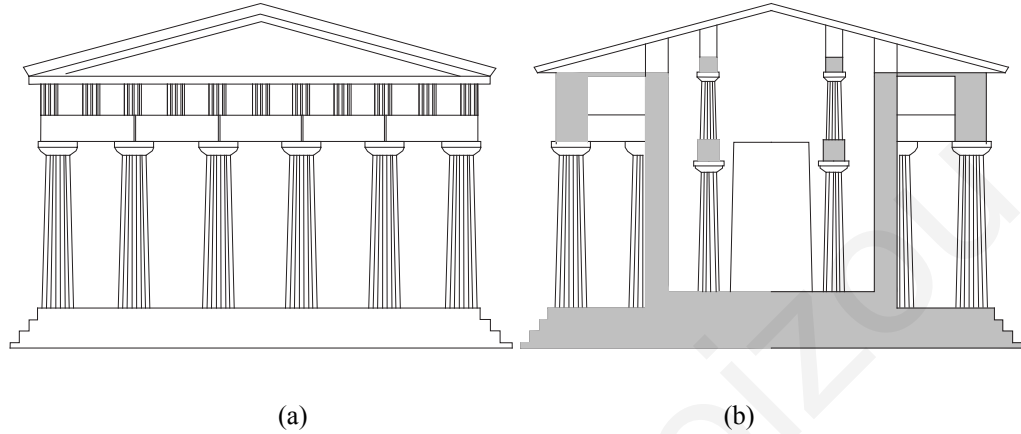


Figure 1.5. (a) Elevation and (b) section illustration of a typical ancient Greek temple.

Today, the remains of the majority of these temples are often limited to series of columns with an entablature or only an epistyle, and in some cases only standalone columns (Figure 1.1 and Figure 1.2).

1.3. Objectives

The main objective of this thesis is a thorough investigation of the seismic behaviour and response of ancient columns and colonnades during strong earthquake excitations using numerical simulations, in particular, the discrete element method (DEM).

The primary goal of the thesis is the development of a specialized software application using the DEM, which will be used to conduct numerical simulations and parametric studies of these structures under harmonic and earthquake ground excitations. The modern object-oriented design and programming will be utilized to develop an extendable software application that will allow the efficient and effective performance of relevant numerical simulations and parametric studies.

A critical step in this work is the extensive validation of the custom-made software application by comparing the computed responses of various simple problems with

corresponding analytical solutions and experimental observations. This will verify that the methodology used is suitable for analysis of multi-drum structures under dynamic loadings, providing sufficiently reliable and accurate results, taking into account the complexity of the problem.

After the development and validation of the custom-made DEM software, a large number of simulations of multi-drum columns and colonnades with varying mechanical and geometrical characteristics will be conducted under the action of various harmonic and earthquake ground excitations. In this way, the influence of several parameters in the seismic response of these structures will be systematically investigated.

Firstly, standalone multi-drum columns will be examined, investigating the effect of the acceleration and frequency of different types of the ground excitation. In addition, the effect of the number of drums per column, the shape of the drums, the coefficient of friction, as well as different frictional levels between different block assemblies will be investigated.

Moreover, various parameters that affect a structural system of multi-drum colonnades with epistyles will also be examined.

Specifically, the following parameters will be studied:

- The effect of the frequency of the ground excitation
- The effect of the number of colonnades
- The effect of the number of drums per column
- The type of epistyle
- The distance between colonnades
- The epistyle mass
- The shape of the colonnades
- The acceleration required to overturn a system
- The effect of a capital at the upper level of a column

Furthermore, a comparison with standalone columns will be conducted, in order to investigate similarities or variations in their responses under earthquake ground motions.

Finally, a more complex system of a row of columns placed on top of another row of columns will be studied under both harmonic and earthquake excitations. Specifically, the effect of the frequency content of the ground motion on the response of the upper level columns in respect to the response of the lower level will be examined.

1.4. Outline

The problem that is addressed in this thesis has been briefly presented in this first chapter, discussing the motivation and some very basic architectural elements of Greek ancient temples. The objectives of the thesis have been presented along with the expected contributions.

Previous relevant research work that has been conducted is summarized in *Chapter 2*. Firstly, relevant studies on the analytical and experimental dynamic response of rigid bodies are discussed. Secondly, an extensive review of the previous work concerning experimental and numerical investigation of the dynamic response of multi-drum columns is presented.

Subsequently, *Chapter 3* describes the methodology adopted to address the problem, covering various aspects of modelling discontinuous systems, contact interactions and forces. The discrete element method (DEM) is utilized to investigate the response of ancient multi-drum columns during harmonic and earthquake excitations by simulating the individual rock blocks as distinct rigid bodies.

The design and development of the software application are then described in *Chapter 0*. The specialized software application has been developed, using modern object-oriented technologies and computer graphics, to efficiently and effectively perform seismic simulations of multi-block structures. Various aspects, such as, the software

design, the selection of the programming language, as well as, the limitations of the developed software application are discussed.

In *Chapter 5* of this thesis, the developed software is thoroughly validated by comparing the computed responses of various fundamental problems, such as sliding, rocking and free vibration dynamics of rigid bodies, with corresponding analytical solutions that are available in the literature. Furthermore, small-scale experiments are carried out in order to assess the response of multiple rigid bodies under harmonic excitations. The results are then compared to corresponding numerical simulations that are conducted with the developed software application.

Subsequently, in *Chapter 6*, numerical simulations of standalone columns are carried out, using the developed application. Various analyses are conducted with different types of standalone columns and several types of ground motion excitations. Specifically, columns with different numbers of drums, various values of the coefficient of friction, as well as numerous shapes are considered. A large number of parametric studies is performed in order to examine the influence of the frequency content and the peak ground acceleration (PGA) of excitations, as well as the geometric and mechanical characteristics of standalone multi-drum columns in their responses to harmonic excitations. A comparison is made between the occurrences of sliding and rocking of the drums, aiming at understanding how various parameters may influence the dominance of either of the two phenomena. In addition to harmonic excitations, strong earthquake ground motions are also used to simulate and evaluate the seismic response of such columns. Various earthquake records, with different characteristics are used, comparing the computed responses to those under harmonic excitations.

In *Chapter 7*, the dynamic behaviour of multi-drum colonnades with epistyles under earthquake excitations is examined through planar numerical simulations. Parameters such as the number of drums that assemble a column, the number and distance between the columns of a colonnade, the type of an epistyle, as well as the loading conditions appear to be defining parameters that affect the dynamic response of colonnades with epistyles. For ground motions with relatively low predominant frequencies, rocking dominates the response, while, with the increase of the excitation frequency the response

becomes even more complex involving both sliding and rocking phenomena. The numerical simulations show that earthquakes with relatively low predominant frequencies seem to endanger both standalone columns and colonnades with epistyles more than earthquakes with higher predominant frequencies. Finally, two series of columns placed the one on the top of the other, representing the lower and upper rows of columns in ancient temples that supported a wooden roof, are investigated. These systems are analyzed under both harmonic and earthquake ground motion excitations.

Chapter 8 presents a summary of the work that has been carried out, followed by conclusions and contributions that have been made. Finally, the chapter concludes with some remarks and suggestions regarding future work in this research area.

2. Literature review

The dynamic behaviour of rigid blocks under dynamic loading is an extremely complicated phenomenon and can be characterized as highly non-linear, as these systems involve complicated rocking and sliding phenomena. Each body can undergo rocking, either individually, or in groups, resulting in several different and alternating shapes of oscillations of the entire system. Such multi-block systems can represent ancient monumental structures, such as multi-drum classical columns, water tanks, large machinery, containers, electrical equipment or even tombstones.

2.1. *Rigid body motion*

The dynamic response of rigid blocks is complex even for a single rigid body. Figure 2.1 shows the response of a rigid body left from an initial inclination angle to oscillate freely. The position of the block at different time increments reveals that the motion involves both rocking and sliding motion.

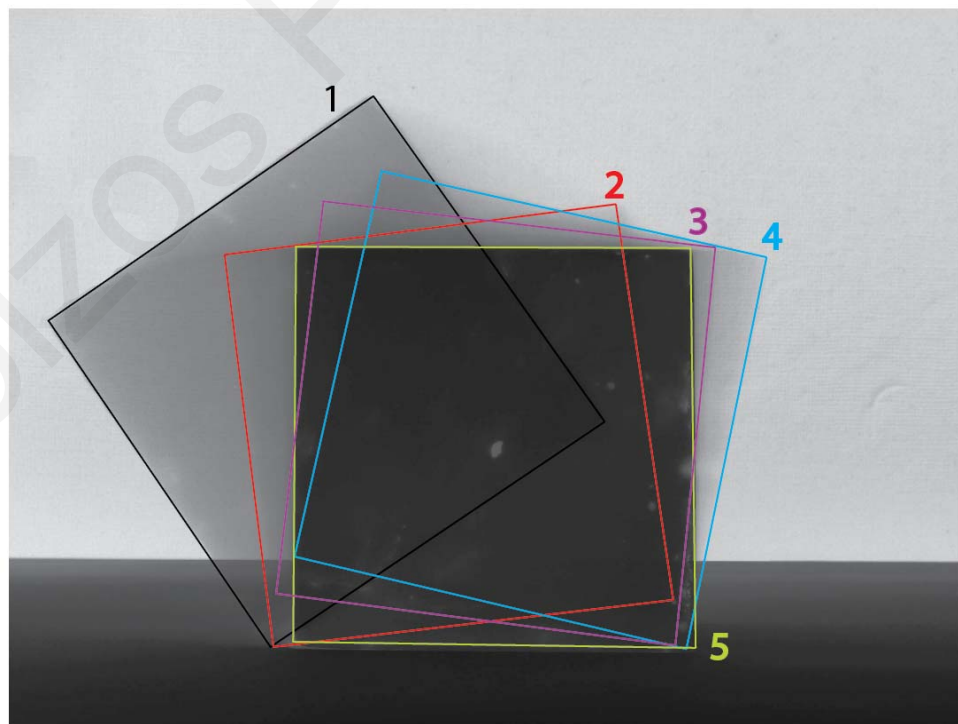


Figure 2.1. Motion of a rigid body left to oscillate freely from an initial inclination angle.

Many researchers have approached the problem of the dynamic response of rigid bodies in different ways. Since 1900, F. Omori [59], [60], one of the first scientists to investigate experimentally the effect of earthquakes on rectangular columns, had stated that the phenomenon is extremely complex and is affected by the input motion. He simplified the problem by focusing on ground motions that had frequency content capable to overturn the columns. A few decades later, other scientists studied the effect of the shape of a rectangular column on its dynamic response, while others, much later, investigated further criteria that affect the overturning of single rigid bodies.

A fundamental analytical study on the rocking response of a rigid block was provided by Housner [29] in 1963. Specifically, Housner considered a rigid body with sufficiently large coefficient of friction so that it can rock, but not slide. Assuming that there is no energy loss during impacts, Housner computed the required time T for a rigid block to complete a full cycle (period) of oscillation, after the rigid body is left to freely oscillate from an initial rotation angle. Furthermore, he computed the reduction of the kinetic energy, during each half-cycle of the oscillation of the body, due to impact.

Aslam et al. [7] studied the rocking and overturning response of rectangular blocks under strong earthquake motions. Aslam et al. suggested that it may be difficult to use data from observations on standing and overturned rigid bodies after an earthquake to provide much useful information on the intensity of the ground motion. They also pointed out the sensitivity of overturning to small changes in the base geometry and the coefficient of restitution as well as to the form of the ground motion.

Ishiyama [31] experimented with motions of rigid bodies on a rigid floor subjected to sinusoidal and earthquake excitations. His study included both experimental and numerical frequency sweep tests, concluding that the horizontal ground velocity, as well as the horizontal ground acceleration must be taken into account as criteria for overturning. He stated that it is possible to estimate the lower limits of the maximum horizontal ground acceleration and velocity needed to overturn rigid bodies.

Psycharis and Jennings [69] studied the dynamic behaviour of a rocking rigid block supported by a flexible foundation that permits uplift, proposing simplified methods

of analysis. Moreover, the study showed that, in general, uplift leads to a softer vibrating system that behaves nonlinearly, although the response of such systems is composed of a sequence of linear responses.

Tso and Wong [82], [83] studied both analytically and experimentally the rocking response of rigid bodies. The experiments were conducted using sinusoidal base motions, showing that for each type of steady-state response, the system may respond in either a symmetric or an asymmetric mode.

Spanos and Koh [79] studied in detail the rocking response of free-standing blocks subjected to harmonic steady-state loading, identifying ‘safe’ and ‘unsafe’ regions and developing analytical methods for determining the fundamental and sub-harmonic modes of the system. Hogan [28], extended this study, by expanding the mathematical structure of the problem, introducing the concepts of orbital stability.

Psycharis [67] presented an analysis of the dynamic behaviour of systems consisting of two blocks placed the one on top of the other, free to rock without sliding, stating that during vibration, the system continuously changes from one mode to another, making the response non-linear. The equations of motion for each ‘mode’ of vibration are derived and criteria for the initiation of rocking and the transition between modes are given. This transition between ‘modes’ includes impacts, in which case dissipation of energy occurs and the amount of which depends on the relative velocities and the dimensions of the blocks. The study showed that in most cases, the contribution from the upper block to the system energy increases, which results in a larger and longer response of the top block, compared to the vibration of the lower block.

The impact problem has been also approached by Sinopoli [78] by adopting a unilateral constraint, according to a “kinematic approach”, while the influence of nonlinearities associated with impact on the behaviour of slender rigid objects subjected to horizontal base excitations was studied by Yim and Lin [91].

Furthermore, a general, two-dimensional formulation for the response of free-standing rigid bodies to base excitation was presented by Shenton and Jones [73] to [75]. That formulation assumes rigid body, rigid foundation, and Coulomb friction, while the

behaviour was described in terms of the five possible modes of response: rest, slide, rock, slide-rock, and free-flight. Impacts with the foundation were assumed to be perfectly plastic and frictional impulses were included. The study found that periodic solutions exist in general only for relatively high amplitudes of the ground accelerations and coefficients of friction less than the inverse aspect ratio of the block. Also, the rock component of the response is sensitive to changes in the aspect ratio and the coefficients of friction, while it is insensitive to changes of the ground acceleration. The slide component of response is approximately equal to the amplitude of the ground displacement and it is insensitive to changes in the friction and the aspect ratio.

Allen and Duan [4] investigated the reliability of linearizing the equations of motion of rocking blocks. Shi et al [76] studied the rocking and the overturning of precariously balanced rocks by earthquake, while Scalia and Sumbatyan [72] examined the slide rotation of rigid bodies subjected to a horizontal ground motion.

Zhang and Makris [93] studied the rocking response of a freestanding block to one-sine and one-cosine acceleration pulses. These two trigonometric pulses are physically realizable and resemble in several occasions the fault-parallel and fault-normal component of motions recorded near the source of strong earthquakes (Makris and Roussos [49]). The study showed that under these pulses a free-standing block can overturn by exhibiting one or more impacts, or without exhibiting any impact. The existence of the second mode results in a safe region that is located over the minimum overturning acceleration spectrum. It was found that the shape of this region depends on the coefficient of restitution and is sensitive to the nonlinear nature of the problem. Furthermore, Makris and Zhang [50] investigated the rocking response and the overturning of anchored blocks under pulse-type motions. Pombei et al. [66] also studied the dynamics of a rigid block subjected to a horizontal ground motion, aiming to formulate criteria that separate the various patterns of the motion.

A probabilistic approach to the problem of rocking of rigid blocks was pursued by Yim et al. [92]. In their study a numerical procedure and computer program were developed to solve the non-linear equations of motion that govern the rocking motion of rigid blocks on a rigid base subjected to horizontal and vertical ground motion. The

presented response results demonstrate that the response of a block is very sensitive to small changes in its size and slenderness ratio, as well as to the details of ground motion. It was stated that the overturning of a block by a ground motion of particular intensity does not imply that the block will necessarily overturn under the action of more intense ground motion.

Koh and Spanos [35], [36] presented an analysis of random rocking of a block on rigid, as well as on flexible, foundation. Kim et al. [33] investigated experimentally the vibration properties of a rigid body placed on sand ground surface. It was found that the natural vibration period depends not only on the mechanical properties of the rigid body and the ground, but also on the magnitude of the vibration amplitude. This finding suggested the notable effect of nonlinear strain dependent stiffness of ground material. A physical model with distributed spring-dashpot element was used to model the interactive mechanical behaviour between the rigid body and the ground. The stiffness of the spring-dashpot element was evaluated through modal analysis of observed vibration behaviours. The effects of the base shape, size and pressure on the stiffness of the spring-dashpot element were discussed. The spring-dashpot model was verified with the behaviour observed in forced vibration tests. Finally, Makris [50] stated that the response of a rigid block involves complex dynamics, even with a simple problem of the simplest man-made structures, the free-standing block.

2.2. *Dynamic response of multi-drum columns*

Experimental research work has been conducted for the investigation of the dynamic behaviour of free standing multi-drum columns and colonnades using metal [21], [51], as well as marble [55], small-scale models. However, it has been shown that rocking of rigid bodies is a size dependent phenomenon and, thus, reliable results can be obtained only from tests with real full-scale dimensions and not from models with significantly smaller dimensions. In particular, it has been observed that among multi-block systems with varying sizes, but with the same relative dimensions, the ones with larger absolute dimensions have a larger capacity against overturning, under certain excitations.

Therefore, for the response of rocking systems, the experimental results cannot be extrapolated using similarity rules [55].

Nevertheless, certain trends of the seismic response and behaviour of such structures can be qualitatively identified and understood. Physical experiments reveal that the response of multi-drum structures under dynamic loadings is generally affected from the predominant frequency of the ground motion, where rocking dominates the response under earthquakes with low predominant frequency content.

Physical experimental tests of full-scale models are very difficult to perform and monitor. In addition, differences in the response have been observed among experiments with ‘identical’ models, due to the high sensitivity of the behaviour to slight changes of the geometry or input motion characteristics. Mouzakis et. al. [55] conducted an experimental investigation of the earthquake response of a model of a marble classical column. The model was a 1:3 scale replica of a column of the Parthenon on the Acropolis of Athens, made from the same material as the original. The base motion was applied in plane, in one horizontal and the vertical direction, and in space, in two horizontal and the vertical direction, using a shaking table. Several earthquake motions, scaled appropriately in order to cause significant rocking but no collapse of the column, were used as ground excitations. The results showed that the column might undergo large deformations during the shaking. Also, for planar excitations, significant out-of-plane displacements can happen, triggered by the inevitable imperfections of the specimen and that the response is very sensitive, even to small changes of the geometry or the input motion parameters. For this reason, the experiments were not repeatable, while ‘identical’ experiments produced different results.

Demosthenous and Manos [21], [51], investigated the dynamic response of rigid bodies, representing ancient columns and colonnades, to various types of horizontal base motions. The used rigid bodies were made of steel and were assumed to be small-scale models of prototype structures that were 20 times larger. Two basic configurations were examined: a single steel truncated cone assumed to be a model of a monolithic free-standing column and two steel truncated cones of the same geometry as the first one, supporting a rectangular solid steel and representing the simplest unit of a colonnade. The

experimental results were compared with predictions from numerical simulations. More recently, Manos et. al. [52] studied the shear transfer mechanism through the horizontal contact surface of two rigid blocks experimentally, as well as numerically using the Finite Element Method (FEM). The experimental sequence included specimens without any connection between the rigid blocks and specimens with poles and empolia connecting the rigid blocks under cyclic loading.

A more realistic, rational and cost-effective approach to investigate the response of multi-drum monuments is through numerical methods, especially since the computing power has been significantly increasing. An extensive overview of the usage of finite and boundary element methods for the analysis of monuments was published by Beskos [11], [12]. However, Finite Element Methods (FEM) are not the most suitable approach for the analysis of multi-block systems that are characterized by continuous changes of their geometry and the contact conditions among individual bodies, although they can be used for the analysis of problems with some discontinuities [53]. Discrete Element Methods (DEM), on the other hand have been specifically developed for systems with distinct bodies that can move freely in space and interact with each other with contact forces, providing an automatic and efficient recognition of all contacts [8], [16], [22].

The DEM have already been employed, through the usage of commercial general-purpose software in recent publications [3], [44], [62], [61], [70], concerning the response of ancient columns. Numerical studies of the earthquake response of ancient columns have been conducted in two dimensions by Psycharis et al. [71], as well as in three dimensions by Papantonopoulos et al. [62], using the commercial software *2DEC* and *3DEC*, respectively. In their work [71], typical sections of two ancient temples were modelled and studied parametrically, in order to identify the main factors affecting their stability and to improve our understanding of the earthquake behaviour of such structures. The analyses showed that, for frequencies usually encountered in earthquakes, free-standing columns can withstand large amplitude harmonic excitations without collapse. The dynamic resistance decreases as the period of the harmonic excitation increases. It was also found that the columns are particularly vulnerable to long-period impulsive

earthquake motions. Their study also showed that the response of two columns coupled with an architrave, did not deviate systematically from that of the single multi-drum column or indeed of the equivalent single block. Therefore, a much simpler single block analysis was suggested that can be used to assess the seismic threat to a monument. Furthermore, imperfections, such as initial tilt of the column or loss of the contact area due to edge damage, were also found to reduce the stability of the system significantly.

Psycharis [68] also investigated the seismic response of monuments with fractured structural elements. The distinct element method was used for the analysis of a model that corresponds to a part of the columns of the Olympiou Dios Temple in Athens, Greece. The results indicated that the degree of the crack opening during an earthquake increases almost linearly with the peak velocity of the ground motion and the number of repetitions of the excitation. If significant shear and tensile strength exist at the crack interface, a stronger seismic excitation is, in general, required to cause failure. It was also concluded that cracks at column drums do not endanger the stability of the structure, unless they produce wedge-type pieces, which may slide during the earthquake.

Psycharis et al. [70] reported that the behaviour displayed by the numerical simulations of standalone columns confirms the conclusions drawn from the shaking table tests. A salient feature is the association of drum rocking with movements of twisting of the column around its vertical axis, leading to the patterns of permanent displacements observed in the experiments [55]. They also observed that reinforcement of the column drums, by titanium dowels that offer shear resistance, may reduce the permanent displacements under typical earthquake motions. For more severe base excitations, however, they concluded that their effect is not important due to the uplift that occurs. They suggested that in some cases, the presence of titanium dowels may be unfavourable to the safety of the structure against collapse.

Konstantinidis and Makris [42] also examined the seismic response of multi-drum columns and the effect that wooden poles might have in their responses, by using the commercial software *Working Model 2D* [89]. In their work, this specific software was validated by comparing selected computed responses with scarce analytical solutions. The most important conclusion of that paper was that relative sliding between the drums

occurs, even when the value of the peak ground acceleration, expressed as a fraction of the gravitational acceleration, is less than the coefficient of friction along the sliding interfaces.

Mitsopoulou et. al. [53] investigated numerically the seismic response of multi-block structures by discretizing the blocks in a two dimensional finite element mesh with discrete nodes. The contact interfaces were handled by applying friction. Both monolithic and multi-drum standalone columns were studied, under various seismic and harmonic ground motions, and the computed responses pointed out that the considered monuments were stable under the selected ground motions.

Columns with an architrave (epistyle) were also investigated by Psycharis et al. [70] with the systems displaying considerable stability when the architraves were properly connected by reinforcement elements. Titanium connections, linking the architraves between themselves and with the column capital, showed a good performance under severe seismic excitations. However, they concluded that if the architraves are left free, they are susceptible to falling under input motions lower than those that lead to failures of the columns. Finally, the analyses indicated that the existence of imperfections, such as split drums, reduced sections or asymmetric architrave placement, adversely affect structural safety. They suggested that when it is not possible to eliminate these deviations from the original state, it is important that they are taken into account in the safety assessment models.

The above studies demonstrated that the DEM can be used, although a sensitivity of the response to small perturbations of the characteristics of the structure or the excitation has been reported. Nevertheless, such sensitivities have also been observed in experimental investigations of multi-drum columns and colonnades.

In order to investigate parameters that affect the response of such multi-drum structures, it is necessary to efficiently perform large numbers of numerical simulations, where earthquake characteristics and design parameters are varied [38]. In this research work a custom-made DEM software has been specifically designed and implemented to efficiently and effectively perform large numbers of numerical simulations with varying

parameters, modelling the individual rock blocks as distinct bodies. The theory, methodology, as well as assumptions and limitations used to implement the custom-made application are explained in the following chapters.

Loizos Papaloizou

3. Formulation of the physical problem

3.1. *Discrete Element Methods (DEM)*

The DEM were originally proposed in 1971 for the solution of problems of rock mechanics [18], where distinct elements were used to simulate rock masses. According to the DEM, each distinct body has its own geometric boundaries that separate it from all other bodies. The distinct bodies are usually assumed infinitely rigid, although it is possible to consider them deformable. Contact forces are applied only when a contact between two bodies is detected. The interactions between two bodies can be due to recently detected contacts, existing contacts, or relative displacements and rotations between bodies that are already in contact.

3.2. *Contact modelling*

In order to simulate multi-body structural systems, the contact model must have the ability to automatically recognize the existence of any contacts between any discrete bodies of the system. Relevant numerical methods are classified into two groups according to the way with which they treat the contact behaviour in the normal direction of motion at the points of contacts. The first group uses a “soft-contact approach”, where, a finite normal stiffness is taken into account to represent the local deformability that exists at a contact, allowing some slight overlapping of colliding bodies. The second group uses a “hard-contact approach”, with which, any interpenetration of the two bodies that are in contact is prevented by enforcing certain constraints, which increase substantially the computational cost. The choice of the contact assumption to be used is usually made on the basis of the physical problem under consideration, depending on the circumstances that are involved, the requirements of the analysis and the numbers of the simulated distinct bodies. The soft contact approach is selected to be used since it is more efficient for the simulation of large number of colliding discrete bodies.

The contact location is an important factor that must also be taken into account. For point contacts, the location of the resultant force vector clearly is at the point of contact. But, where contact conditions exist over a finite surface area on both bodies, the exact point where the contact force should be applied is not so obvious. It is reasonable to assume that the resultant force acts at the centre of the interpenetration volume or area. Cundall [18] suggested that the location should be regarded as an independent constitutive property, depending on the relative rotation of the two surfaces in contact. Even if a computer program can relate force location to geometric variables, there is, at present, very little data from physical tests to substantiate any physical assumption [32].

For the specific problem of the dynamic response of ancient columns and colonnades under dynamic loading, the contact forces are computed based on the overlapping region of the bodies in contact. The contact forces in the normal and tangential contact planes are assumed to act on the centroid of the overlapping region, and applied at the corresponding position of the bodies in contact.

3.3. Block deformability

There are two approaches for modelling the mechanical behaviour of the solid discrete bodies of a discontinuous system. The simulated discrete bodies can be considered to be either infinitely rigid, i.e. without any deformations, or deformable. Either of the two approaches can be used according to the details of the specific problem under investigation and the response quantities that need to be computed.

If the deformation of each solid discrete body cannot be neglected, two main methods can be used to take into account its deformability. In the direct method of introducing deformability, each discrete body is subdivided internally into finite or boundary elements in order to consider its internal deformations. Due to the large displacements of the simulated bodies, a nonlinear formulation should be used to express the equations of motion on the deformed rather than the initial undeformed configuration of the system. In addition to the geometric nonlinearities due to the large displacements, the deformations of each body may be substantial, requiring a nonlinear constitutive law

to consider the large strains. Another difficulty of this approach is that a body of complex shape must necessarily be subdivided into many zones, even if only a simple deformation pattern is required [32].

An alternative scheme to consider the deformability of the individual bodies was devised by Shi [77] in his “Discontinuous Deformation Analysis” (DDA). According to that approach a series of approximations are used to supply an increasingly complex set of strain patterns that are superimposed for each block. However, Williams and Mustoe [88] noted that the use of direct strain modes may be inconsistent.

The assumption that the material of each discrete body is infinitely rigid is appropriate when most of the overall deformations in a physical system are due to movements on discontinuities and rearrangements of the individual bodies rather than due to internal deformations of the simulated discrete bodies. Such a condition applies, for example, in an unconfined assembly of rock blocks at low stress levels. In that case, the deformations of the simulated system are due to the movements that are caused mainly due to sliding and rotation of the individual blocks, as well as, due to the opening and interlocking of interfaces, but not due to internal deformations of the individual bodies.

For the dynamic analyses of ancient columns and colonnades the bodies are assumed infinitely rigid, considering that the overall deformation of a system with distinct bodies is due to the relative displacements and rearrangements of the simulated bodies rather than due to the deformations of the individual bodies. The system is dominated by discontinuities between the drums of the columns and consequently, the material is assumed to be infinitely rigid and its elastic properties are taken into account only indirectly through the stiffness of the corresponding contact springs. The basic formulation for infinitely rigid blocks was given by Cundall et al. [20], where the medium is dealt as a set of distinct blocks that do not change their geometry as a result of the applied loadings.

3.4. Contact interactions

The contact interactions between colliding bodies constitute an extremely complicated phenomenon that involves stress and strain distributions within the colliding bodies, thermal, acoustical and frictional dissipation of energy due to contacts, as well as plastic deformations. In our simulations, the contact interactions are modelled using soft contact springs and dashpots to evaluate the contact and damping forces based on the interpenetration between bodies in contact. A unique ability of the DEM is the automatic and efficient recognition of contacts between simulated bodies, as well as detachments of bodies that were previously in contact.

In particular, the interactions between two rigid distinct bodies in contact are automatically generated in the DEM as soon as a contact is detected, kept as long as the bodies remain in contact and removed as soon as the bodies are detached from each other (Figure 3.1.a). In order to be able to consider potential sliding according to the Coulomb law of friction, normal and tangential directions are considered during contact. The normal and tangential directions are based on a contact plane, which is determined at each simulation step (Figure 3.1.b). The bodies may slide along the contact plane relatively to each other, when the tangential force reaches the maximum allowable force in that direction, as computed by the Coulomb Law of Friction.

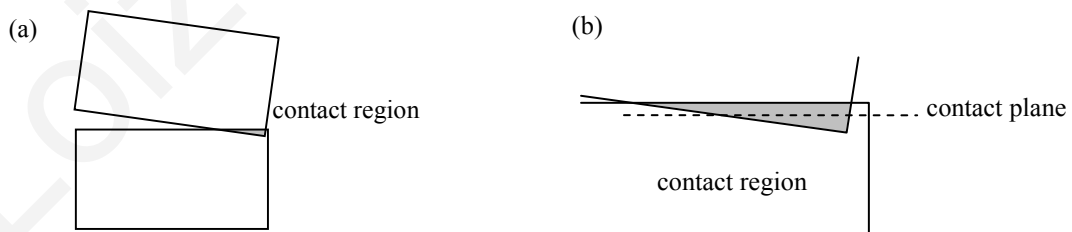


Figure 3.1. Contact between two bodies: (a) contact region and (b) contact plane.

At any simulation step, when two bodies come in contact, equivalent springs and dashpots are automatically generated, in the normal and tangential directions, to estimate the respective contact forces that are applied to the bodies pushing them apart (Figure 3.2). Some overlapping of the bodies in contact is allowed, which is justified by the

deformability at the vicinity of the contact. The interactions between bodies may involve new contacts, renewed contacts, slippages and complete detachments from other bodies with which they were, until that time, in contact.



Figure 3.2. Contact springs and dashpots: (a) in the normal and (b) tangential directions.

3.5. Simulating discontinuous systems

Many software applications are based on a continuum mechanics formulation, such as the finite element methods and the Lagrangian finite-differences method, that can simulate the variability in material types and nonlinear constitutive behaviour. However, the representation of discontinuities requires a discontinuum-based formulation. There are several finite element, boundary element and finite difference general purpose programs available that have interface elements or “slide lines”, which enable them to model a discontinuous material to some extent. Their formulation is usually restricted in one or more of the following ways. Firstly, the logic may break down when many intersecting interfaces are used. Secondly, there may not be an automatic scheme for recognizing new contacts and thirdly, the formulation may be limited to small displacements and rotation. Finally and most importantly the computational cost of contact problems is substantial, not allowing simulations of more than a couple of distinct bodies.

Computer programs described as *discrete element* codes provide the capability of analyzing the motion of multiple, intersecting discontinuities explicitly. Cundall and

Hart [19], [32] provided the following definition of a discrete element method, where the name “discrete element” applies to a computer program *only* if:

1. It allows finite displacements and rotations of discrete bodies, including complete detachments
2. It recognizes new contacts automatically as the calculation progresses.

A discrete element code typically will embody an efficient algorithm for detecting and classifying contacts. It will maintain a data structure and a flexible memory allocation scheme that can handle many hundreds or thousands of discontinuities.

Cundall and Hart [19], [32] also identified the following four main classes of codes that conform to the definition of a discrete element method.

1. Distinct element programs use an explicit time-marching scheme to solve the equations of motion directly. Bodies may be rigid or deformable.
2. Modal methods are similar to the distinct element method in the case of rigid blocks but, for deformable bodies, modal superposition is used.
3. Discontinuous deformation analysis assumes that contacts are infinitely rigid. The simulated bodies may be rigid or deformable.
4. Momentum-exchange methods assume that both the contacts and the bodies are infinitely rigid. Friction sliding can be represented.

Another class of codes, defined as limit equilibrium methods, can also model multiple intersecting discontinuities, but does not satisfy the requirements for a discrete element code. These codes use vector analysis to establish whether it is kinematically possible for any block in a multi-body system to move and become detached from the system. This approach does not examine subsequent behaviour of the system of blocks or redistribution of loads, while all blocks are assumed rigid.

3.6. Contact detection

Since the contact forces are computed based on the overlapping area of two bodies in contact, an efficient contact detection algorithm has been developed. The algorithm computes whether two bodies are in contact providing the overlapping region of the bodies in contact. The overlapping region is then used to compute the magnitude, position, and direction of the contact forces (Figure 3.3).

The main computational demand during the simulation of multiple bodies is usually the contact detection [87], [58]. If the interacting bodies have simple geometric shapes, such as circles, the contact detection as well as the definition of the contact plane is simple. For more complex shapes this procedure becomes more complicated. The contact detection process requires special caution in order to avoid exhaustive tests of each discrete body against all other bodies in the simulated system. This process is computationally very costly especially for a large number of bodies, N , as it requires an order $O(N^2)$ checks. A contact detection scheme that consists of a spatial reasoning and identification phase followed by a detail pairwise contact detection and resolution phase is used to avoid exhaustive checks of each body against all other simulated bodies.

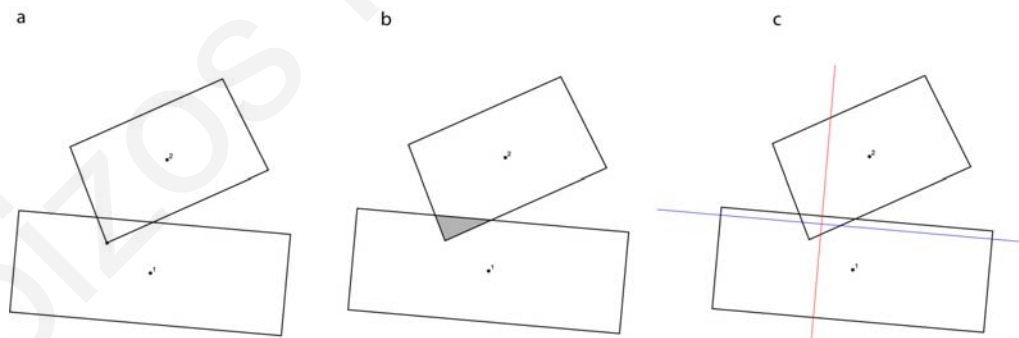


Figure 3.3. Calculation of the normal and tangential contact plane.

In particular, a spatial reasoning and identification phase is used to exclude all bodies that cannot be in contact. This phase is based on a spatial sorting of the bodies followed by a spatial searching. The former uses overlapping tests to identify potential pairs of bodies that are candidates to be in contact. Figure 3.4 demonstrates a simple spatial reasoning method, where the rigid bodies can be approximated by forming rigid

Formulation of the physical problem

circles around them. For each pair of bodies the algorithm checks whether these circles overlap, in which case the two bodies can be potentially in contact in the overlapping region of these circles (Figure 3.4b).

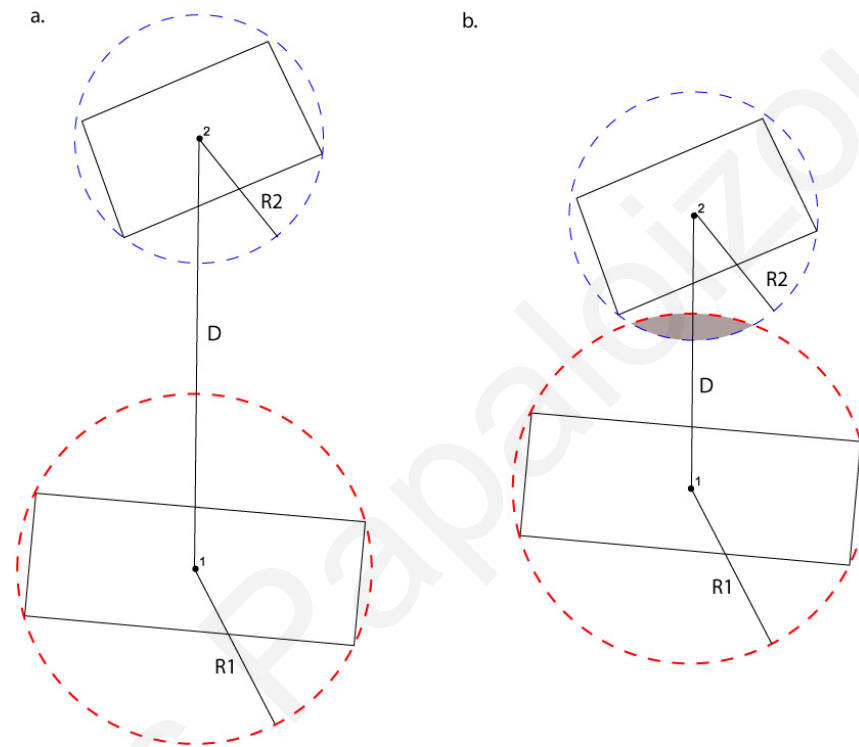


Figure 3.4. Contact checks for each body using only adjacent bodies.

Having identified pairs of bodies that may be in contact, the pairwise contact detection and resolution phase follows. The checks in this phase are done for each body using only adjacent bodies, which are selected during the spatial reasoning phase. The pairwise contact detection phase makes detailed contact checks for each selected pair of bodies that has been selected to be potentially in contact and determines whether the bodies under consideration are indeed in contact. Whenever two bodies are verified to be in contact, the contact resolution determines the contact geometry of the overlapping region and the directions of the relative movements of the two bodies. This information is used for the computation of the normal and tangential contact forces that are applied by the contact springs and dashpots during the formulation of the equations of motion.

These contact detection checks between distinct bodies are performed at every time step Δt during the simulation. The time step is sufficiently small with respect to the expected velocities and the dimensions of the simulated bodies in order to avoid omitting any contact detection.

Depending on the geometric characteristics of the bodies that are used in the problem, various algorithms of spatial reasoning can be used in order to identify potential contacts between bodies. For multi-drum columns in particular, where the distinct bodies that represent the drums are placed on each other, spatial reasoning can be computed based on the position of each body and the diameter of the corresponding circle that encloses it (Figure 3.5). Therefore, if the circles that enclose two bodies overlap, the corresponding bodies may potentially be in contact. Otherwise, the bodies are definitely not in contact and should not be checked further.

Another algorithm of spatial reasoning that can be selected for different problems is based on the projection of each body bounds on a horizontal and a planar vertical axis. Specifically, the selection of potential bodies in contact is performed by comparing the projections of the minimum and maximum bounds of the bodies on the X and Y axes (Figure 3.6). This spatial reasoning based on a sorting of the bounds of each body in order to expedite the search processes reduces substantially the computational cost. If the projections on both axes of a body's bounds lie within the corresponding projections of another body, then the two bodies are selected for detailed contact detection, since they may potentially be in contact. Otherwise, if their bounds in any of the axes do not overlap, the bodies are definitely not in contact and there is no need for detailed contact detection.

These spatial reasoning methods significantly reduce the computational time required for contact detection, since they exclude all bodies that are obviously not in contact from the more detailed checks. Furthermore, the ability to select a specific spatial reasoning algorithm for a specific geometry increases the overall efficiency of the developed application.

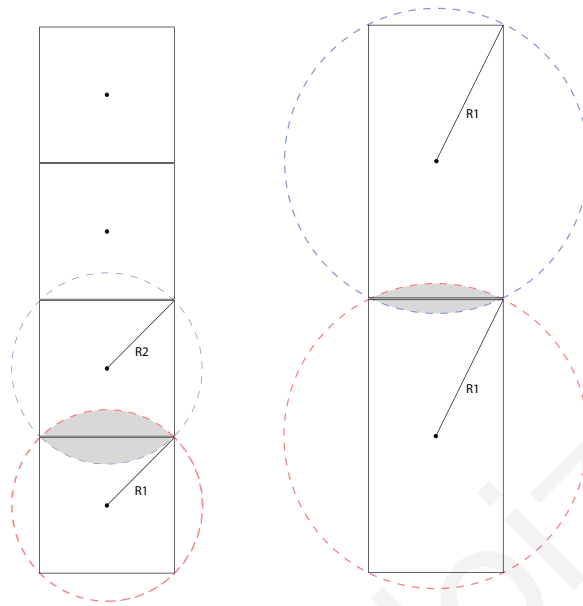


Figure 3.5. Spatial reasoning based on the body's position and boundary diameter.

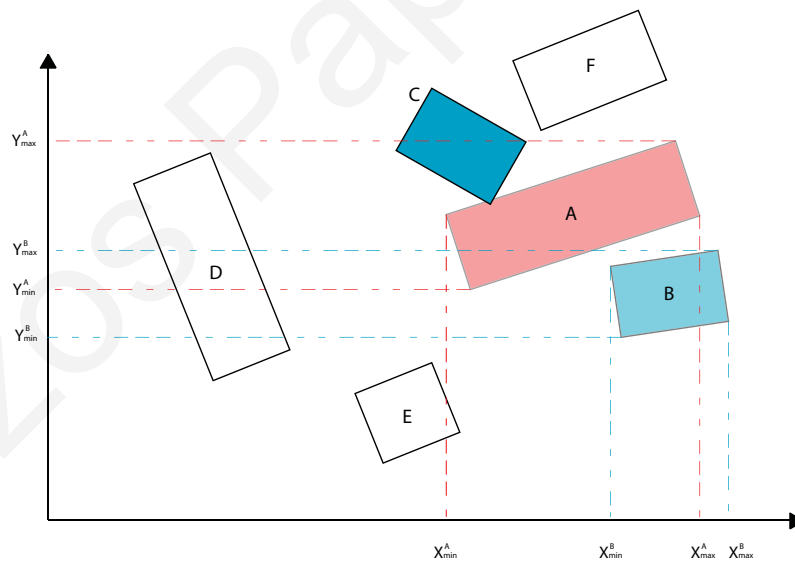


Figure 3.6. Spatial reasoning based on the projection of each body's bounds on the X and Y axes.

3.7. Contact plane

In addition to the determination of the contact area of the bodies in contact, it is necessary to determine the normal and tangential contact planes in order to be able to apply the normal and tangential contact forces as well as the Coulomb Law of Friction.

For rectangular bodies the contact plane is a contact line. The orientation of the contact plane, can be defined by a normal vector to that plane. The normal vector is determined by the features of each of the two bodies that are in contact. Specifically, a specialized algorithm has been developed for the calculation of the contact plane between bodies of various shapes. The algorithm takes into account the overlapping area of the bodies in contact and their position in space. Figure 3.7 illustrates different cases of contact between two rectangular bodies with the corresponding contact planes.

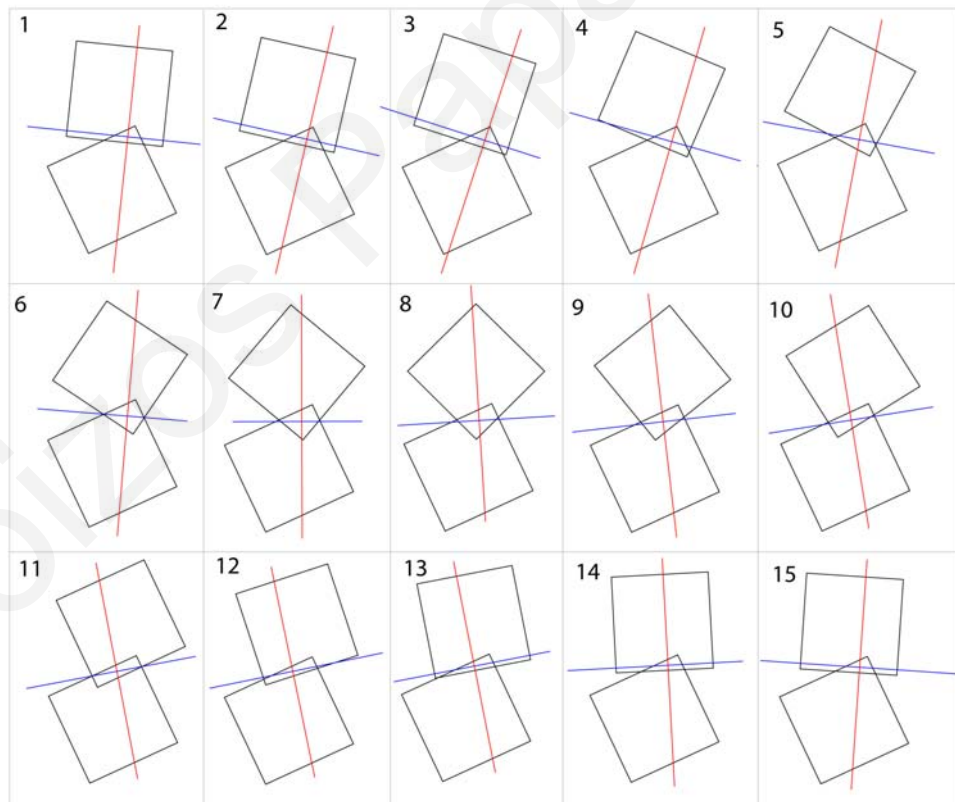


Figure 3.7. Normal (red) and tangential (blue) plane.

Formulation of the physical problem

Specifically, the developed algorithm is a “corner - corner” contact algorithm that uniquely defines the normal and tangential plane, as well as the reference position of the contact forces for a pair of rigid bodies (A and B) that are in contact. The bodies in contact are considered to be convex polygons with three or four faces, resembling individual drums of multi-drum columns as well as different type of epistyles. Therefore, the contact overlapping area can be either triangular or quadrilateral (Figure 3.8).

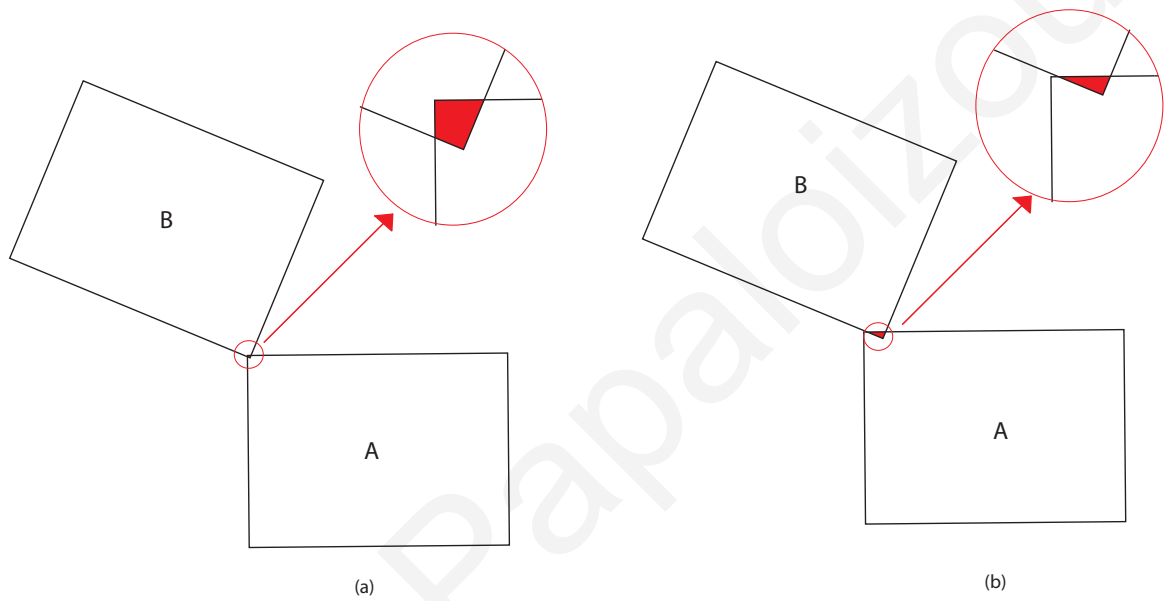


Figure 3.8. Contact resolution: (a) quadrilateral and (b) triangular overlapping contact area.

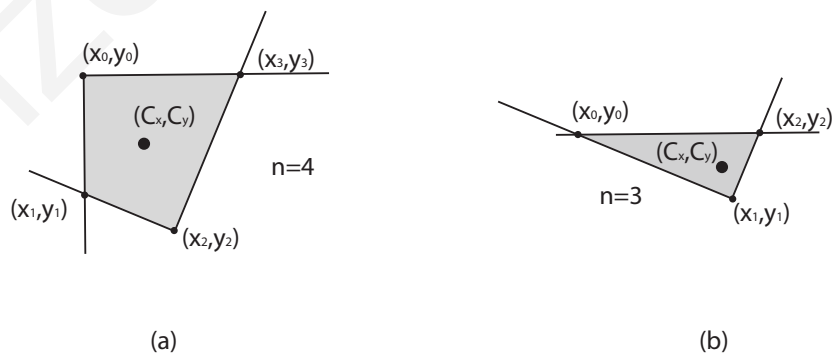


Figure 3.9. Calculation of the contact area of (a) a quadrilateral and (b) a triangular contact region.

Formulation of the physical problem

The methodology that is used defines a normal (N) and a tangential (T) plane in such a way that no directional jump occurs, at any case. Specifically, the two contact planes smoothly change direction, while the overlapping contact area changes from triangular to quadrilateral. The area (A) and the coordinates of the centroid (C_x, C_y) of the overlapping contact region are given by the following equations:

$$A = \frac{1}{2} \sum_{i=0}^{n-1} (x_i \cdot y_{i+1} - x_{i+1} \cdot y_i) \quad (3.1)$$

$$C_x = \frac{1}{6 \cdot A} \sum_{i=0}^{n-1} (x_i + x_{i+1})(x_i \cdot y_{i+1} - x_{i+1} \cdot y_i) \quad (3.2)$$

$$C_y = \frac{1}{6 \cdot A} \sum_{i=0}^{n-1} (y_i + y_{i+1})(x_i \cdot y_{i+1} - x_{i+1} \cdot y_i) \quad (3.3)$$

For a triangular overlapping contact region, the direction of the tangential contact plane (T) is defined to be parallel to the longest side of the triangle. For a quadrilateral contact region, the tangential contact plane (T) is defined to be parallel to the longest line joining two non-consecutive vertices of a polygon. The direction of the normal contact plane (N) is defined to be perpendicular to the tangential contact plane ($N \cdot T = 0$). The contact forces in the normal and tangential directions are applied at the centroid of the contact region (C_x, C_y) according to the normal and tangential contact planes.

The formulation of the methodology that is used is based on the assumption that the overlapping contact region will be relatively small. Consequently, the time-step used in the analysis is required to be sufficiently small.

The developed software is designed to handle contact between multiple bodies. For each set of contacting bodies and for each time step, the application stores a normal and tangential contact vector, which is used for the calculation of the corresponding normal and tangential contact forces, respectively.

3.8. Contact forces

When damping is taken into account the increment of the contact forces consists of two parts, the elastic and the damping force increments. The elastic and damping contact forces in the normal (N) and tangential (T) directions are computed in terms of the elastic and the damping force components, using the following equations, respectively, based on the area of the overlap region and considering the interpenetrations and the relative velocities, in both directions, between the colliding bodies:

$${}^{t+\Delta t}F_N = {}^{t+\Delta t}F_N^{elastic} + {}^{t+\Delta t}F_N^{damp} = {}^tA_c \cdot K_N + V_N^{rel} \cdot C_N \quad (3.4)$$

$${}^{t+\Delta t}F_T = {}^{t+\Delta t}F_T^{elastic} + {}^{t+\Delta t}F_T^{damp} = {}^tF_T^{elastic} + V_T^{rel} \cdot \Delta t \cdot K_T + V_T^{rel} \cdot C_T \quad (3.5)$$

Similarly, the indices N and T in the above equations, indicate the normal and the tangential directions, respectively. K_N and K_T are the stiffnesses in the normal and tangential directions, respectively. A_c is the area of the contact region, V_N^{rel} , V_T^{rel} , C_N and C_T are the relative velocities and the damping coefficients in the normal and tangential directions, respectively. Damping is velocity-proportional and the magnitude of the damping force is proportional to the corresponding relative velocity of the rigid blocks that are in contact.

The Coulomb friction law is used to limit the tangential contact force, ${}^{t+\Delta t}F_T$, below a certain magnitude taking into account the magnitude of the normal contact force, ${}^{t+\Delta t}F_N$, and the minimum of the coefficients of friction, μ , of the bodies in contact.

$$\left| {}^{t+\Delta t}F_T \right| \leq \left| {}^{t+\Delta t}F_N \cdot \mu \right| \quad (3.6)$$

Damping is velocity-proportional and the magnitude of a damping contact force is proportional to the relative velocity of the rigid blocks that come in contact, representing the dissipation of energy during contacts. In the way the energy dissipation is modelled, velocity-proportional contact dampers are automatically generated and act between bodies that are in contact. The coefficient of damping for the velocity-proportional contact

dampers has Ns/m units, so that when multiplied with the relative velocity between the bodies in contact to derive the corresponding contact damping force.

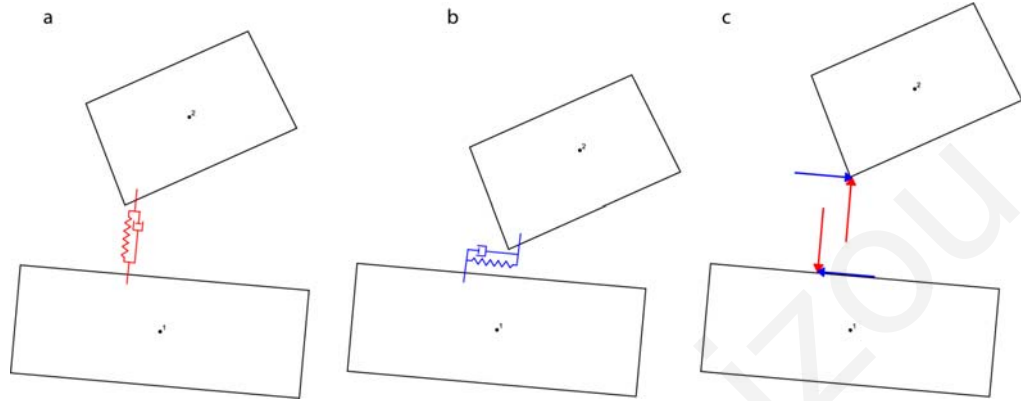


Figure 3.10. Contact springs and dashpots: (a) in the normal direction and (b) in the tangential direction.(c) Contact Forces.

3.9. Equations of motion

The contact forces, which are applied at the corresponding contact points during impact, are taken into account, together with the gravity or any other forces, in the formulation of the equations of motion. The contact forces from each contact point as well as any other forces acting on each body are then transformed to the centre of mass of the body, as shown in Figure 3.11.

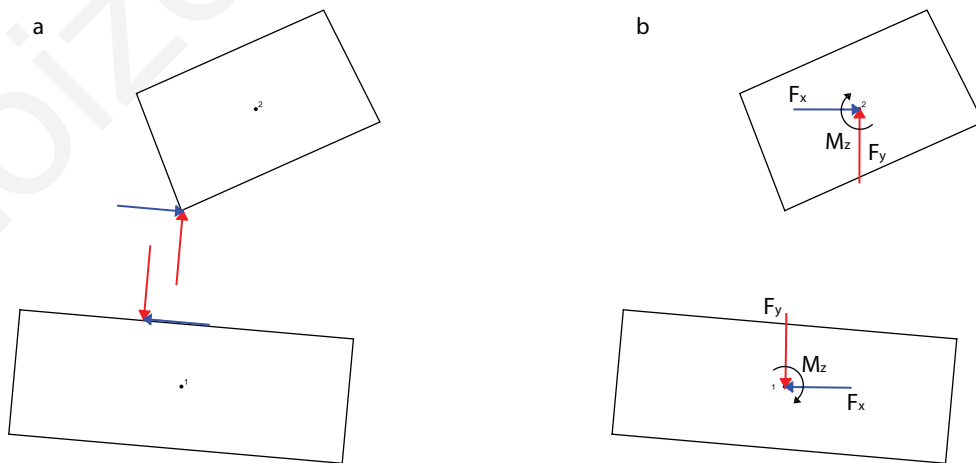


Figure 3.11. Transformation of the contact forces to the centre of mass of each rigid body.

Formulation of the physical problem

The motion of a discrete body at time $t + \Delta t$ is determined from the dynamic equilibrium equations at time t , which are integrated using an explicit direct integration numerical method (Bathe [9]). In particular, the equations of motion are numerically integrated using the Central Difference Method (CDM) computing the displacements at time $(t + \Delta t)$ from the following Equations:

$$U_x(t + \Delta t) = \frac{\Delta t^2}{m} \cdot \left\{ F_x - \frac{m}{\Delta t^2} U_x(t - \Delta t) + \frac{2m}{\Delta t^2} U_x(t) \right\} \quad (3.7)$$

$$U_y(t + \Delta t) = \frac{\Delta t^2}{m} \cdot \left\{ F_y + m \cdot g - \frac{m}{\Delta t^2} U_y(t - \Delta t) + \frac{2m}{\Delta t^2} U_y(t) \right\} \quad (3.8)$$

$$\Theta_z(t + \Delta t) = \frac{\Delta t^2}{I_o} \cdot \left\{ M_z - \frac{I_o}{\Delta t^2} \Theta_z(t - \Delta t) + \frac{2I_o}{\Delta t^2} \Theta_z(t) \right\} \quad (3.9)$$

In the above equations of motion, U_x and U_y are the displacements at the X and Y directions, respectively, while Θ_z is the rotation about the Z axis. Similarly, F_x and F_y are the forces acting on the body at the centre of mass in the X and Y directions, respectively, and M_z is the moment acting on the body about the Z axis. The time step, Δt , is selected to be sufficiently small to satisfy the stability requirements of the numerical method accurately and to capture all contact interactions. Finally, m and I_o are the mass and the rotational inertia at the centre of mass of the body, respectively. This process is iteratively repeated with new cycles of contact detection, contact resolution and numerical solution of the formed equations of motion until the simulation procedure ends.

The numerical analysis is based on the assumption that velocities and accelerations are constant within each time step. The motion of each individual body is computed using the CDM, which is an explicit time stepping integration method, based on the following approximations for the velocity:

Formulation of the physical problem

$$\underline{\dot{U}}(t + \Delta t / 2) = \frac{\underline{U}(t + \Delta t) - \underline{U}(t)}{\Delta t} \quad (3.10)$$

therefore,

$$\underline{\dot{U}}(t - \Delta t / 2) = \frac{\underline{U}(t) - \underline{U}(t - \Delta t)}{\Delta t} \quad (3.11)$$

where,

$$\underline{U}(t) = \begin{bmatrix} U_x(t) \\ U_y(t) \\ \Theta_z(t) \end{bmatrix} \quad (3.12)$$

Accordingly the acceleration can be computed by the equations:

$$\underline{\ddot{U}}(t) = \frac{\underline{\dot{U}}(t + \Delta t / 2) - \underline{\dot{U}}(t - \Delta t / 2)}{\Delta t^2} \quad (3.13)$$

$$\underline{\ddot{U}}(t) = \frac{\underline{U}(t + \Delta t) - 2\underline{U}(t) + \underline{U}(t - \Delta t)}{\Delta t^2} \quad (3.14)$$

Considering the equations of motion, the displacements, including the two translational and the rotational degrees of freedom, at time $t + \Delta t$ can be derived:

$$\underline{F}(t) = \underline{M} \cdot \underline{\ddot{U}}(t) = \underline{M} \frac{\underline{U}(t + \Delta t) - 2\underline{U}(t) + \underline{U}(t - \Delta t)}{\Delta t^2} \quad (3.15)$$

Therefore,

$$\underline{U}(t + \Delta t) = \Delta t^2 \cdot \underline{M}^{-1} \cdot \underline{F}(t) + 2 \cdot \underline{U}(t) - \underline{U}(t - \Delta t) \quad (3.16)$$

The matrix \underline{M} is diagonal and has the following form for a planar body of mass m and rotational inertia I_0 :

$$\underline{M} = \begin{bmatrix} m & & \\ & m & \\ & & I_o \end{bmatrix} \quad (3.17)$$

The DEM are based on the concept that the time step Δt is sufficiently small so that during a single step, disturbances cannot propagate between one discrete element and its immediate neighbours. Therefore, very small time steps are used, of the order of 1E-6 sec, so as to satisfactorily capture the collisions and contacts among the individual discrete bodies of the simulated system. Such small time step satisfies both the stability and the accuracy requirements of the CDM.

After computing the displacements and rotations of all bodies, for each time step, their corresponding positions and orientations are determined and updated. Then, a new cycle of contact detection, contact resolution, application of forces and solution of the equations of motion follows, based on the updated positions of the bodies. This iterative procedure continues until the end of the simulation.

Considering for simplicity in Figure 3.12 only the normal direction, the magnitude of the contact forces starts from zero, when the bodies first come in contact (Figure 3.12 and Figure 3.13, Stage 1), and increases during the approach phase, as the bodies "interpenetrate" each other up to a maximum value (Figure 3.12 and Figure 3.13, Stage 2). Then, during the restitution phase the contact force decreases and eventually becomes equal to zero when the bodies detach from each other (Figure 3.12 and Figure 3.13, Stage 3).

At each contact point, pairs of equal and opposite contact forces in the normal and the tangential directions are computed from the relative motions of the bodies in contact. Any residual contact forces from the previous time steps are also taken into account. The normal and tangential contact forces are stored at each time step with respect to the associated normal and tangential vectors to the contact plane, in a way that their magnitudes are invariable to rigid body rotations. The bodies are eventually pushed apart due to the action of the contact forces. As soon as there is no overlap between the two bodies, the memory corresponding to the contact data, which are used in the software, is

Formulation of the physical problem

released by the program. After that point, no contact forces are applied between the two formerly-in-contact bodies.

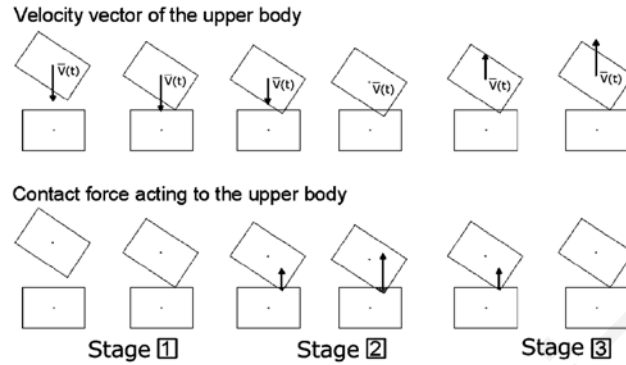


Figure 3.12. Variation of the relative impact velocity in the normal direction during impact.

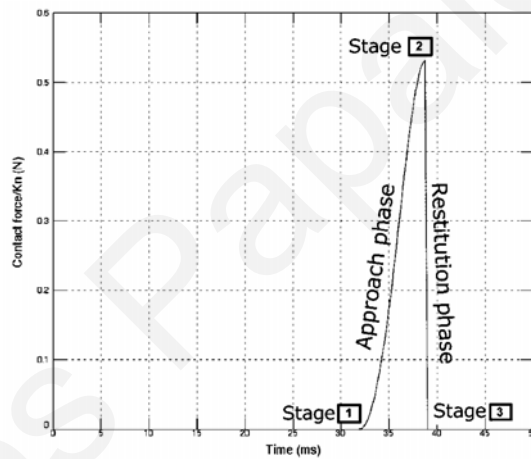


Figure 3.13. Build-up of the contact force in the normal direction during impact.

3.10. Analysis procedure

During the analysis, at each simulation step, all of the bodies are checked with each other for contact. If no contact for a body is detected, gravitational, or any other surface or body, forces are applied on the body.

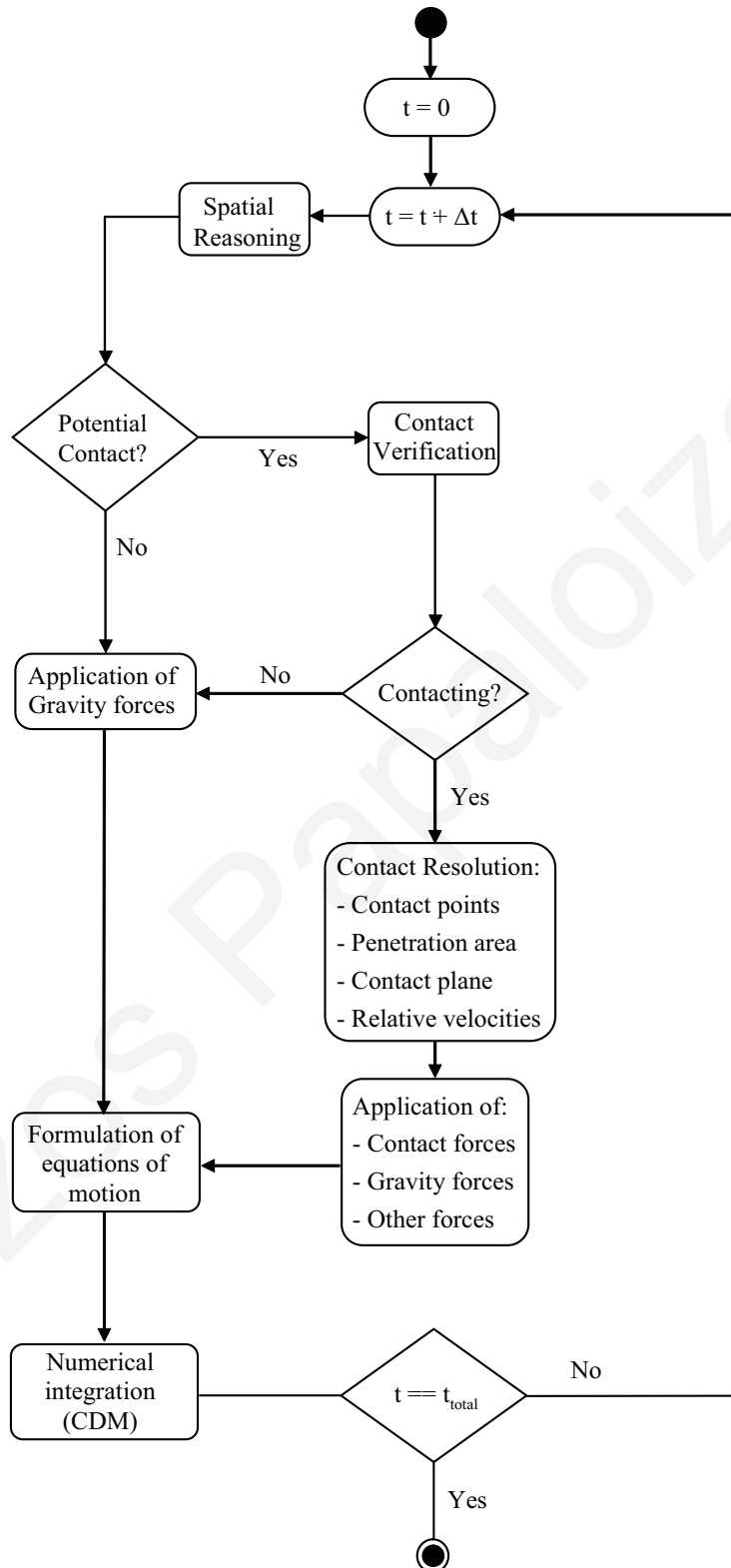


Figure 3.14. Flow of control of the developed algorithms.

Formulation of the physical problem

If contact is detected, the contact area and contact planes are determined and the relative velocities of the bodies in contact are computed. Using the contact springs and dashpots, the contact area and planes and the relative velocities, the contact forces are calculated and applied at each body, in addition to any other forces acting on the bodies.

Taking into account all forces and moments applied at the centroid of each body, the equations of motion are formed and numerically solved using the Central Difference Method. After computing the displacements and rotations of all bodies, for each time step, their corresponding positions and orientations are determined. Then, a new cycle of contact detection, contact resolution, application of forces and numerical solution of the equations of motion follows, based on the updated positions of the bodies. This iterative procedure, which is shown graphically in Figure 3.14, continues until the end of the simulation.

4. Software development

Performing large numbers of dynamic simulations of columns with varying mechanical and geometrical characteristics of drums and columns under the action of various harmonic oscillations and earthquake excitations provides an insight into the behaviour of these structures during strong earthquakes. The custom-made software application (Figure 4.1) that has been developed facilitates the specific needs of this work, without being limited to the general capabilities of a commercial general-purpose DEM program.

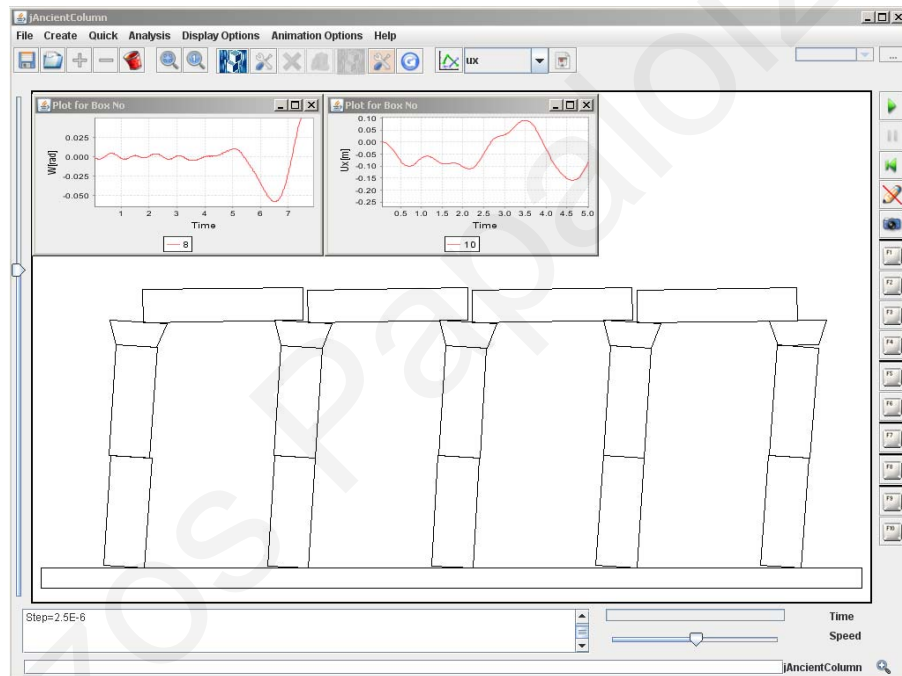


Figure 4.1. Graphical-user interface of the developed software.

The DEM software application, which is used in the simulations, has been specifically designed and implemented to enable efficient performance of two-dimensional (2D) seismic simulations of multi-block structures, while maintaining extensibility towards future spatial (3D) capabilities. The developed DEM software has the capability of enforcing displacements of the support base in order to simulate harmonic and seismic excitations of the latter. In addition, customized distinct elements and the respective contact detection algorithms are used for the modelling of ancient columns and colonnades.

A major requirement for the developed software is the ability to perform effectively and efficiently large numbers of dynamic simulations and parametric studies of monolithic or multi-drum columns and colonnades with an epistyle, with varying mechanical and geometrical characteristics, under the action of earthquake excitations. Modern object-oriented design and programming approaches have been employed using Java technologies, in order to benefit from the significant advantages that these technologies offer to modern engineering software.

4.1. Software design

Conventional engineering software often lacks the desired flexibility for modifications and extensions as it is habitually developed using Procedure-Oriented Programming (POP) languages, which are inherently based on tightly coupled procedures. A minor modification to tightly coupled software may inadvertently introduce bugs in other parts of the code that have already been exhaustively debugged, unless the engineer has detailed knowledge and complete understanding of the entire software application. POP is based on a number of elementary procedures, also called methods or functions, which are invoked to perform certain tasks on data that are not associated with the procedures and without any prevention mechanisms against accidental data corruption.

A few decades ago, most engineering software applications had been initially developed in Fortran, since it was the most suitable programming language to use at that time. POP and Fortran served well the needs of engineers and researchers, as the engineering applications of that era were based heavily on numerical analysis and algorithms. Many structural engineering programs still maintain their original procedure-based orientation using code that had been written in Fortran when the available computing resources were just a tiny fraction of what is available nowadays. Since then, the demands of engineering software have considerably increased with remarkable advances in computing power, such as the increased processor speeds, number of processors and the substantial increase of the available memory, as well as the utilization of the internet and web services.

Researchers call for more functionalities and different characteristics of modern engineering software that cannot be provided with classical software design approaches and POP languages. Due to the increased needs, engineering software has become very large and complex, requiring an entire team of structural and computer engineers to be properly developed and maintained. While frequent changes and extensions are routinely requested in engineering applications, especially if they are used for research purposes, POP software is inherently not easily reusable, modifiable, or extendable. Sometimes it becomes preferable to rewrite a software application, adopting designs that facilitate future modifications, rather than to struggle with major revisions and extensions by retaining the inherent constraints of the POP paradigm.

In spite of the significant advances in software engineering and computing hardware, structural engineering software, especially when used for research purposes, still does not provide the desirable levels of maintainability and extensibility to facilitate the state-of-the-art knowledge and the constantly changing needs of the researchers. Modern research requires frequent revisions, customizations and extensions to accommodate the latest findings and facilitate the changing research needs. The increased demands and requirements of modern engineering applications well exceed the adequacy of POP and justify the utilization of recent advances in software design and modern development methodologies in engineering software. POP languages, such as Fortran, have already been pushed well beyond their capability limits, trying to imitate, often unsuccessfully, characteristics and capabilities of Object-Oriented Programming (OOP).

Complicated engineering systems can be easier modelled with the OOP paradigm utilizing the provided abstraction, encapsulation, information hiding, inheritance and polymorphism mechanisms.

Encapsulation of data and methods improve the adaptability and extensibility of software to accommodate potential revisions and future extensions. Information hiding of unnecessary knowledge about the data and the actual implementations of methods that act on them avoids unintentional interfering with data that may lead to introduction of bugs or data corruption. Restricting the access to data is readily available in OOP languages in the form of data scoping and access specifiers, such as public, protected, package and private that control the access to members of a class.

Inherent complexity can be addressed through a direct correspondence between the classes and objects with the real-world entities of the engineering system that is simulated. Obscuring details that are not necessary can be bypassed with the usage of abstraction and association, allowing the engineer to easily comprehend and effectively debug and modify engineering software. Method overloading allows the existence of a large set of methods with the same name, but with different number, type and sequence of arguments, which define which version of the method to be actually invoked.

Inheritance enhances the reuse of common properties and behaviour, avoiding unnecessary code duplication, which often constitutes a source of errors when revisions are attempted without realizing that the code that must be modified may appear in multiple locations of the program. Polymorphism, a very powerful feature of OOP, allows programming for an interface or a superclass rather than for a concrete implementation, which uses dynamic binding to determine at run-time the method that should be invoked based on the actual type of the object that makes the method call.

OOP was introduced in structural engineering software in the 1990's, although OOP languages were available much earlier. In the last decade, OOP principles have been promoted by the work of several researchers [1], [5], [25], [26], [46], [47], [48], [94], [95]. The OpenSees (Open System for Earthquake Engineering Simulation) [23], [64], [81] constitutes a major contribution for the promotion of a wider use of OOP in structural engineering, especially for research purposes. It has been shown that OOP can be used in structural engineering, specifically in finite element analysis (FEA), without sacrificing the computational efficiency that is required in solving such computationally demanding problems. However, the advantages of OOP have been appreciated mostly by a very small number of researchers. In addition, the code of many Object Oriented (OO) structural engineering applications is still tightly coupled without fully utilizing the advances in OOP and software engineering to develop flexible and extendable applications.

Although the term OOP is used to collectively represent Object-Oriented Analysis (OOA), Object-Oriented Design (OOD), and Object-Oriented Programming (OOP), in engineering software emphasis is given primarily to the OOP aspect and much less to the OOA and OOD. In particular, OOA is used to identify the objectives of a software

system, while with the OOD the software is designed to fulfil these objectives. In order to fully utilize the advantages of OOP, it is not sufficient to use an OOP language, such as C++, Java and C#, but certain OOA and OOD principles should also be followed, from the initial software design phase, to achieve the desired flexibility. Furthermore, the next logical step to code-reusability is to achieve OOD reusability, which may offer the experience that is obtained through optimized solutions of recurring software design problems.

The last decade has experienced significant advances in the area of software engineering, especially concerning OOP and modern software design and development techniques. One relatively recent advancement is the design approach based on Design Patterns (DPs), which can be used to design and develop flexible software applications that achieve the desired maintainability and extensibility. Although DPs have been progressively utilized in other scientific and business sectors, there has been very limited utilization of this advanced OOP design approach in civil engineering, in particular in the areas of structural and earthquake engineering. This research work aims to motivate the obvious next step after the OOP paradigm, the utilization of DPs in the design and development of flexible OO engineering software.

4.2. *Design Patterns (DPs)*

With the substantial increase of the capabilities of modern computers, engineering software applications are becoming very sizable and complicated, in order to support different simulation models, analysis approaches and solution methods. Furthermore, engineering software nowadays must be able to facilitate various interactions with the user, between different modules of the application, or even with other applications that may run either locally or remotely. These objectives can be achieved more effectively with the proper design of engineering software in order to better manage the size and complexity of modern engineering software applications.

The Design Patterns (DPs) can be used to design and develop engineering software in ways that manage the size and complexity of modern engineering software applications.

Although the DPs had originated from Architecture, thanks to the relevant work of Christopher Alexander [2], they have been utilized in the design of large OO software applications only after a set of 23 specific DPs was defined in the “*Design Patterns: Elements of Reusable Object-Oriented Software*” book [27]. However, the exploitation of DPs in the design and development of engineering software has remained very limited.

The DPs take advantage of the experience gained by software developers to recurring problems [27], [17]. The aim is to design and develop flexible software that can be easily reused, modified and extended to fulfil the continually changing needs of academic research or engineering practice. In particular, the DPs provide proven effective designs to organize classes and objects, regarding their responsibilities and relations, in order to achieve the desired maintainability and extensibility. However, it is our responsibility to properly adjust the suggested DPs in order to adapt them to engineering research and practice.

OOP and DPs can be used to substantially reduce the development time, considering future revisions and extensions, especially as the size and complexity of the code increases. More importantly, future modifications and extensions can be performed with the minimum possible impact on existing code, avoiding unintentional introduction of bugs. In addition, the DPs provide a concise vocabulary that facilitates the communication and collaboration among software designers, developers and users of engineering applications, not only during development time, but also during expected revision and extension phases.

Most DPs enable the isolation, through encapsulation, of parts of software applications from the rest of the code, by keeping the classes separated and uninformed about the others, so as to avoid the possibility of accidentally introducing bugs during modifications. Although OOP provides both composition and inheritance, it is preferable, whenever it is meaningful, to use composition over inheritance in order to enhance the flexibility of the software. This can be achieved by encapsulating the behaviour in an object that can be easily changed with some other behaviour that implements the proper behaviour interface, essentially “inheriting” dynamically behaviour through composition and delegation at run-time.

The DPs can be categorized in three major categories:

- *The creational DPs*, which provide different flexible ways to instantiate objects dynamically at run-time without providing any creation details.
- *The structural DPs*, which organize classes and objects into larger structures in ways that facilitate future modifications and extensions.
- *The behaviour al DPs*, which define the communication and interactions of objects and classes so as to facilitate encapsulation of the relevant processes and distribute responsibilities.

The last few years many additional DPs and categories have been identified, involving specific types of OOP, such as programming for concurrent or distributed systems. In the developed software application, DPs have been used to achieve the desired maintainability of the code.

4.2.1. Creational design patterns

The Creational DPs include the *Factory Method*, the *Abstract Factory*, the *Builder*, the *Prototype* and the *Singleton* patterns. These DPs provide adaptable ways to create instances of classes so that the system that uses them is independent of how the objects are created, composed and represented. Essentially, the Creational DPs encapsulate information regarding the concrete classes that are instantiated and how they are configured, hiding this information from the system that uses them, in order to provide the loose-coupling that is essential to facilitate future extensions of the application. For example, the Factory Design Pattern (DP) and Abstract Factory DP offer a flexible way to instantiate objects without specifying their concrete classes in order to avoid explicit binding of the code to concrete subclasses, which would limit the extensibility of the code.

Specifically, the *Abstract Factory DP* delegates, through composition, the instantiation to another object that creates and returns one of several families of related objects, without letting the client know about the actual objects that are created. The abstract factory superclass defines the interface that all concrete factories must implement to create the families of related objects. Each of the methods of the specified interface is responsible to create the corresponding concrete object. In essence, the *Abstract Factory*

DP can be used to instantiate one of a number of concrete implementations of an abstract factory class, returning one of the several factories. Subsequently, each concrete factory returns a set of instances of several related classes by implementing the methods that are defined in the abstract factory for creating a family of objects. Consequently, the actual concrete classes that are instantiated and used in an application are isolated from the client, which facilitates straightforward modifications and transparent additions of new families of concrete classes. In addition, this DP allows the implementation and use of a variety of factories that can instantiate different objects, depending on the current and future needs of the engineering application, to obtain various behaviours.

The Unified Modelling Language (UML) class diagram in Figure 4.2 demonstrates the utilization of the Abstract Factory (*creational*) DP in order to facilitate the instantiation of a set of related objects, without explicit binding of the code to concrete subclasses, in order to assist future modifications and extensions of the concrete classes. In particular, a drum and an excitation can be instantiated by the concrete factory named *ConcreteFactory1*.

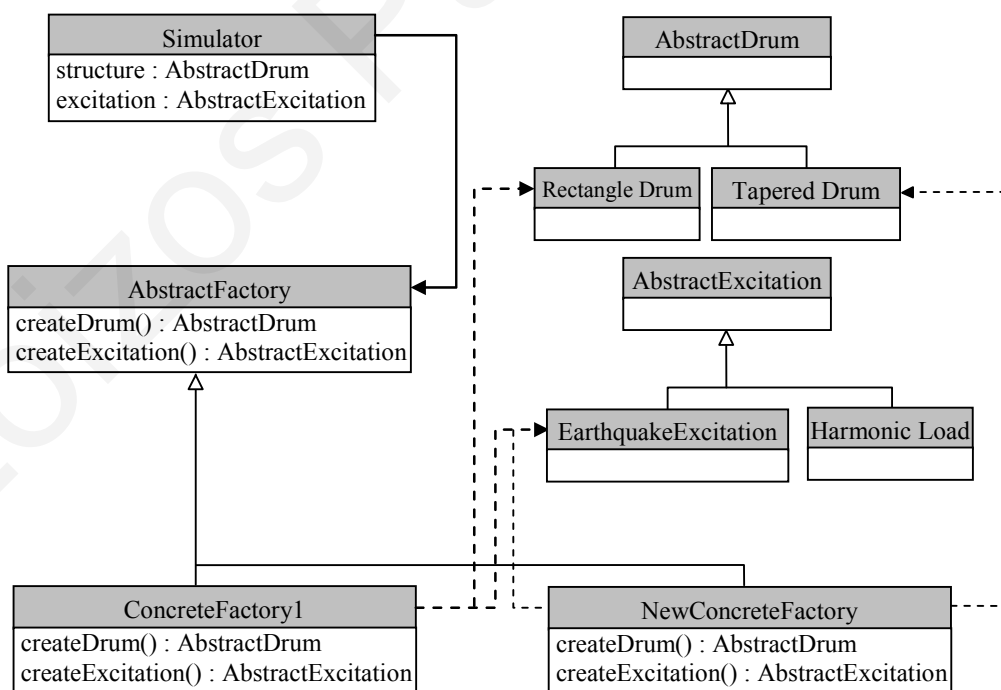


Figure 4.2. Utilization of the Abstract Factory DP.

Subsequently, due to the changing needs of the user, a supplementary concrete factory named *NewConcreteFactory*, can be added to enable the instantiation of a different kind of drum, such as a rectangular drum, and an excitation, which also could have been of a different type. This added feature of the software can be achieved by simply adding the concrete implementations of new types of structures and excitations, together with the corresponding new concrete factories that instantiate them, but without any need to modify the classes of the existing code.

4.2.2. Structural design patterns

The Structural DPs, which include among others the *Adapter*, *Composite*, *Proxy*, *Facade*, *Bridge* and *Decorator* patterns, use inheritance and aggregation to provide effective interfaces, and to organize better or form larger classes and objects in ways that facilitate future changes and extensions.

The *Composite DP* enables the creation of tree structures using composition of objects that each of them may be an individual object or a composite object with a tree structure itself. The formed trees may contain both individual objects and trees or sub-trees of objects, on which the same operations can be applied uniformly. The Composite DP can be used to represent either an individual object or a collection of objects, by allowing the objects to be leaf nodes or to have additional branches. New kinds of components can be simply added as long as they implement the same interface, which is common for simple and composite objects.

For example an object representing an earthquake excitation may be used to represent either an individual excitation or a composite of excitations, in order to optionally contain a collection of excitations, which can be used by the Simulator in the analysis. Figure 4.3 shows a potential usage of the Composite DP to represent earthquake excitations in a way that either an individual excitation or a collection of excitations can be represented and used uniformly, by implementing a common interface for simple and composite objects.

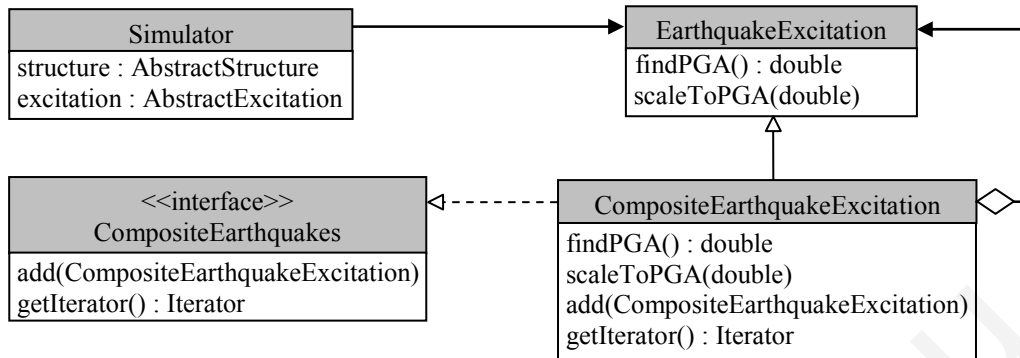


Figure 4.3. Example of using the Composite DP to represent earthquakes.

4.2.3. Behavioural design patterns

The Behavioural DPs, which include the *Command*, *Iterator*, *Mediator*, *Observer*, *Template Method*, *State* and *Strategy* patterns, facilitate the communication between objects in a system, defining the responsibilities and interactions between them. The *Strategy DP* can be used to encapsulate in a superclass or an interface, known as strategy, a set of interchangeable algorithms, or numerical methods, with the same functionality. Subsequently, subclasses that implement the defined interface of the strategy provide different implementations that can be selected by instantiating the proper strategy instead of direct calling the corresponding algorithm.

For example Figure 4.4 provides a UML class diagram that shows the usage of the Strategy DP to define various contact detection strategies in a set of interchangeable algorithms with the same functionality that can be easily modified and extended.

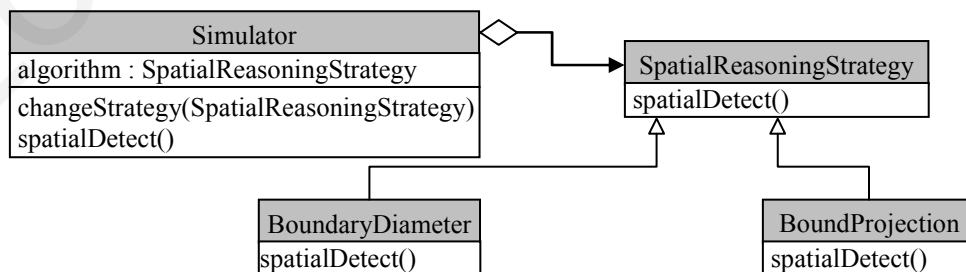


Figure 4.4. Use of the Strategy DP to define various contact detection algorithms.

4.3. Software development

Java technologies are employed in the software development, taking into account the significant advantages that these technologies offer [6]. Specifically, the *Java* language is used for the computational part, while the Java application programming interfaces *Java Swing* and *JDBC* are employed for the computer graphics, the graphical user interface and the database connectivity, respectively.

The Java programming language is a pure Object-Oriented Programming (OOP) language that combines the best ideas, concepts and mechanisms of other OOP languages, such as virtual functions and polymorphism, inheritance, function overloading, garbage collection and exception handling. Java offers modularity, robustness, reusability, portability, architectural neutrality, superior memory management and multithreading capabilities. In addition, the various Java APIs allow efficient development of applications with graphics, database connectivity and graphical user interfaces without a need to use any other programming language or library.

The Java Media Framework API can be used to capture images from the simulations and stream video to create animations of the simulations. The Swing API provides several components that can be used for the development of graphical user interfaces (GUI) and the Java2D API for high quality two-dimensional (2D) graphics.

The developed DEM software requires large sets of input data and generates huge amounts of output data that need to be efficiently managed, which can be achieved by utilizing database technologies. The Java database connectivity (JDBC) API [85] will be used as it provides an interface between the simulation program and a conventional relational database management system. Since data is stored in the database, it is available from the query language that enables a variety of capabilities to compose queries for searching, retrieving, combining, constraining, and transforming data.

The use of the Java programming language in engineering and scientific applications sometimes encounters scepticism regarding the performance limitations and scalability of Java. A detailed comparison of the performance of Java and corresponding C/C++ software implementations of certain algorithms, which are typically used in DEM

simulations, demonstrated that although the Java implementations are relatively slower than the C/C++ ones, the difference is not that significant compared to the advantages that this programming language offers [40]. In addition, varying the order of the size of the problems proved that Java shows the same scalability as C/C++, which is very important for the intensive computational demands of the DEM.

The expected performance difference between Java and other high-level programming languages, such as C/C++, is due to the fact that C/C++ programs are compiled into executable machine instructions for the underlying architecture and operating system, while Java code is compiled into bytecode. During execution, the bytecode is translated into machine instructions by the Java Virtual Machine (JVM). Although this two-phase compilation-interpretation has some overhead on the computational performance, it provides the desired portability to Java programs. Furthermore, the latest JVM allows just-in-time compilation and run-time optimizations that achieve performance comparable to that of a compiled language due to the profiling and recompilation of Java programs during execution. In contrast, any optimization of C/C++ programs is done during compilation. The run-time optimizations are more powerful as they can take advantage of given conditions during execution of the program, while static compilation can take advantage of only what the compiler can predict based on certain predefined rules. Finally, the concept of virtual machines and run-time optimizations are recent advances that are expected to be improved in the near future.

4.4. Graphical User Interface (GUI)

The Java Foundation Classes (JFC) are employed for the development of a graphical user interface (GUI) which is shown in Figure 4.5. The JFC consists of the Abstract Window Toolkit (AWT), Swing and Java 2D. Together, they provide a consistent user interface for Java programs, regardless whether the underlying user interface system is Windows, Mac OS X or Linux. The GUI is developed in a way that allows a user to efficiently define and perform large numbers of parametric dynamic analyses, mainly concerning multi-drum columns and colonnades.

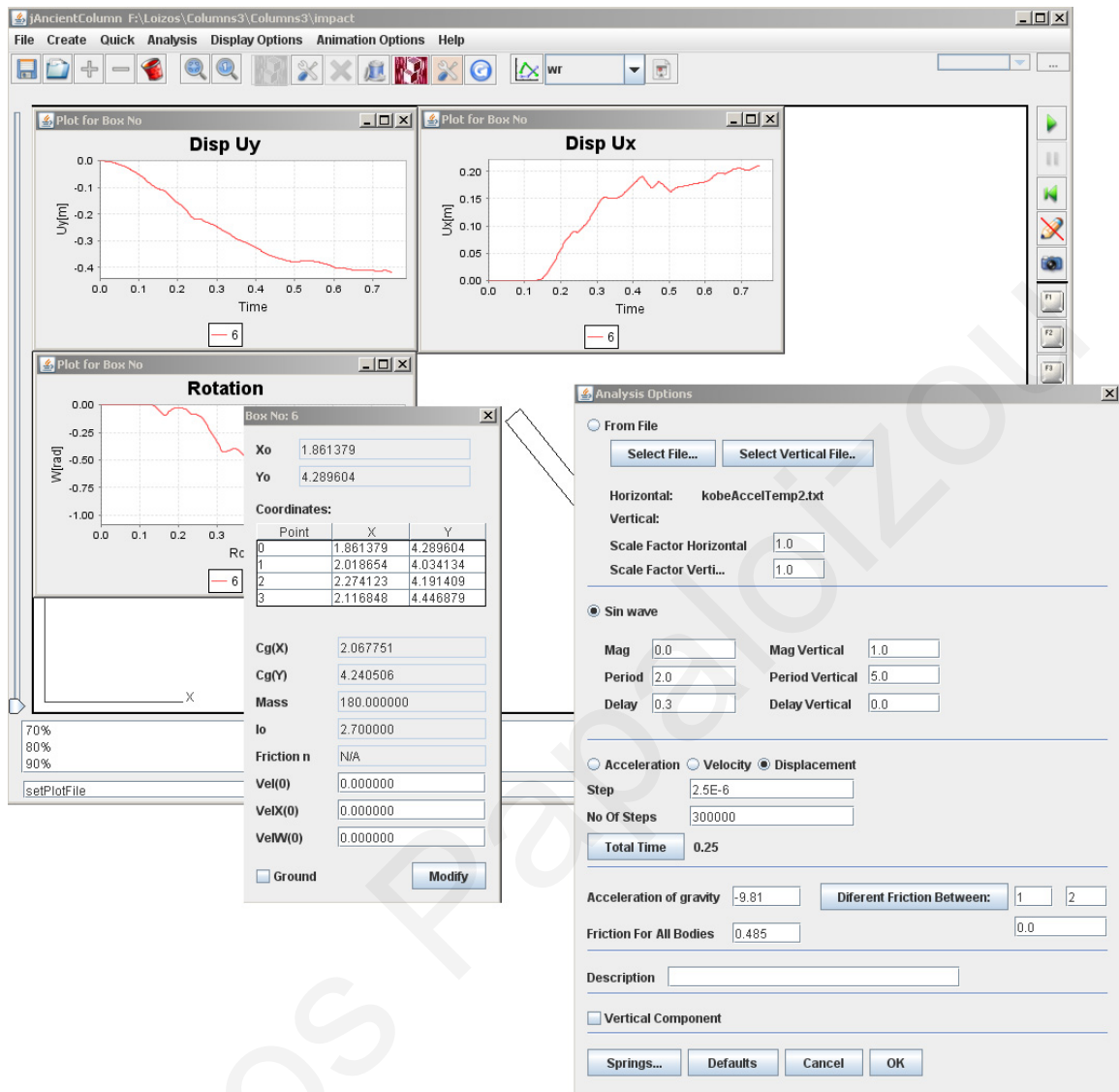


Figure 4.5. Graphical-user interface of the developed software.

Some of the pre-processing and post-processing capabilities of the developed application are briefly described:

1. *The GUI pre-processing*

- Input geometry and material properties can easily be defined using the GUI. Initial velocities or ground motion parameters can be assigned to specific bodies. Automated routines are programmed in order to rapidly produce colonnade systems with a given number of drums or columns.

- Input motion can be selected in two directions by either using an input file or a harmonic excitation. Input can be directly defined either as displacement or as acceleration. The acceleration motion is integrated and base line corrected by the application.
- Analyses parameters, such as the contact parameters, the time-step size and the friction between different bodies can also be defined.
- A command-line input option is available and can be used to input a specific command, similar to those that can be provided in an input file.

2. *Post processing.*

- Saving the analyses results into a single file that can be, later on, loaded back into the application, which can display it as an animation.
- Output graphs for each body can be produced with an option to export the graph's data to a text file.
- Vector drawing files (eps) can be produced at any time of the response.
- Animation of the response can be displayed during execution of the program or stored in animation files, which can be produced through a sequence of snapshots at different time steps.
- Parametric investigation can be easily handled. Plots of how a specific parameter affects the response can be obtained from a large number of analyses with the same geometry and configuration.

4.5. Input files

The developed software has the capability of user input through the GUI or by using an input file. In this way, several input files can be prepared and batch analyzed by the application, without the need of any user interaction to define the parameters of the

problem. A wide variety of parameters can be changed, such as the ground motion, the coefficient of friction, the frequency and amplitude of the harmonic motion, the contact parameters and the mass.

Figure 4.6 shows a typical input file, demonstrating how different input parameters can be used. The software is also designed for parametric investigation, in which, a single geometry can be given, and a specific parameter can be varied within a range of values set by the user. The application will then perform a number of analyses changing only the desired parameter by a small increment.

```
//Base
createDrum(20,0.5,0,0,2000);

//First Column
createTaperColumn(1,5.4,1.0,3,-8,0,2000)
createTaperColumn(1,.60,1.4,1,0,0,2000)

//Second Column
createTaperColumn(1,5.4,1.0,3,4,-6,2000)
createTaperColumn(1,.60,1.4,1,0,0,2000)

//Third Column
createTaperColumn(1,5.4,1.0,3,4,-6,2000)
createTaperColumn(1,.60,1.4,1,0,0,2000)

//Fourth Column
createTaperColumn(1,5.4,1.0,3,4,-6,2000)
createTaperColumn(1,.60,1.4,1,0,0,2000)

//Fifth Column
createTaperColumn(1,5.4,1.0,3,4,-6,2000)
createTaperColumn(1,.60,1.4,1,0,0,2000)

//Epistyle
createTaperColumn(3.9,0.8,3.9,1,-1.95,0,2000)
createTaperColumn(3.9,0.8,3.9,1,-4,-0.8,2000)
createTaperColumn(3.9,0.8,3.9,1,-4,-0.8,2000)
createTaperColumn(3.9,0.8,3.9,1,-4,-0.8,2000)

//Time Step Parameters
setDelay(0.0);
setStep(2E-6);
setNoOfSteps(5000000);

//Ground motion Parameters
setAnalysisUnit(a);
setEqFile(Mexcit_Accel.txt);
setScaleFactor(1.5);
setAnalysisType(File);

//Set a Description
setDescription(Mexico City Earthquake. Scale Factor=1.5);

//Starts the analysis and saves all results to a file
analysisStart;
save(C5x3x4_mexico);

//Plots to a file the X displacements of the base
sel(1);
setPlotFile("output_UX.txt");
plot(ux);
exit();
```

Figure 4.6. Typical input file.

4.6. Limitations of the two dimensional analysis

The developed software application has been specifically designed and implemented to enable efficient performance of 2D seismic simulations of multi-block structures, while maintaining extensibility towards future spatial (3D) capabilities. It is well known that the results obtained by 2D dynamic analysis of rigid block assemblies are not capable of

providing phenomena that may appear in the actual 3D response of such systems, such as off-plane movements and oscillations. Numerical studies of the earthquake response of ancient columns by Papantonopoulos et al. [70], using commercial 3D software, reported significant differences in the response of 2D and 3D analysis, even for plane excitations, although the models used were symmetrical about the vertical axis. The researchers also observed that very small disturbances, in the direction normal to the plane of rocking, may cause significant amplification of the response and that 2D analysis may underestimate the response, predicting greater stability. In addition, the collapse mechanisms of colonnades in many cases appear in the out-of-plane direction. Experimental work regarding the response of a scaled model of a marble classical column, presented by Mouzakis et al. [55], also reported this ‘3D sensitivity’ inherent in the rocking phenomenon.

Nevertheless, numerical studies by Psycharis [71] and Konstantinidis [42] showed that 2D analysis can be used to capture the overall phenomenon and various parameters that affect the seismic response of multi-drum columns. Moreover, 2D can be used more efficiently and effectively when it is necessary to perform large numbers of simulations in order to study the effect of various parameters and characteristics, as 2D idealizations analysis is much more time efficient and is less sensitive to the selection of the values of the contact parameters.

4.7. Other uses of the developed software

4.7.1. Masonry structures

Analysis tools for masonry structures are very important for the maintenance and restoration of historic structures [43]. The dynamic analysis of masonry structures is a challenging problem due to the discontinuities of these structures. DEM analysis can capture the discrete behaviour of these structures providing a better understanding of their response and their potential failure mechanisms under earthquake excitations. Old masonry buildings were, typically, built without any consideration to earthquake resistant design. In addition, the excessive masses of masonry structures owing to over-sized walls

and high material densities, results in high seismic loads. Finally, inappropriate design, e.g. eccentricities and deterioration of the quality of the materials (stone, bricks and mortars) make these structures very vulnerable to earthquake excitations. Therefore, a better understanding of the dynamic behaviour of such structures is very important. These structures exhibit a highly nonlinear behaviour when subjected to earthquake excitations which is very difficult or even impossible to capture with classical methods.

Although some FEM (using smeared cracks or special "gap elements"), finite difference methods (FDM) and boundary element methods (BEM) models have been used for simulations of these discontinuous structures, certain difficulties arise mainly due to the inherent discontinuities of the problem. These methods are ineffective in modelling many interacting bodies, especially for dynamic analysis, since they are based on continuity assumptions [54]. The "smeared cracking technique", and the "gap elements" or the "no-tension contact elements" that have been used in FEM have limited capabilities and the analysis often becomes unstable. Figure 4.7 shows results of a FEM analysis of a masonry building under dynamic loading. Although cracking of the material can be represented, it is very difficult, if not impossible, to capture the collapse mechanism, something that can be well represented with the DEM.

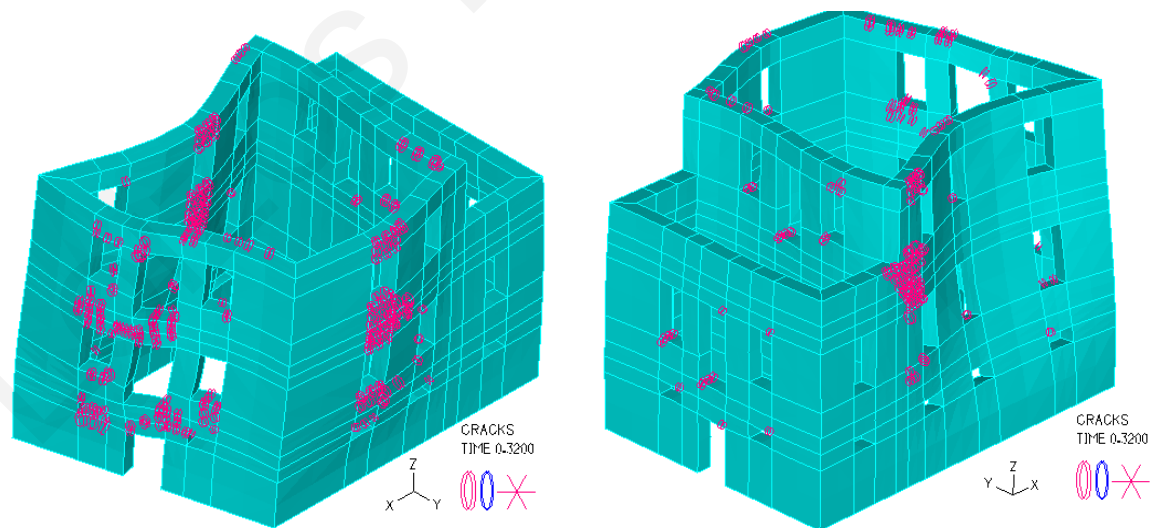


Figure 4.7. Masonry building under dynamic loading using FEM [54].

With the DEM, the structure can be modelled as a system of many distinct bodies put together in the same way that the structure had been physically constructed, and allowed to interact through contact stresses with their adjacent bodies. Each distinct body can be modelled as a single rigid, or deformable, discrete element, while element interactions are modelled using idealized contact and cohesive springs. DEM can be used to more realistically simulate blocks, such as bricks or stones, separated by joints, as well as joint-mortar using cohesion bonds, which can be defined between adjacent bodies with certain strength. The opening and closure of joints, crack formations, sliding and rocking can be modelled with the DEM, which is almost impossible with other standard numerical methods. Phenomena such as cracking and separation of parts of the structure into various smaller parts that vibrate in different ways due to different frequencies, which result in further destruction, can be potentially studied using the DEM.

4.7.2. Rock masses – Land slides

The developed software, based on the DEM, can also simulate rock formations, such as those studied in rock mechanics. Dynamic stability analysis to consider seismic excitations and other dynamic loadings can be performed using DEM instead of the currently used equivalent static analysis. Figure 4.8 demonstrates a land slide problem, with multiple rectangular bodies of different sizes, simulated using the developed software application.

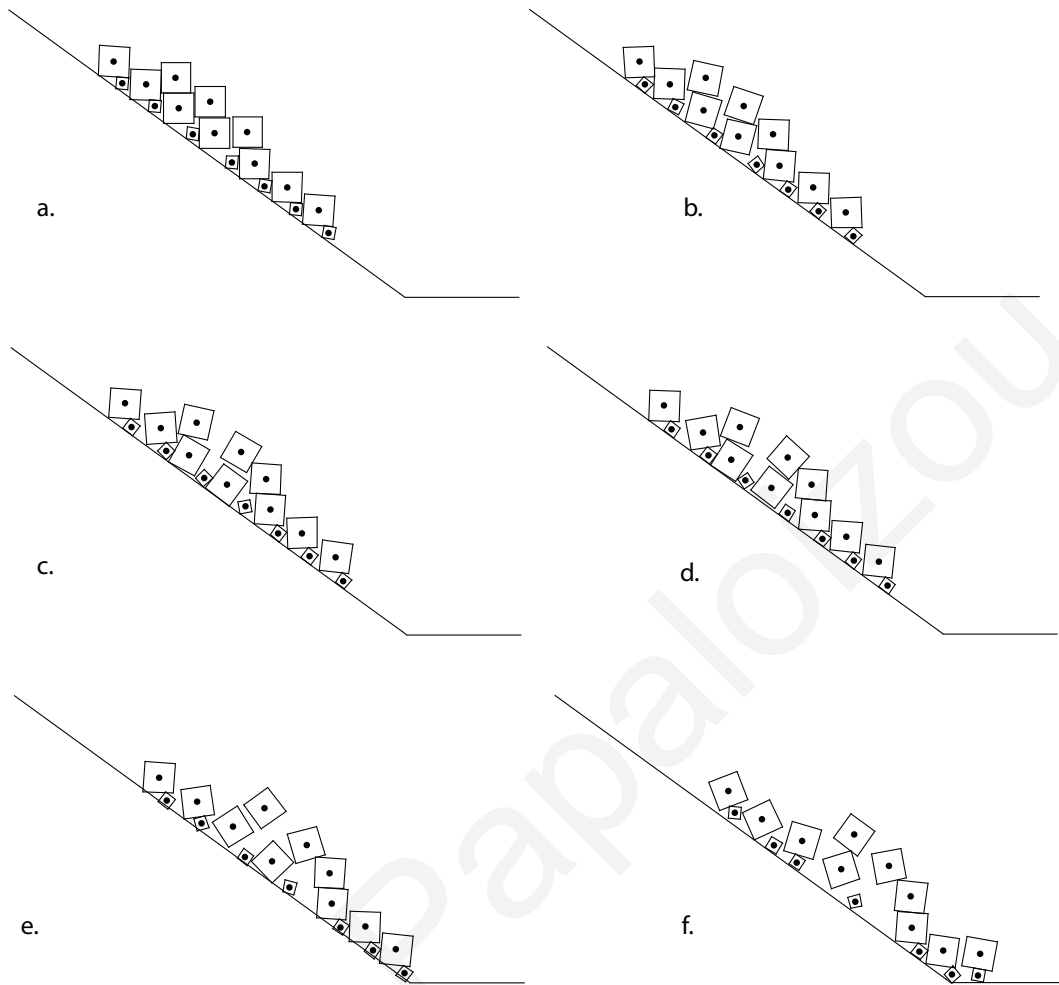


Figure 4.8. Sliding of multiple bodies of various sizes sliding on an inclined surface.

4.7.3. Realistic multi-body animations

DEM may also be used to create more realistic multi-body animations used in computer graphics, virtual reality and video games by incorporating mechanics into the animations. In recent years, there is an increased interest in developing realistic physical animations in computer-aided design and virtual reality environments, e.g. for educational and training simulations. More realistic multi-body animations and more meaningful numerical simulations can be performed by combining engineering-oriented numerical techniques with computer graphics capabilities supplemented with contact detection algorithms, as shown in Figure 4.9.

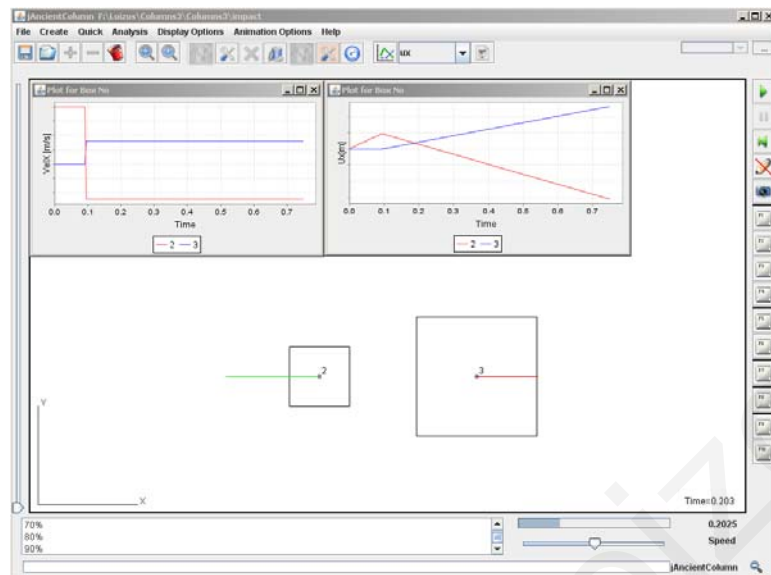


Figure 4.9. Multi-body animations of colliding bodies.

4.7.4. Multi-body dynamic and mechanical systems

There are practical applications that involve both mechanical systems and large numbers of particles that interact together. Simulations of such systems may be possible by incorporating in DEM simple mechanical system formations, which allow optimization of the design product prior to actual manufacturing. Figure 4.10 shows simulations performed with the developed software concerning objects getting blocked while moving down a cone.

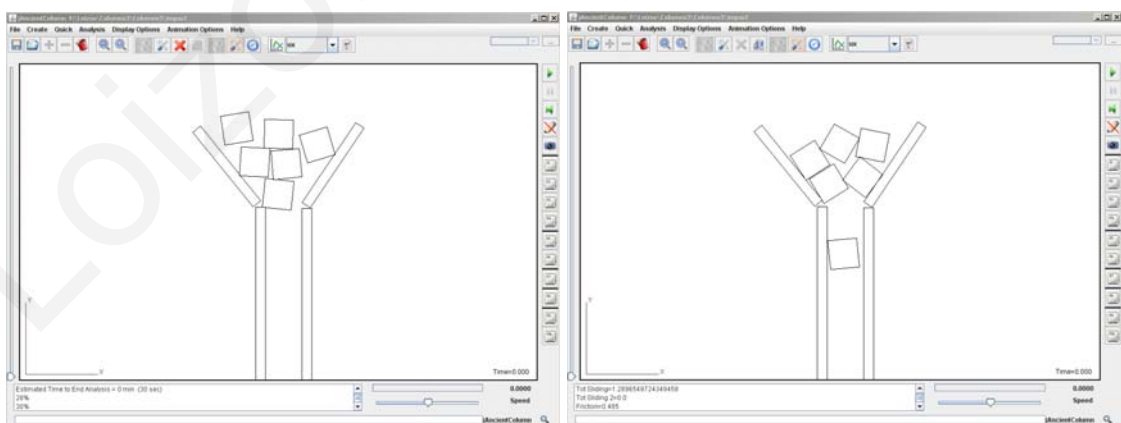


Figure 4.10. Objects getting blocked while moving down a cone.

5. Verification of the developed software

The initial goal of this thesis is the development of a specialized software tool using the DEM, which can be used to conduct numerical simulations and parametric studies of multi-body structures under harmonic and earthquake ground motions. A critical step in pursuing this research work is the validation of the custom-made software application by comparing the computed responses of various problems with corresponding analytical solutions and experiments that are available in the scientific literature. Such validation is important so as to verify that the methodology used is suitable for the analysis of multi-drum bodies under dynamic loading and that the computed responses are sufficiently accurate.

In particular, numerical simulations of multi-drum standalone columns, using the previously described methodology, have been performed in order to verify the developed software and the validity of the numerical simulations, under the described assumptions. Values for the contact parameters can be estimated by performing analyses of problems for which either an analytical solution is known, or experimental results are available, in order to properly calibrate the contact parameters.

5.1. *Analytical validation*

5.1.1. *Free vibration rocking period*

An initial validation test of the developed software is performed by comparing the theoretical rocking period, T , of a rigid body that is left to oscillate freely from an initial rotation angle with the corresponding rocking period computed by the developed application.

Housner [29] considered a rigid body with sufficiently large coefficient of friction so that it can oscillate about the centres of rotation O and O' (Figure 5.1), without sliding. Assuming that there is no energy loss during impacts, Housner computed the required

time T for a rigid block to complete a full cycle (period) of oscillation, after the rigid body is left to freely oscillate from an initial rotation angle:

$$T = \frac{4}{\sqrt{\frac{W \cdot R}{I_o'}}} \cdot \cosh^{-1} \left(\frac{I}{I - \frac{\theta_o}{a}} \right) \quad (5.1)$$

θ_o is the initial rotation angle, W is the weight of the block and I_o' is the moment of inertia about the point O. R and a are the geometric characteristics of the block, as shown in Figure 5.1.

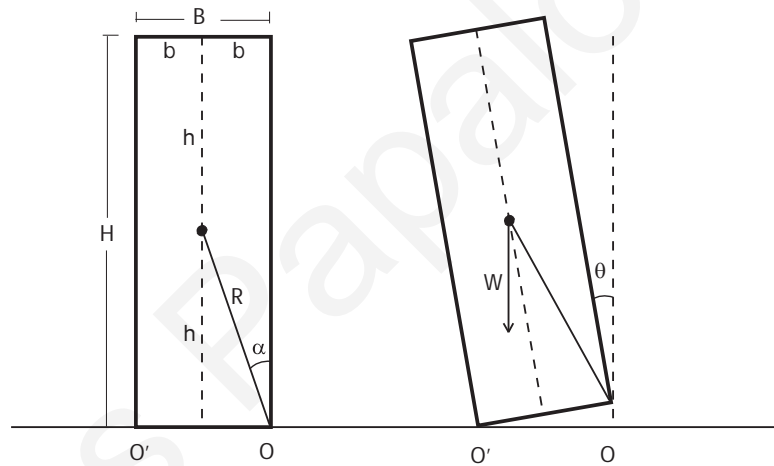


Figure 5.1. Rocking block.

Figure 5.2 plots with a blue line the calculated values of the term $\frac{T}{4} \cdot \sqrt{\frac{W \cdot R}{I_o'}}$ for a rigid body that is left to oscillate freely from an initial rotation angle. T is the theoretical rocking period, while $\frac{W \cdot R}{I_o'}$ is constant. Therefore, the graph shows the variation of the theoretical rocking period, T , with respect to the initial rotation angle θ_o .

The points presented in Figure 5.2 show various results acquired from analyses performed by the developed software, using different geometric characteristics. In

particular, for each analysis the period T of a rigid block is computed for three different block geometries, while varying the initial rotation angle, θ_o .

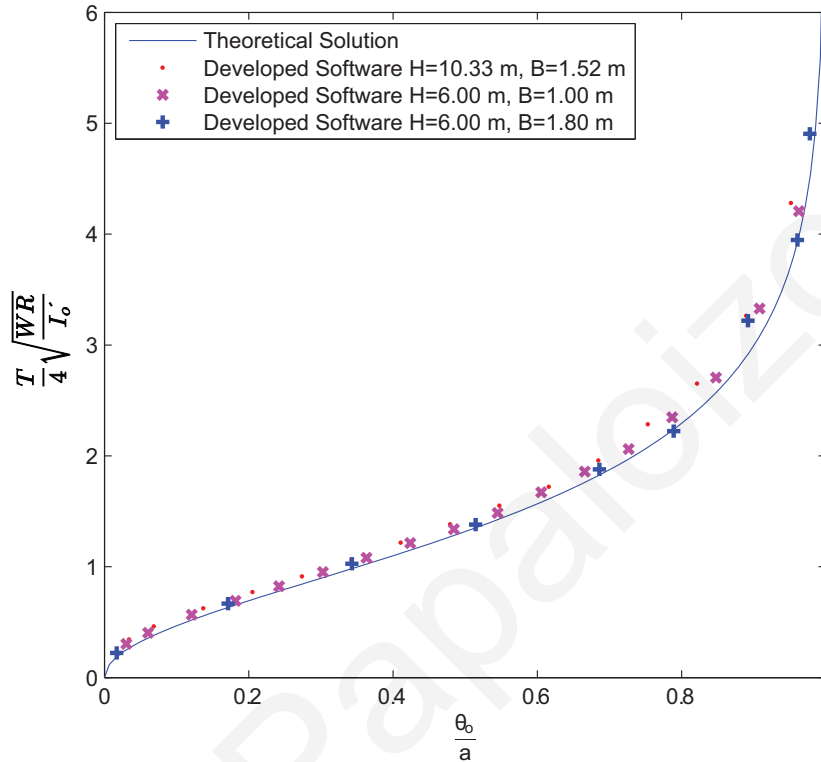


Figure 5.2. Period T of a block rocking with amplitude θ_o .

The results in Figure 5.2 show that the developed software captures sufficiently well the theoretical solution provided by Housner [29], considering the complexity of the problem.

5.1.2. Energy loss during impact

Further validation of the developed application, based on the methodology described earlier, is performed on the energy loss during impact of a rotating rigid body according to the theory that is also provided by Housner [29]. During each half-cycle of the oscillation of the body, the vibration energy is decreased due to each impact. The reduction of the kinetic energy is given by the following equation:

$$r = \frac{\left(\frac{I}{2} \cdot I_o' \cdot \dot{\theta}_2^2\right)}{\left(\frac{I}{2} \cdot I_o' \cdot \dot{\theta}_1^2\right)} = \left(\frac{\dot{\theta}_2}{\dot{\theta}_1}\right)^2 \quad (5.2)$$

Where $\dot{\theta}_1$ and $\dot{\theta}_2$ are the angular velocities just before and after impact, respectively. For slender blocks the reduction of the angle of rotation, θ_n , for each impact n is proven by Housner [29] to be equal to:

$$\theta_n = \alpha \cdot \left(1 - \sqrt{1 - r^n \cdot \left[1 - \left(1 - \frac{\theta_o}{\alpha} \right)^2 \right]} \right) \quad (5.3)$$

where θ_o is the initial angle of rotation. Furthermore, the dissipation of energy, during impacts of the block, results in a reduction of the period of each half cycle as shown in Figure 5.3.

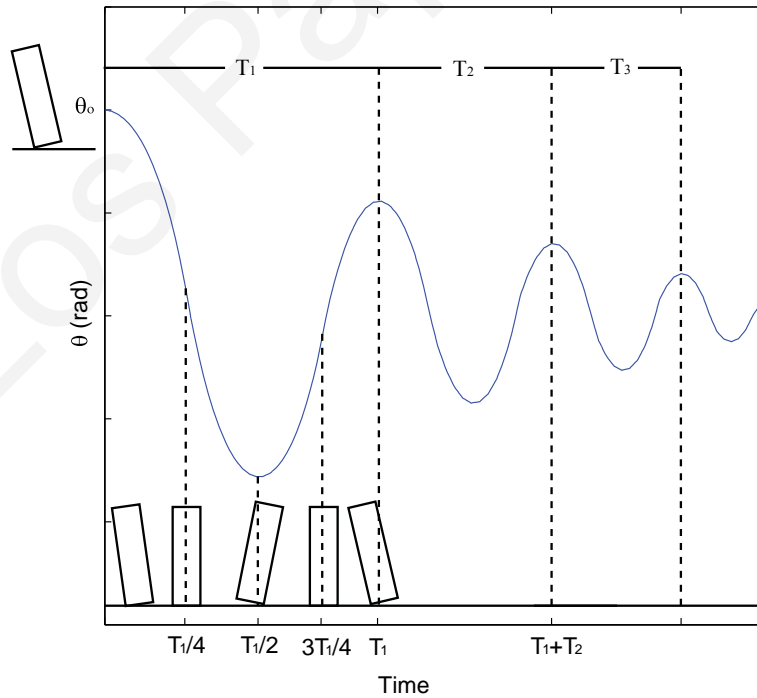


Figure 5.3. Time-history response of a rigid block left to freely vibrate from an initial angle, with energy loss during impacts.

The half-periods of vibration during free rocking are given by:

$$\frac{T}{2} = 2\sqrt{\frac{I_o'}{W \cdot R}} \cdot \tanh^{-1} \left(\sqrt{r^n \left[1 - \left(1 - \frac{\theta_o}{\alpha} \right)^2 \right]} \right) \quad (5.4)$$

A rigid block left to rock freely from an initial rotation angle has been analyzed using the developed software. The reduction of the kinetic energy in each cycle is set equal to $r = 0.85$, by setting the contact parameters appropriately. Specifically, for the numerical analyses, a contact stiffness of the order of 10^8 N/m^2 and a damping coefficient of 10^3 N s/m have been used. The time-history response of the rotation angle of the block is given in Figure 5.4.

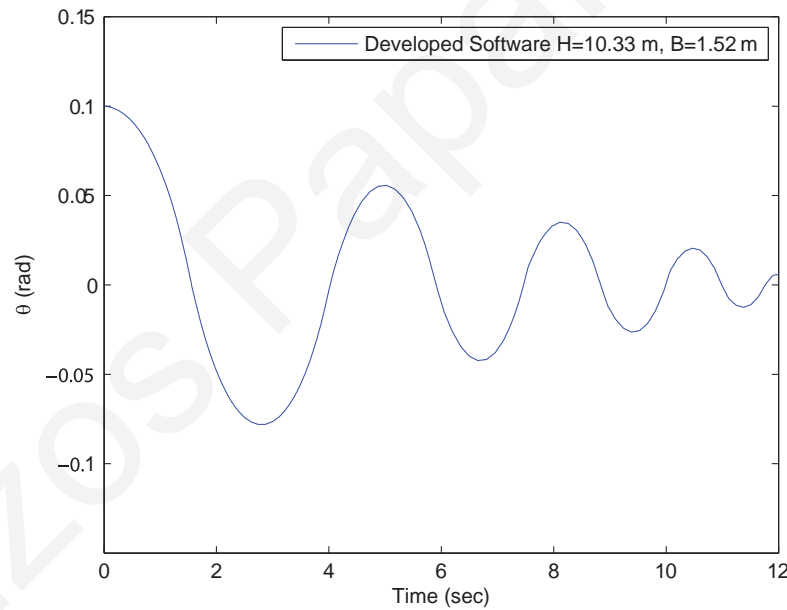


Figure 5.4. Computed time-history response of a rigid block left to freely vibrate from an initial angle, with energy loss during impacts.

The reduction of the angle with each impact is given in Figure 5.5. The latter figure shows that the computed reduction of the rotation angle, therefore the kinetic energy at each impact, is satisfactorily close to the theoretical solution provided by Housner [29].

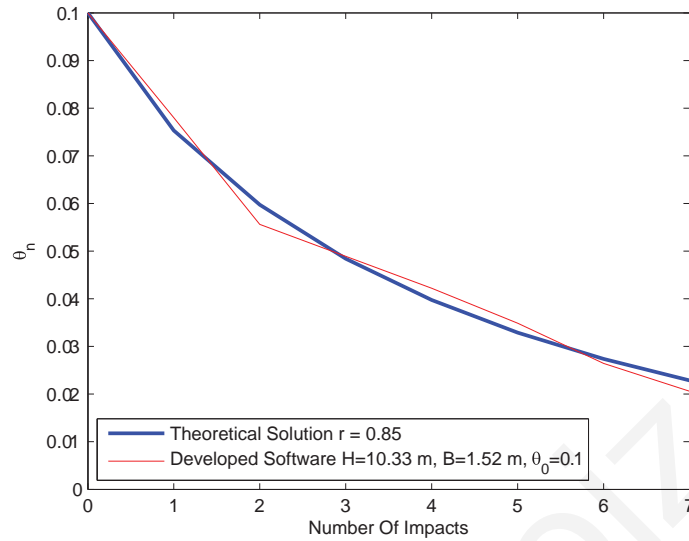


Figure 5.5. Reduction of the maximum rotation angle of each cycle due to impact.

5.1.3. Sliding response to acceleration pulses

To validate the developed software, rigid bodies that are resting on a horizontal plane with a coefficient of friction, μ , are subjected to rectangular pulse accelerations (Figure 5.6). An analytical solution of this problem was given by Newmark [57], as well as Younis and Tadjbakhsh [90]. A similar validation process was carried out by Konstantinidis and Makris [42] in order to validate a commercially available software [89] capable of performing simulations of multiple rigid bodies that can undergo rocking and sliding under dynamic and earthquake loadings.

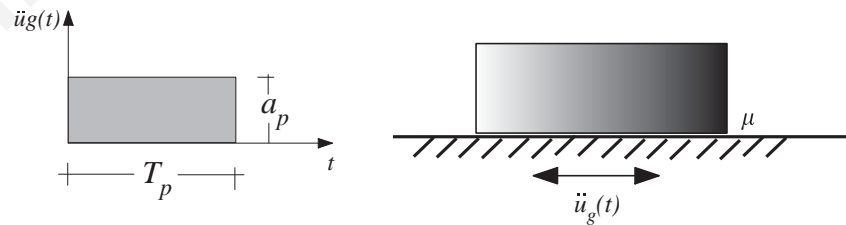


Figure 5.6. Rigid body on a horizontal plane subjected to a rectangular pulse acceleration.

Figure 5.7 shows the normalized maximum relative displacements of a rigid body, resting on a surface with a coefficient of friction μ , subjected to rectangular acceleration pulses with an amplitude a_p and a duration T_p . The theoretical maximum relative displacement of the rigid body with respect to the base is given by the following equation, the solution of which is presented with a continuous blue line in Figure 5.7.

$$u_{max} = \frac{a_p \cdot T_p^2}{2} \cdot \left(\frac{a_p}{\mu \cdot g} - 1 \right) \quad (5.5)$$

The points presented in Figure 5.7 correspond to various results acquired from numerical simulations performed by the developed software. For each analysis, a rectangular acceleration pulse of an amplitude a_p and a duration T_p is applied to the base with a coefficient of friction μ between the base and the rigid body. Specifically, various values μ are used in the analyses with a combination of the pairs: $a_p = 0.8g$, $T_p = 1.5sec$ and $a_p = 0.5g$, $T_p = 1.0sec$, respectively. The maximum relative displacement, u_{max} , is obtained from the analysis once the relative velocity between the base and the body becomes zero. Regardless of the parameters a_p , T_p and μ that have been used in the analysis, the relative displacement u_{max} scales to a single governing curve as the response is self-similar [42]. The value of the $\Pi_1 = \frac{U_{max}}{a_p \cdot T_p^2}$ is plotted in Figure 5.7, showing that the developed software captures sufficiently well the theoretical solution.

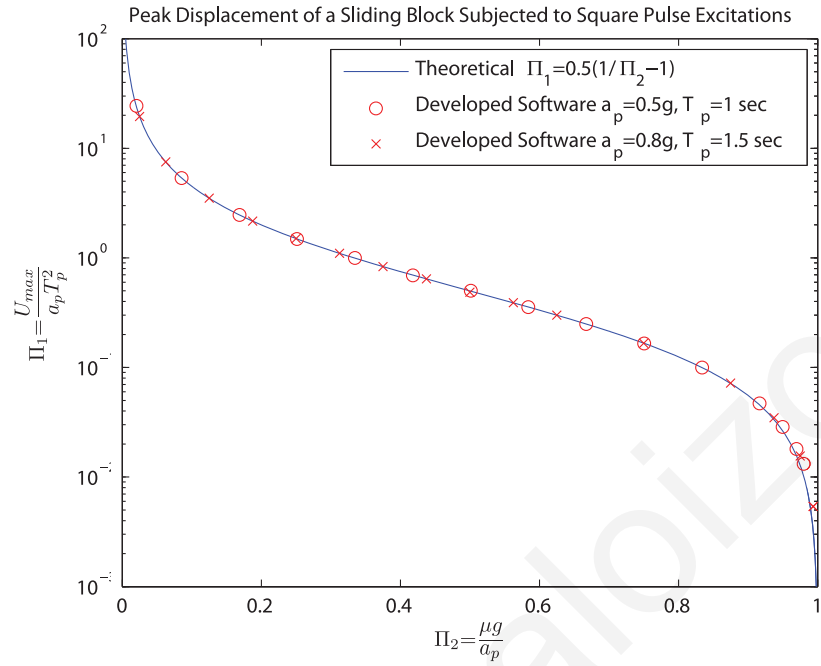


Figure 5.7. Normalized maximum relative displacements of a rigid body, resting on a surface with coefficient of friction μ , subjected to rectangular acceleration pulses.

Figure 5.8 shows the time-history relative displacement, u , of the body, with respect to the base, for different coefficients of friction, μ , and for a rectangular pulse of $a_p = 0.8g$ and $T_p = 1.5\text{ sec}$. As μ increases, the time required for the body to reach a “full stop” decreases.

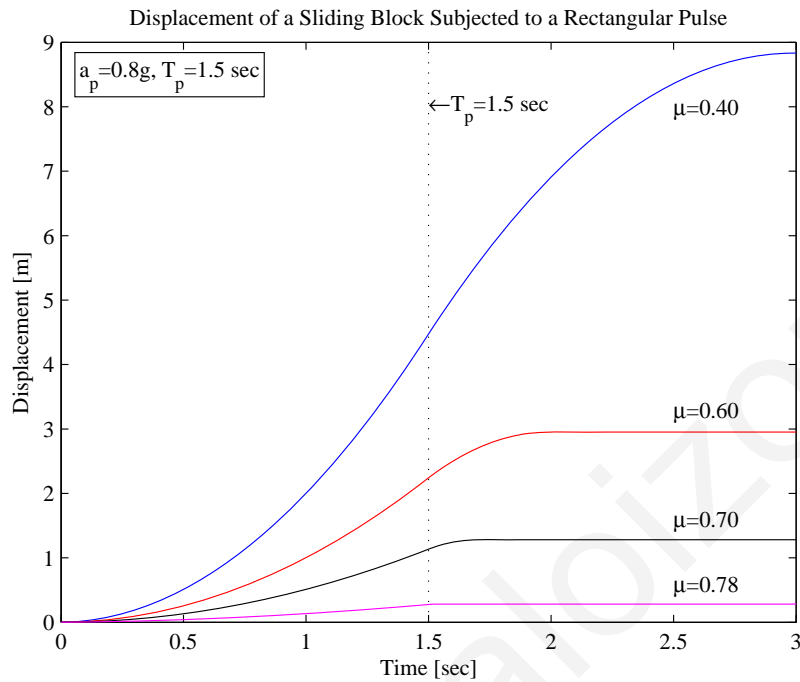


Figure 5.8 Time-history relative displacements of a sliding block under rectangular pulse accelerations.

5.1.4. Sliding response to earthquake motions

A similar validation process for the developed software is performed using earthquake ground motions as excitations (Figure 5.9). Specifically, two different earthquake excitations are used as base acceleration motions, and the results that have been obtained from the analyses using the software application are presented in Figure 5.10 and Figure 5.11 along with the theoretical responses.

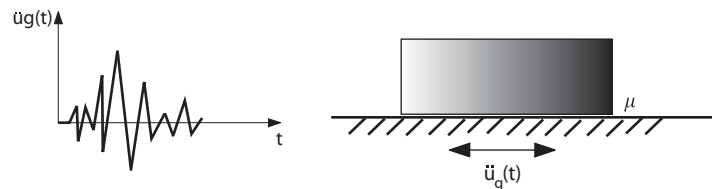


Figure 5.9. Rigid body on a horizontal plane subjected to earthquake excitations.

In particular, horizontal components of the 1994 Northridge and the 1995 Aigion earthquakes have been used. This validation process had also been carried out by Konstantinidis and Makris [42] using the same earthquake excitations with a commercially available software providing the theoretical results given by the following equations, which are a specific case of the Bouc-Wen elastoplastic model [84].

$$\ddot{u}(t) + \mu \cdot \gamma \cdot \dot{z}(t) = -\ddot{u}_g(t) \quad (5.6)$$

$$u_y \cdot \dot{z}(t) + \gamma \cdot |\dot{u}(t)| |z(t)| |z(t)|^{n-1} + \beta \cdot \dot{u}(t) \cdot |z(t)|^n - \dot{u}(t) = 0 \quad (5.7)$$

where $z(t)$ is the hysteretic dimensionless quantity, u_y is a yield displacement for the case of rigid-plastic behaviour, which is set to a small value of $u_y = 10^{-6} m$, and β , γ and n are dimensionless quantities that control the shape of the hysteretic loop. The specific solution presented for the response of a sliding mass has been acquired for $\gamma = \beta = 0.5$ and $n = 50$, while the value of the coefficient of friction was set to $\mu = 0.3$.

Figure 5.10 and Figure 5.11 show that the response computed by the developed software for the displacements due to sliding of a rigid body, under earthquake excitations, is sufficiently similar to the corresponding results provided by Konstantinidis and Makris [42].

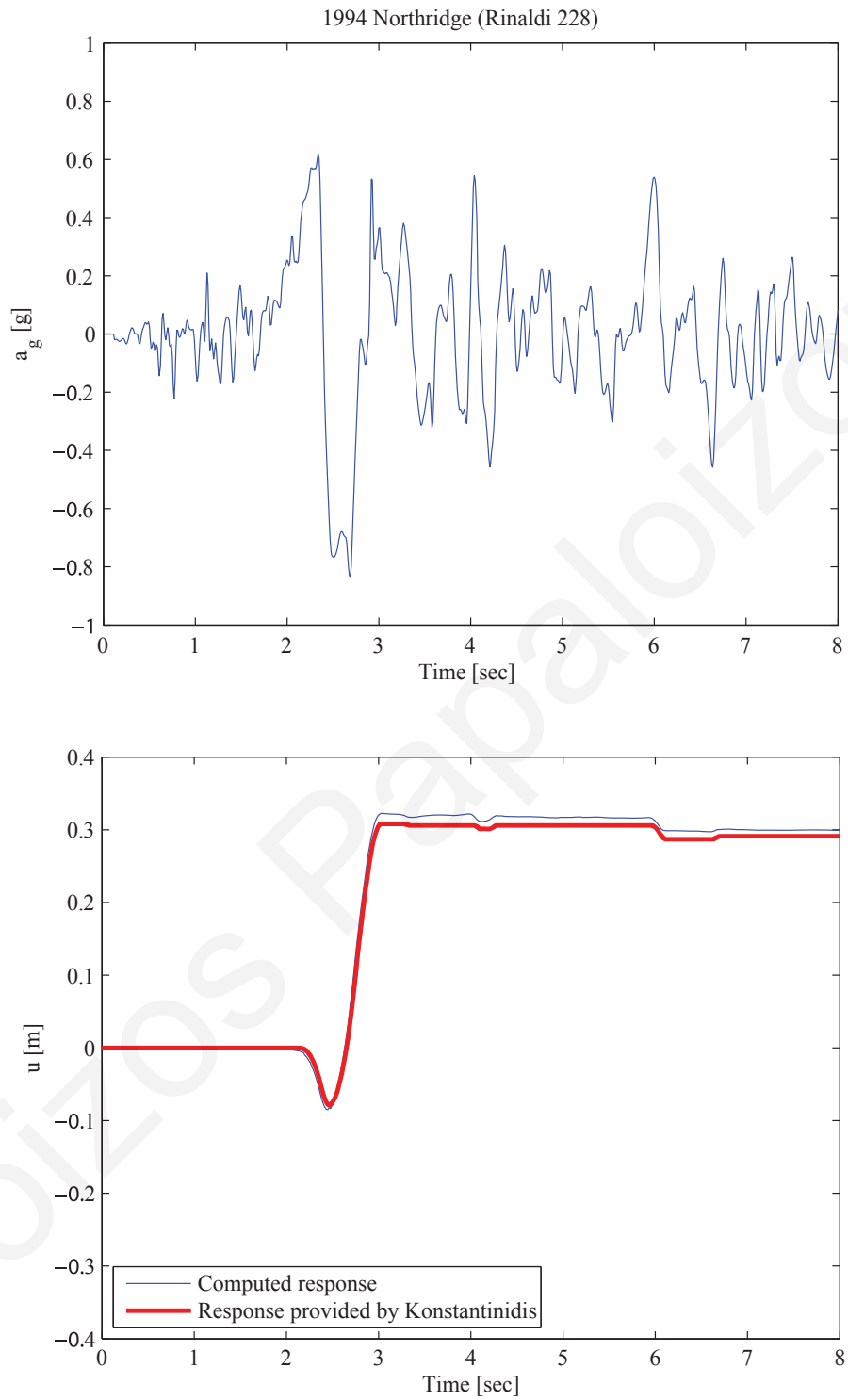


Figure 5.10. Sliding response of a rigid body under an earthquake excitation.

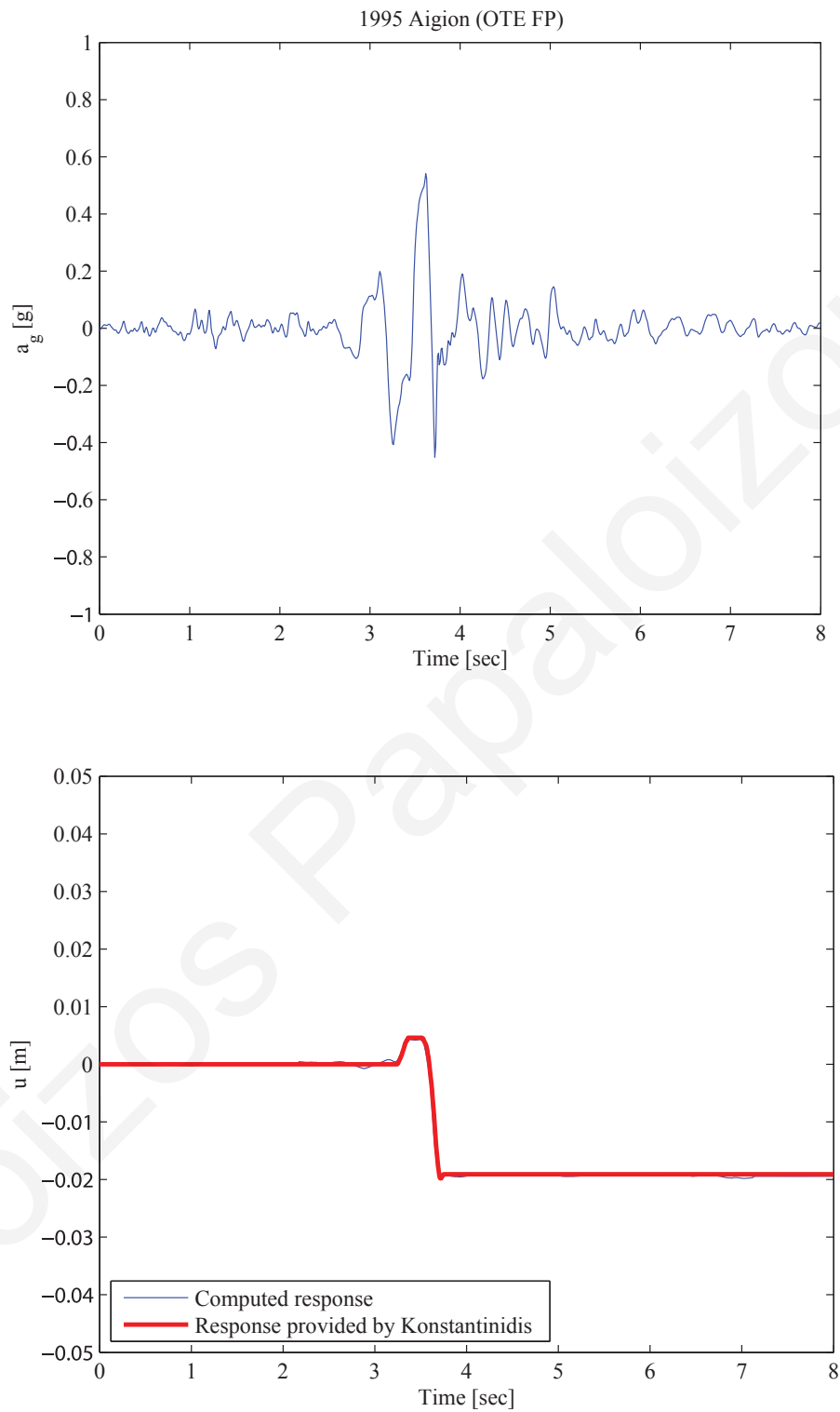


Figure 5.11. Sliding response of a rigid body under an earthquake excitation.

5.1.5. Rocking response to earthquake motions

Pure rocking of a rigid body has also been studied by Shenton [75], who indicated that, in addition to pulse sliding and pure rocking, there is a slide-rock mode, and its manifestation depends not only on the width to height ratio, but also on the magnitude of the base acceleration.

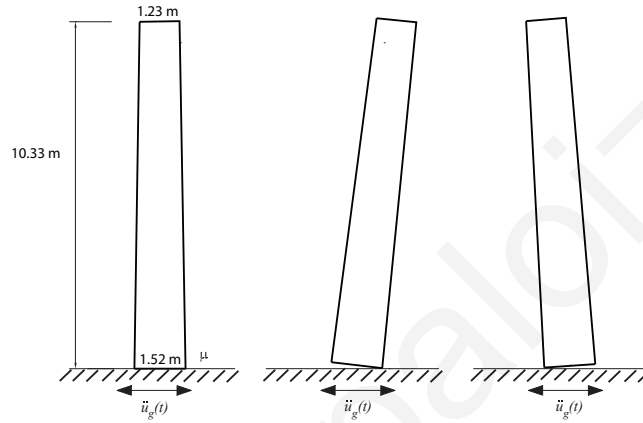


Figure 5.12. Model of a rigid block used for the validation under earthquake motions.

These ideas were further refined by Zhang and Makris [93] who demonstrated that under a trigonometric pulse with acceleration amplitude a_p , the condition for a block to enter rocking motion without sliding is

$$\frac{\lambda \cdot a_p - \frac{3}{4} \cdot g \cdot \cos(\alpha) \cdot \sin(\alpha) \left(\lambda \cdot \frac{a_p}{g} \cdot \tan(\alpha) - 1 \right)}{g + \frac{3}{4} \cdot g \cdot \sin^2(\alpha) \cdot \left(\lambda \cdot \frac{a_p}{g} \cdot \tan(\alpha) - 1 \right)} \leq \mu \quad (5.8)$$

where the fraction $\frac{g}{a_p} \cdot \tan(\alpha) < \lambda \leq 1$ gives the level of the ground acceleration, $\lambda \cdot a_p$, at the instant when a block with slenderness α is about to enter rocking motion. The above equation indicates that under an excitation pulse with acceleration amplitude a_p , the condition for a block to enter a rocking motion without sliding depends on the value of a_p . However, this is true only for pulses that have a finite acceleration at the initiation of

the motion. For pulses where the acceleration builds up gradually, such as a one-sine pulse, the value $\lambda \cdot a_p$ at the initiation of rocking is equal to $g \cdot \tan \alpha$, and the previous equation reduces to $\tan(\alpha) < \mu$, which is the traditional expression that one derives from static equilibrium analysis [93].

Figure 5.13.b shows the time-history rotation of a monolithic column (Figure 5.12) under the 1977 Bucharest earthquake (Figure 5.13.a). The coefficient of friction, μ , at the base of the rigid column is sufficiently large so that no sliding is observed. The dashed line represents the theoretical solution provided by Konstantinidis and Makris [42], while the solid line plots the response obtained by the developed software. Comparison of the results obtained from the analysis methods is deemed satisfactory.

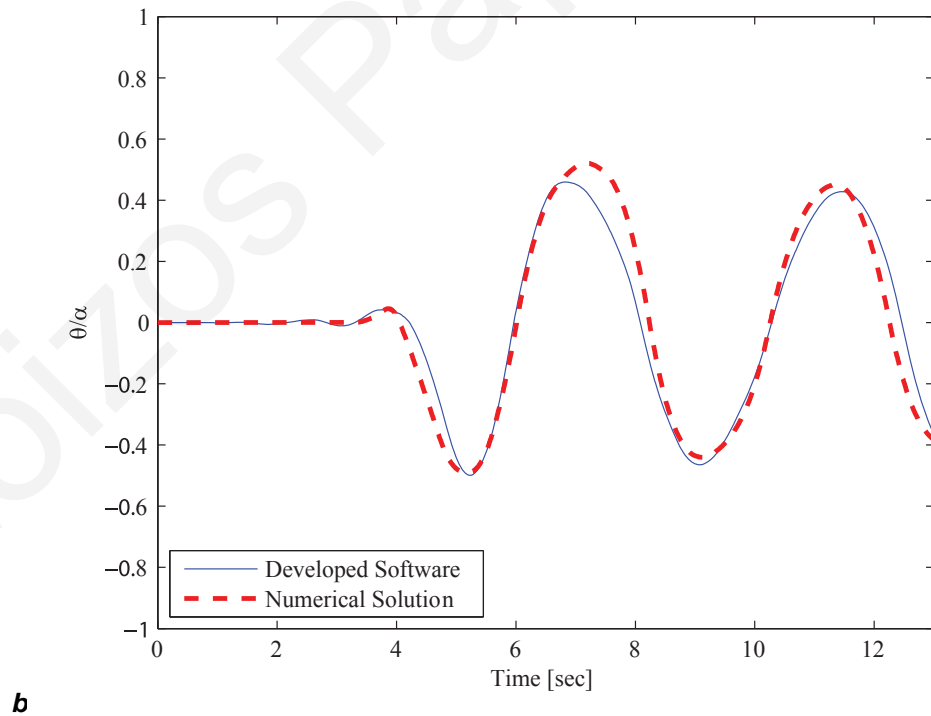
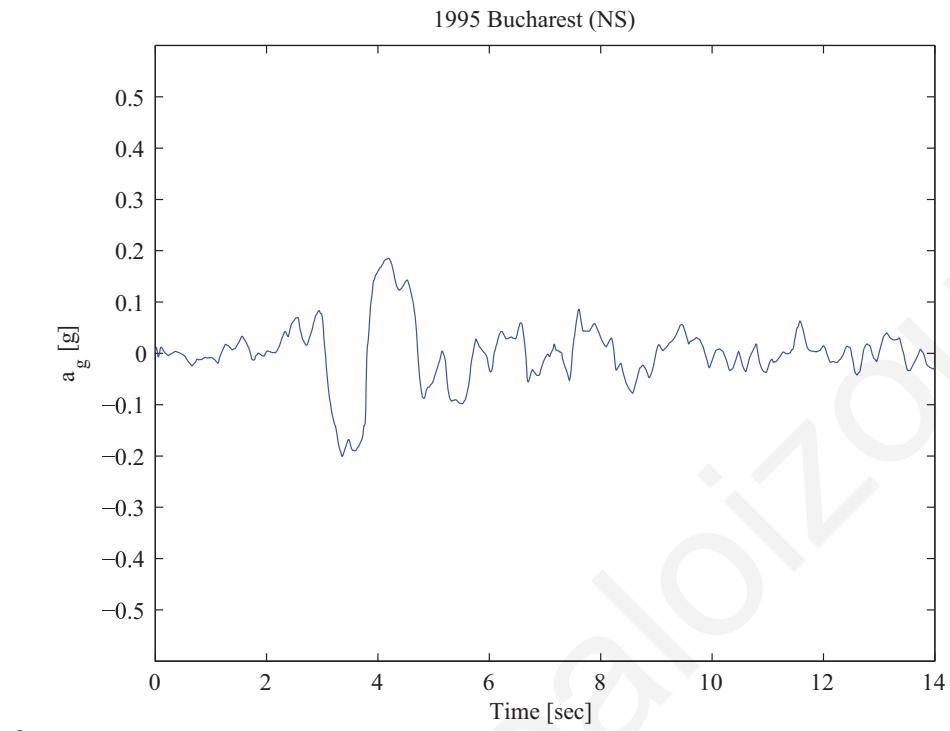


Figure 5.13. Rocking response of a rigid body under earthquake excitations.

5.1.6. Rocking response during free vibration of two rigid bodies

For verification purposes, a comparison is made between results obtained by the developed software with corresponding results that are derived from analytical solutions of simplified problems with two rigid bodies conducted by Psycharis [67]. Specifically, the free oscillation response of two rigid bodies (Figure 5.14) that are left to oscillate from an initial inclination angle of 0.1 rad is examined numerically and the computed response is compared with the corresponding analytical results.

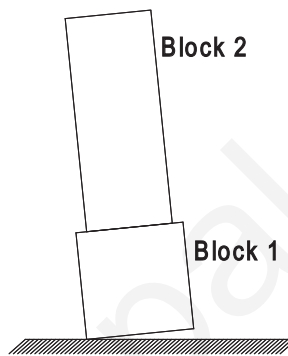


Figure 5.14. Free oscillation of two rigid bodies released from an initial inclination angle of 0.1 rad .

In particular, the dimensions of the bodies, which are placed freely the one on top of the other, are $b_1=1.25 \text{ m}$, $h_1=1.25 \text{ m}$, $b_2=1.0 \text{ m}$, $h_2=2.5 \text{ m}$. For the numerical analyses, a contact stiffness of the order of 10^8 N/m^2 and a damping coefficient of 10^3 N s/m have been used. Figure 5.15.a shows the results that are obtained from the analytical solutions [67], while the results that are computed from the respective simulations using the developed software are presented in Figure 5.15.b.

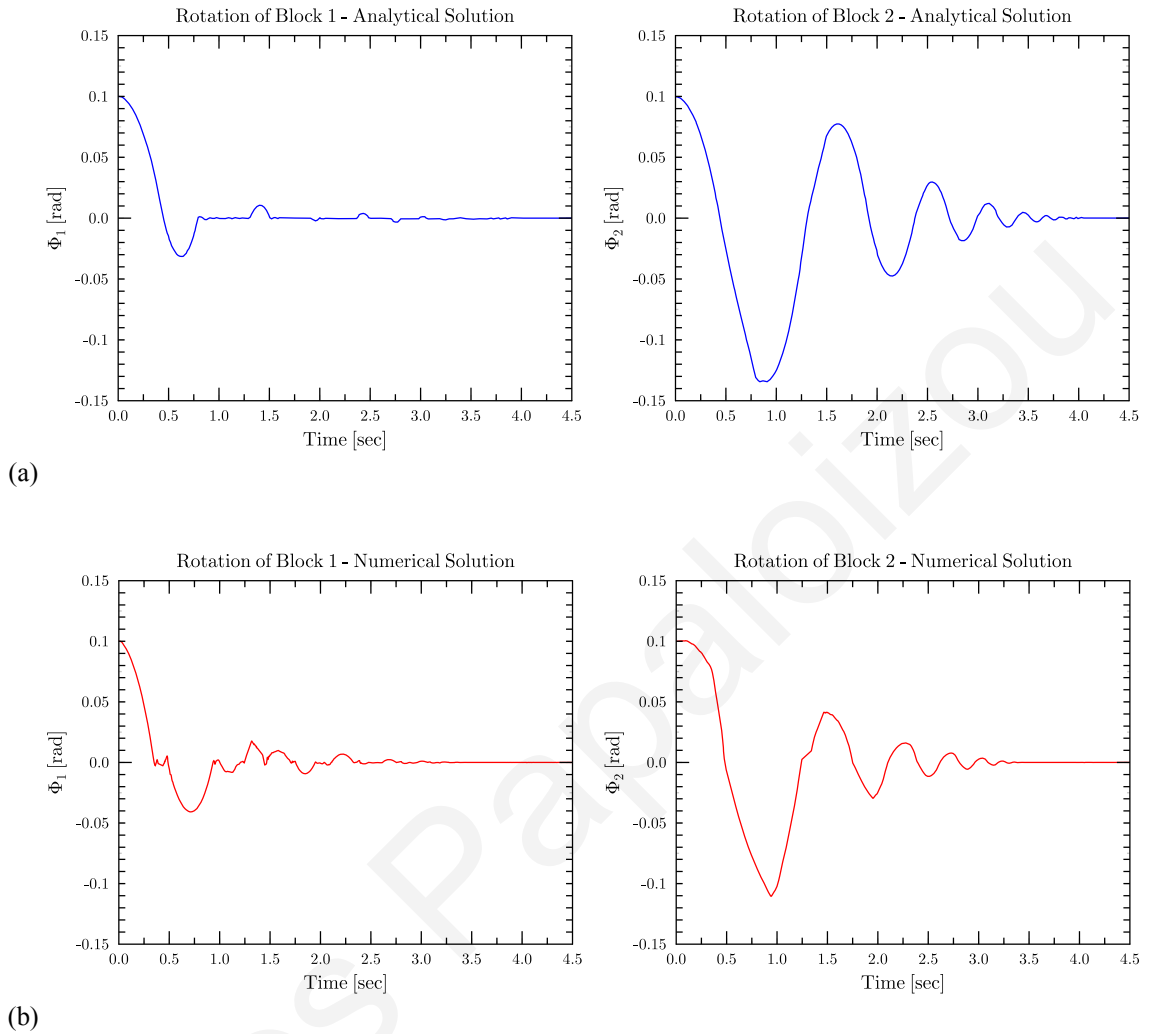


Figure 5.15. Rotation of the two bodies obtained analytically and numerically.

The results of the analyses, both qualitatively and quantitatively, demonstrate the satisfactory convergence of the numerical simulations with the analytical solutions of the rotations of the two oscillating bodies. The small differences that are observed can be justified by the fact that the numerical solution includes sliding phenomena, which were limited, but not completely avoided, by considering a high value of the coefficient of friction in order to compare the two solutions, since sliding had not been considered in the analytical solution.

Similarly, for the same geometry, Figure 5.16 and Figure 5.17 show the rotation of Block 1 as it has been computed from a non-linear analytical formulation as well as by the developed software, respectively. The non-linear formulation is provided by Spanos et. al. [80]. These results confirm the satisfactory convergence of the numerical simulations with analytical solutions of the rotations of the two oscillating bodies.

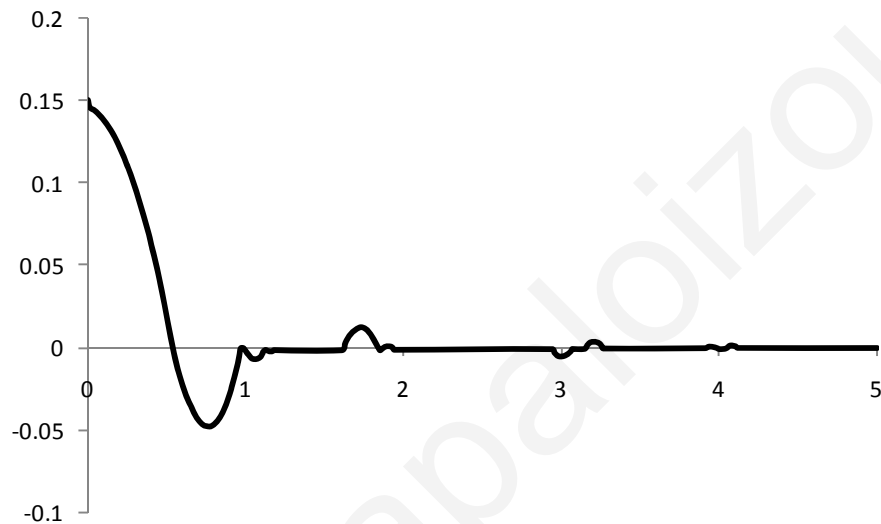


Figure 5.16. Rotation of Block 1 from an initial rotation angle of 0.15 rad as computed by a nonlinear analytical formulation provided by Spanos [80].

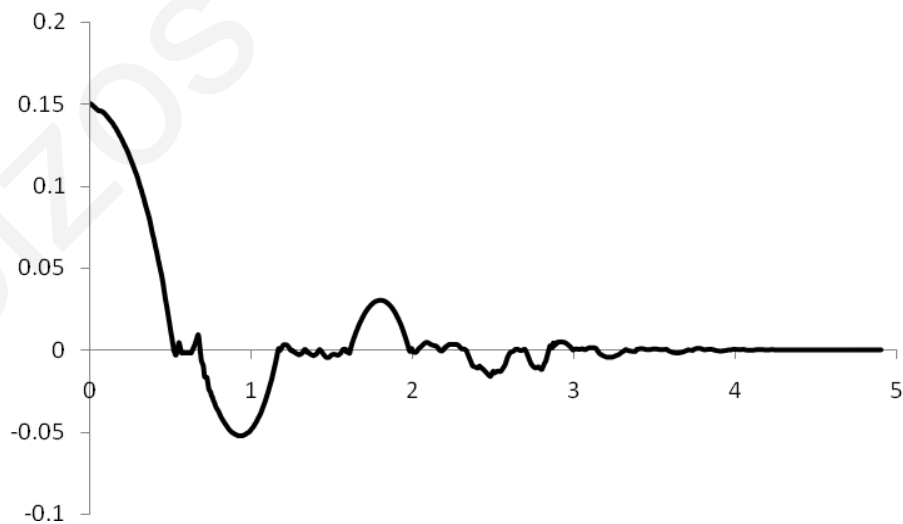


Figure 5.17. Rotation of Block 1 from an initial rotation angle of 0.15 rad as computed using simulation with the developed software.

5.2. Experimental validation

5.2.1. Rigid body free vibration

In this paragraph the developed software application is validated with results obtained from experiments conducted with stones under dynamic loading, intended to describe the behaviour of single rigid-block structures. An experimental investigation has been carried out by Peña et. al. [63] to study the rocking response of blue granite stones under free vibration. The results are compared with the computed response of a simulated rigid block with the same dimensions and mass obtained from the custom-made software.

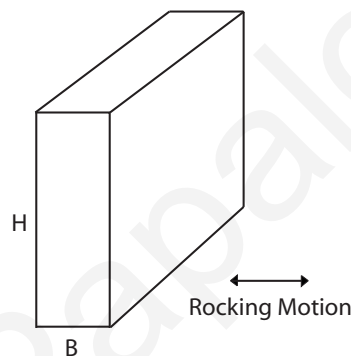


Figure 5.18. Experimental Setup [63].

The rigid block studied has a width of $b=0.25\text{ m}$, a height of $h=1.00\text{ m}$ and a mass of 503 Kg . For the numerical analyses, a contact stiffness of the order of 10^8 N/m^2 and a damping coefficient of 10^6 N s/m have been used in order to obtain the desired energy loss due to impacts (Figure 5.21). The rigid block was left to freely rock from an initial angle of 0.05236 rad . In the numerical analyses a large coefficient of friction is used in order to minimize the sliding between the block and the base during impacts.

Figure 5.19 displays the rotation angle of the block obtained experimentally [63], while Figure 5.20 shows the response computed by the developed software. The results of the analyses, demonstrate the satisfactory convergence of the computed onto the experimental response.

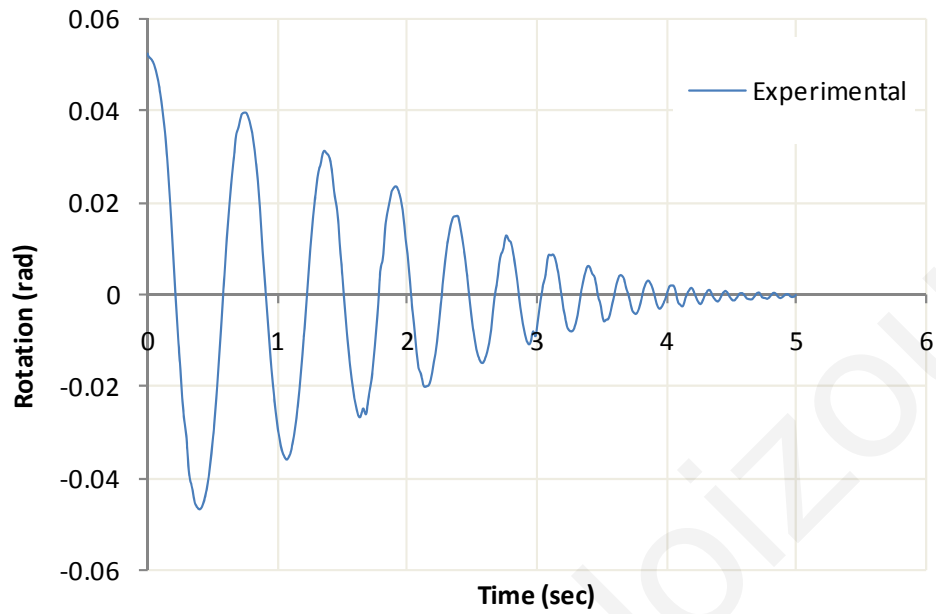


Figure 5.19. Rotation of a rigid body obtained experimentally by Pena et. al. [63].

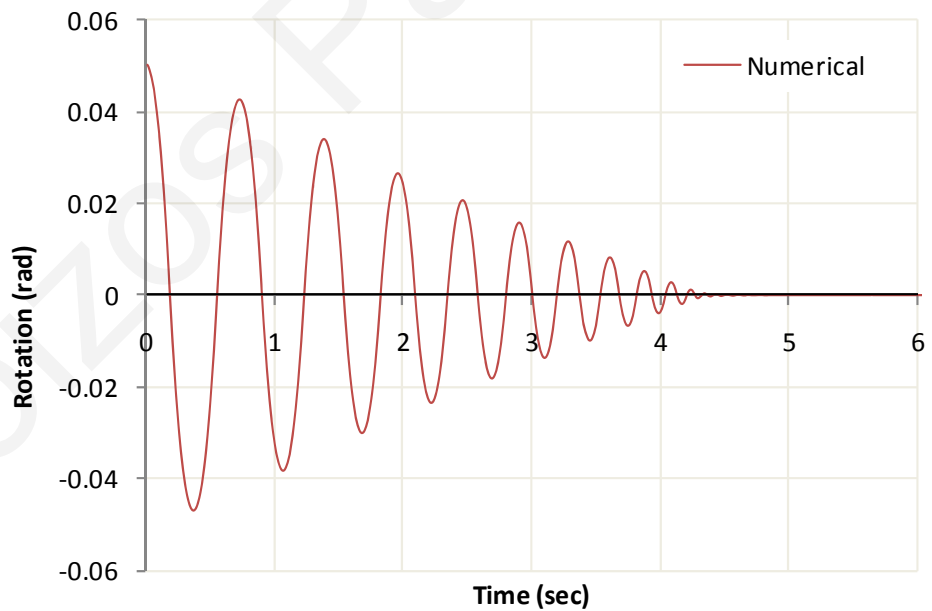


Figure 5.20. Rotation of the rigid body obtained numerically with the developed software.

Moreover, the contact parameters required for the analyses can be derived from such experiments. Figure 5.21 shows the effect of the contact damping coefficient on the response of a rigid block left to freely rock. This coefficient can represent the energy loss during each impact.

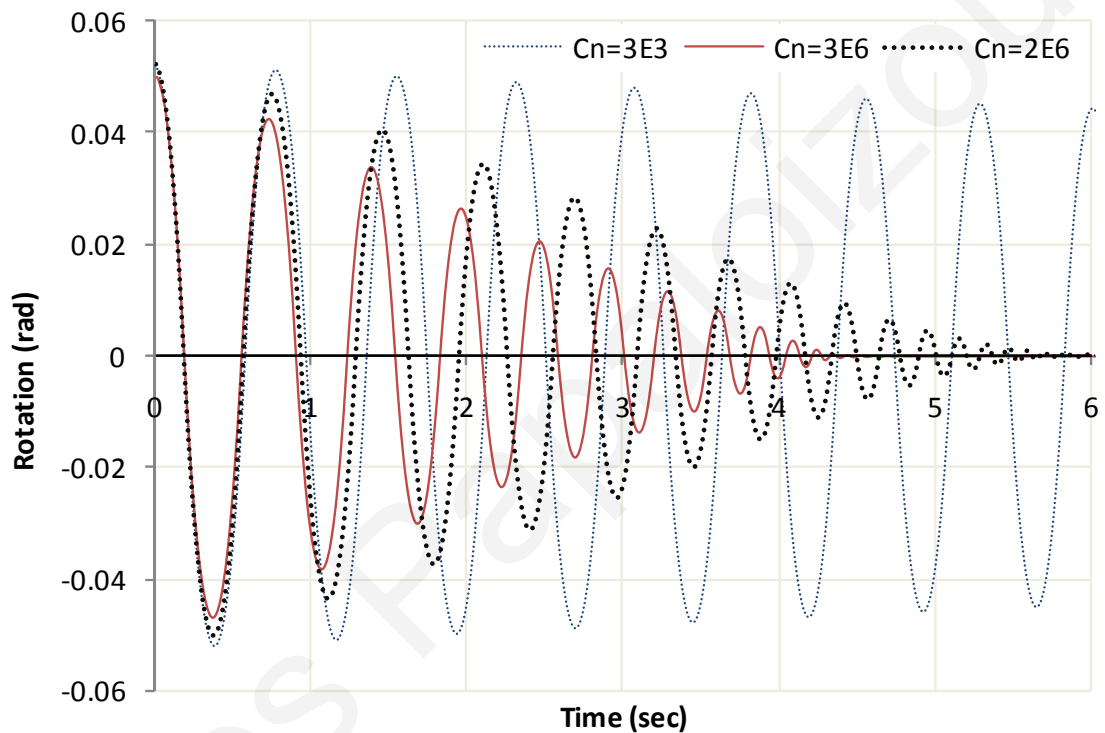


Figure 5.21. The effect of the contact damping coefficient on the free vibration of a rigid body.

5.2.2. Small-scale standalone multi-drum columns

Analyses showed that the response of multi-drum columns, using the methodology described, is extremely sensitive to small perturbations of the contact properties. It is important to correctly assess the contact parameters, such as the contact stiffness and the damping coefficients in order to obtain relatively accurate responses. These parameters can be determined by performing analyses of problems for which an analytical solution is known, calibrating the parameters to obtain the expected results. Another way to estimate these parameters is through the performance of relevant experiments.

Although the response of multi-drum columns depends on scale, small-scale experiments have been conducted, using a “Quanser Shake Table II”, to investigate certain characteristics of the response and validate the developed software (Figure 5.22a). In each experiment, the specimen column is composed of seven individual bodies (48x48x29 mm), with the bottom one fixed on the shake-table. The coefficient of friction μ has been measured to be 0.68. The weight of each drum is 0.135 Kg. A large number of experiments has been conducted using up to 2.15 m/s^2 peak ground accelerations, by changing the frequency and amplitude of harmonic excitations, considering only one horizontal direction. Snapshots have been taken to capture the failure mode at different excitation frequencies.

A parallel set of numerical simulations has been performed, using the developed software, in order to numerically simulate the small-scale columns of the experiments. The numerical simulations exhibit responses similar to the ones observed experimentally (Figure 5.22b). In particular, the results from both experimental and numerical simulations show that the required acceleration to initiate either sliding or rocking decreases as the excitation frequency increases (Figure 5.23).

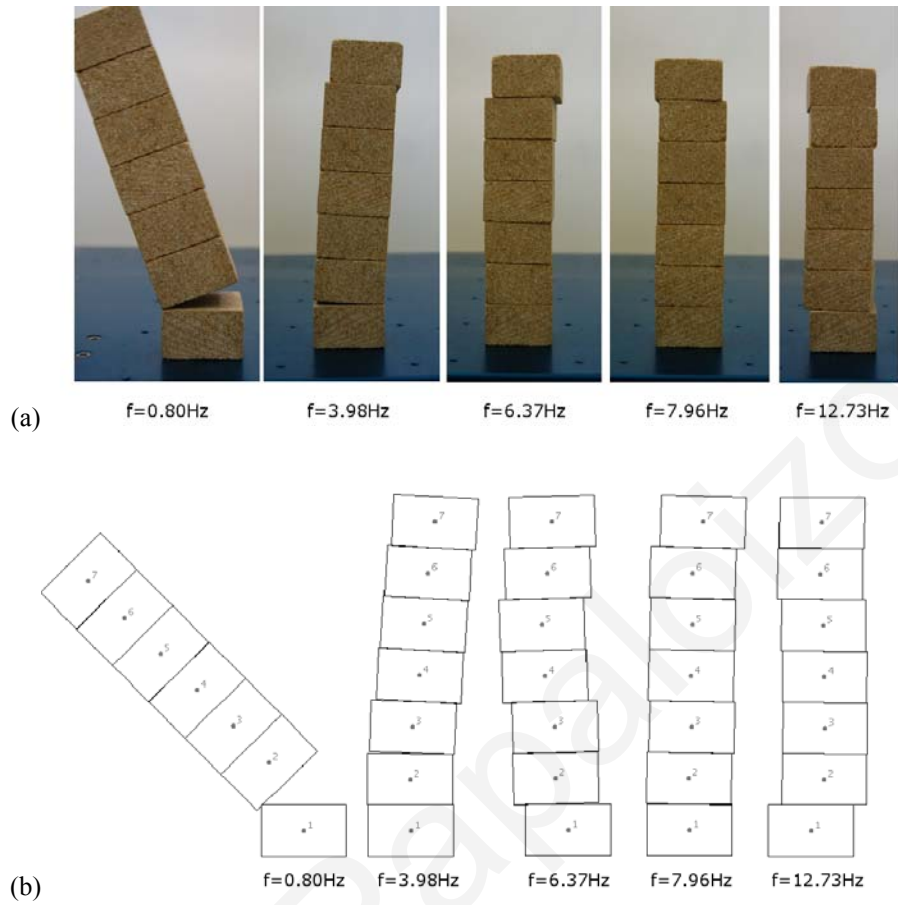


Figure 5.22. (a) Experimental column dynamic response (b) Computed response from numerical simulations.

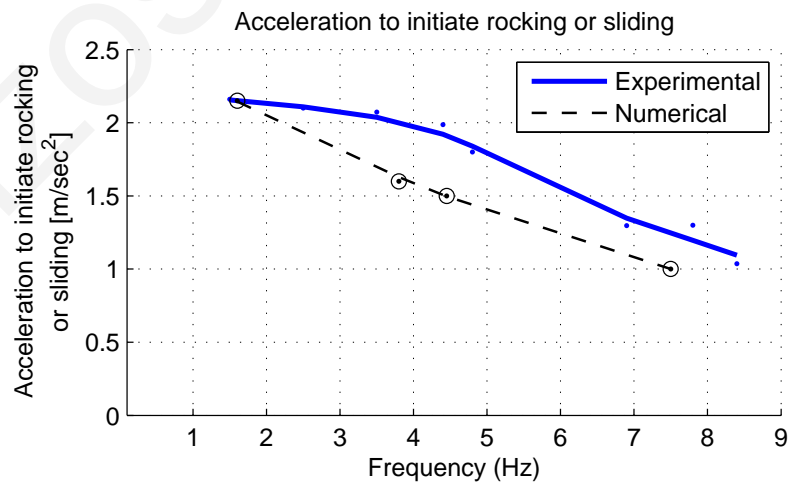


Figure 5.23. Specimen acceleration for sliding or rocking effect.

5.2.3. Small-scale colonnades with epistyles

Experiments of rigid bodies with two columns and a beam placed on top (60x60x150 mm, 1.140 Kg) have been conducted. Specifically, two different cases have been investigated, where the columns are either monolithic (60x60x100 mm, 0.750 Kg) or consisted of two bodies placed serially height-wise (60x60x50 mm, 0.750 Kg).

Firstly, the experiments show (Figure 5.24) that with the increase of the excitation frequency, the required acceleration to initiate either rocking or sliding decreases. Secondly, it is indicated that as the excitation frequency decreases, rocking is more dominant. For extremely low frequencies overturning occurs in the first few excitation cycles. With the increase of the excitation frequency the sliding effect dominates the response without overturning the system.

Furthermore, the conducted small-scale experiments reveal that energy dissipation through sliding mechanisms improves the overall stability of the system with an epistyle. Multi-body columns with a rigid beam placed on top seem to be more stable than monolithic colonnades. It is also observed that for monolithic columns, both the required acceleration to initiate rocking or sliding, and the acceleration required to overturn the system, are less than those required for multi-drum columns. Finally, it is observed that for monolithic columns, the sliding effect appears in higher frequencies compared to the colonnades that are constructed with a greater number of bodies.

6. Numerical simulations of standalone columns

In order to investigate the response of standalone columns, a large number of numerical simulations and parametric studies concerning monolithic and multi-drum columns have been carried out, using the developed software application. Different types of standalone columns and several types of ground motion excitations have been used in the conducted analyses.

Specifically, columns with different numbers of drums, various coefficients of frictions as well as numerous shapes have been considered. A large number of parametric studies have been performed in order to examine the influence of the frequency content and the peak ground acceleration (PGA) of ground excitations, as well as the geometrical and mechanical characteristics of standalone multi-drum columns in their response to harmonic excitations.

A comparison is made between the occurrence of sliding and rocking of the drums, aiming at understanding how various parameters may influence the dominance of either of the two phenomena. In the parametric studies, the sum of the overall sliding of the drums of a column, measured in centimetres, is defined as the “total sliding”. Accordingly, “rocking” is defined as the average absolute rotation of the drums measured in radians.

In addition to harmonic excitations, strong earthquake ground motions are also used to simulate and evaluate the dynamic response of such columns. Various earthquake records with different characteristics are used, enabling comparison between computed responses to those obtained under harmonic excitations. Finally, the effect of different frictional levels between different blocks is investigated through numerical analyses of various assemblies.

All numerical simulations have been conducted with the base of the columns fixed to the ground, moving with the ground during an excitation and in two dimensions. The values of the contact parameters, which depend on the geometry, the masses and the number of blocks as well as on the selected iteration time-step, have been estimated accordingly for each particular configuration so as to prevent excessive overlap between

the rigid bodies as well as to avoid any computational instabilities that may cause abnormal responses.

6.1. Influence of the excitation's PGA and frequency

A large number of numerical simulations of small-scale columns, corresponding to those experimentally tested, has been performed to study the influence of the excitation's peak ground acceleration (PGA) and frequency in the total sliding and rocking of the columns. In particular, using a specific peak ground acceleration (2.15 m/sec^2) and three different values for the coefficient of friction, the total sliding and rocking of the simulated columns is measured with respect to the corresponding excitation frequency (Figure 6.1a).

Furthermore, using a specific coefficient of friction ($\mu=0.68$) and four different values for the amplitude of the peak ground acceleration of a harmonic ground excitation, the total sliding and rocking of the simulated columns is measured with respect to the corresponding excitation frequency (Figure 6.1b).

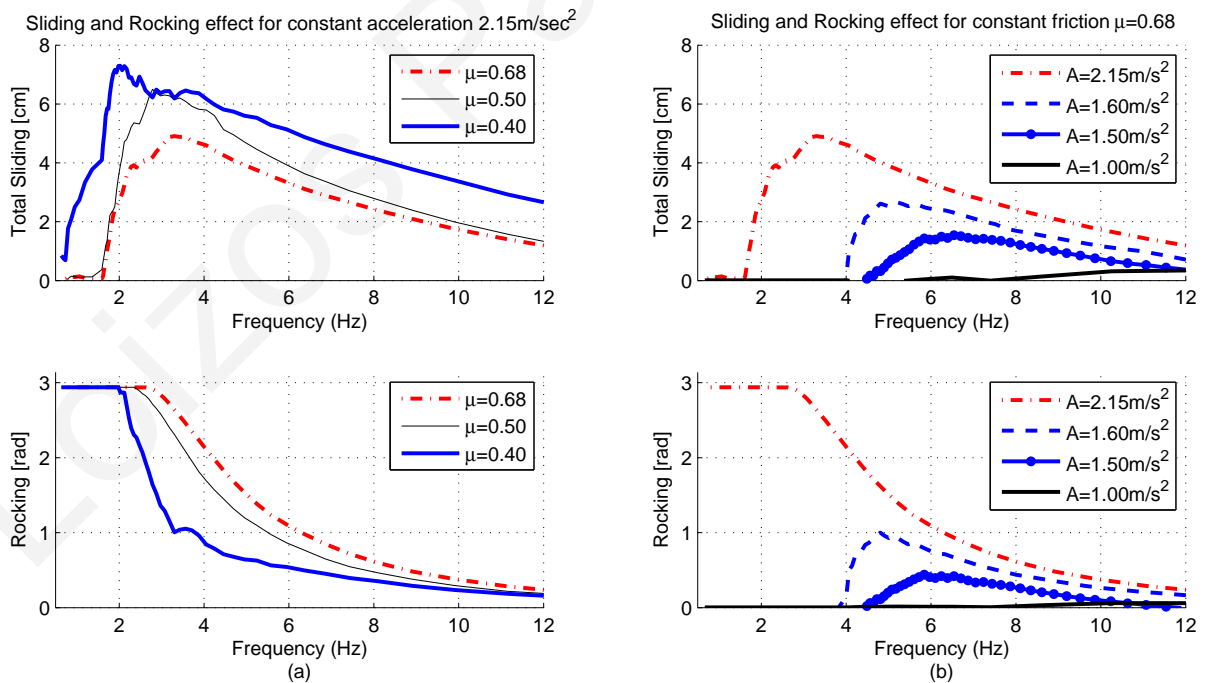


Figure 6.1. Total sliding and rocking computed in numerical simulations for (a) different coefficients of friction and (b) different peak ground accelerations.

The results from the performed numerical simulations exhibit similar responses with those observed in the conducted small-scale experiments (Figure 5.22). In particular, the results indicate that for low frequencies, rocking is the prevailing failure mode. By increasing the frequency, both sliding and rocking occur, while for very high frequencies only sliding occurs.

Furthermore, the computed responses suggest that for lower peak ground accelerations, higher excitation frequencies are required to initiate rocking (Figure 5.23 and Figure 6.1.b). Conversely, as shown from the parametric analyses (Figure 6.1.b) the acceleration needed to overturn a column increases with the excitation frequency.

Subsequently, full-scale multi-drum columns with a total height of 6 m and width of 1 m are numerically simulated, using the developed software, for various harmonic excitations with a displacement amplitude of 0.25 m. Figure 6.2 - Figure 6.4 show time-history snapshots of the computed responses for 0.5, 2 and 20 Hz excitation frequencies, respectively, in order to identify the influence of the excitation frequency, while keeping the displacement amplitude constant.

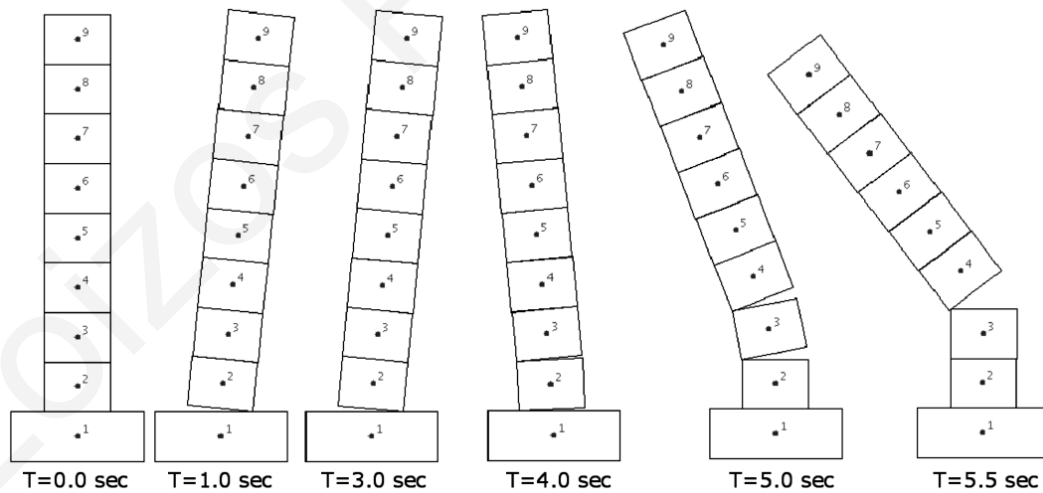


Figure 6.2. Response of a multi-drum column under a harmonic excitation with 0.5 Hz frequency and 0.25 m amplitude.

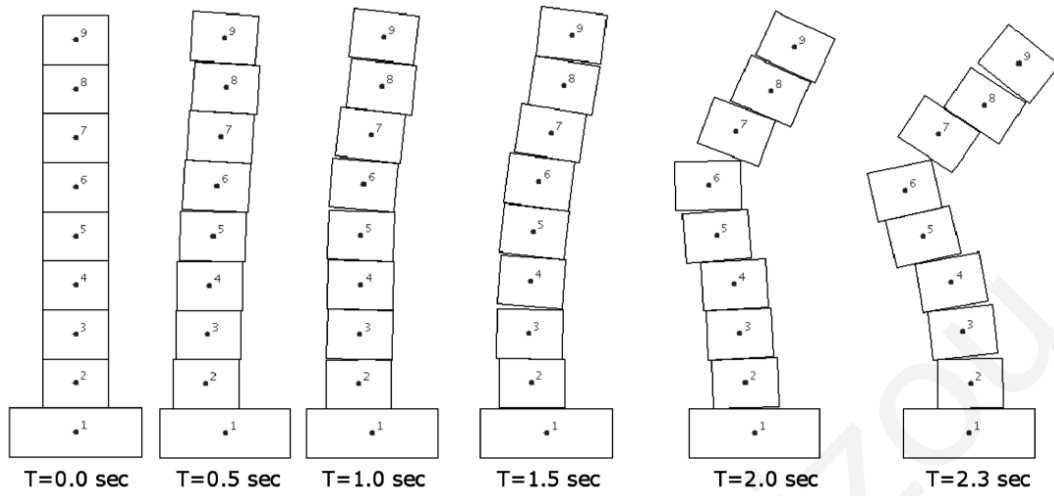


Figure 6.3. Response of a multi-drum column under a harmonic excitation with 2 Hz frequency and 0.25 m amplitude.

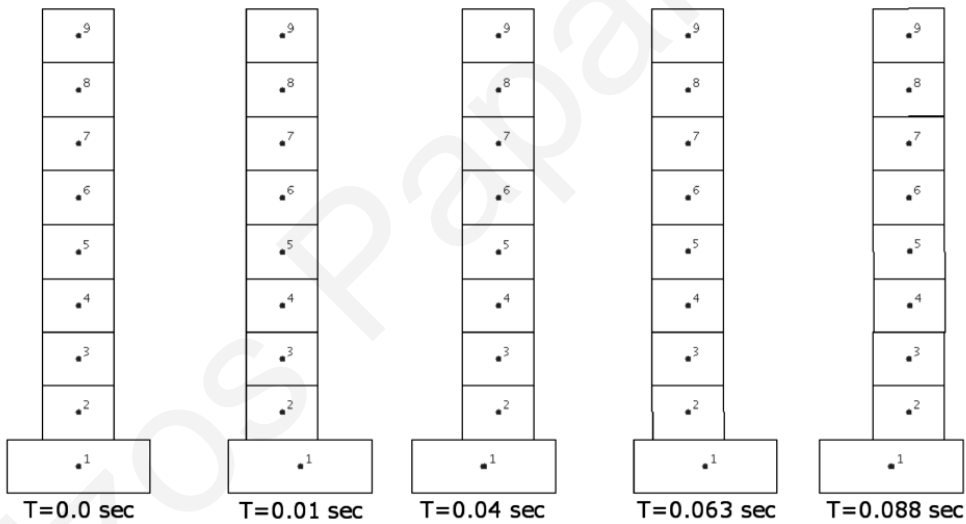


Figure 6.4. Response of a multi-drum column under a harmonic excitation with 20 Hz frequency and 0.25 m amplitude.

The numerical simulations indicate that for very low frequencies, the response does not exhibit any sliding or rocking. In those cases, the entire column moves together with the moving base, remaining essentially undeformed. Conversely, for very high frequencies the base slides from the rest of the column, which seems to not have the time to react to the rapid excitation, remaining essentially undeformed (Figure 6.4). In this case, the ratio of the total sliding to the total base movement is approximately equal to 1.0

(Figure 6.5). Between these frequencies both rocking and sliding occurs, where for lower frequencies rocking dominates the response (Figure 6.2).

6.2. Influence of the coefficient of friction

The material used for the construction of ancient columns varies, depending on the rock formations in the area of the monument. This variation results to different frictional coefficients for each material. The roughness of the drum's surface is an additional parameter that may lead to higher or lower values of the coefficient of friction. Furthermore, in some cases, where retrofitting of ancient monuments is necessary, old destroyed drums are replaced by new ones of the same material, but with different roughness. The values of the coefficient of friction for such monuments are estimated from $\mu=0.4$ to values more than 1.0 .

Parametric analyses reveal (Figure 6.1a, Figure 6.5 and Figure 6.6) that the value of the coefficient of friction affects the response of a column. In particular, for lower values of the frictional coefficients, the sliding effect is greater, while the rocking effect decreases. The acceleration that is required to overturn a column for higher excitation frequencies, increases with the decrease of the coefficient of friction.

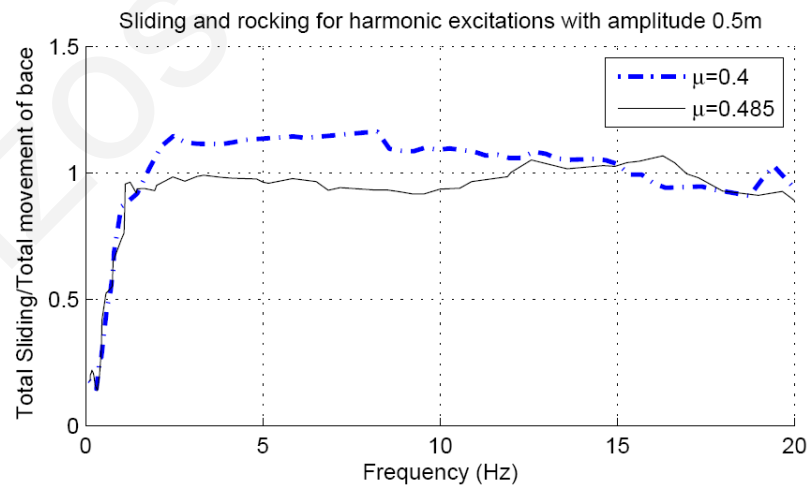


Figure 6.5. Ratio of total sliding to total base movement response under harmonic excitations with an amplitude of 0.5 m for full-scale columns (6 m height and 1 m width) constructed with eight drums.

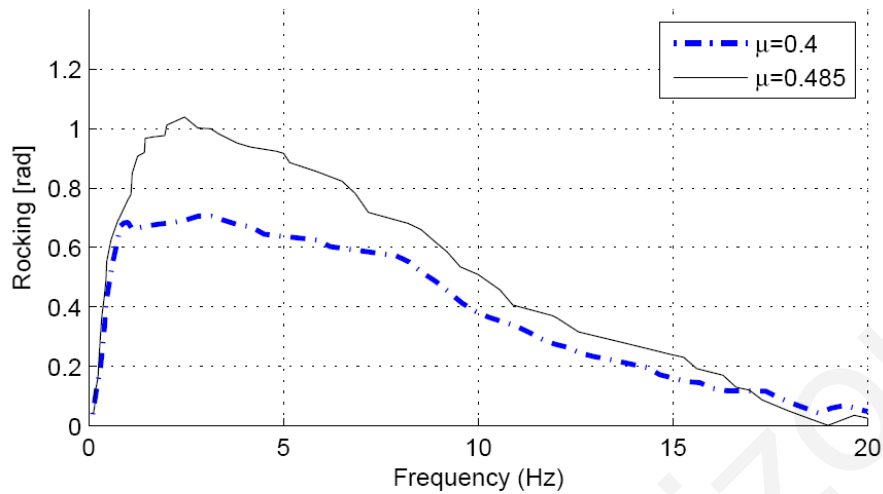


Figure 6.6. Rocking response under harmonic excitations with an amplitude of 0.5 m for full-scale columns (6 m height and 1 m width) constructed with eight drums.

6.3. Influence of the drums

6.3.1. Number of drums

A series of numerical simulations has been performed for columns with the same total height (6 m) and width (1 m), but with different numbers of drums. Figure 6.7 shows the response of a column with four drums, each with a height of 1.5 m under a harmonic excitation with a 0.5 Hz frequency and a 0.25 m amplitude.

Similarly, Figure 6.8 shows the response of a column with two drums, each with a height of 3 m under the same harmonic excitation. It is observed that the response of a column changes considerably as the geometric characteristics of the drums change. Despite the same overall dimensions, the number and position of the discontinuities, between drums, influences significantly the response of the column and in case of failure, the mode of collapse.

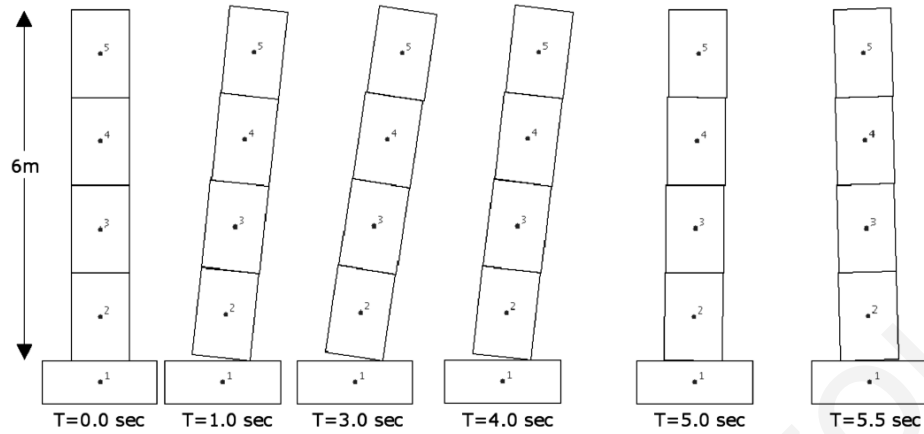


Figure 6.7. Response of a multi-drum (drum height = 1.5 m) column under harmonic excitation with 0.5 Hz frequency and 0.25 m amplitude.

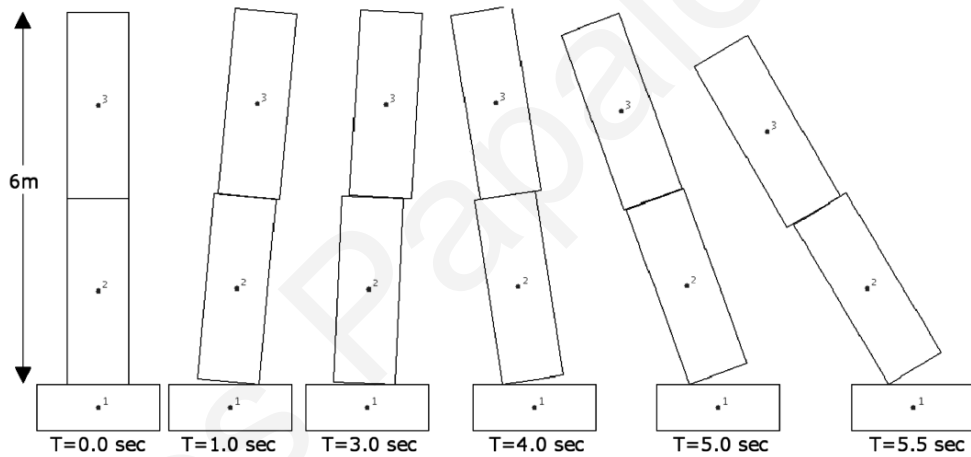


Figure 6.8. Response of a multi-drum (drum height = 3 m) column under harmonic excitation with 0.5 Hz frequency and 0.25 m amplitude.

The numerically evaluated ground acceleration $\ddot{u}_{g,cr}$ to initiate rocking for a monolithic column without sliding is consistent to that given by the following equation [53]:

$$\theta_{cr} = a \cdot \tan\left(\frac{b}{h}\right) = 0.165 \text{ rad} \quad (6.1)$$

where b and h are the total width and height of the column, respectively, and g is the acceleration of gravity.

Initiation of rocking is considered to happen when the column's rotation exceeds the angle of $\theta_{cr}/30$, where θ_{cr} is the critical angle, which when exceeded the column overturns. Instead of using a zero value, the value $\theta_{cr}/30$ is selected and used as a reasonable threshold to designate rocking, in order to ensure that the computed rotation is due to actual rocking and not due to numerical errors. The critical angle is given by the next equation:

$$\ddot{u}_{g,cr} = \pm \frac{b}{h} \cdot g = \pm 1.635m / \text{sec}^2 \quad (6.2)$$

For a column consisting of more than one drum, this phenomenon becomes more complicated. The acceleration that is needed to initiate rocking and to cause overturning of a column, with respect to the number of drums that assemble the column, is examined in a set of parametric analyses (Figure 6.9 and Figure 6.10). A linearly time-increasing acceleration with a rate of $0.5 \text{ m/sec}^2/\text{sec}$ is considered as a monotonic base excitation.

The plot in Figure 6.9 provides the mean rotation of the column in terms of the increasing base acceleration. When the mean rotation of the column exceeds the value of θ_{cr} the structure becomes unstable and the collapse is unavoidable. However, beyond that value, the curve follows the same trend until the time of collapse.

The simulations indicate that the ground acceleration that is required to overturn the column depends on the position of the Centre of Gravity (CoG) and on the energy loss due to friction between sliding drums. Increasing the number of drums, activates sliding between more bodies, resulting to potential dislocation of the CoG of the column, which may lead to instability. On the other hand this sliding effect between drums increases the energy dissipation due to friction. The relationship between the number of drums and the necessary PGA to initiate rocking and to cause overturning, for the column that is examined, are shown in Figure 6.10, in terms of the number of drums of the column.

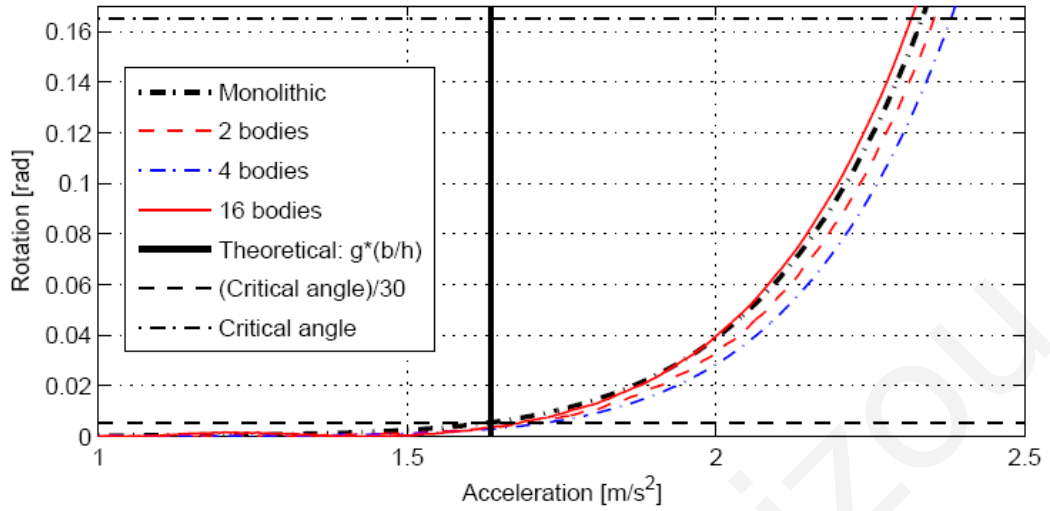


Figure 6.9. Mean rotation of the column with various number of drums under monotonically increasing base acceleration.

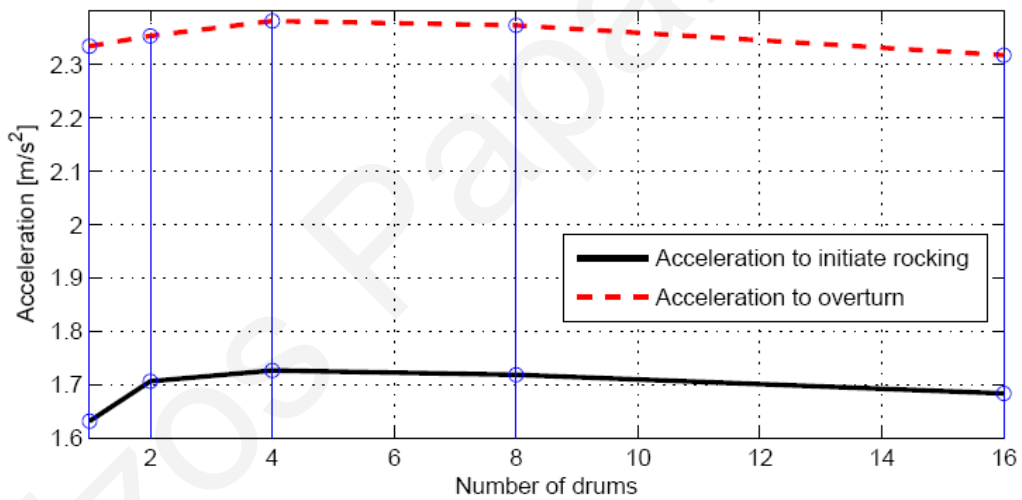


Figure 6.10. Required acceleration to initiate rocking and overturning, in terms of the number of drums of the column.

6.3.2. Shape of drums

In order to investigate the effect of the shape of the individual drums, various simulations have been performed on a set of tapered columns. Three columns with different ratios of the base width W_b to the top width W_t are analyzed, keeping the total mass of the column constant and equal to the mass of a non-tapered column, with base width of 1 m and total

height of 6 m (Figure 6.11). The mean rotation of the columns with the same total height and number of drums, but with different shapes of the drums, under monotonically increasing base acceleration is presented in Figure 6.12.

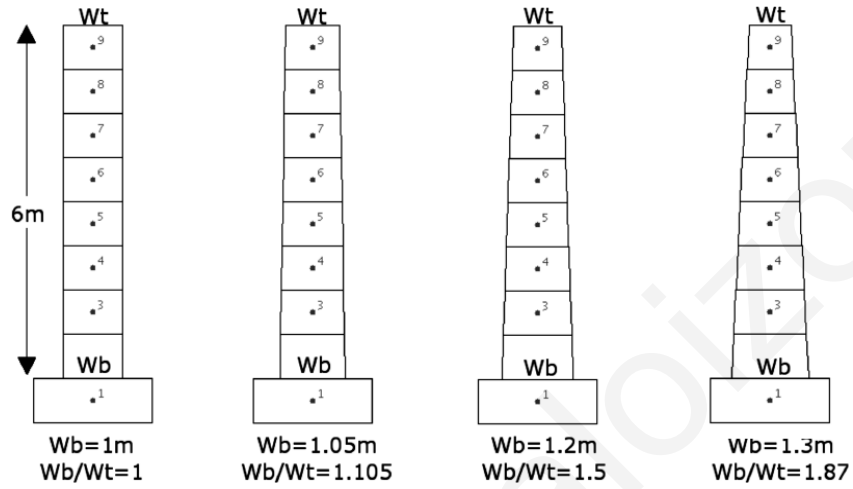


Figure 6.11. Models of the examined tapered columns.

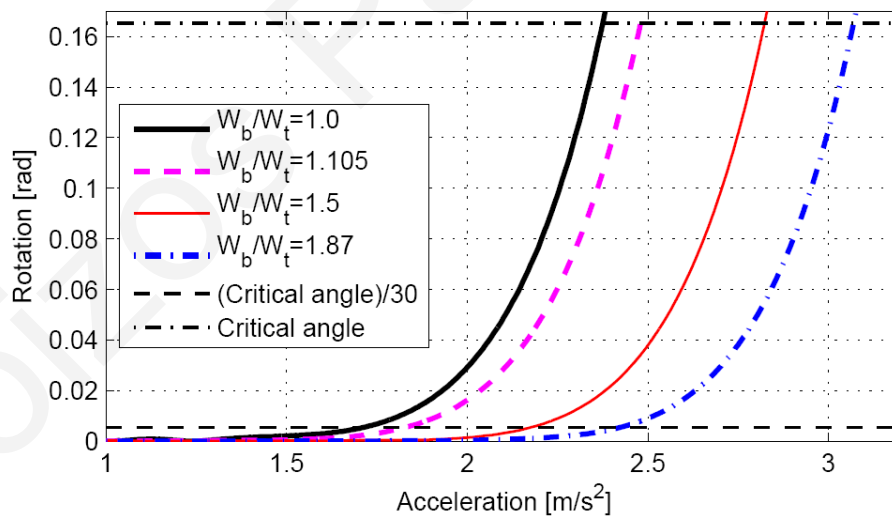


Figure 6.12. Mean rotation of the column with various shapes of the drums under monotonically increasing base acceleration.

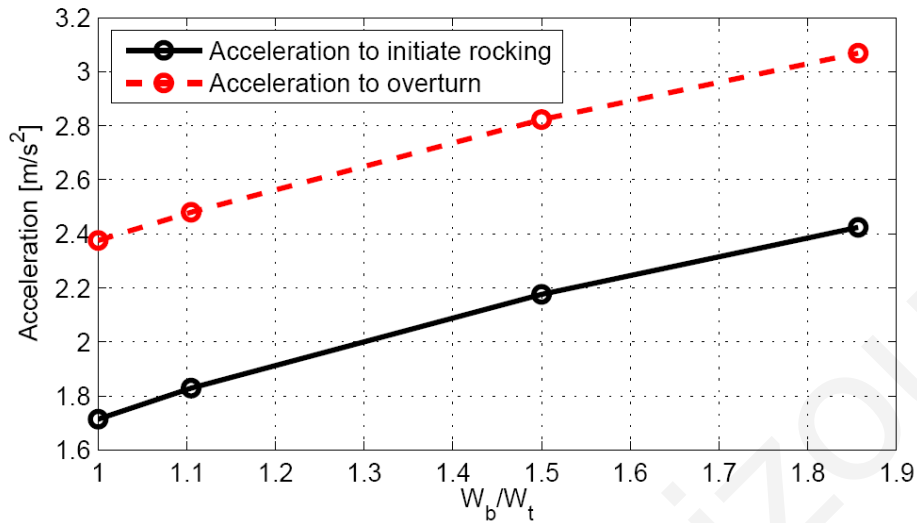


Figure 6.13. Required acceleration to initiate rocking and overturning of the column with various shapes of tapered drums.

Numerical simulations indicate that tapered columns are more stable than corresponding non-tapered columns, probably since the former have the CoG closer to the ground. Both the PGA that is needed to initiate rocking and the PGA that is needed to overturn the column increase, as the ratio W_b/W_t increases, if the total mass is kept constant, as shown in Figure 6.12 and Figure 6.13.

6.4. Response to strong motion excitations

Three ground acceleration records from the Athens, Kalamata, and Mexico City earthquakes, which have different characteristics (Table 6.1), have been selected and used to investigate how the response of these columns under strong seismic motion is influenced by the characteristics of the earthquake excitation. The predominant frequencies of these earthquake records vary from 0.45 to 8.3 Hz. Dynamic analyses are performed after scaling the earthquakes appropriately to cause failure. Figure 6.14 provides the pseudo-acceleration response spectra for three scaled earthquake excitation, assuming 10% viscous damping ratio.

Figure 6.15 to Figure 6.17 show snapshots from the time-history response of the simulated full-scale multi-drum columns, for the Athens, Kalamata, and Mexico City earthquakes, respectively.

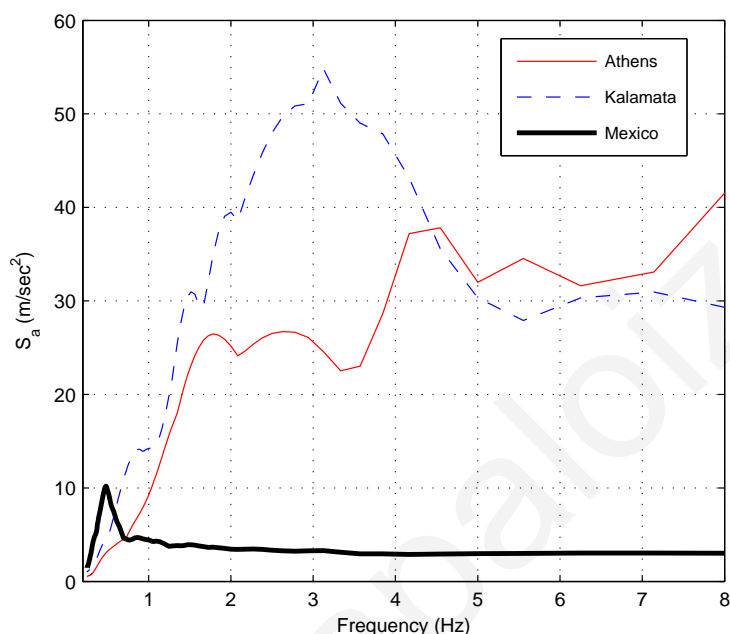


Figure 6.14. Pseudo-acceleration response spectra ($\xi=10\%$) of the scaled earthquake records.

Table 6.1. List of earthquake records that have been used in the analyses.

Record No.	Date and Time	Earthquake Component	PGA (m/sec^2)	Predominant Frequencies (Hz)	Acceleration to overturn (m/sec^2)	Scale Factor
1	9/7/1999 (11:56:50)	ATHENS, Greece (KALLITHEA, N46)	3.01	4.1-8.3	23.4	7.77
2	9/13/1986 (17:24:31)	KALAMATA, Greece (OTE, N10W)	2.67	2.9-3.5	18.7	7.00
3	9/19/1995 (13:19CT)	MEXICO CITY (COMP 270)	0.98	0.45-0.53	2.7	2.76

The simulations indicate that earthquakes with relatively low predominant frequencies need much lower peak ground acceleration to overturn the columns that are considered in our numerical simulations. Conversely, earthquakes with relatively high predominant frequencies, such as the ones that usually occur in regions where many of

these monuments exist such as the eastern Mediterranean region, do not seem to easily endanger the simulated columns.

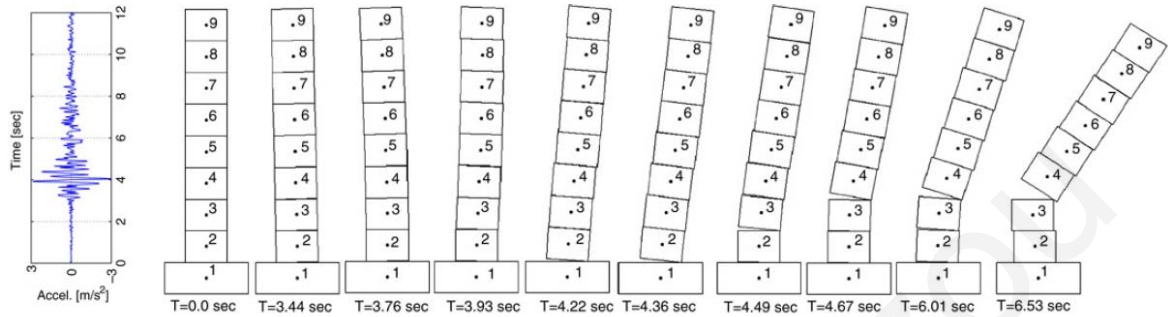


Figure 6.15. Time-history response of a multi-drum column under the Athens Earthquake scaled appropriately to cause collapse.

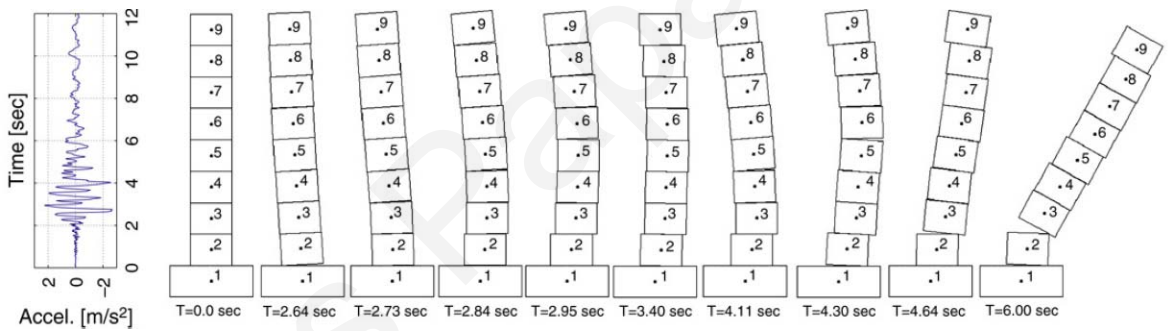


Figure 6.16. Time-history response of a multi-drum column under the Kalamata Earthquake scaled appropriately to cause collapse.

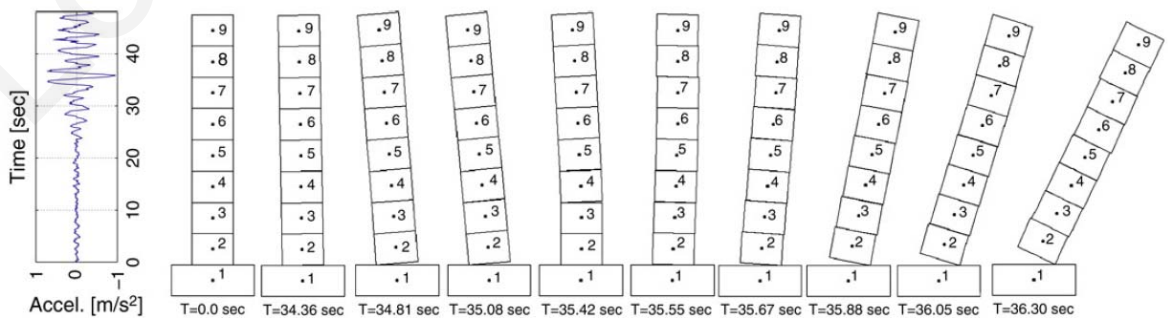


Figure 6.17. Time-history response of a multi-drum column under the Mexico City Earthquake scaled appropriately to cause collapse.

Furthermore, columns with different numbers of drums are examined through numerical analyses that have been performed using the developed software, in order to examine the influence of the frequency content and the peak ground acceleration (PGA) of earthquake excitations. The analyzed columns have a total width of 1 m , a height of 6 m and various combinations of the number of drums of each column. The coefficient of friction that is used for the analyses is set to $\mu = 0.485$. A contact stiffness of the order of 10^8 N/m^2 and a damping coefficient of 10^3 N s/m are used in the simulations.

Several analyses are performed with records scaled to PGAs above those that are needed to cause collapse. The exact PGA that is needed to overturn different arrangements of multi-drum structures is discussed in depth in Paragraph 7.2 of the thesis.

Figure 6.18 to Figure 6.23 show time-history snapshots of the computed responses of multi-drum columns with either one or two drums for the Athens, Kalamata and Mexico City earthquakes, respectively, scaled appropriately to cause failure.

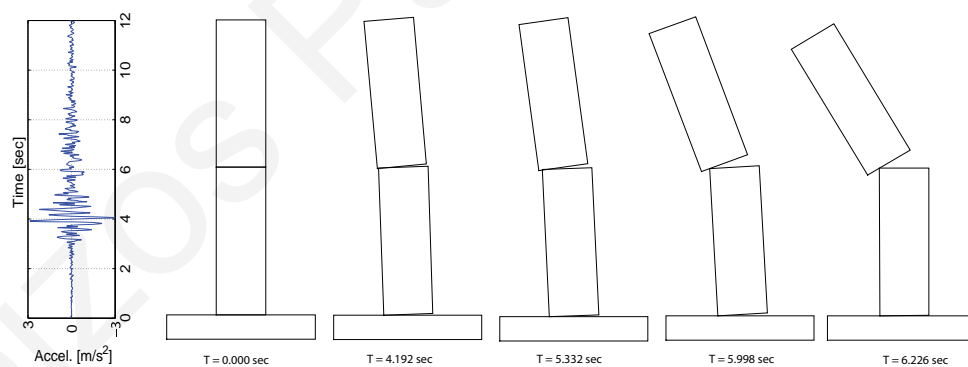


Figure 6.18. Time-history response of a two-drum standalone column under the record from the Athens Earthquake scaled to a PGA of 26.43 m/sec^2 .

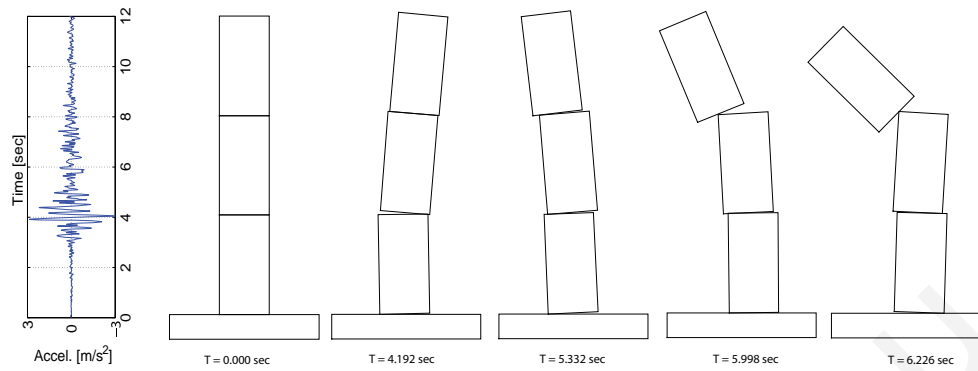


Figure 6.19. Time-history response of a three-drum standalone column under the record from the Athens Earthquake scaled to a PGA of 26.43 m/sec^2 .

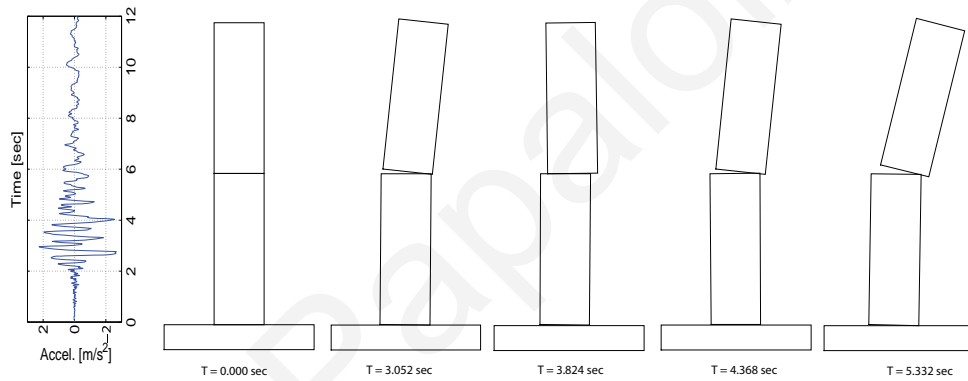


Figure 6.20. Time-history response of a two-drum standalone column under the record from the Kalamata Earthquake scaled to a PGA of 9.35 m/sec^2 .

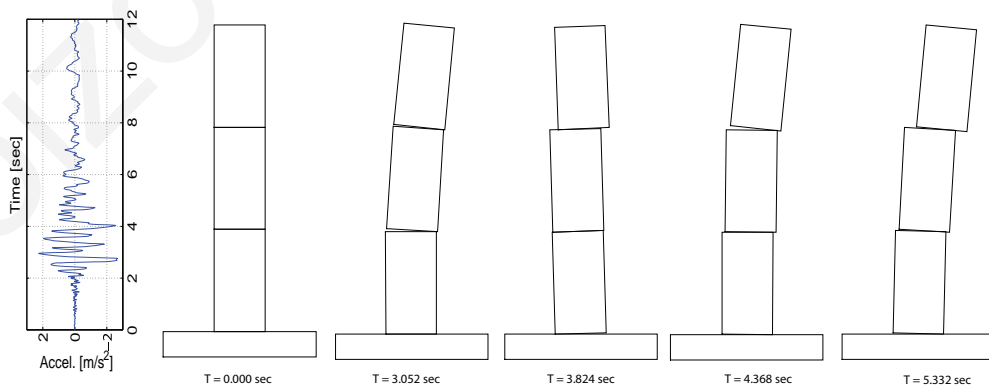


Figure 6.21. Time-history response of a three-drum standalone column under the record from the Kalamata Earthquake scaled to a PGA of 9.35 m/sec^2 .

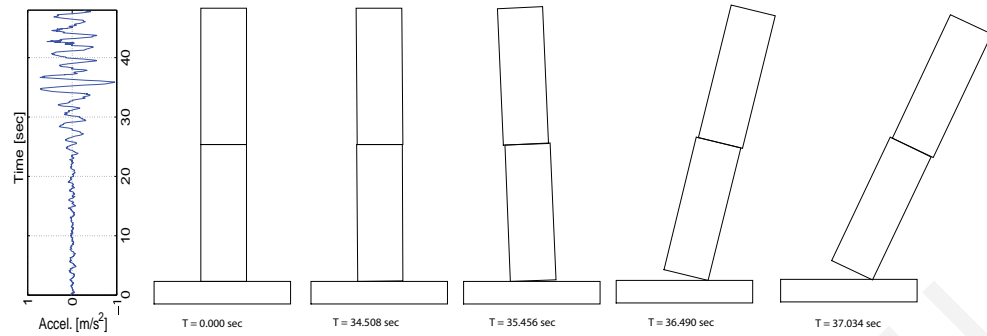


Figure 6.22. Time-history response of a two-drum standalone column under the record from the Mexico City Earthquake scaled to a PGA of 1.47 m/sec^2 .

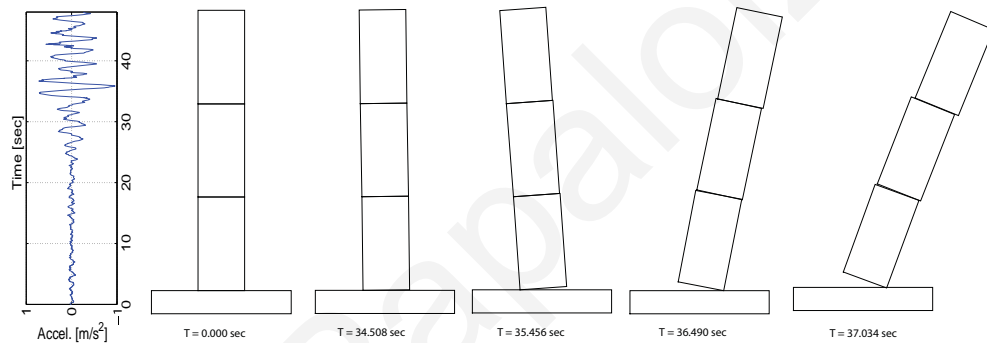


Figure 6.23. Time-history response of a three-drum standalone column under the record from the Mexico City Earthquake scaled to a PGA of 1.47 m/sec^2 .

For the Athens and Kalamata earthquakes, which have high predominant frequencies, the response is very complex, containing both sliding and rocking phenomena. Conversely, for the Mexico City Earthquake, rocking is the dominant response. The number of drums that assemble a column seems to affect the overall response in cases where the response exhibits sliding or both rocking and sliding phenomena. In cases of low predominant frequency earthquakes, like the Mexico City Earthquake, all drums of the column tend to rotate in a single group, with a response similar to that of a monolithic column. It seems that in such cases the energy dissipation mechanism between drums, due to the relative sliding, are not activated to dissipate energy.

Furthermore, the simulations indicate that the Mexico City Earthquake, which has relatively low predominant frequencies, requires much lower acceleration to overturn the column than the Athens Earthquake, which has much higher predominant frequencies.

The PGA that is needed to overturn the simulated columns for earthquakes with low predominant frequencies, like the Mexico City Earthquake, is comparable, as an order of magnitude, to the required acceleration to initiate rocking and overturning of a single rigid body under “static” conditions, given by the following equation:

$$\ddot{u}_{g,cr} = \pm \frac{b}{h} \cdot g = \pm 1.635m / \text{sec}^2 \quad (6.3)$$

Similar responses have been observed for harmonic excitations with frequencies close to the predominant frequencies of the earthquakes. Specifically, the mode of failure of a column under an earthquake excitation seems to be similar with the ones that have been observed under harmonic ground excitations with frequencies similar to the earthquake’s predominant frequencies. For relevantly low earthquake predominant frequencies, mostly rocking occurs (Figure 6.17), where for higher frequencies (Figure 6.15 and Figure 6.16) both rocking and sliding are involved. For earthquakes with low predominant frequencies, such as the Mexico earthquake (Figure 6.17), the column collapses during the first strong cycle of the excitation.

6.5. Different frictional levels between different blocks of the assembly

In order to investigate the effect of different friction levels between different blocks, numerical analyses of various assemblies have been performed. This analysis may be useful in the assessment of proposals for potential seismic isolation of ancient multi-drum columns to protect them, as part of our cultural heritage, from devastating earthquakes. One simple way to change the dynamic characteristics and behaviour of these structures is to change the coefficient of friction at specific interfaces, at the base of the columns, or higher, aiming to improve their seismic response.

Specifically, columns with a height of 6 m consisting of four (Figure 6.24 to Figure 6.27) and eight blocks (Figure 6.28 to Figure 6.31), are analyzed using the developed software. The coefficient of friction between specific surfaces are varied, while, between the rest of the surfaces, the frictional coefficient is set to $\mu=0.48$. Figure 6.24 to Figure 6.31 show the absolute total rotation for all blocks, while varying the coefficient of friction at different levels of the assembly from a smaller value for the coefficient of friction of $n=0.05$ to $n=0.35$. The response of a system for which the coefficient of friction is not varied and equal with $\mu=0.48$ for all of the bodies, is shown with a continuous blue line (marked as 0_0). The numerical analyses are performed with a frequency of 0.5 Hz and amplitude of 0.3 m.

Indicatively, Figure 6.24 provides the absolute total rotation of all blocks for various cases, introducing a coefficient of friction $n=0.05$ at different levels. The plot indicates that having a very low value of a coefficient of friction at the base of the column acts like a sliding isolator system with almost zero total absolute rotation for all drums.

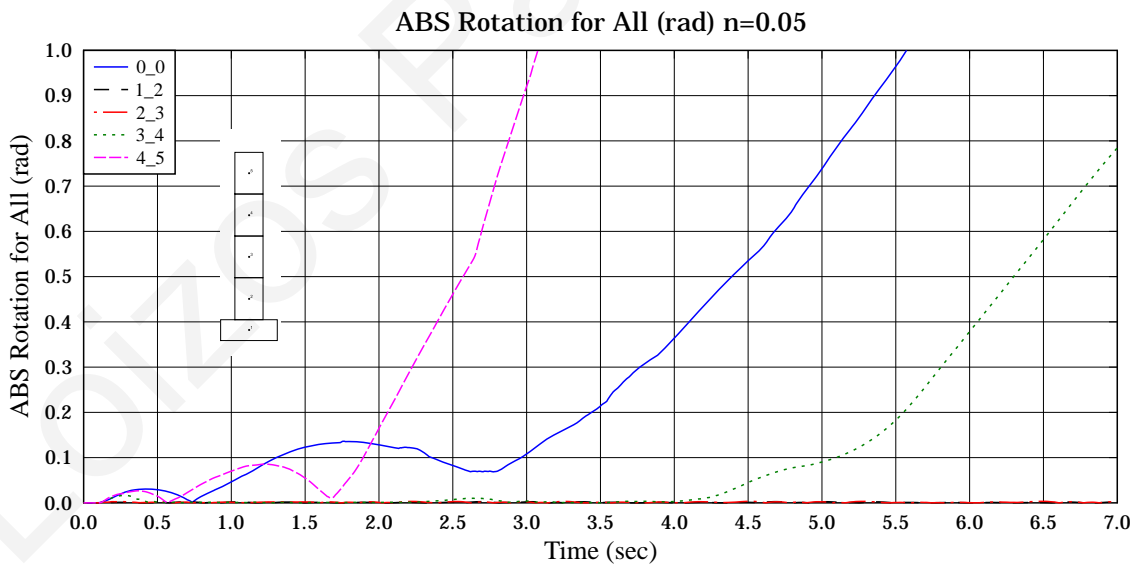


Figure 6.24. Different frictional levels between different blocks for a four block assembly ($n=0.05$).

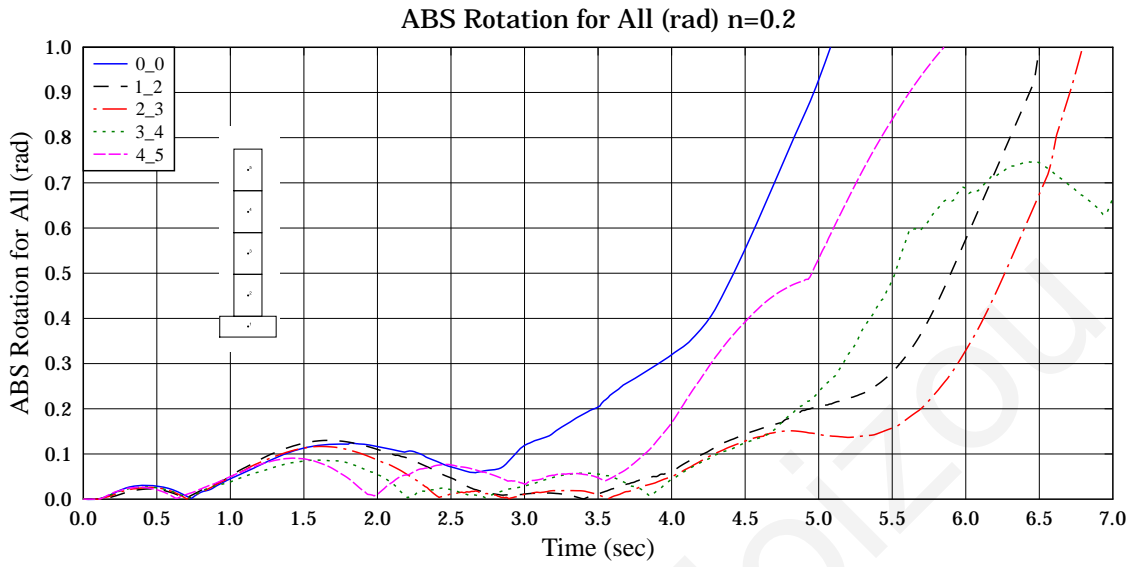


Figure 6.25. Different frictional levels between different blocks for a four block assembly (n=0.2).

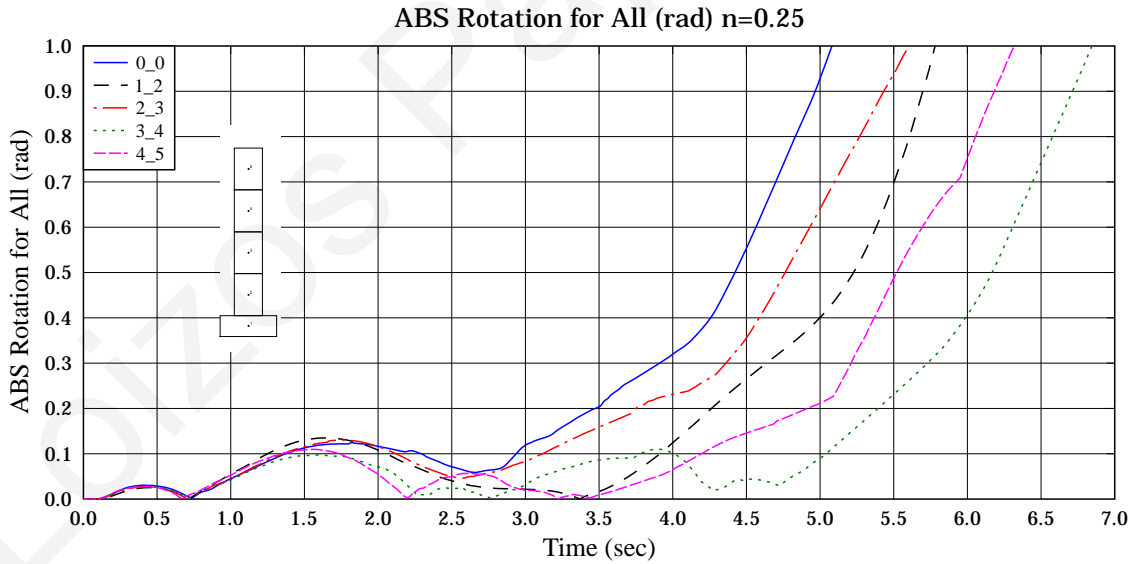


Figure 6.26. Different frictional levels between different blocks for a four block assembly (n=0.25).

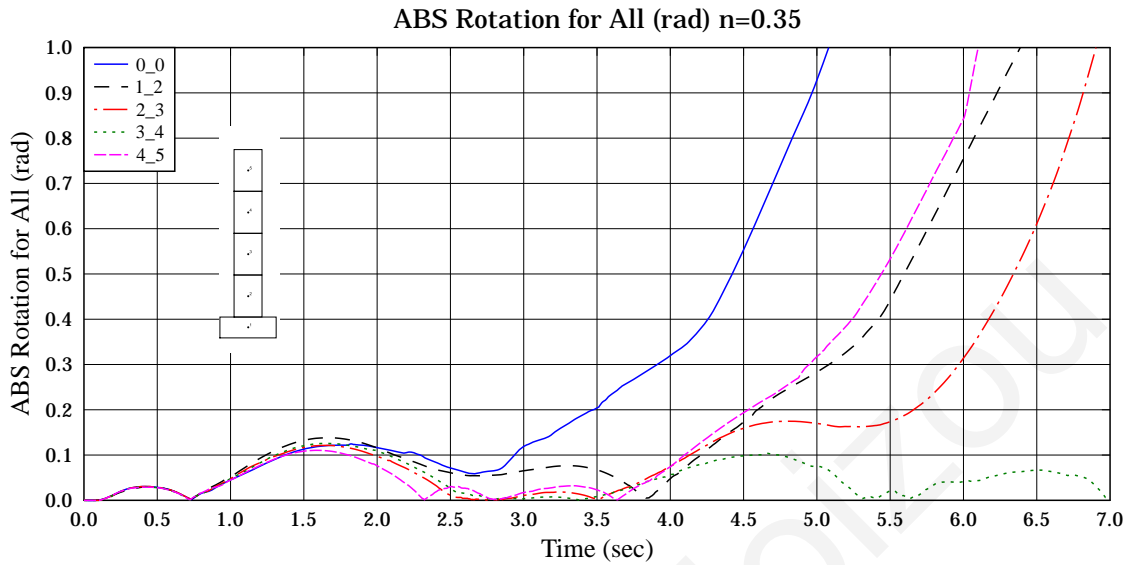


Figure 6.27. Different frictional levels between different blocks for a four block assembly ($n=0.35$).

The results show that the assemblies that are composed of four rigid bodies seem to be more stable when a very small value of the coefficient of friction ($\mu=0.05$) is applied at the base of the structure. Such case resembles seismic isolation based on a sliding mechanism installed at the base of the multi-drum column.

Furthermore, it is observed that for values of the coefficient of friction that are greater than $\mu_l=0.2$ the absolute total rotation of the bodies is reduced compared to the corresponding system with identical friction between all individual blocks (Figure 6.28- Figure 6.31).

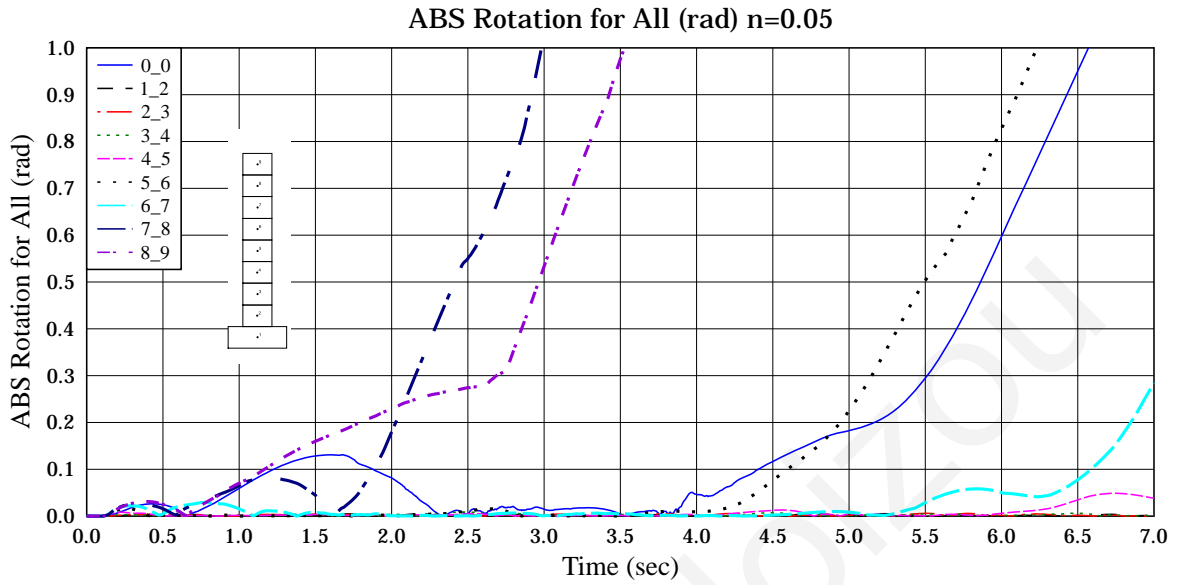


Figure 6.28. Different frictional levels between different blocks for an eight block assembly.

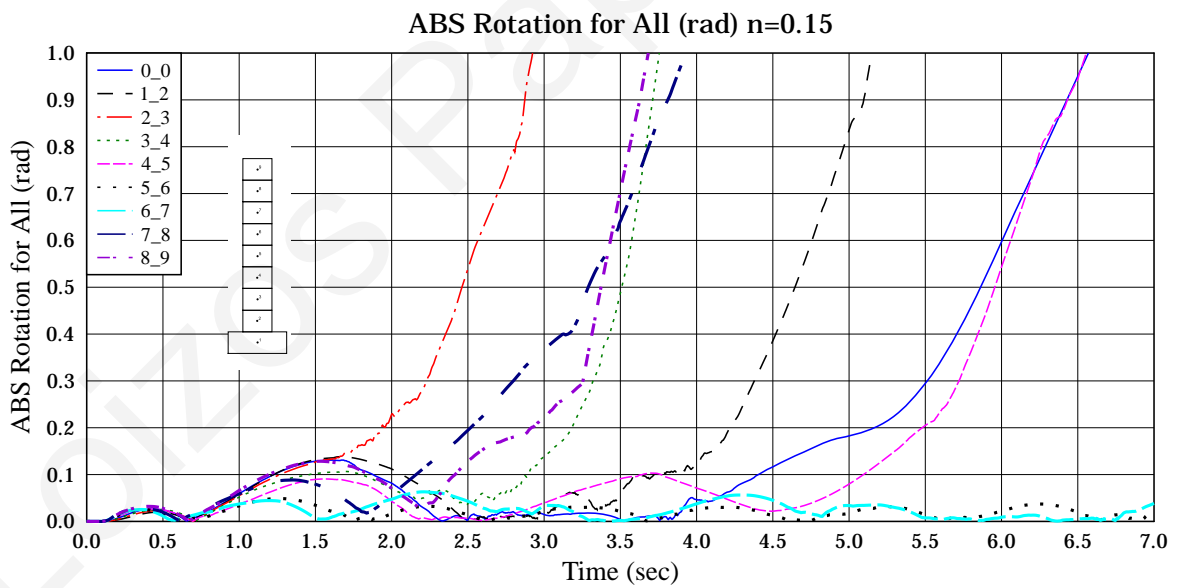


Figure 6.29. Different frictional levels between different blocks for an eight block assembly.

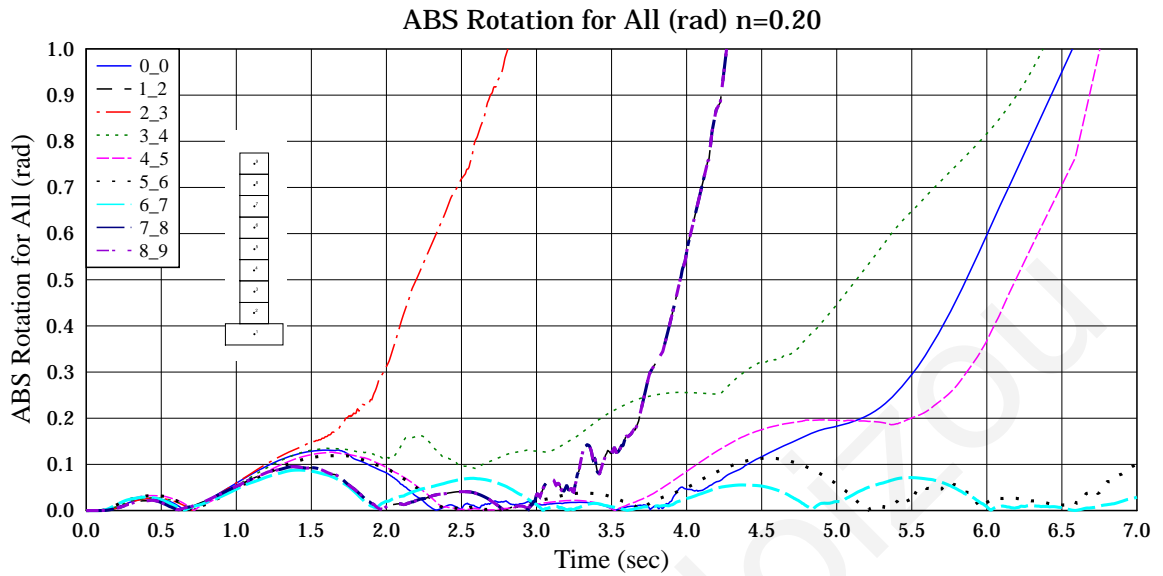


Figure 6.30. Different frictional levels between different blocks for an eight block assembly.

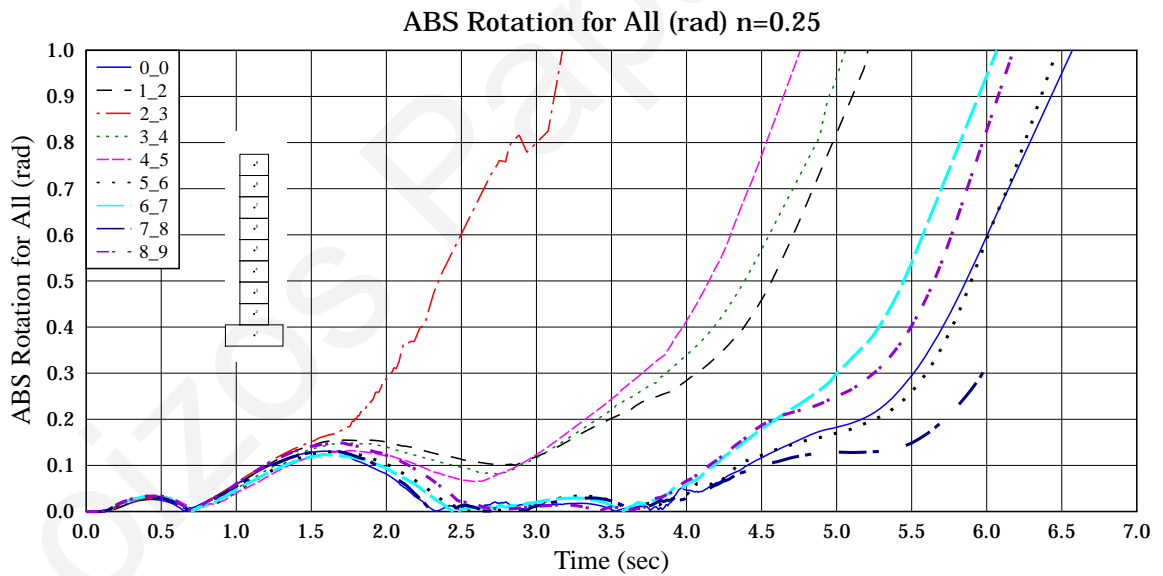


Figure 6.31. Different frictional levels between different blocks for an eight block assembly.

For assemblies with eight rigid blocks, the response that is observed (Figure 6.28 - Figure 6.31) differs from that of the assemblies of four blocks. Similarly to the observations for the four block assemblies, the total absolute rotation of the bodies is minimized when a very small value of the coefficient of friction ($\mu=0.05$) is applied at the base of the structure.

7. Numerical simulation of colonnades with an epistyle

In order to investigate various parameters that may affect the response of multi-drum colonnade systems with epistyles under strong motion excitations, a large number of simulations has been conducted using the developed software application. In the performed simulations several arrangements of colonnades with base width of 1 *m* and total height of 6 *m* have been examined.

Figure 7.1 to Figure 7.6 show snapshots from the computed time-history responses of multi-drum colonnades with epistyles for the Athens, Kalamata and Mexico City earthquakes, scaled appropriately to cause failure to the simulated structures.



Figure 7.1. Time-history response of a colonnade with two drums under an accelerogram from the Athens Earthquake scaled to a PGA of 32.21 m/sec^2 .

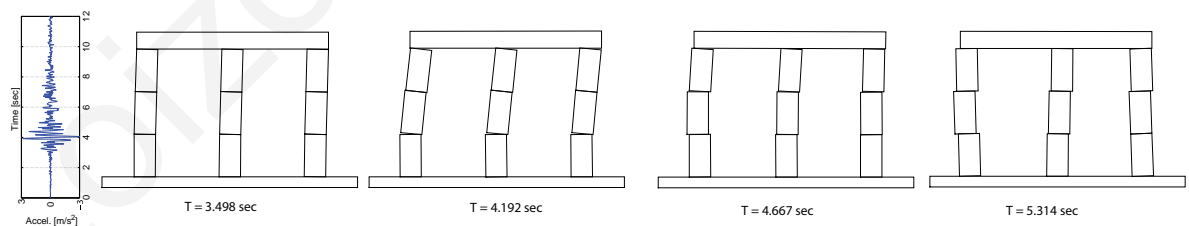


Figure 7.2. Time-history response of a colonnade with three drums under an accelerogram from the Athens Earthquake scaled to a PGA of 32.21 m/sec^2 .

Numerical simulation of colonnades with an epistyle

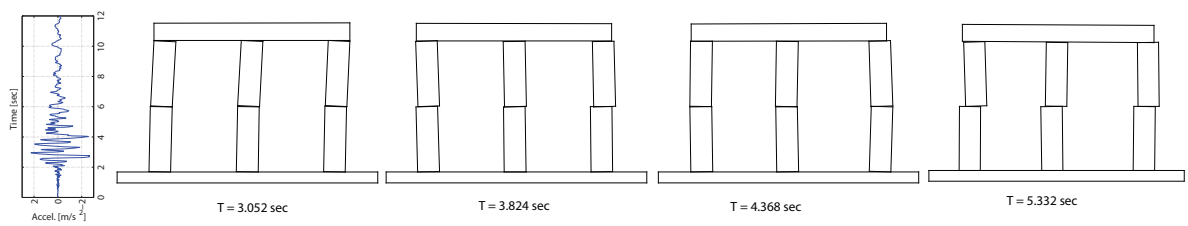


Figure 7.3. Time-history response of a colonnade with two drums under an accelerogram from the Kalamata Earthquake scaled to a PGA of 17.35 m/sec^2 .

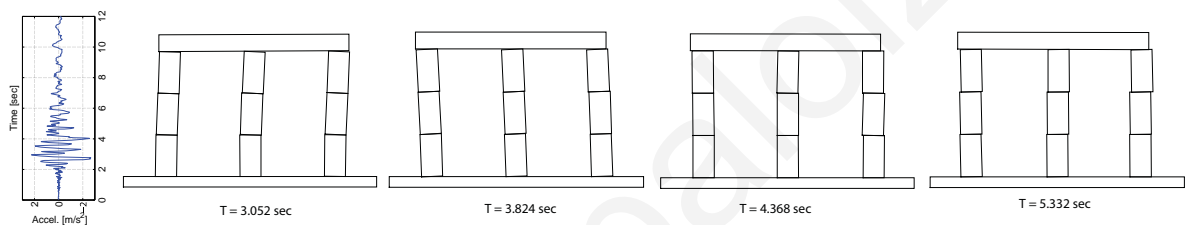


Figure 7.4. Time-history response of a colonnade with three drums under an accelerogram from the Kalamata Earthquake scaled to a PGA of 17.35 m/sec^2 .

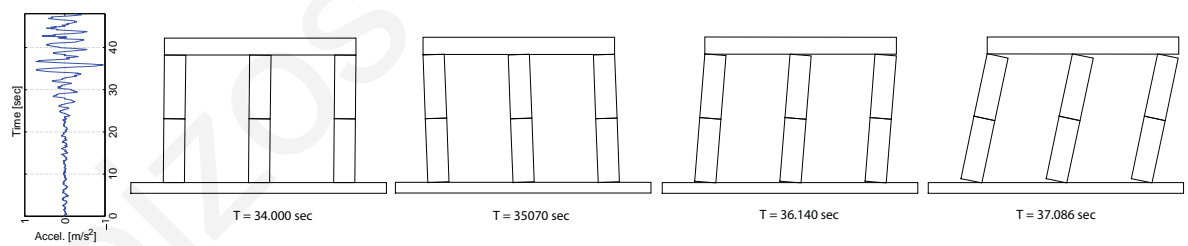


Figure 7.5. Time-history response of a colonnade with two drums under an accelerogram from the Mexico City Earthquake scaled to a PGA of 2.45 m/sec^2 .

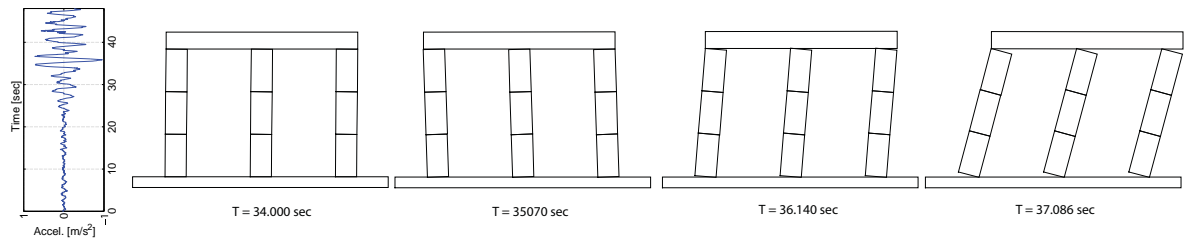


Figure 7.6. Time-history response of a colonnade with three drums under an accelerogram from the Mexico City Earthquake scaled to a PGA of 2.45 m/sec^2 .

The response of multi-drum colonnades with an epistyle exhibits important similarities with the response of standalone multi-drum columns. For earthquakes with higher predominant frequencies, the response contains both sliding and rocking phenomena. For the Mexico City Earthquake, which has lower predominant frequencies, rocking dominates the seismic response. Moreover, earthquakes with relatively low predominant frequencies require lower acceleration to overturn the colonnades than earthquakes with higher predominant frequencies.

As observed in the response of standalone columns, in cases of low predominant frequency earthquakes, like the Mexico City Earthquake, the number of drums that assemble a colonnade does not affect the seismic response of the system, since all of the drums of the columns tend to rotate in a single group, similar to a monolithic column. Therefore no seismic energy is dissipated at the interfaces between each block, since no sliding occurs between adjacent discrete bodies.

Furthermore, the conducted analyses show that colonnade systems with epistyles require higher accelerations to overturn than the corresponding standalone columns with the same dimensions and number of drums.

Figure 7.7 to Figure 7.10, Figure 7.11 to Figure 7.14 and Figure 7.15 to Figure 7.18 provide the time history response of colonnades with various numbers of drums and capitals for the Athens, Kalamata and Mexico City earthquake.

Athens Earthquake

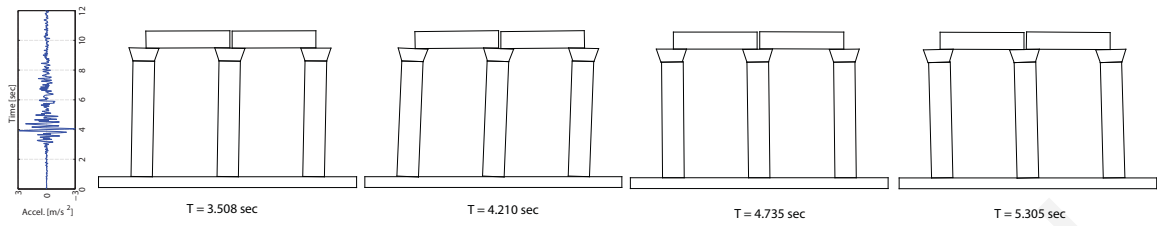


Figure 7.7. Time-history response of a colonnade with each column having one drum and a capital under the Athens Earthquake scaled to a PGA of 32.21 m/sec^2 .

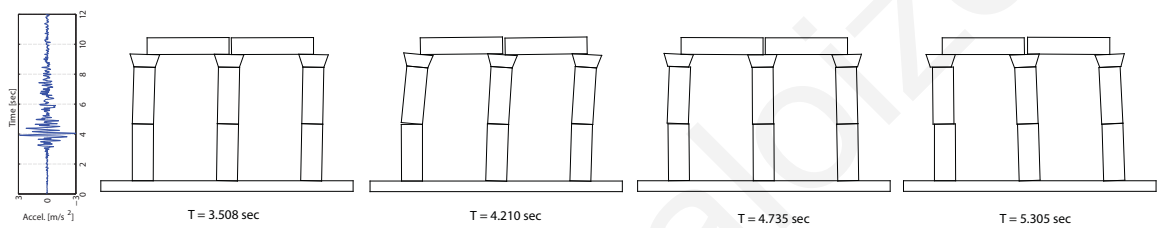


Figure 7.8. Time-history response of a colonnade with each column having two drums and a capital under the Athens Earthquake scaled to a PGA of 32.21 m/sec^2 .

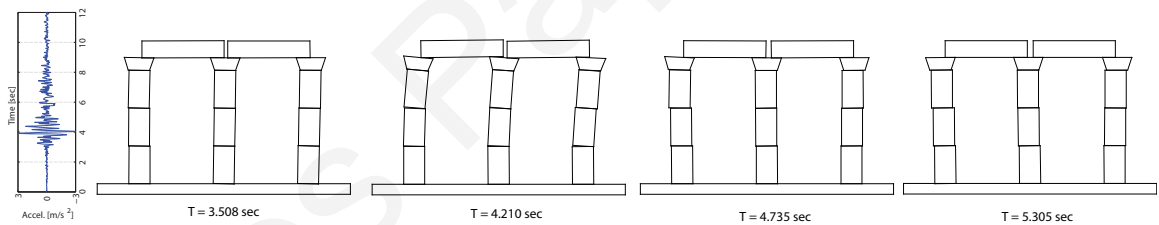


Figure 7.9. Time-history response of a colonnade with each column having three drums and a capital under the Athens Earthquake scaled to a PGA of 32.21 m/sec^2 .

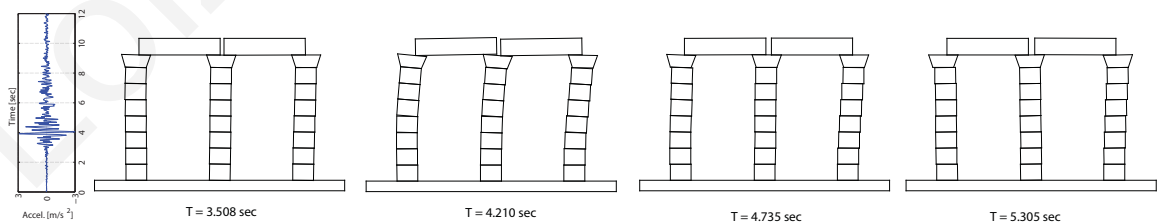


Figure 7.10. Time-history response of a colonnade with each column having seven drums and a capital under the Athens Earthquake scaled to a PGA of 32.21 m/sec^2 .

Kalamata Earthquake

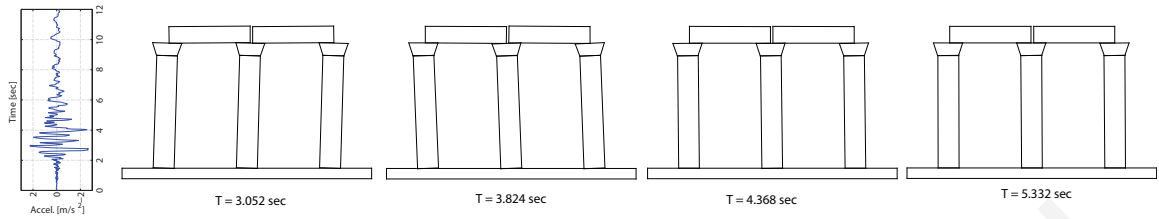


Figure 7.11. Time-history response of a colonnade with each column having one drum and a capital under the Kalamata Earthquake scaled to a PGA of 17.35 m/sec^2 .

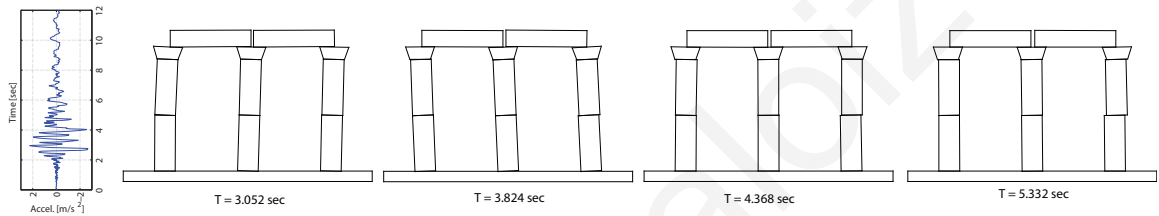


Figure 7.12. Time-history response of a colonnade with each column having two drums and a capital under the Kalamata Earthquake scaled to a PGA of 17.35 m/sec^2 .

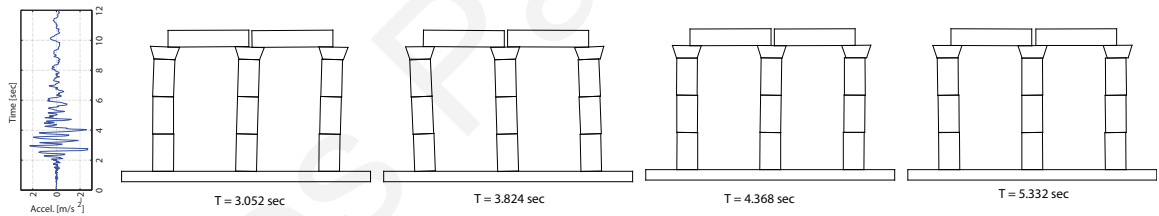


Figure 7.13. Time-history response of a colonnade with each column having three drums and a capital under the Kalamata Earthquake scaled to a PGA of 17.35 m/sec^2 .

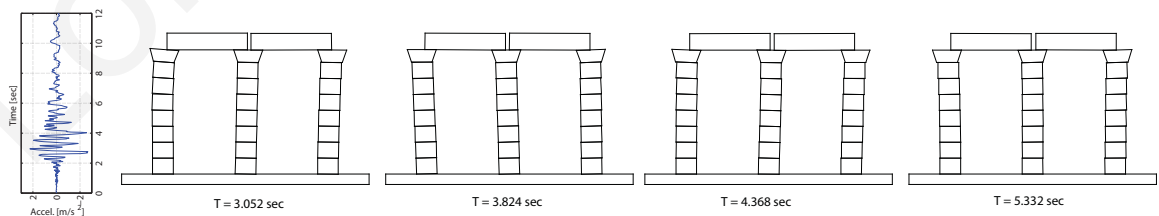


Figure 7.14. Time-history response of a colonnade with each column having seven drums and a capital under the Kalamata Earthquake scaled to a PGA of 17.35 m/sec^2 .

Mexico City Earthquake

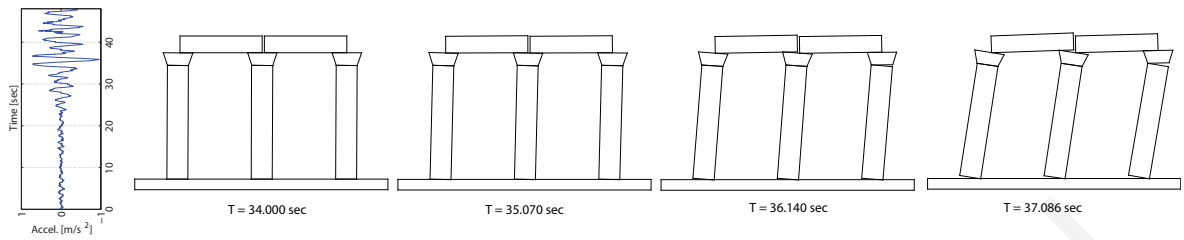


Figure 7.15. Time-history response of a colonnade with each column having one drum and a capital under the Mexico City Earthquake scaled to a PGA of 2.45 m/sec^2 .

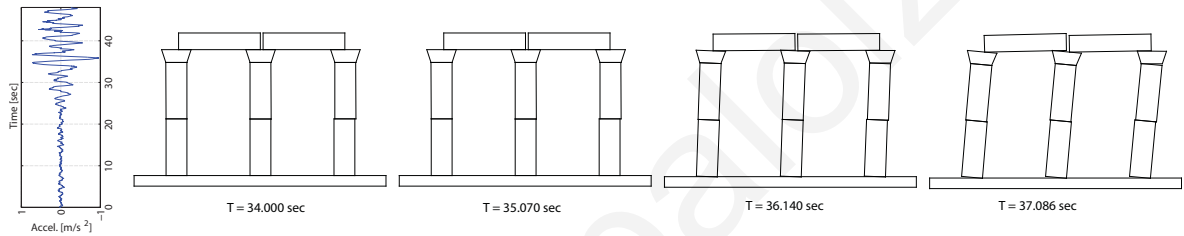


Figure 7.16. Time-history response of a colonnade with each column having two drums and a capital under the Mexico City Earthquake scaled to a PGA of 2.45 m/sec^2 .

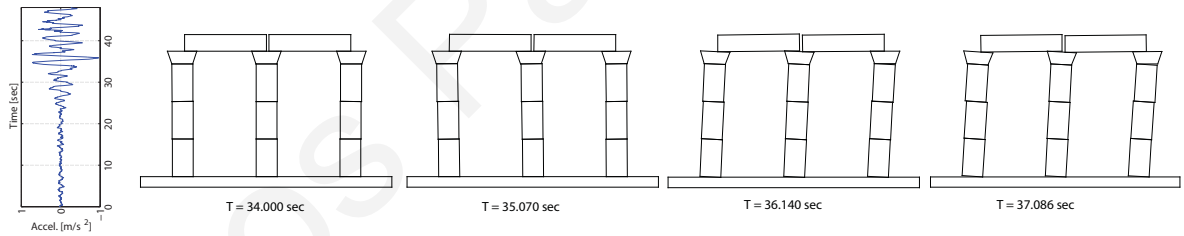


Figure 7.17. Time-history response of a colonnade with each column having three drums and a capital under the Mexico City Earthquake scaled to a PGA of 2.45 m/sec^2 .

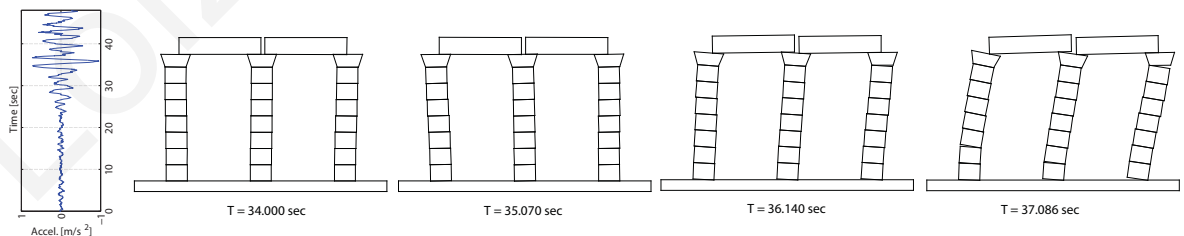


Figure 7.18. Time-history response of a colonnade with each column having seven drums and a capital under the Mexico City Earthquake scaled to a PGA of 2.45 m/sec^2 .

A series of numerical simulations has been performed for colonnades with the same total height (6 m) and width (1 m), but with different numbers of drums. Figure 7.19 to Figure 7.21 show the horizontal displacements of the epistyle for an arrangement of three, four and five colonnades with epistyles. Three different earthquake excitations (Table 1) have been used in each simulation. In most cases, it is observed that, as the number of drums of the columns of a colonnade increases, the maximum displacement of the epistyle is reduced and the stability of the system seems to accordingly increase. Most of the simulation results also reveal that a larger number of columns in a colonnade leads to smaller displacements of the epistyles. These observations, however, are not always the case and cannot be generalized. The response of multi-drum monuments is highly nonlinear and depends on numerous parameters. Therefore, the response of such structures should be studied for the specific characteristics of each structure and for specific earthquake excitations.

Athens Earthquake

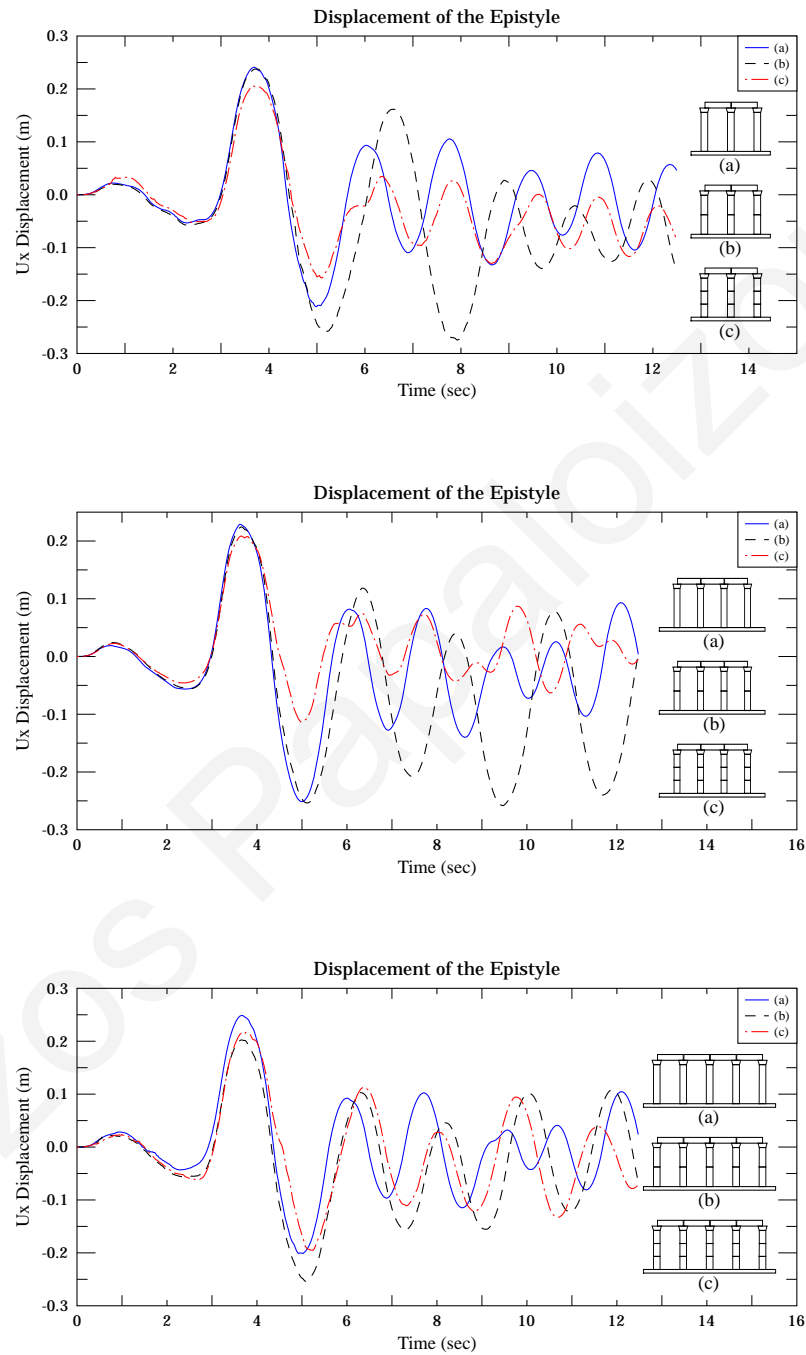


Figure 7.19. Horizontal displacements of the epistyle for different arrangements of multi-drum colonnades under the Athens Earthquake scaled 9.0 times.

Kalamata Earthquake

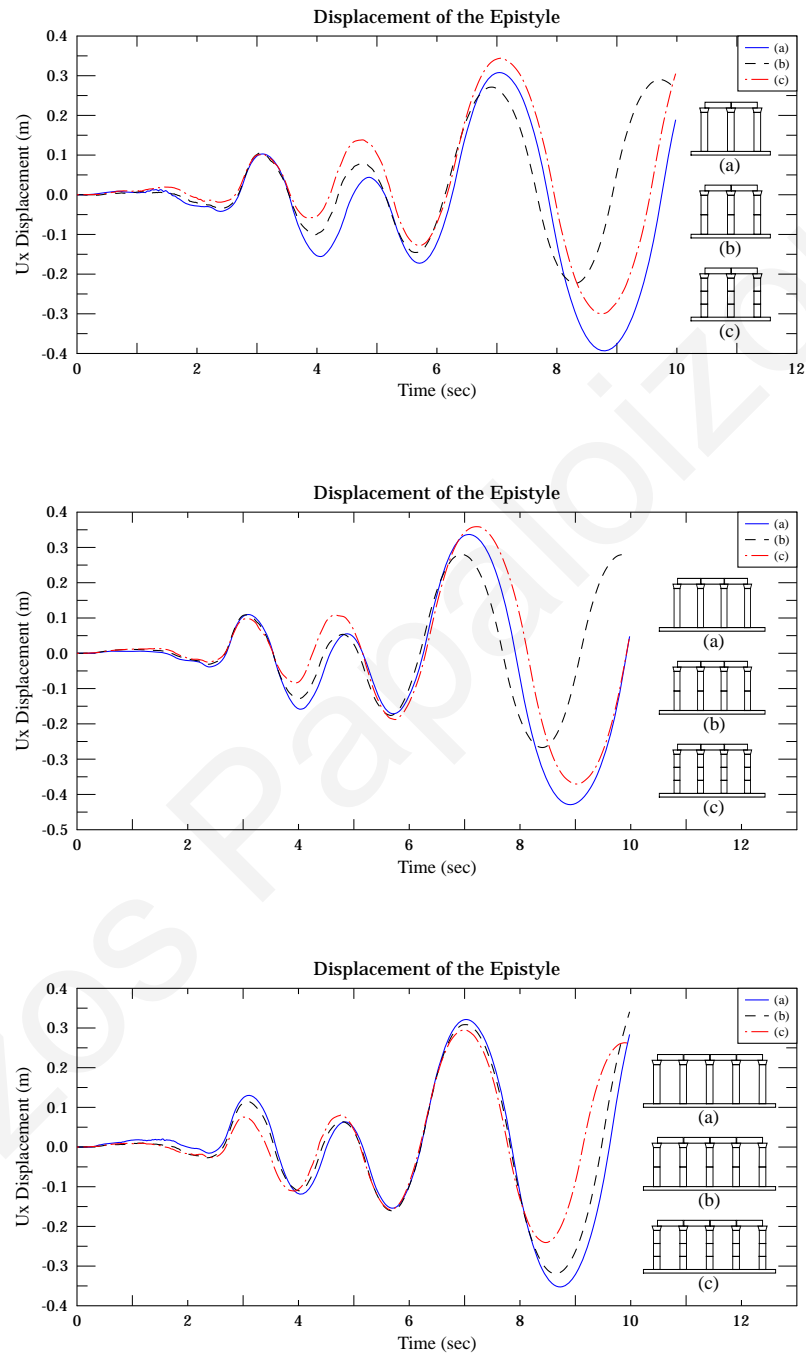


Figure 7.20. Horizontal displacements of the epistyle for different arrangements of multi-drum colonnades under the Kalamata Earthquake 3.5 times.

Mexico City Earthquake

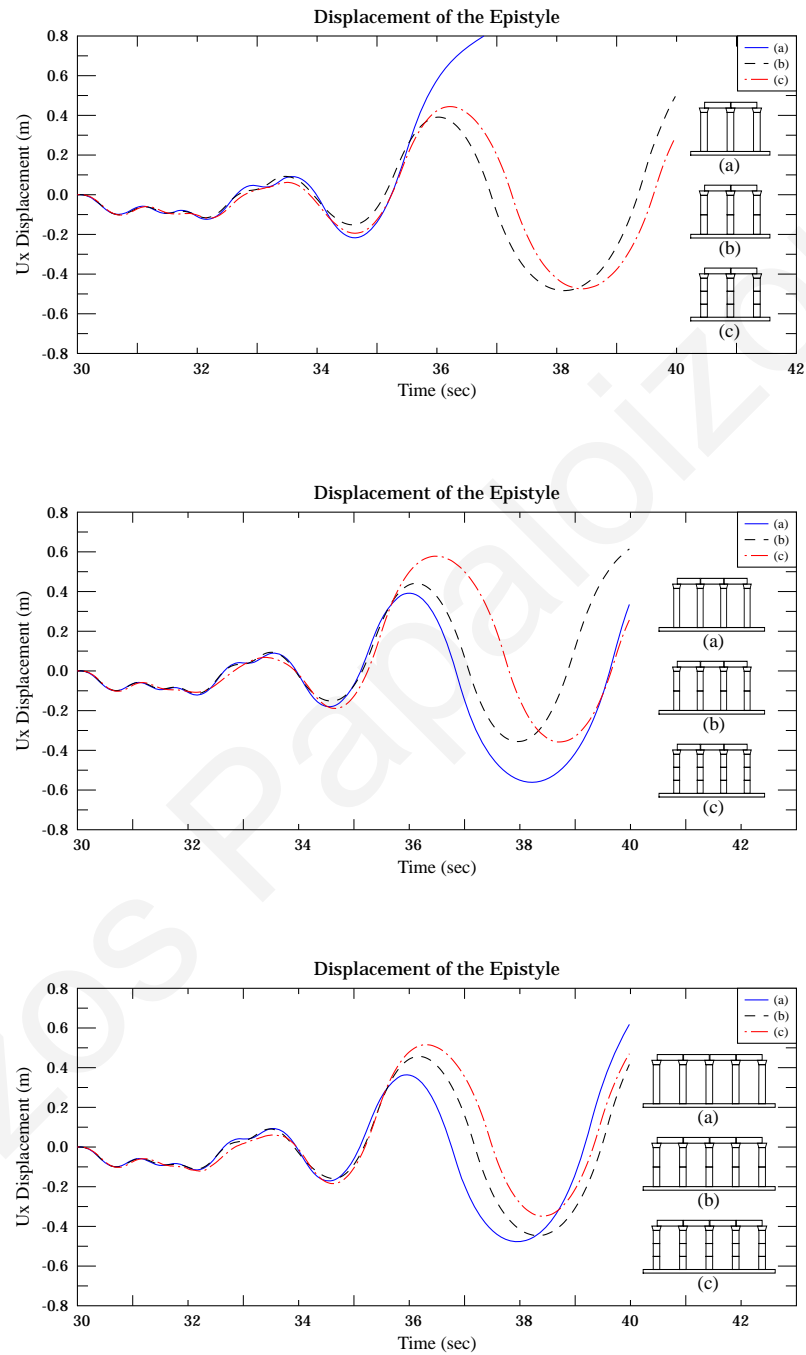


Figure 7.21. Horizontal displacements of the epistyle for different arrangements of multi-drum colonnades under the Mexico City Earthquake scaled 1.4 times.

7.1. Comparison with standalone columns

Figure 7.22 shows the rotation of a standalone column compared to the rotation of a colonnade with an epistyle. Furthermore, the graph shows the rotation of a standalone column having an additional vertical load, applied at its top, equal to the extra load carried by the colonnade with an epistyle.

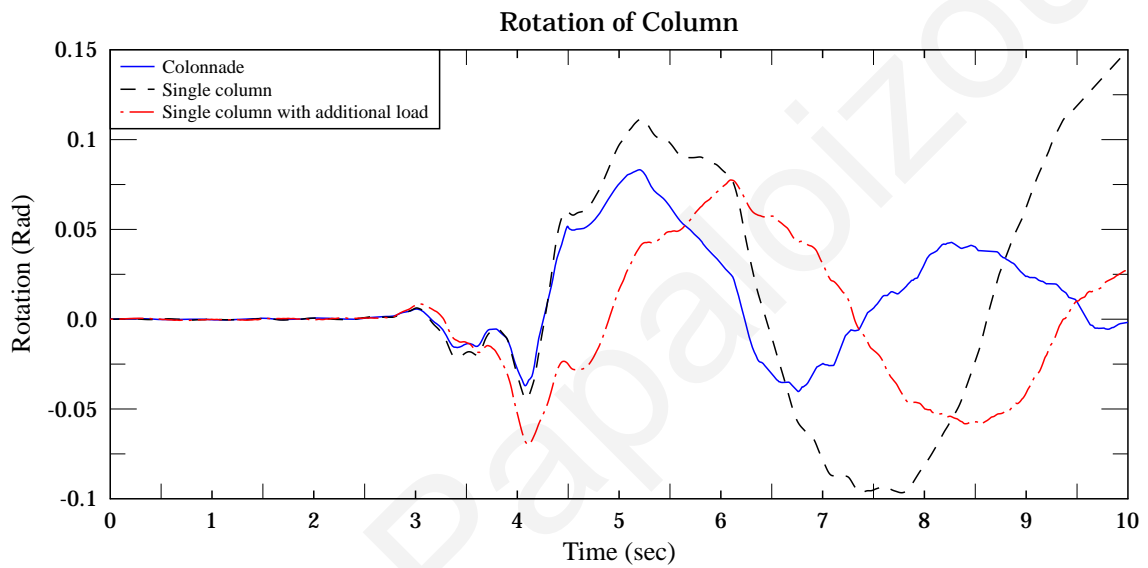


Figure 7.22. Rotation of a standalone column compared to the rotation of a colonnade with an epistyle.

For the selected earthquake excitation, the rotation of a colonnade is less than that of a standalone column with no additional vertical load. Furthermore, it is observed that the standalone column with the additional vertical load, taking into account the loading conditions due to an epistyle, is more stable than the corresponding standalone column without extra load. However, the computed results indicate that the improved stability, due to the additional load, does not exceed the stability of the corresponding colonnade with an epistyle.

7.2. Acceleration required to overturn a system

A number of numerical analyses has been performed in order to investigate the acceleration that is required to overturn a system of colonnades compared to the

acceleration required to cause collapse to the equivalent standalone columns. The standalone columns have been analyzed considering the loading conditions of a colonnade with an epistyle. Figure 7.23 shows the different arrangements that have been simulated, and Table 2 provides the required acceleration to overturn these arrangements for the various earthquake excitations that have been used.

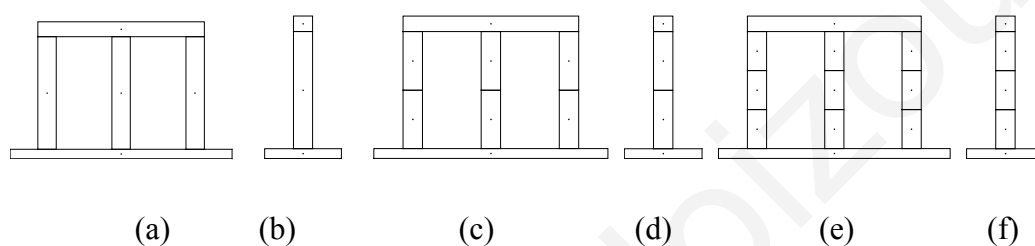


Figure 7.23. Arrangements of the simulated systems.

Table 7.1. Acceleration that is required to cause failure.

(Figure 7.23)	Type of System Analyzed	Acceleration to cause failure (m/sec^2)		
		Mexico City	Kalamata	Athens
a	3 Colonnades (1 drum) with a single epistyle	1.39	16.02	27.69
b	Single Column (1 drum)	1.15	8.94	20.77
c	3 Colonnades (2 drums) with a single epistyle	1.42	16.42	28.60
d	Single Column (2 drums)	1.15	9.01	21.37
e	3 Colonnades (3 drums) with a single epistyle	1.42	17.30	31.91
f	Single Column (3 drum)	1.15	9.28	24.98

As mentioned previously, it has been observed that under the Mexico City Earthquake, which has relatively low predominant frequencies, the mode of failure is characterized by rocking, with all drums of a column tending to rotate together in a single group, as a monolithic column. Therefore, the acceleration that is needed for a single column to overturn does not vary with the number of the drums of the column. In addition, the analyses reveal that for the Athens Earthquake, which has higher predominant frequencies than the Mexico City Earthquake, energy is dissipated through the sliding

effect. Consequently, for the Athens as well as for the Kalamata Earthquake and for colonnades that are constructed with a larger number of drums, the acceleration needed to cause failure is higher.

7.3. Number of drums of columns

A series of numerical simulations has been performed for colonnades with the same total height (6 m) and width (1 m), but with different numbers of drums under the Athens Earthquake scaled to a PGA of 29.09 m/sec^2 . Figure 7.24 shows the horizontal displacement of the epistyle for an arrangement of three colonnades with a single epistyle. It is observed that as the number of drums constructing a colonnade increases, the maximum displacement of the epistyle, as well as the stability of the system, seem to accordingly increase.

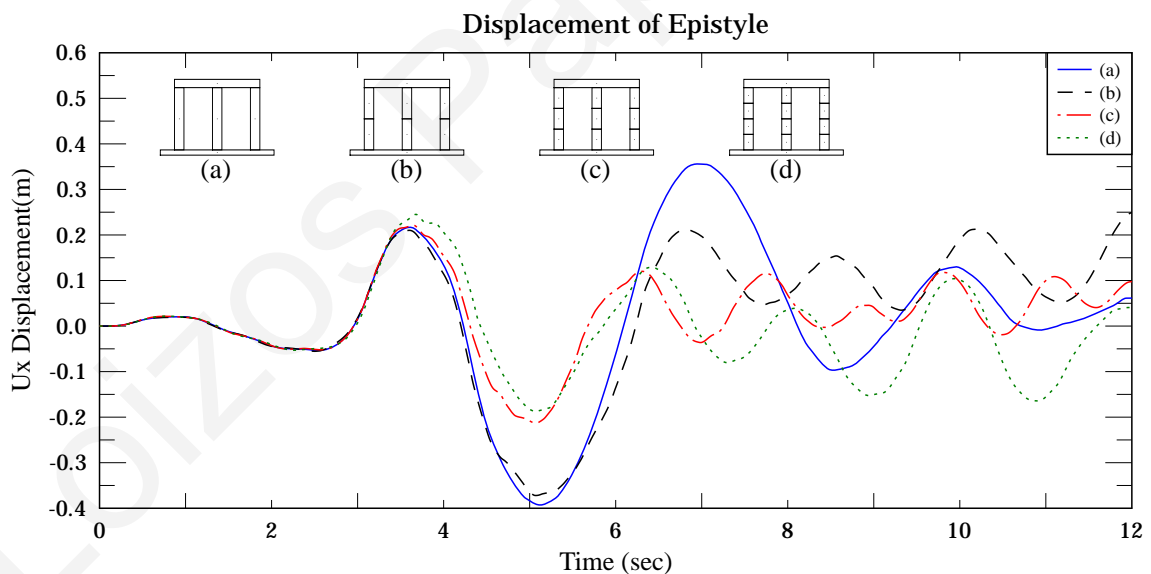


Figure 7.24. Horizontal displacements of the epistyle for an arrangement of three colonnades with a single epistyle with different numbers of drums.

Similarly, Figure 7.25 and Figure 7.26 show the absolute horizontal displacements of the centre of gravity of the epistyle for an arrangement of four and five colonnades, respectively, with a single epistyle. It is observed that, despite the same overall

dimensions, the number and position of the discontinuities between drums, influences significantly the response of the structural system.

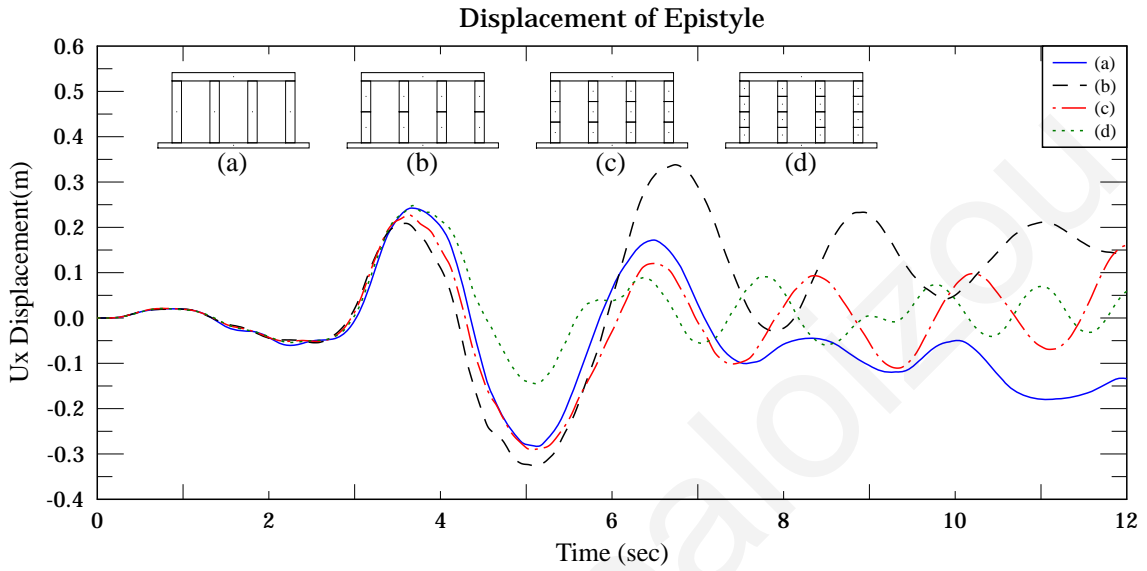


Figure 7.25. Horizontal displacements of an epistyle for an arrangement of four colonnades with a single epistyle with different numbers of drums.

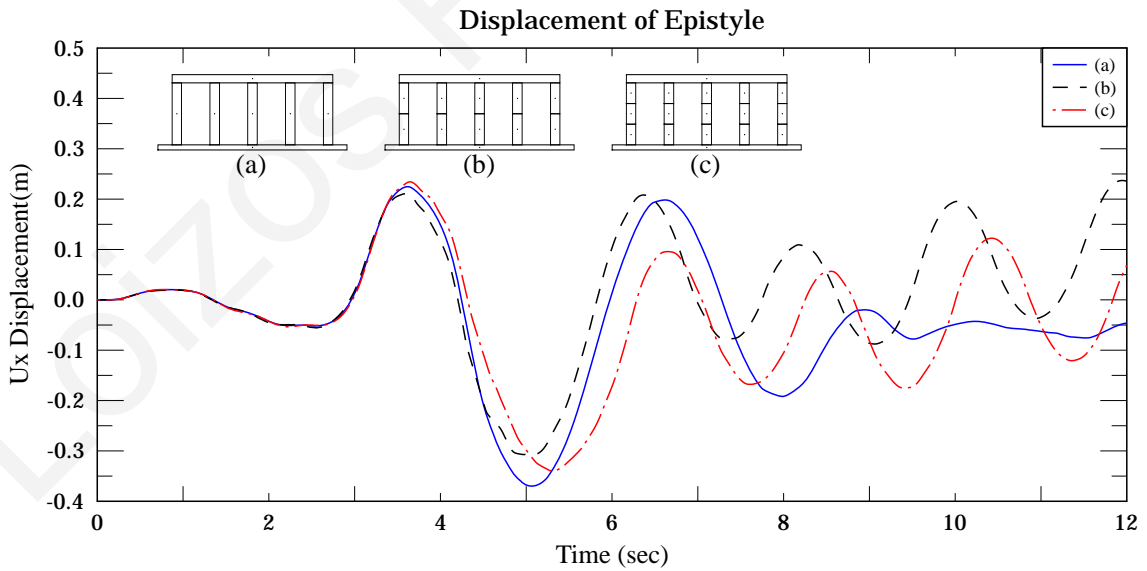


Figure 7.26. Horizontal displacements of an epistyle for an arrangement of five colonnades with a single epistyle with different numbers of drums.

7.4. Number of columns of colonnades

Systems of colonnades with epistyles exhibit different responses under dynamic loadings compared to standalone columns with the same dimensions. The number of columns in a colonnade system has been examined in various analyses. Figure 7.27 and Figure 7.28 show the horizontal displacements of the epistyle for different arrangements of monolithic colonnades with epistyles that are considered to be either multi-body (Figure 7.27) or single body (Figure 7.28). It appears that for colonnades with a single monolithic epistyle (Figure 7.28) a larger number of monolithic columns increases the stability of the overall structural system.

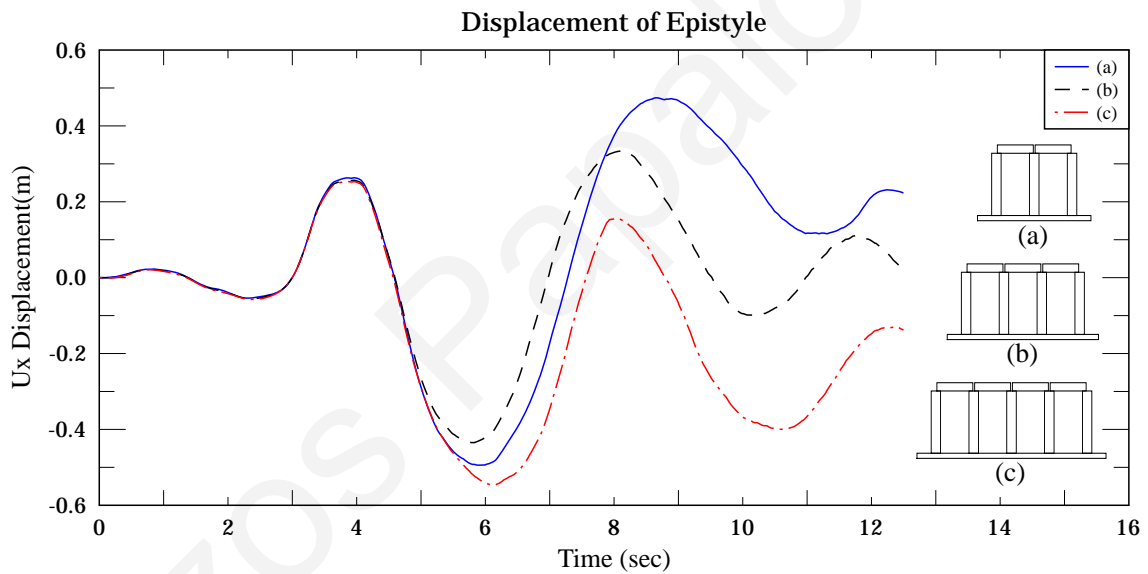


Figure 7.27. Horizontal displacements of the epistyle for different arrangements of monolithic colonnades considering multiple epistyles under the Athens Earthquake, scaled to a PGA of 29.09 m/sec^2 .

Figure 7.29 and Figure 7.30 show the horizontal displacements of the epistyle for different arrangements of multi-drum columns of the colonnades, assembled with two and four drums respectively, and the with monolithic epistyles. The results show that the number of drums can change the response of multi-drum systems with epistyles under earthquake loading.

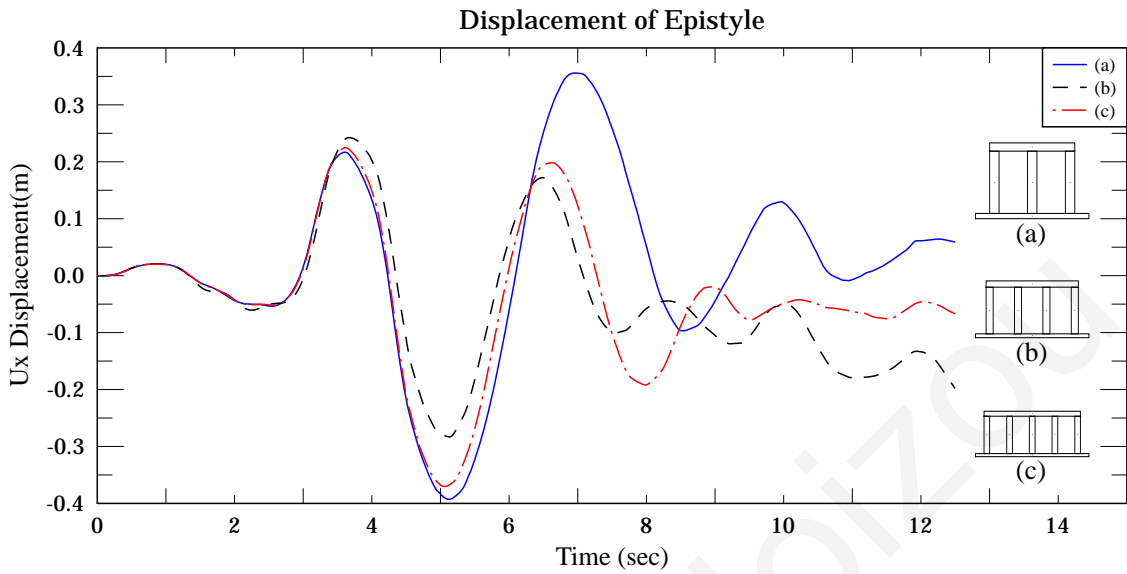


Figure 7.28. Horizontal displacements of the epistyle for different arrangements of monolithic colonnades considering single body epistyles under the Athens Earthquake, scaled to a PGA of 29.09 m/sec^2 .

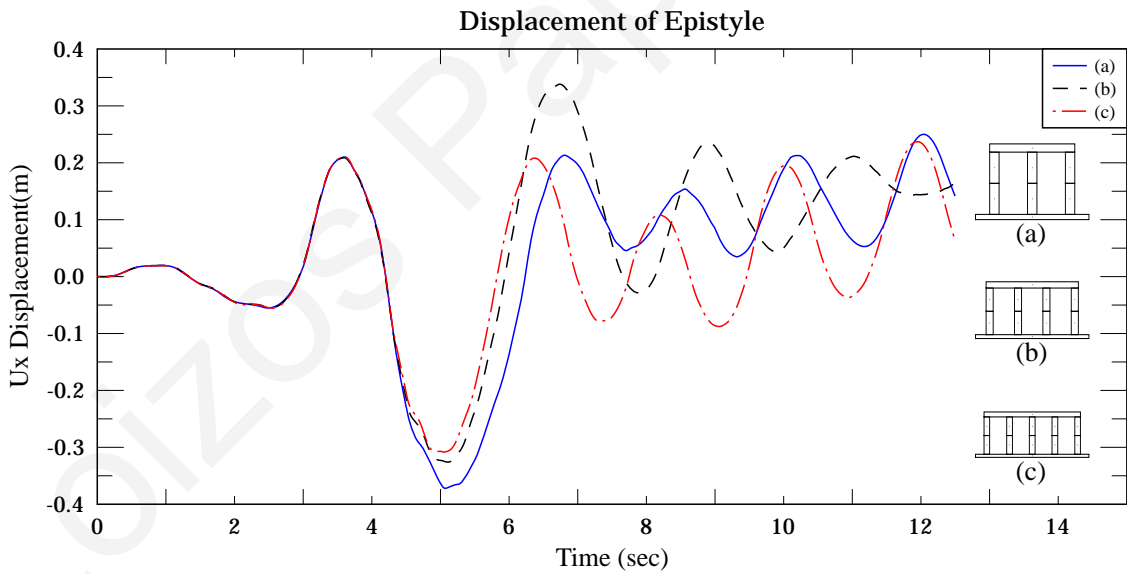


Figure 7.29. Horizontal displacements of the epistyle for different arrangements of two-drum colonnades with monolithic epistyle under the Athens Earthquake, scaled to a PGA of 29.09 m/sec^2 .

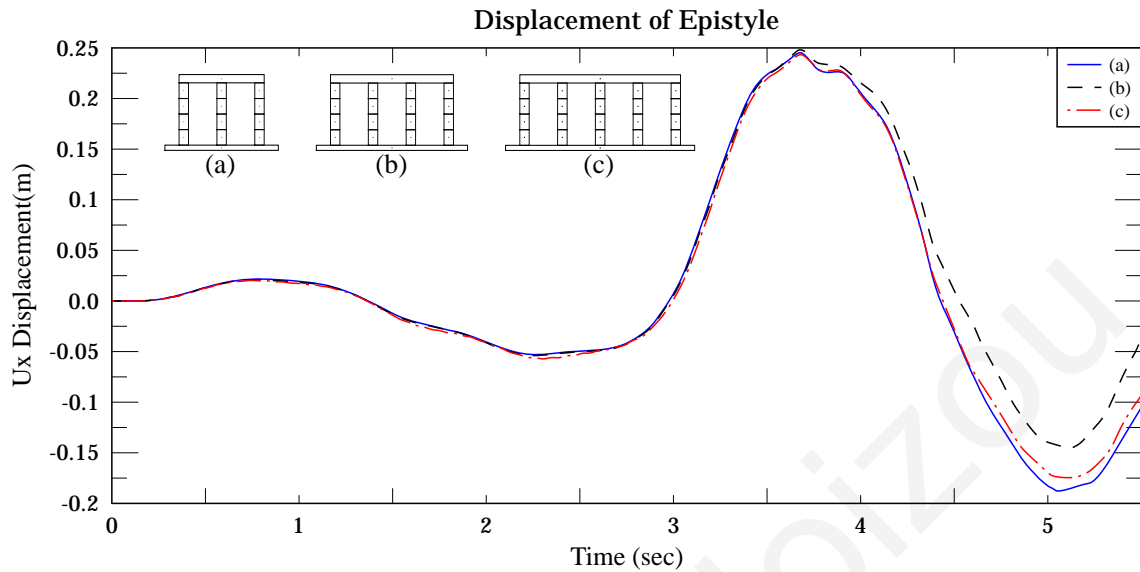


Figure 7.30. Horizontal displacements of the epistyle for different arrangements of four-drum colonnades with monolithic epistyle under the Athens Earthquake, scaled to a PGA of 29.09 m/sec^2 .

7.5. Distance between columns of colonnades

A colonnade system of three monolithic columns and a single epistyle has been parametrically investigated by varying the clear distance between the columns. Figure 7.31 shows the response of the systems under the scaled Athens Earthquake for distances varying between 1.5 m and 4.0 m . The simulation results reveal that the distance between the columns can be a defining parameter to the overall response of the system. As the distance increases, smaller horizontal displacements of the epistyle are observed.

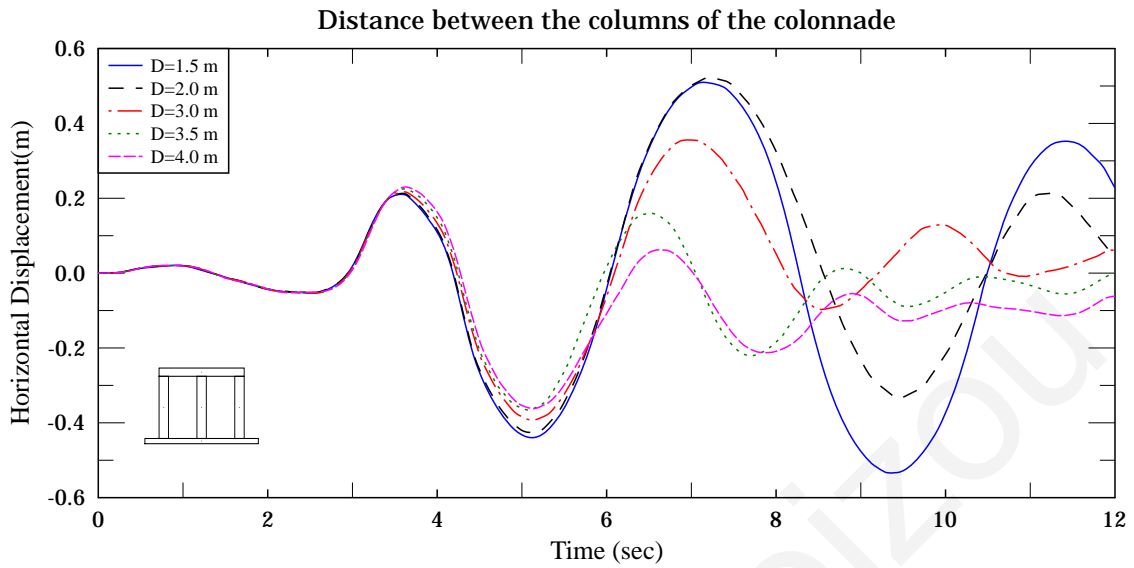


Figure 7.31. Variation of the distance between monolithic columns of colonnades with an epistyle.

In order to examine the contribution of the additional vertical load, the response of a colonnade system with a distance of 2 m between the columns and a mass of an epistyle that corresponds to a colonnade system with columns at a distance of 4 m is shown in Figure 7.32. It seems that the additional vertical load, provided by the wider epistyle, results in smaller displacements than those that are observed with the narrower colonnade.

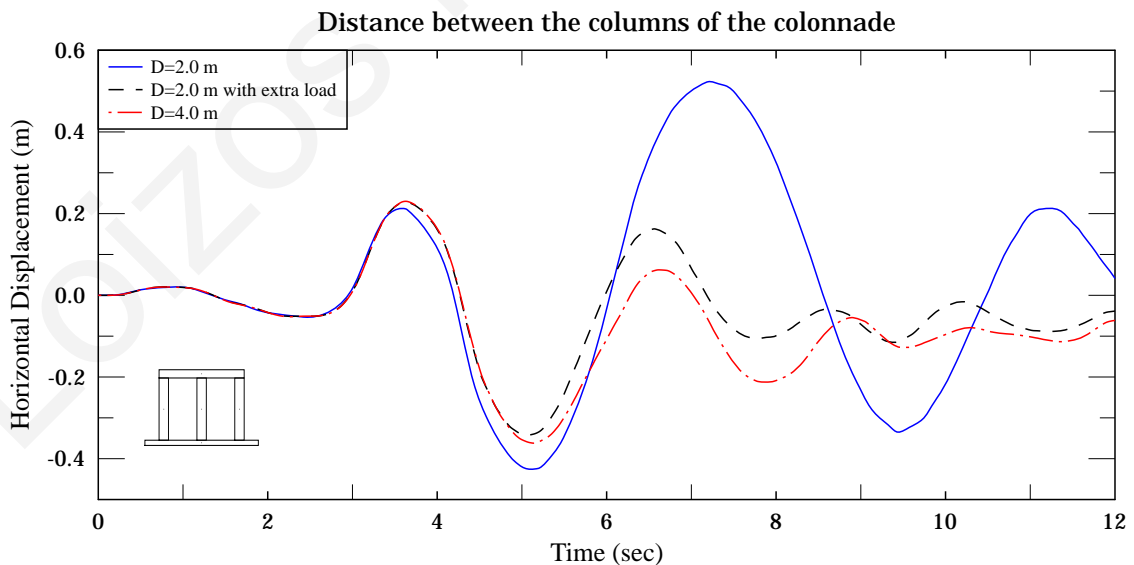


Figure 7.32. Variation of the distance between monolithic columns of colonnades and the load of the epistyle under the Athens Earthquake, scaled to a PGA of 29.09 m/sec^2 .

7.6. Types of epistyles

The type of an epistyle resting on a series of columns may also alter the seismic response of the colonnade system. Four types of epistyles described in Table 7.2 have been analyzed in order to examine their influence in the overall response of the structural systems. Single monolithic epistyles have been examined, considering the possibility of artificially linking epistyles, e.g. through titanium bars, during future rehabilitation or seismic upgrading of such monuments.

Table 7.2. Types of epistyles that have been analyzed.

Type (Figure 7.34)	Description
(a)	Single epistyle extending to the entire width of the external colonnades
(b)	Two epistyles extending to the entire width of the external colonnades
(c)	Single epistyle extending to the centroid of the external colonnades
(d)	Two epistyles extending to the centroid of the external colonnades

Figure 7.33 and Figure 7.34 show the horizontal displacements of the epistyle for different types of epistyles considering three and four columns respectively. The performed simulations indicate that epistyles that extend to the entire width of the external columns have increased stability as compared with corresponding epistyles that extend only to the centre of the columns of the colonnades.

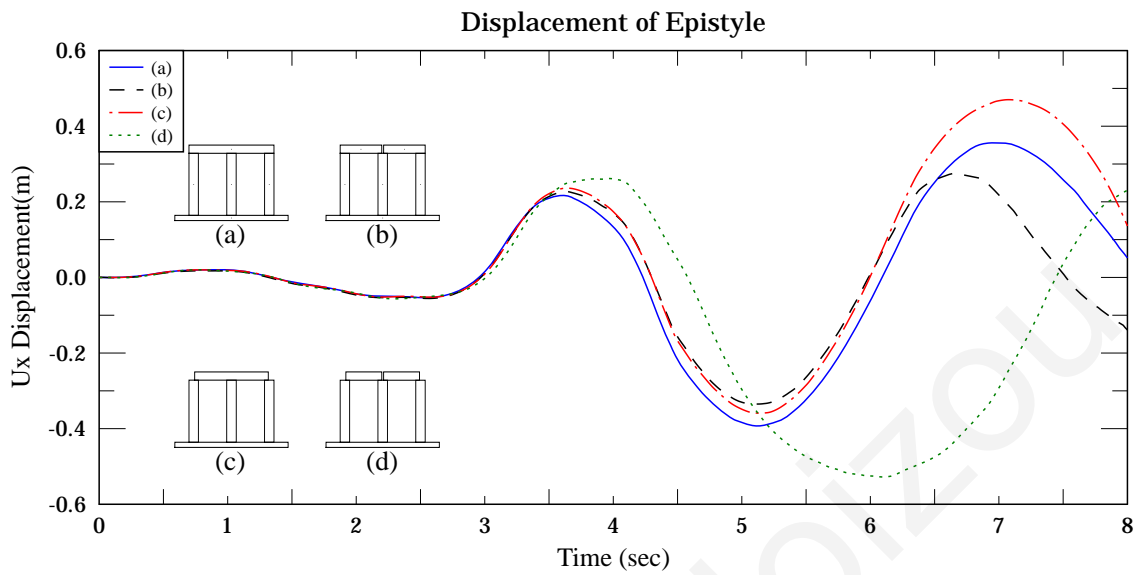


Figure 7.33. The effect of different types of epistyles considering three monolithic columns with various types of epistyles under the Athens Earthquake, scaled to a PGA of 29.09 m/sec^2 .

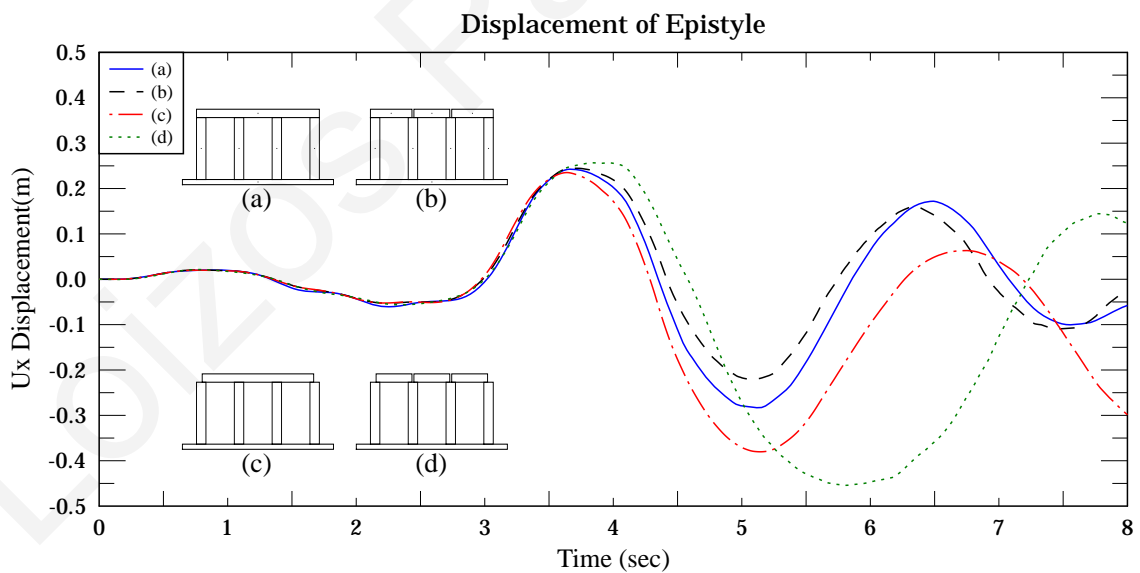


Figure 7.34. The effect of different types of epistyles considering four monolithic columns with various types of epistyles under the Athens Earthquake, scaled to a PGA of 29.09 m/sec^2 .

7.7. Epistyle mass

Ancient classical columns and colonnades were originally designed to carry the weight of the entablature, which is composed of two parts, the epistyle (architrave) and the frieze in the long sides, plus the tympanon on the short sides (Figure 1.3).

Today, the loading condition of the remains of these monuments has changed significantly mainly due to missing parts of the frieze. The addition of mass to these systems can alter the response to earthquake excitations of their bases. Numerical analyses have been conducted in order to examine the behaviour of colonnades with an epistyle under different loading conditions.

Figure 7.35 to Figure 7.40 show the horizontal displacements of the epistyle under the Athens Earthquake for three, four and five columns in a row respectively, constructed of one and two drums, for different epistyle masses (EM). The density of an epistyle is varied between 5000 Kg/m^3 to 10000 Kg/m^3 .

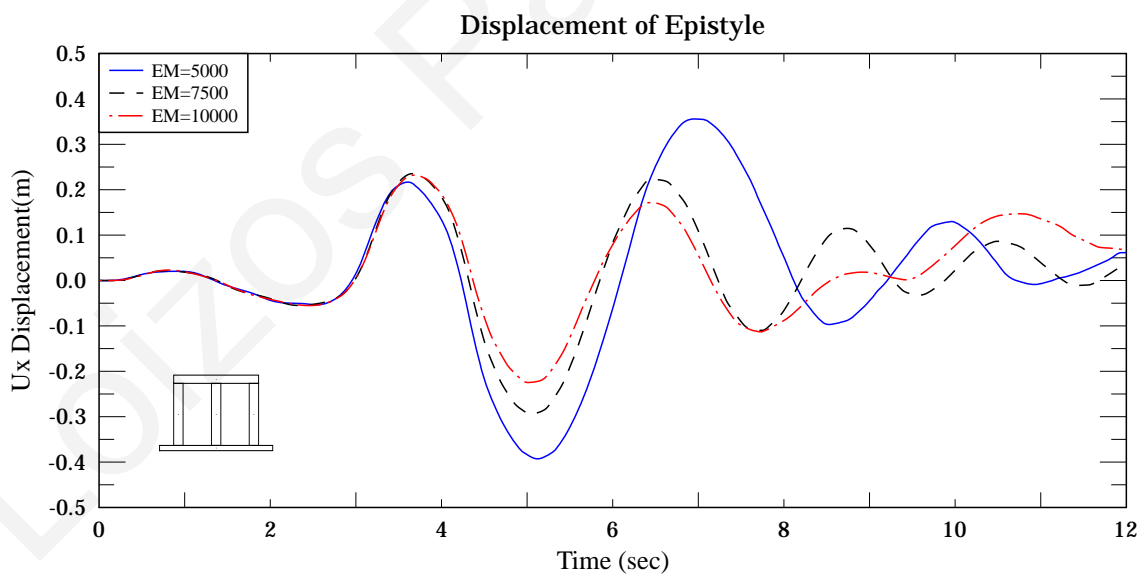


Figure 7.35. Effect of the epistyle mass for a colonnade system with three monolithic columns and a single epistyle under the Athens Earthquake, scaled to a PGA of 29.09 m/sec^2 .

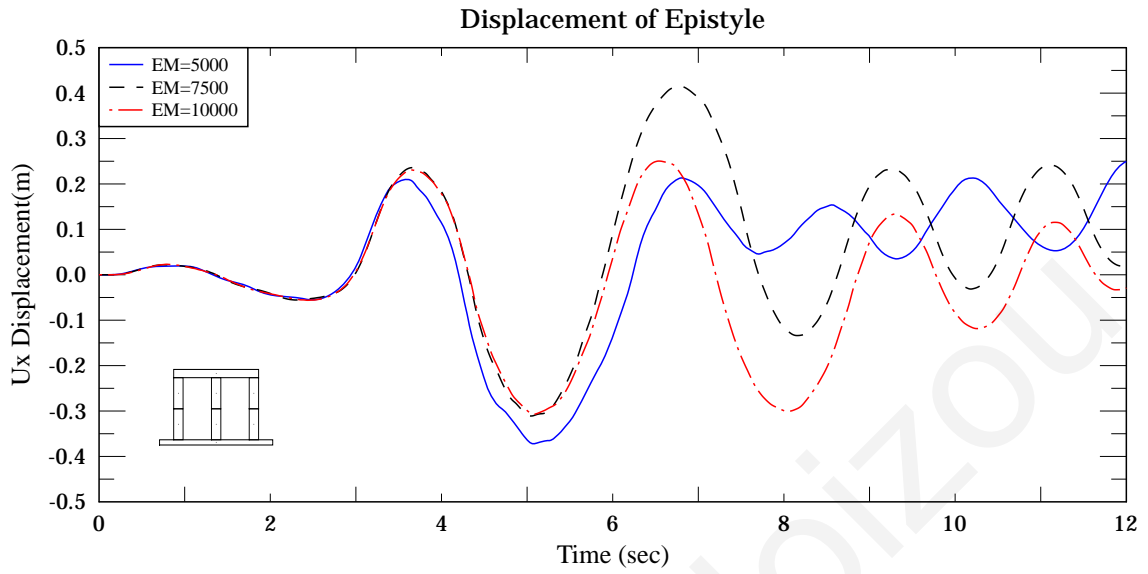


Figure 7.36. Effect of the epistyle mass for a colonnade system with three (two drum) columns and a single epistyle under the Athens Earthquake, scaled to a PGA of 29.09 m/sec^2 .

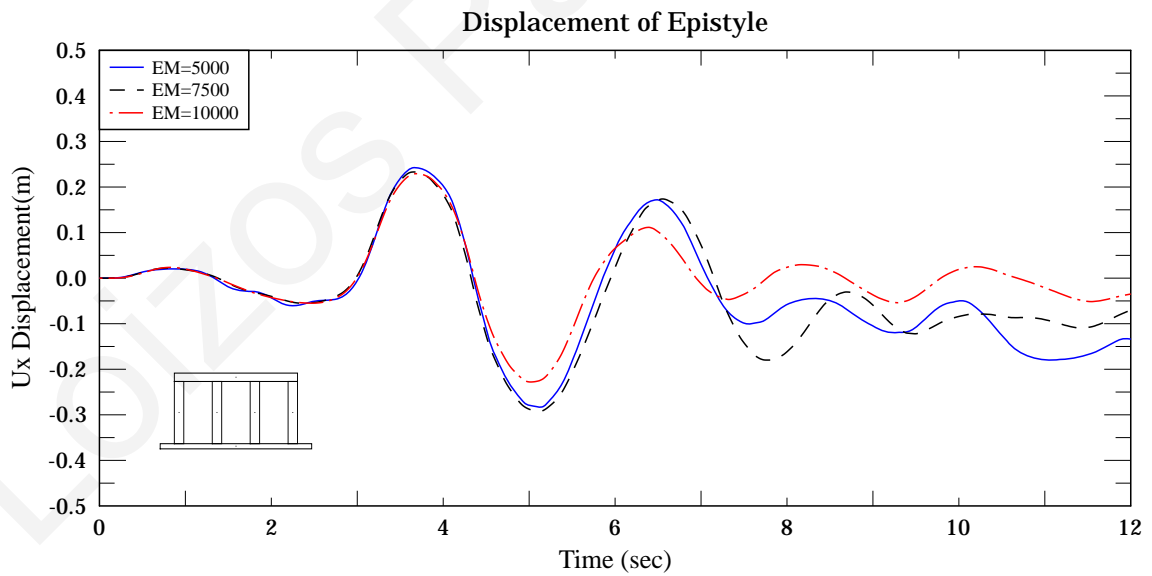


Figure 7.37. Effect of the epistyle mass for a colonnade system with four monolithic columns and a single epistyle under the Athens Earthquake, scaled to a PGA of 29.09 m/sec^2 .

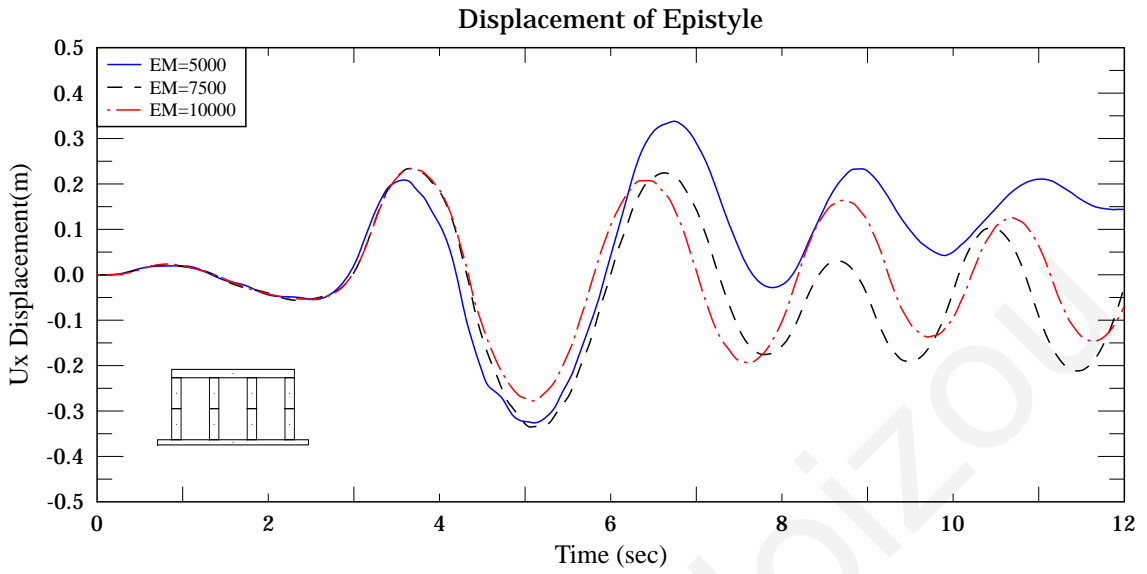


Figure 7.38. Effect of the epistyle mass for a colonnade system with four (two drum) columns and a single epistyle under the Athens Earthquake, scaled to a PGA of 29.09 m/sec^2 .

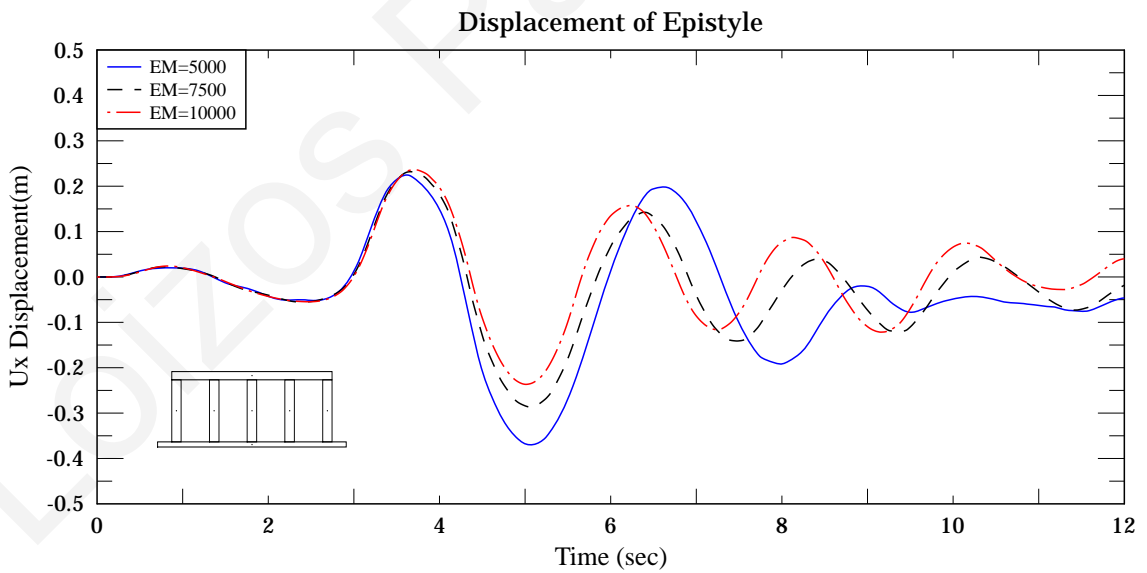


Figure 7.39. Effect of the epistyle mass for a colonnade system with five monolithic columns and a single epistyle under the Athens Earthquake, scaled to a PGA of 29.09 m/sec^2 .

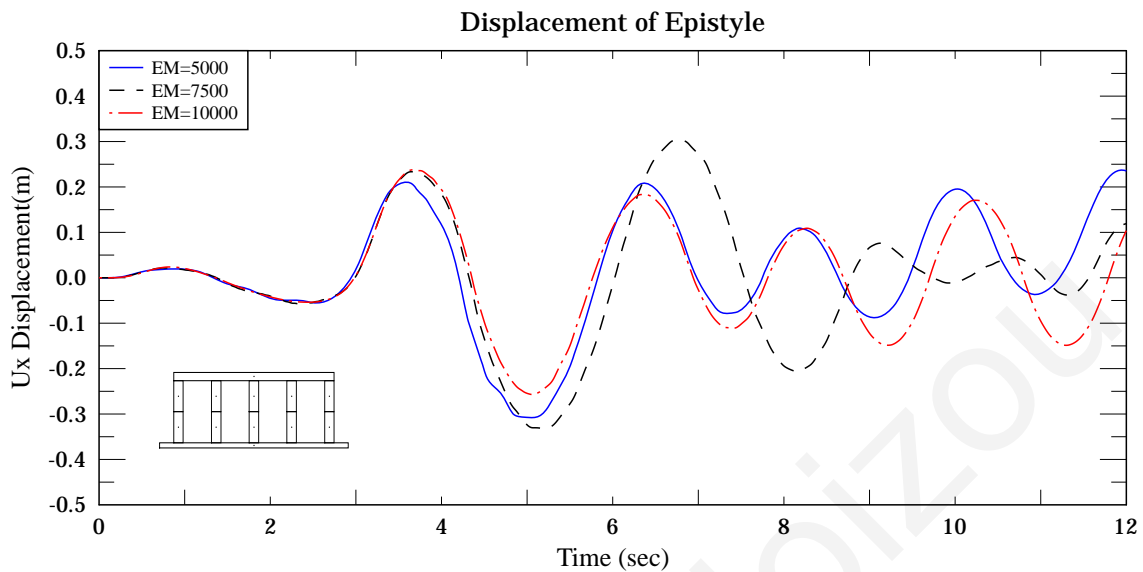


Figure 7.40. Effect of the epistyle mass for a colonnade system with five (two drum) columns and a single epistyle under the Athens Earthquake, scaled to a PGA of 29.09 m/sec^2 .

The analyses show that the increase of the mass of the epistyle, which is closer to the original design loading condition, causes a reduction of the maximum horizontal displacement of the epistyle.

7.8. Tapered shape colonnades with an epistyle

In order to investigate the effect of the shape of the colonnades with an epistyle, various simulations have been performed on a set of tapered columns. Three columns with different ratios of the base width, W_b , to the corresponding top width, W_t , have been analyzed, keeping the total mass of the column constant and equal to the mass of a non-tapered column, with base width of 1 m and total height of 6 m (Figure 7.41).

The numerical simulations indicate that for colonnades with monolithic columns, the tapered columns reduce the maximum horizontal displacement of the epistyle, therefore increasing the stability corresponding to non-tapered columns (Figure 7.41).

Figure 7.42 to Figure 7.49 show the effect of tapered colonnades in different arrangements, epistyle masses and number of drums of the colonnades. The numerical simulations again show that the increase of the epistyle's mass, both for monolithic and for multi-drum colonnades, decreases the maximum horizontal displacement of the epistyle (Figure 7.43).

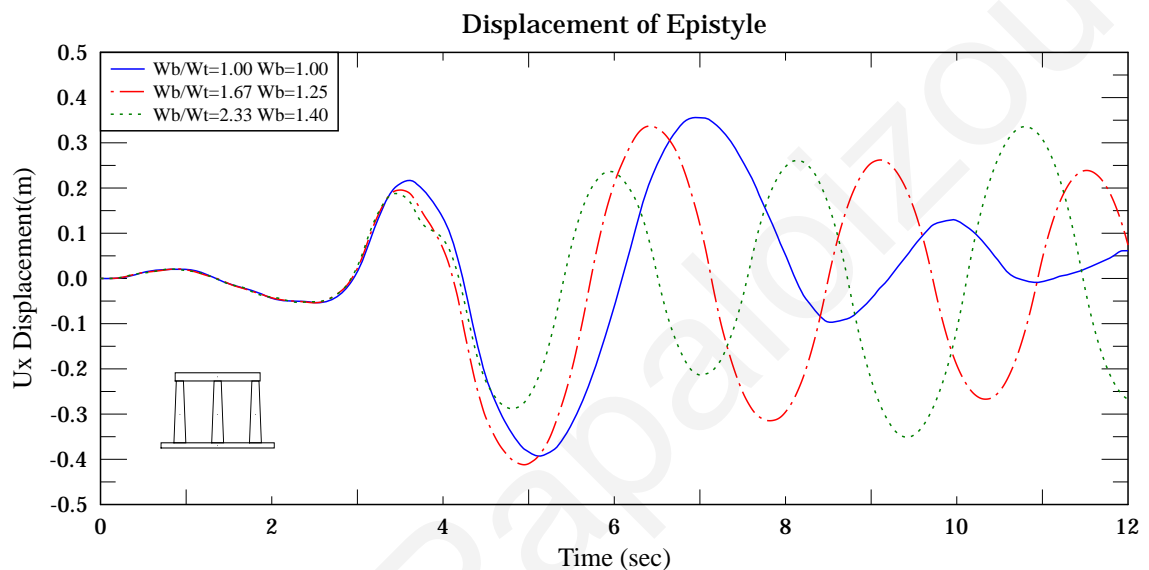


Figure 7.41. The effect of monolithic tapered colonnades under the Athens Earthquake, scaled to a PGA of 29.09 m/sec^2 .

Furthermore, the numerical simulations show that tapered multi-drum colonnades are not as stable as the corresponding non-tapered multi-drum colonnades. The analyses also reveal that as the number of colonnade drums increases, the maximum horizontal displacement of the epistyle increases.

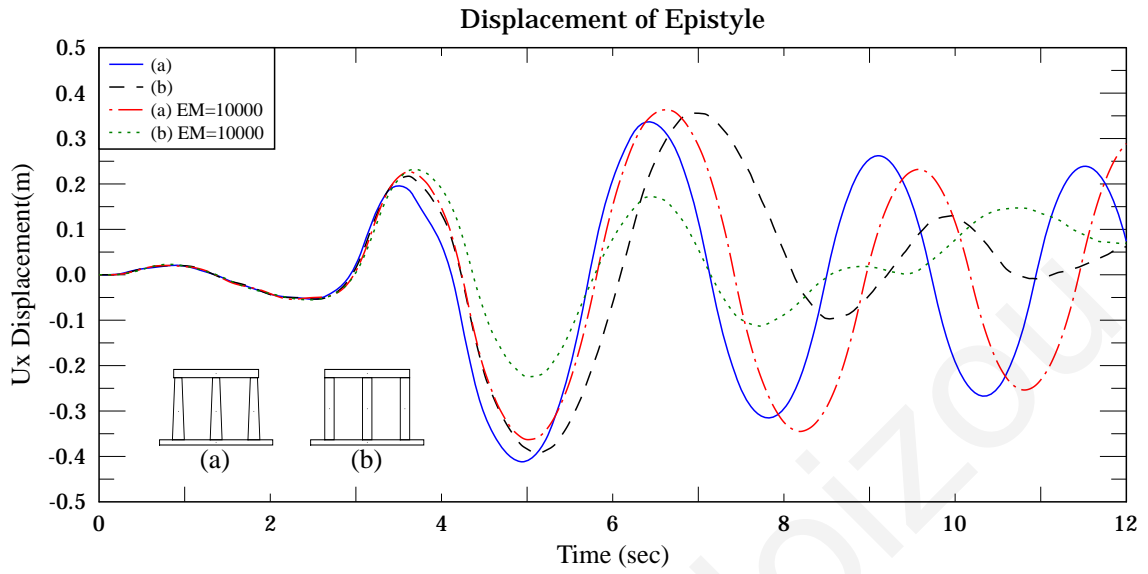


Figure 7.42. Displacements of monolithic tapered and non-tapered columns with various epistyle masses under the Athens Earthquake, scaled to a PGA of 29.09 m/sec^2 .

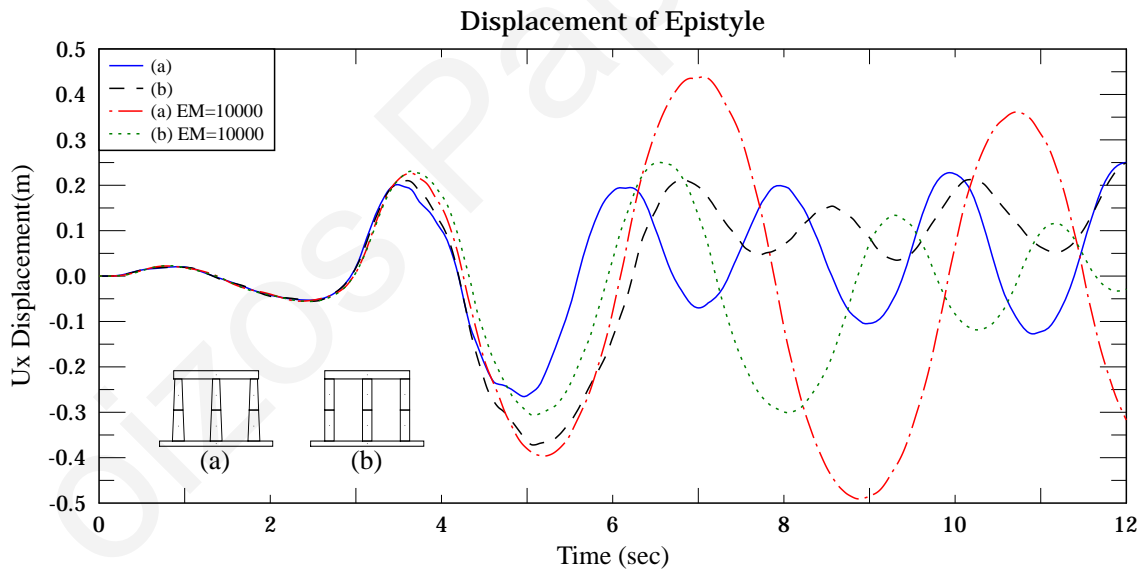


Figure 7.43. Displacements of (two-drum) tapered and non-tapered columns with various epistyle masses under the Athens Earthquake, scaled to a PGA of 29.09 m/sec^2 .

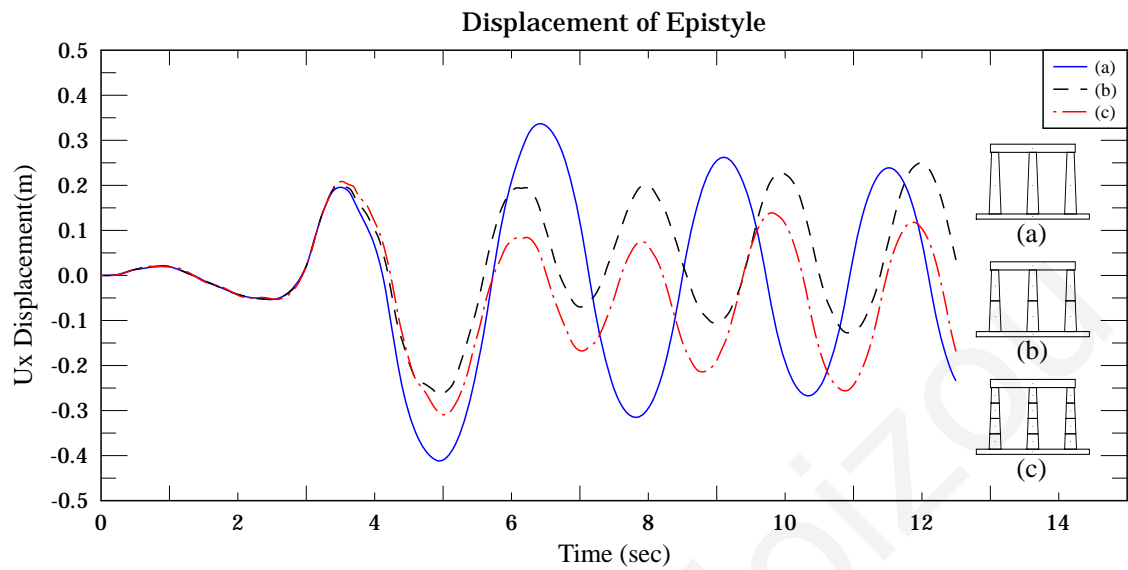


Figure 7.44. Displacements of monolithic, as well as, two and four drum tapered columns under the Athens Earthquake, scaled to a PGA of 29.09 m/sec^2 .

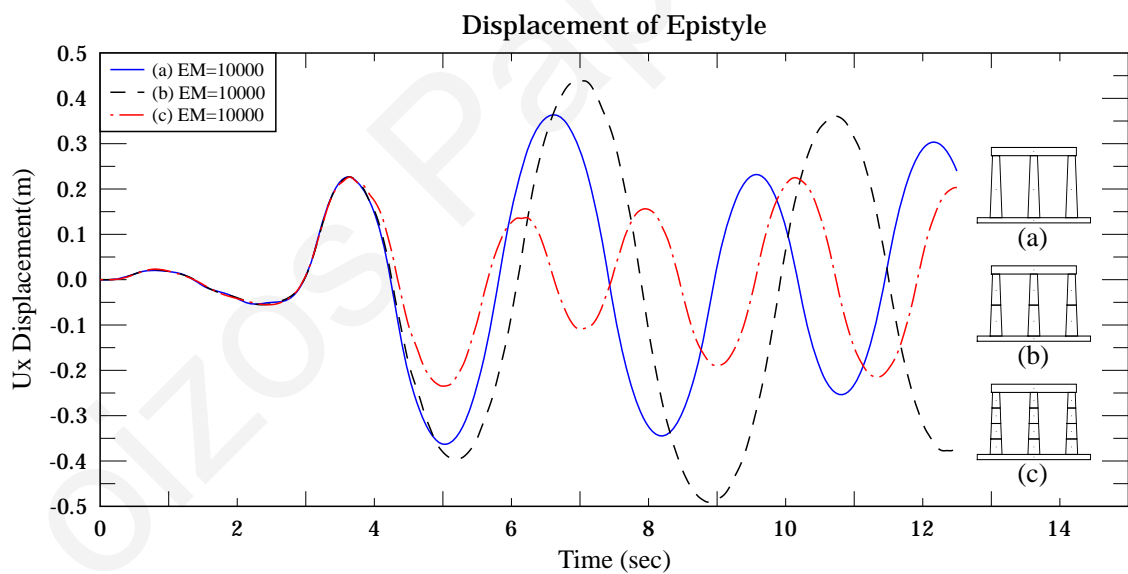


Figure 7.45. Displacements of monolithic, as well as, two and four drum tapered columns for increased epistyle mass under the Athens Earthquake, scaled to a PGA of 29.09 m/sec^2 .

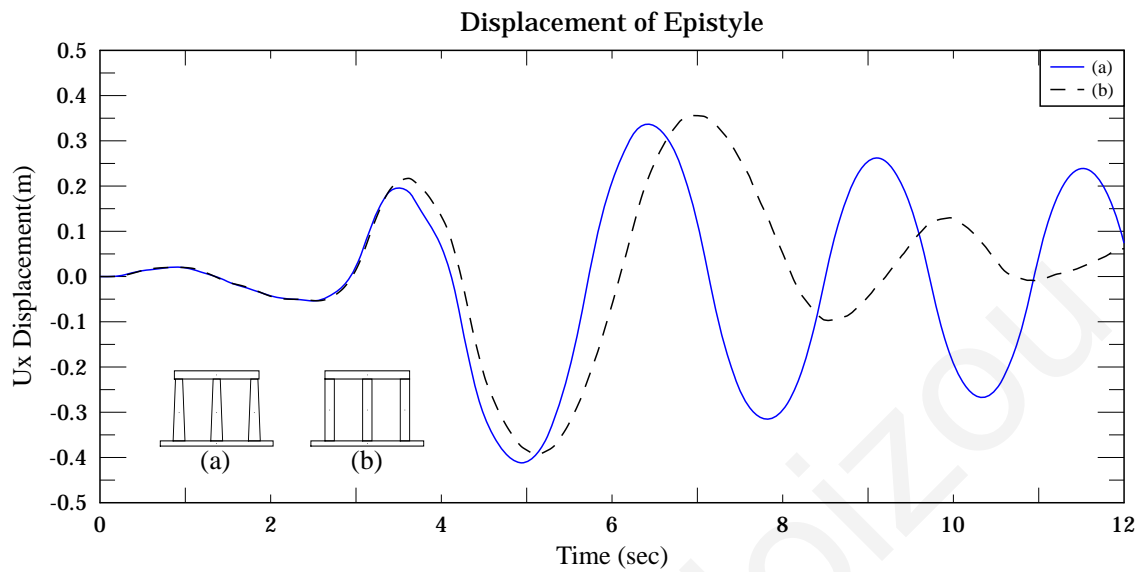


Figure 7.46. Comparison of tapered colonnades with a non-tapered monolithic colonnades under the Athens Earthquake, scaled to a PGA of 29.09 m/sec^2 .

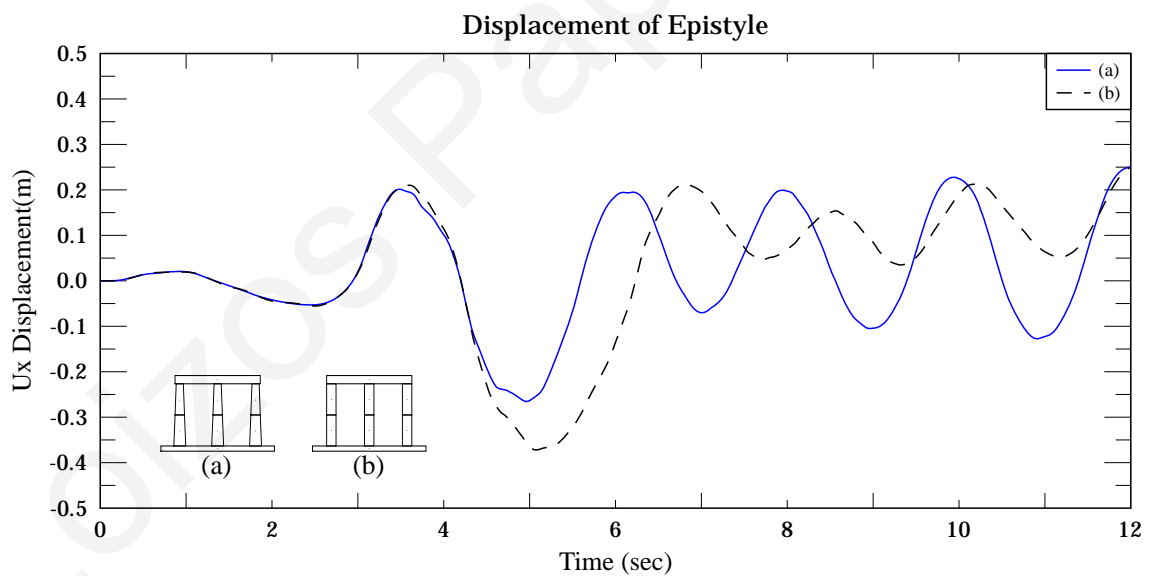


Figure 7.47. Comparison of tapered multidrum (two drum) colonnades with a non-tapered ones under the Athens Earthquake, scaled to a PGA of 29.09 m/sec^2 .

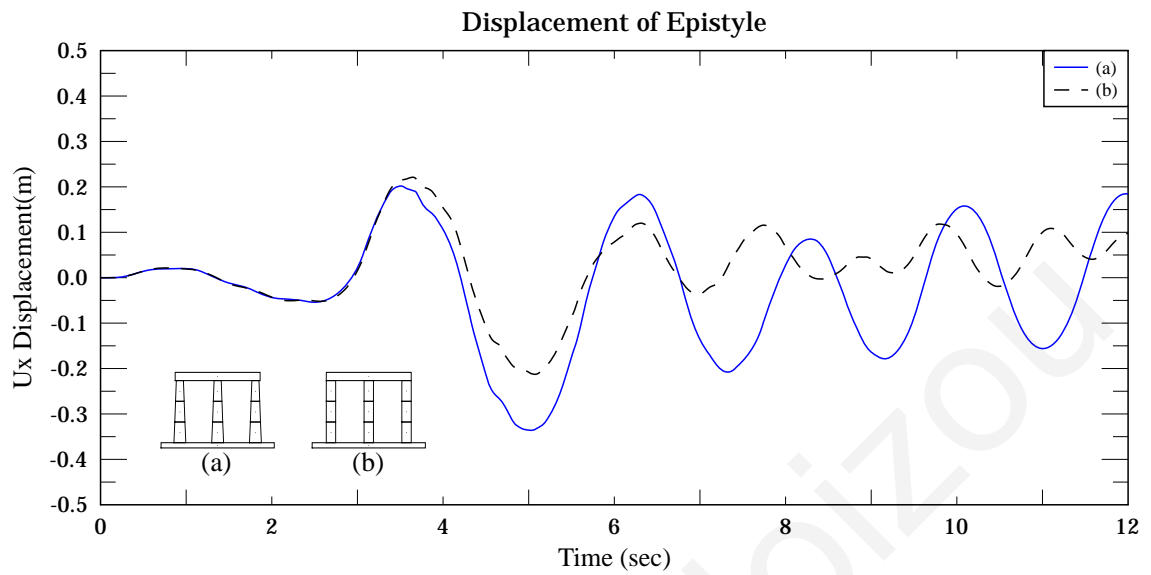


Figure 7.48. Comparison of tapered multidrum (three drum) colonnades with a non-tapered ones under the Athens Earthquake, scaled to a PGA of 29.09 m/sec^2 .

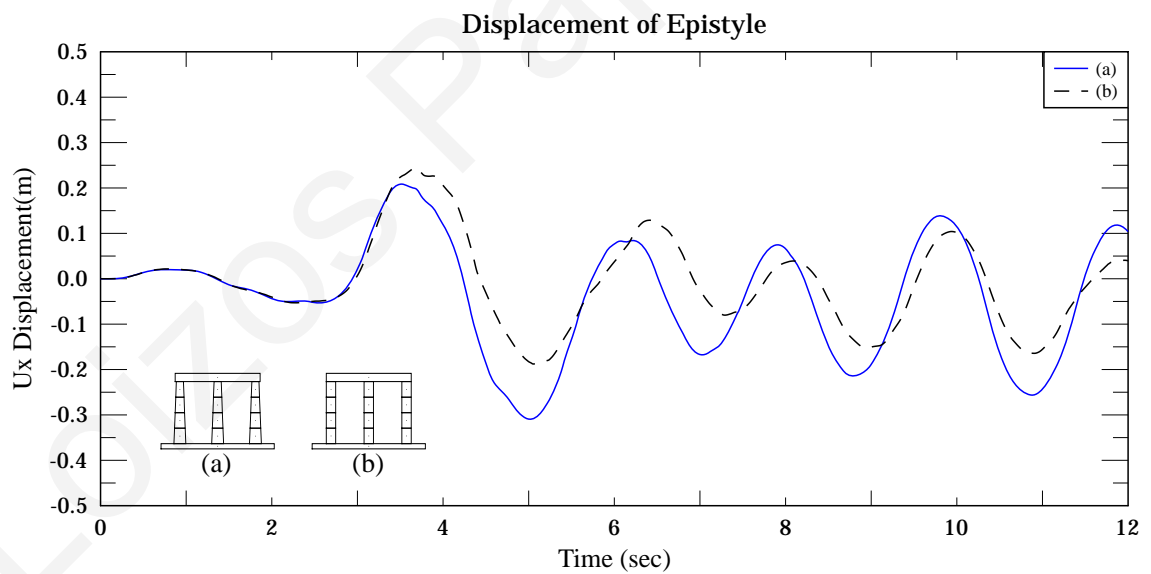


Figure 7.49. Comparison of tapered (four-drum) colonnade with a non-tapered one under the Athens Earthquake, scaled to a PGA of 29.09 m/sec^2 .

7.9. Colonnades with two rows of columns

In ancient Greek temples the internal columns supported an upper row of smaller columns carrying the timber roof. The remains of this upper row of columns can be seen today in several ancient Greek monuments, such as, the temple of Aphaia in Aegina.

Figure 7.50 and Figure 7.51 show snapshots of the response of such systems for the Athens and the Mexico City Earthquakes, respectively. The upper row of columns alters the response of the overall system, compared to colonnade systems with only one lower row of columns.

Moreover, Figure 7.52 to Figure 7.55 show the response of these systems under harmonic excitations. In particular, various excitation frequencies have been used for the analyses. The results show that the frequency content of the ground motion affects significantly the response. The displacements of the upper level columns in respect to the displacements of the lower level column are affected by the frequency content of the excitation. Specifically, for the geometry examined, as the frequency of a harmonic ground motion increases the upper level columns seem to have greater displacements than the lower columns. The maximum acceleration that is required to overturn the system of columns increases as the excitation frequency decreases. This has also been observed in the analyses of standalone multi-drum columns, as well as, for a single row of colonnades with an epistyle.

Such phenomenon also appears under earthquake excitations. For the Mexico City earthquake, which has low predominant frequencies, the upper level columns overturn. On the other hand, for the Athens Earthquake, which has higher predominant frequencies, and for a much larger maximum acceleration the upper level columns are not as much affected.

Numerical simulation of colonnades with an epistyle

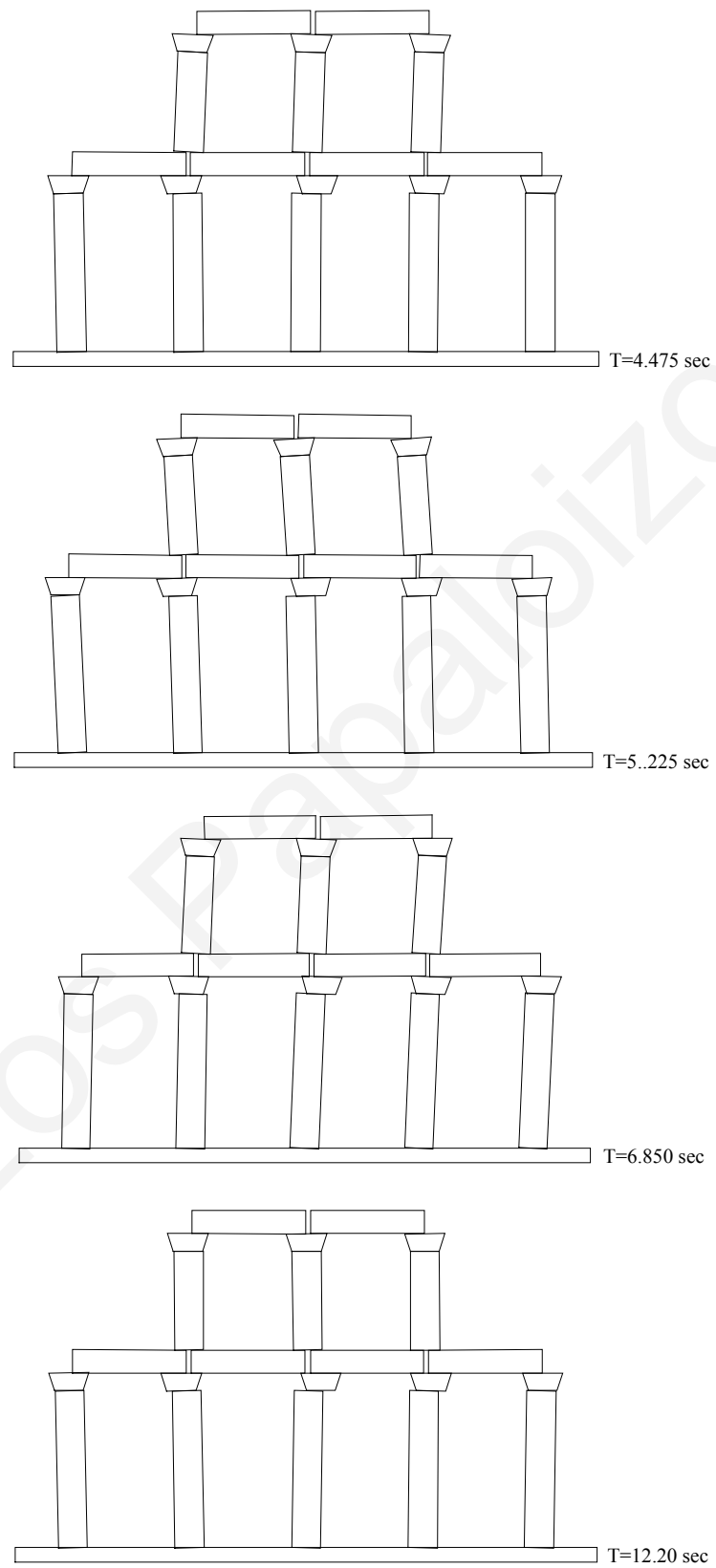


Figure 7.50. Athens Earthquake (scaled acceleration by 9.0).

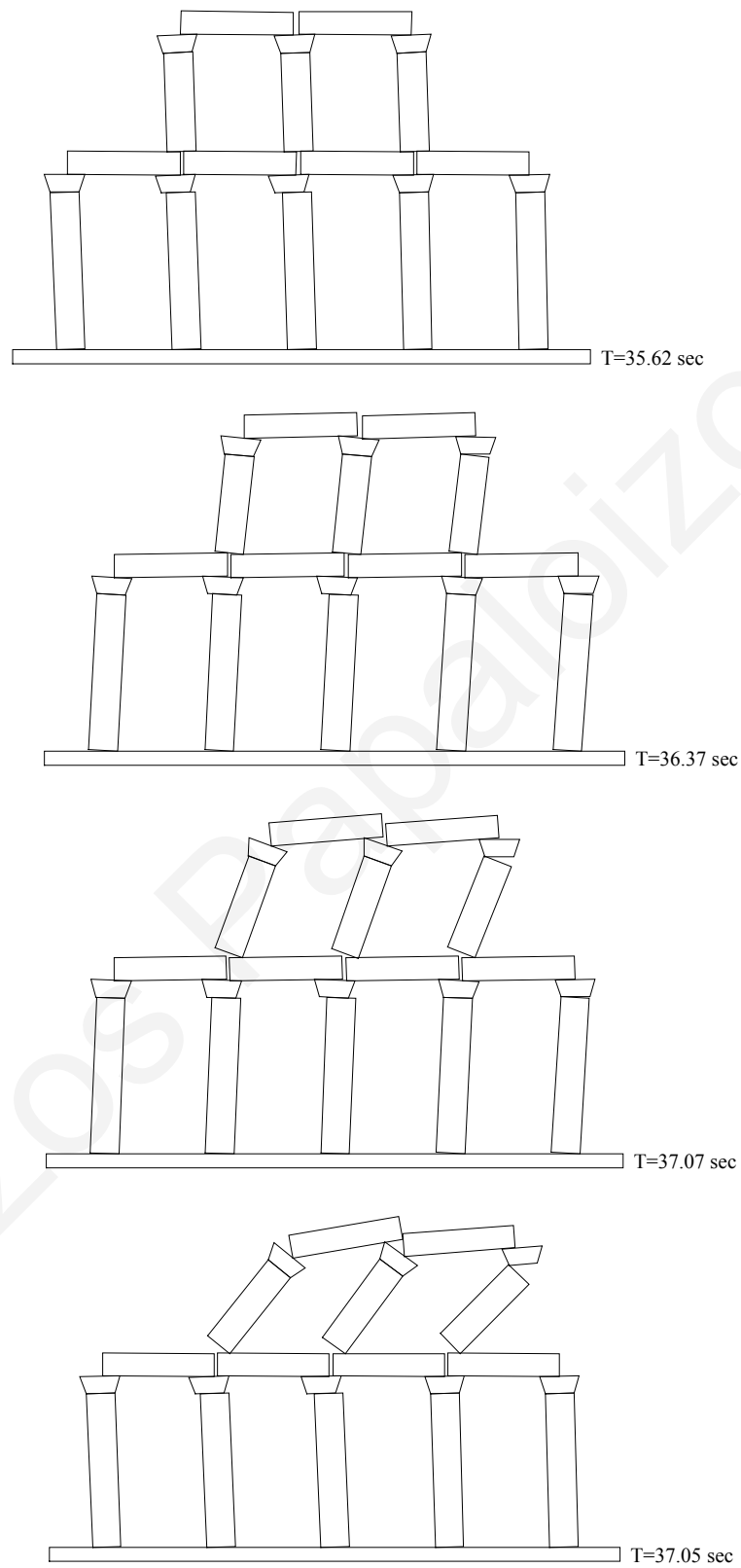


Figure 7.51. Mexico City Earthquake (scaled acceleration by 1.5).

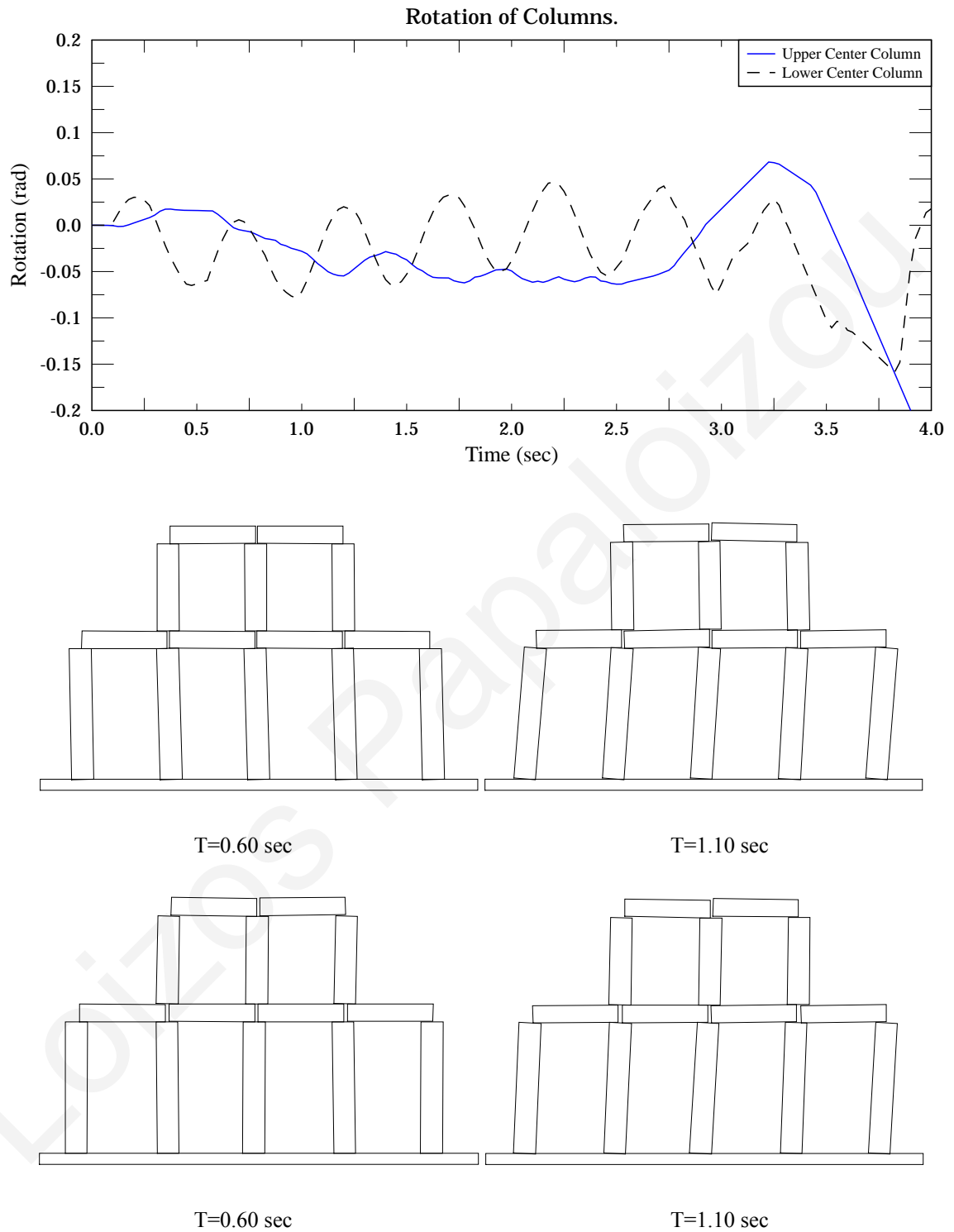


Figure 7.52. Response of a two level column system under a harmonic excitation with 2 Hz frequency and 0.25 m amplitude.

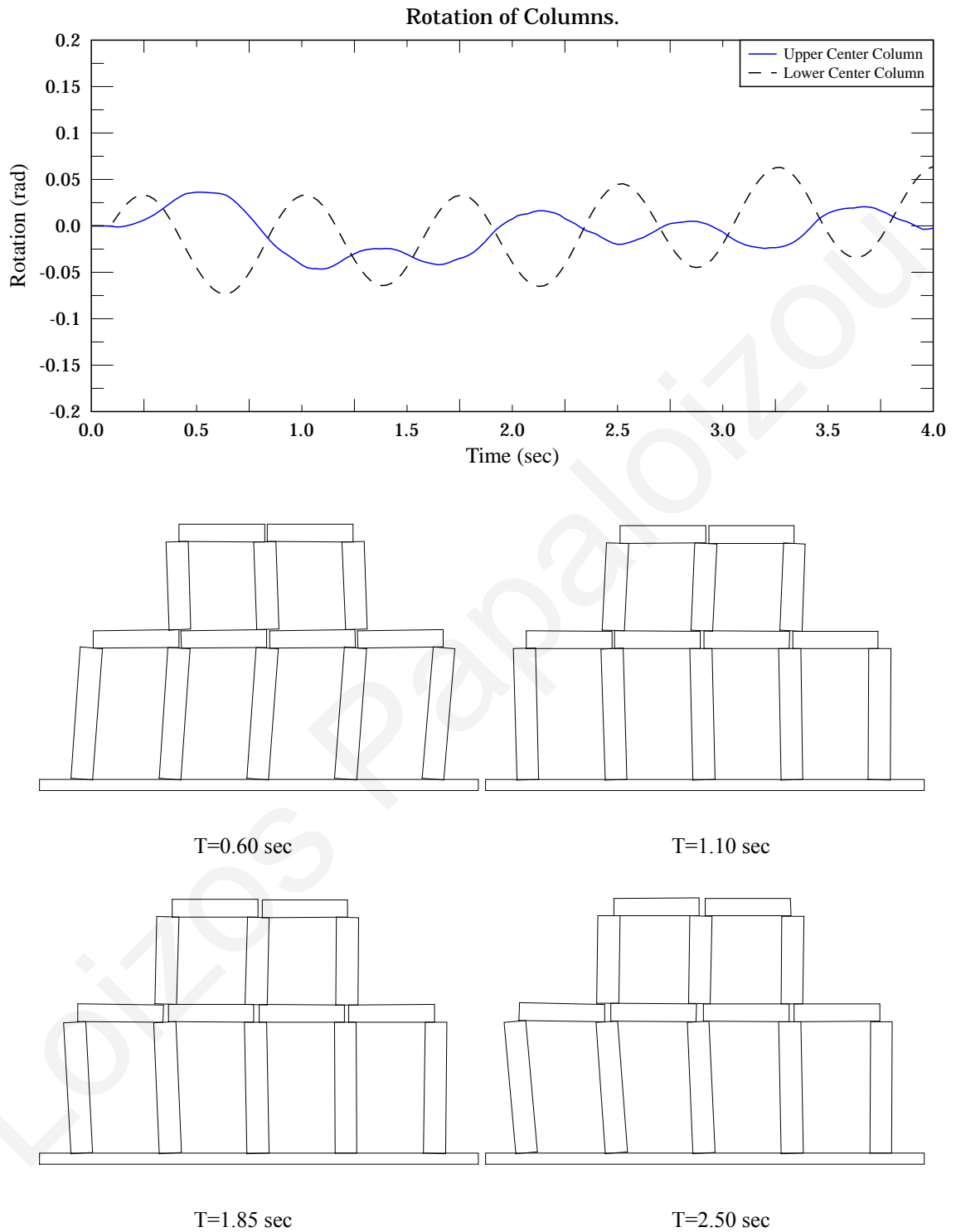


Figure 7.53. Response of a two level column system under a harmonic excitation with 1.33 Hz frequency and 0.25 m amplitude.

Numerical simulation of colonnades with an epistyle

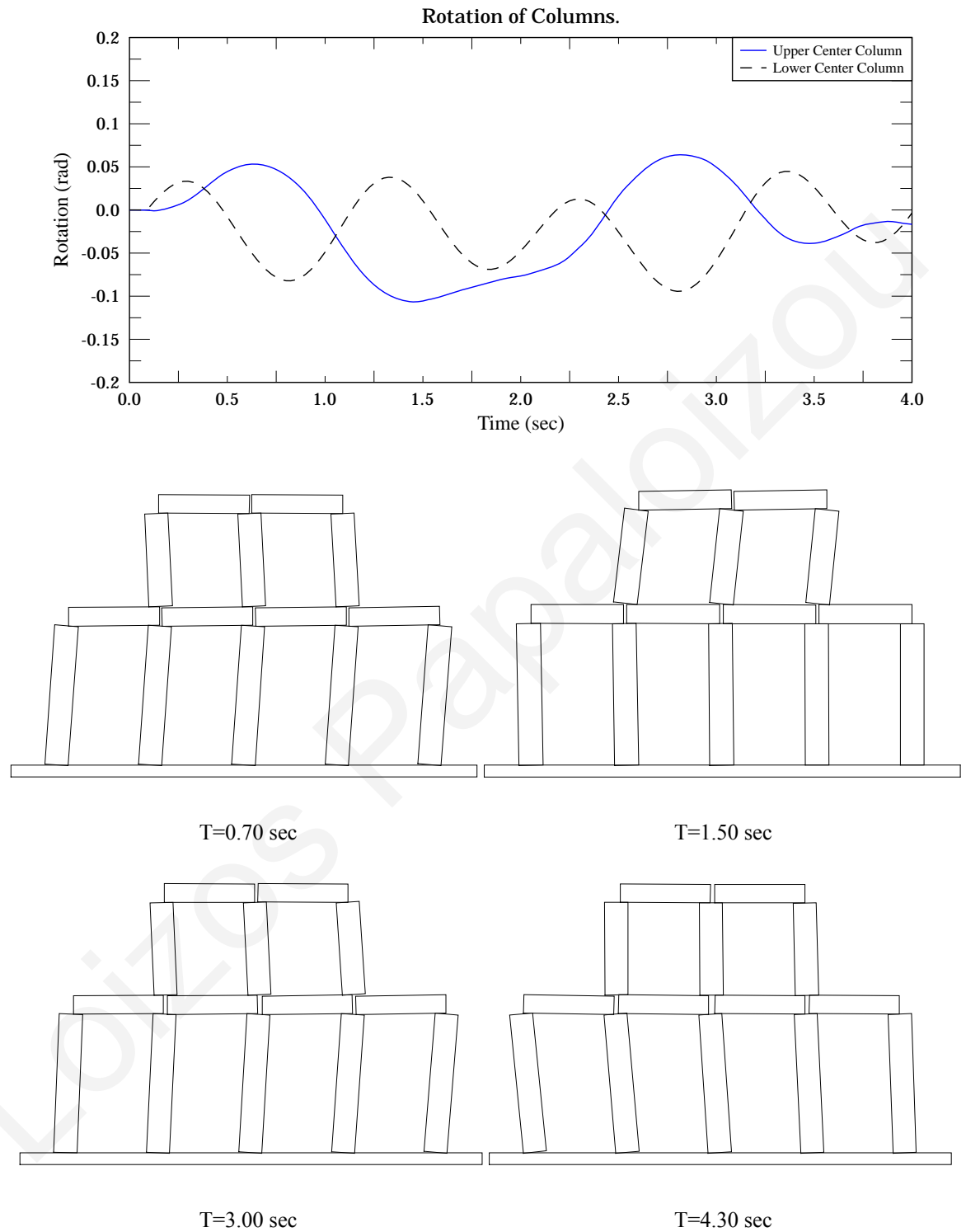
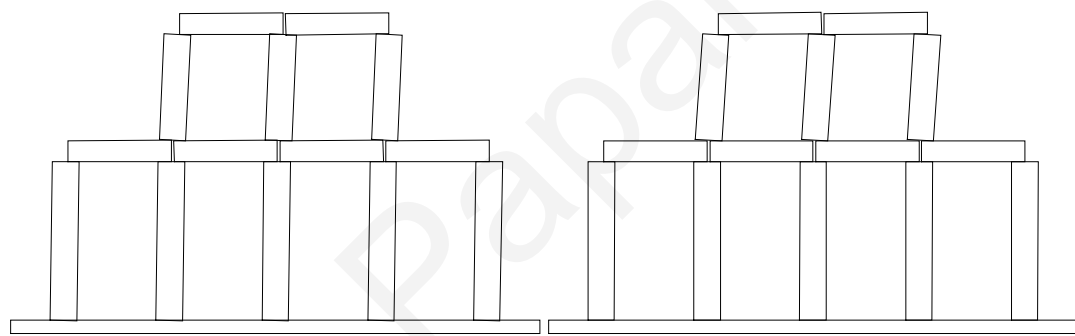
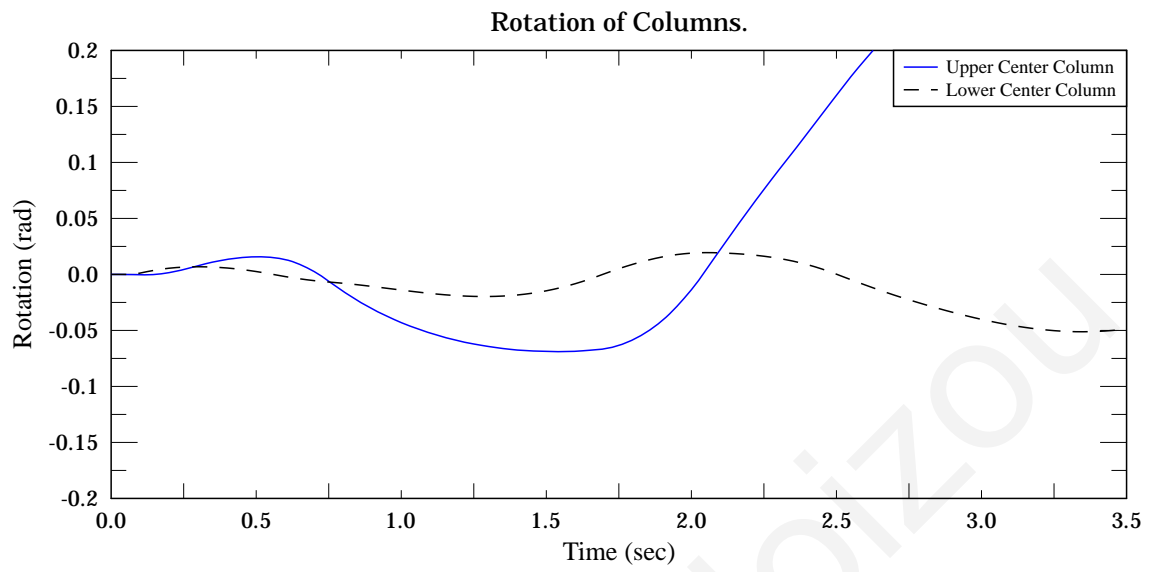
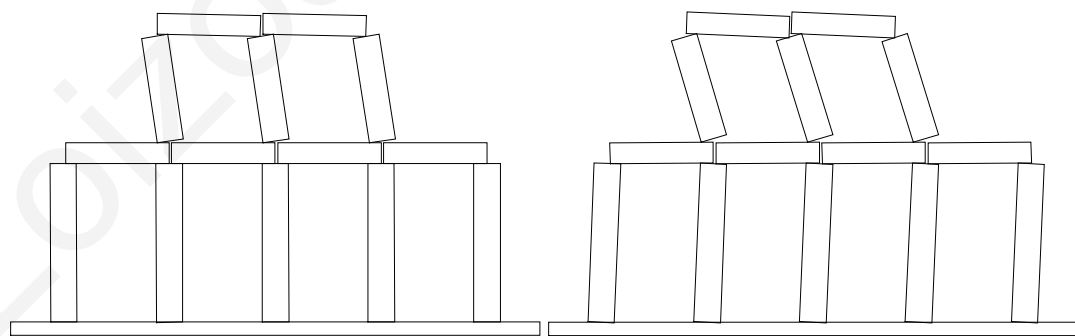


Figure 7.54. Response of a two level column system under a harmonic excitation with 1.00 Hz frequency and 0.25 m amplitude.



T=1.000 sec

T=1.675 sec



T=2.475 sec

T=3.000 sec

Figure 7.55. Response of a two level column system under a harmonic excitation with 0.5 Hz frequency and 0.1 m amplitude.

Further analyses of these more complex systems, which consist of a lower and an upper series of columns, have been conducted to investigate the effect of a larger number of drums. Figure 7.56 to Figure 7.58 show snapshots of the responses of two-drum column system, under harmonic excitations. Firstly, the results reveal that for higher harmonic excitation frequencies, rocking and sliding of the individual drums of the lower columns is more intense, especially for the outermost lower columns, which have a lower vertical load.

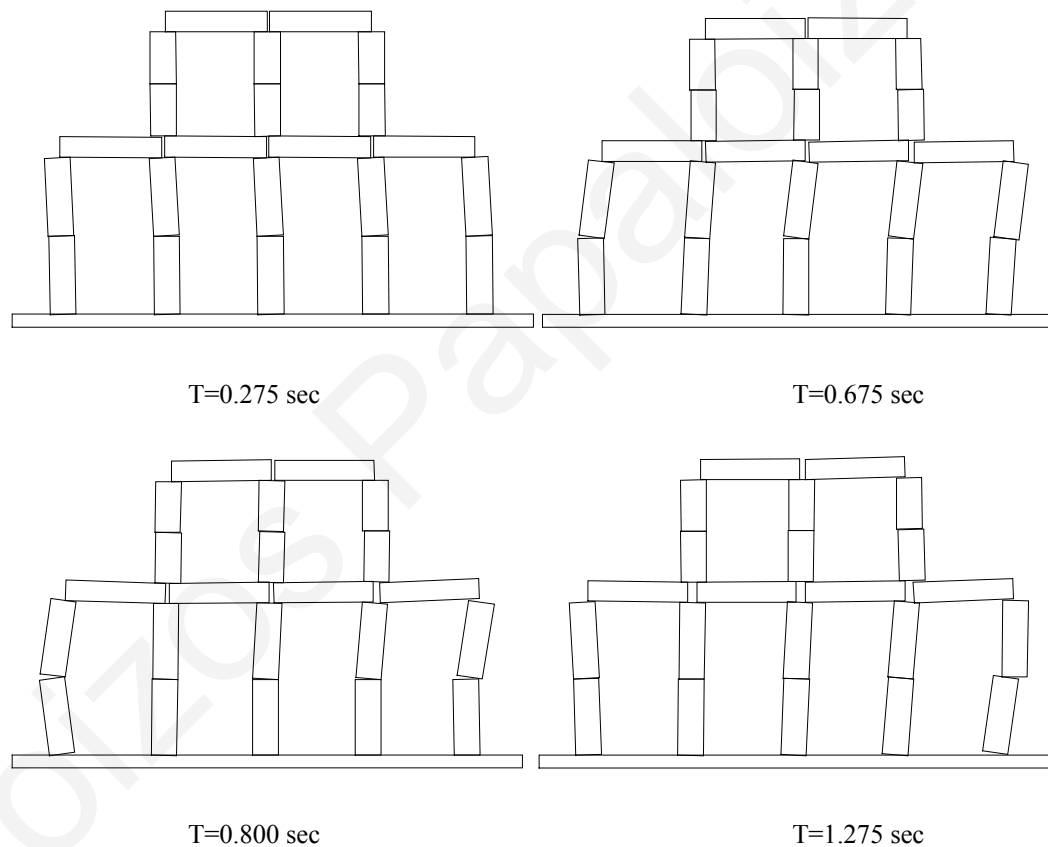


Figure 7.56. Response of a two series (2 drum) column system colonnade, under a harmonic excitation with 1.33 Hz frequency and 0.25 m amplitude.

As the excitation frequency decreases (Figure 7.57) the sliding phenomenon seems to degrade. The lower series of columns continues to have larger relative displacements than the upper row of columns.

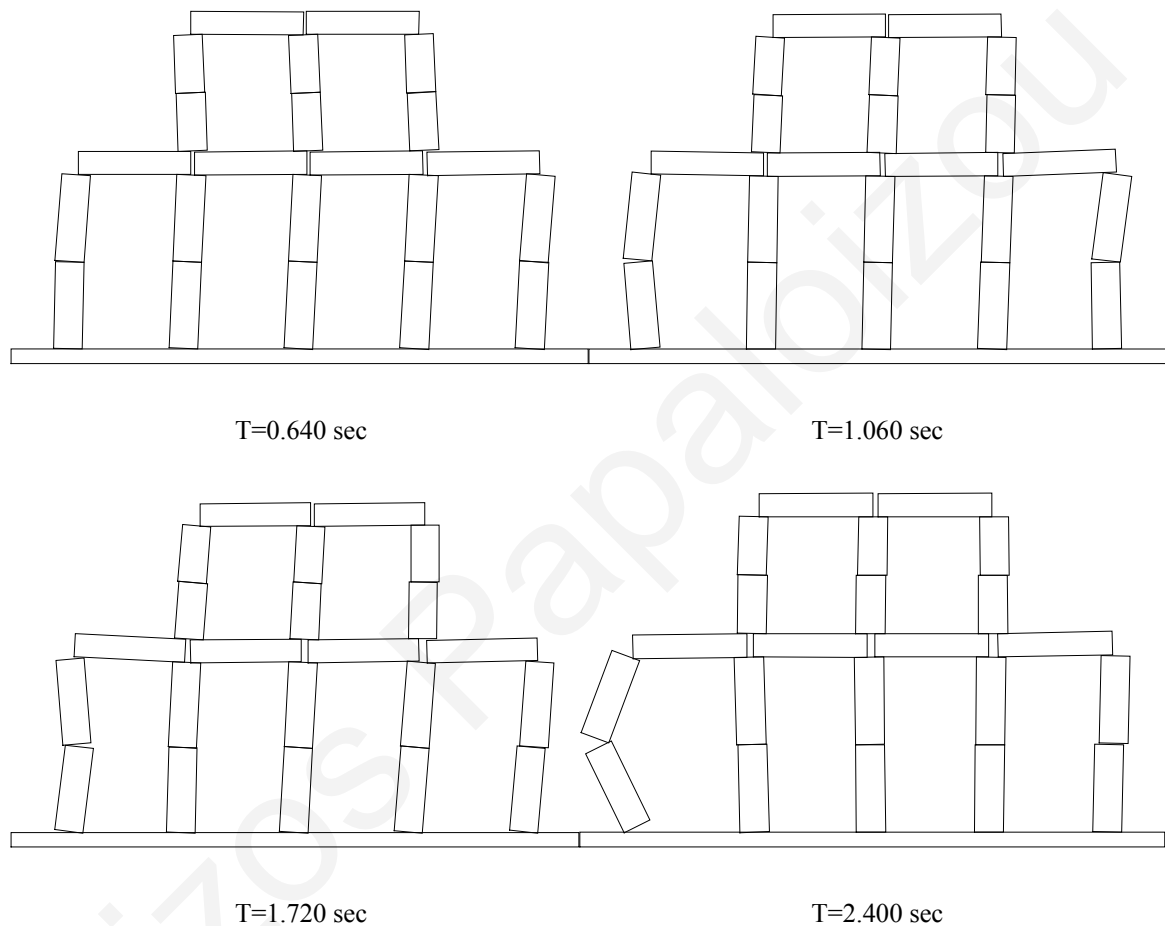


Figure 7.57. Response of a two series (2 drum) column system colonnade, under a harmonic excitation with 1 Hz frequency and 0.1 m amplitude.

Finally for an even lower harmonic excitation of 0.5 Hz , the lower columns rock as a monolithic column with both drums having the same rotation. The upper set of columns has greater relative displacements than the lower row.

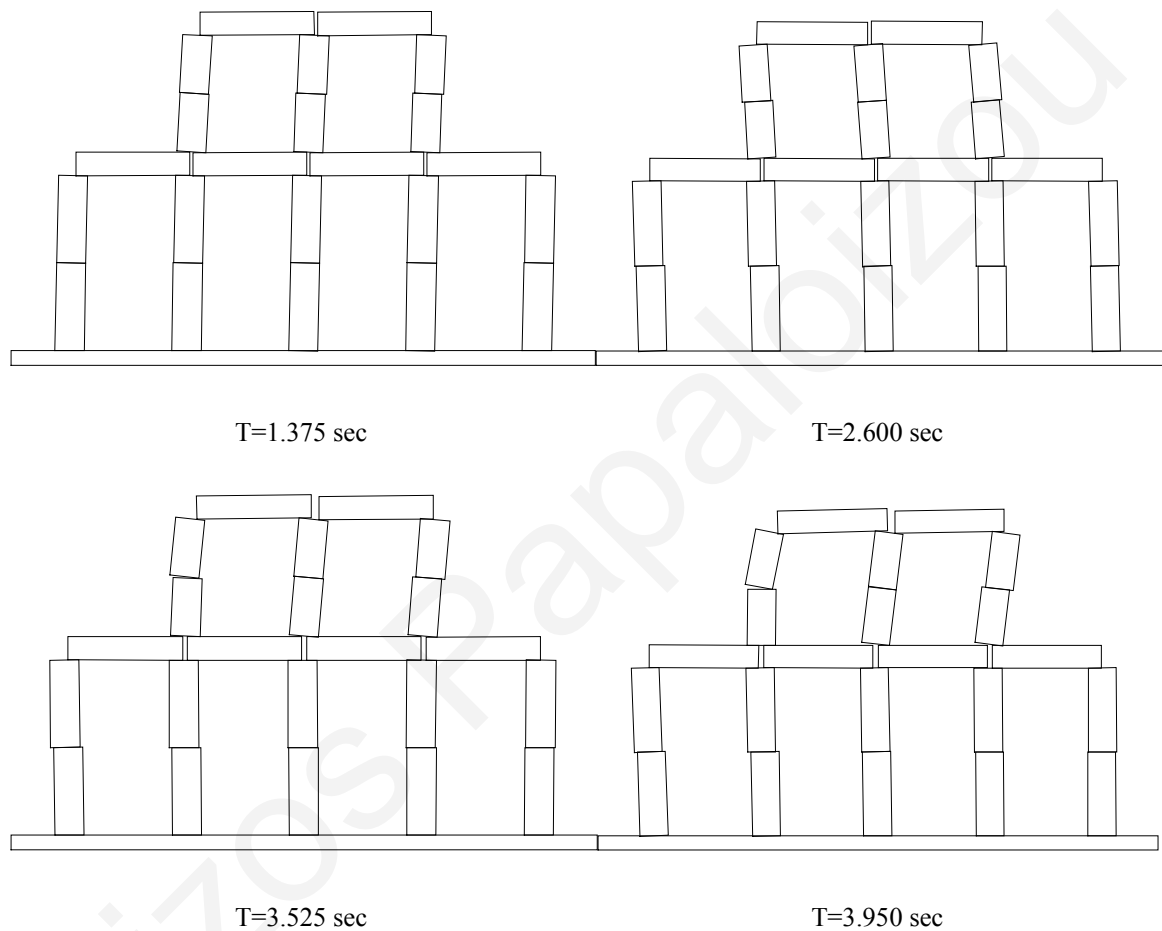


Figure 7.58. Response of a two series (2 drum) column system colonnade, under a harmonic excitation with 0.5 Hz frequency and 0.25 m amplitude.

8. Concluding remarks

8.1. Summary

This thesis has examined the response and behaviour of ancient columns and colonnades under various ground excitations. For this purpose, the DEM has been utilized to investigate their response during harmonic and earthquake excitations by simulating the individual rock blocks as distinct rigid bodies. A specialized software application has been designed and developed, using modern object-oriented technologies to perform efficient seismic simulations of multi-block structures. The developed software has been extensively validated by comparing the computed responses of various fundamental problems, such as sliding, rocking and free vibration dynamics of rigid bodies, with corresponding analytical solutions as well as results obtained from experiments that are available in the literature.

Numerical simulations of standalone columns have been carried out, using the developed application. Various analyses have been conducted with different types of standalone columns and several types of ground motion excitations. Specifically, columns with different numbers of drums, various coefficients of friction, as well as numerous shapes have been considered. A large number of parametric studies has been performed in order to examine the influence of frequency content and peak ground acceleration of the excitations, as well as the geometrical and mechanical characteristics of standalone multi-drum columns in their responses to harmonic and earthquake excitations.

Furthermore, the dynamic behaviour of multi-drum colonnades with epistyles under earthquake excitations is examined through planar numerical simulations using the developed application. Parameters such as the number of drums that assemble a column, the number and distance between the columns of a colonnade, the type of an epistyle, as well as the loading conditions appear to be defining parameters that affect the dynamic response of colonnades with epistyles.

Finally, two series of columns placed the one on the top of the other, representing the lower and upper rows of columns in ancient temples that supported a wooden roof, are investigated. These systems are analyzed under both harmonic and earthquake ground motion excitations.

8.2. Contributions and conclusions

A major contribution of this research work is the development of a flexible object oriented software that is specifically developed for the numerical investigation of the response of multi-drum columns and colonnades under harmonic and earthquake ground excitations. The developed application is based on the DEM, utilizing contact detection algorithms, object-oriented-design and programming as well as, Design Patterns to address effectively the specific problem, while maintaining the necessary flexibility and extensibility of the program.

In particular, a modern object-oriented design and programming approach has been used to develop an architecturally neutral, platform independent, robust object-oriented software that can be easily extended. Therefore, the developed cross-platform application may run on Microsoft Windows, Linux, Mac OS, or even future operating systems on either 32-bit or 64-bit architectures. Design Patterns together with the OOP paradigm have been utilized for the implementation of this software application that easily enables future modifications and extensions.

Analyses conducted with the developed software show that both multi-drum standalone columns and colonnades, with or without epistyles, exhibit very complicated seismic responses that involve rocking and sliding behaviour, depending on certain influencing parameters. Parametric studies have been performed by varying the excitation frequency and acceleration, as well as the frictional coefficient and the geometric characteristics of the simulated columns and colonnades in order to assess the influence of these parameters in their seismic response and behaviour. The analysis results indicate that the frequency and the peak ground acceleration of the excitation, significantly affect the seismic response of monolithic and multi-drum standalone columns and colonnades.

In particular, for low frequency harmonic excitations, the exhibited response is dominated by rocking, while sliding prevails in cases of harmonic excitations with very high frequencies. In between the two extremes, the response contains both rocking and sliding phenomena. Furthermore, according to the conducted simulations the required acceleration to initiate rocking or sliding decreases as the excitation frequency increases. The acceleration that is needed to overturn the column also increases as the frequency increases.

An extensive investigation of colonnades with epistyles reveals that several parameters affect their dynamic response under ground excitations. Geometrical characteristics, such as, the number of columns in a system, the number of drums of a column, the shape of the drums and the distance between the columns are important parameters in their dynamic response. Furthermore, the frequency of the ground motion is a key parameter of their dynamic behaviour. Other characteristics, such as the epistyle type and mass as well as the tapering of the column can also affect their response.

In particular, the numerical simulations and parametric analyses suggest that:

- The methodology described as well as the developed software can be used to evaluate the response of both monolithic and multi-drum column and colonnade systems, which have a great archaeological significance. The computed responses using numerical simulations compare sufficiently well with analytical equations, providing relatively accurate results, considering the high complexity and nonlinearities of the problem.
- The numerical analysis results indicate that the frequency and the PGA of an excitation can significantly affect the seismic response of multi-drum columns. The required PGA to overturn a column decreases as the predominant frequency of the earthquake decreases. In particular, for low frequency harmonic excitations, the exhibited response is dominated by rocking, while sliding prevails in cases of harmonic excitations with very high frequencies. In between the two extremes, the response engages both rocking and sliding phenomena.

- In cases of low predominant frequency earthquakes, like the Mexico City Earthquake, all drums of a standalone column tend to rotate as a single group and the multi-drum column behaves similarly to the corresponding monolithic column. This phenomenon is also observed for multi-drum colonnade systems with an epistyle. Therefore, the acceleration that is needed to overturn these systems under such conditions is not influenced by the number of the drums of a column.
- Colonnades with an epistyle seem to require higher accelerations to be overturned as compared to standalone columns.
- Geometric characteristics of colonnades with an epistyle, such as tapering, the number of drums of a column, the number of columns of a colonnade system, the distance between the columns, as well as the type of epistyles affect their response.
- The original loading conditions of these monuments that are still standing today are usually different than their current conditions, which alter the response of systems with epistyle.
- By examining the stability of multi-drum colonnades for earthquakes that were selected from regions, where these monuments are still standing, such as the Eastern Mediterranean region, the simulations reveal that such monuments have the capacity to successfully withstand strong earthquakes with high frequency content.

In addition, colonnade systems with two rows of columns, one over the other, have been examined with ground motions of various excitation frequencies. Specifically, earthquake ground motions as well as harmonic excitations have been used. The results show that the frequency content of the ground motion affects mostly the response. The displacement of the upper level columns with respect to the displacement of the lower level column is affected more by the frequency content of the excitation. At last, based on the results obtained from the conducted simulation, as the frequency of a harmonic ground motion increases the upper level columns seem to have greater displacements than

the lower columns. The maximum acceleration that is required to overturn systems with two rows of columns increases as the excitation frequency decreases. This has also been observed in the analyses of standalone multi-drum columns, as well as, for a single row of colonnades with an epistyle.

8.3. Future work

By using the existing developed application, planar analyses can be readily carried out to investigate the influence of the vertical component of earthquake excitations in the response of classical columns and colonnades. This can be done by applying, at the base of the column or colonnade, simultaneously the earthquake excitation in both the horizontal and the vertical directions.

Furthermore, analyses can be easily performed to examine how these structures can perform during a second earthquake excitation, taking into account residual deformations from previous seismic actions. Other parameters such as the effect of possible column inclination due to differential settlements can also be examined, with the developed software.

Having direct access and control to the source code of the specifically developed software, allows the addition of suitable discrete elements and algorithms in order to fulfil future research objectives. Some of them can be achieved with minor modifications and extensions to the program. Others may require wider extensions of the software, as well as further advances in the available computing resources.

Specifically, with minor additions to the existing code the investigation of the effect of wooden poles that used to be installed in ancient times between the individual drums, can be enabled, by considering the shear strength of the pole within the sliding mechanism. Moreover, the effect of metallic shear links that replace the wooden poles when retrofitting multi-drum columns can also be studied with a minor extension of the program.

Further development of the discrete element formulation can include body deformability, so that both stresses and strains could be computed at any point within a deformable element. In order to achieve the consideration of deformability of the individual discrete blocks, a combination of discrete and finite elements can be employed, introducing deformable bodies through finite element expansion of the displacement field within each discrete element. A combination of a small-strains and large-displacements finite element formulation with the discrete element method will enable the evaluation the stress and strain distributions within simulated bodies during simulations. However, the consideration of deformability will substantially increase the complexity and the computational cost of the analyses of multi-body systems.

Moreover, the software can also be extended in three dimensions, using three-dimensional customized elements, such as cylindrical elements and truncated cones. The latter represent more realistically the geometric characteristics of ancient columns and their drums than the polygonal elements that the general-purpose DEM programs usually provide. Although the computational requirements will be significantly increased, with the dramatic increase of the computing speed and available computing resources, such extensions may be reasonable and realistic to perform in the near future.

References

- [1] Adeli H, Yu G. “An integrated computing environment for solution of complex engineering problems using the object-oriented programming paradigm and a blackboard architecture”, *Computers and Structures*, 1995;54(2):255-265.
- [2] Alexander C., Ishikawa S., Silverstein M., “A Pattern Language: Towns, Buildings, Construction”, Oxford University Press, 1977.
- [3] Alexandris A, Psycharis IN, Protopapa EA. The collapse of the Temple of Zeus at Olympia. Back analysis using the Distinct Element Method, *Proceedings of the Second Greek National Conference on Earthquake Engineering and Seismology 2001*;1:297-306.
- [4] Allen R and Duan X. Effects of linearizing on rocking block. *Journal of Structural Engineering* 1995;12(7):1146-9.
- [5] Archer G. C, Fenves G, Thewalt C, “A new object-oriented finite element analysis program architecture”, *Computers and Structures*, 1999;70(1):63-75.
- [6] Arnold K, Gosling J and Holmes D. *The Java Programming Language*, 3rd edition, Addison-Wesley Pub Co, 2000.
- [7] Aslam M, Godden W, Scalise D. Earthquake rocking response on rigid bodies. *Journal of the Structural Division of the ASCE* 1980;106(ST2):377-92.
- [8] Barbosa R, Ghaboussi J. Discrete finite element method, *Proceedings of the 1st U.S. Conference on Discrete Element Methods* 1989.
- [9] Bathe KJ. *Finite Element Procedures*, Prentice-Hall Inc. Englewood Cliffs, New Jersey 1996.
- [10] Beck, K, Crocker R, Meszaros G, Coplien J.O, Dominick L, Paulisch F and Vlassides J. *Proceedings of the 18th International Conference on Software Engineering*, 1996;25-30.

References

- [11] Beskos D. Use of finite and boundary elements in the analysis of monuments and special structures, Bulletin of the Association of Civil Engineers of Greece 1993/4; No. 216 [in Greek].
- [12] Beskos D. Use of finite and boundary elements in the analysis of monuments and special structures, Bulletin of the Association of Civil Engineers of Greece 1993/4; No.217 [in Greek].
- [13] Borchers, Jan. A Pattern Approach to Interaction Design. John Wiley & Sons. ISBN 0-471-49828-9, 2001.
- [14] Brown K. and Petersen D. "Ready to Run Java 3D", Wiley & Sons Inc, 1999.
- [15] Cook, B.K., and Jensen, R.P. (Editors). Discrete Element Methods: Numerical Modelling of Discontinua, Proceedings of the Third International Conference on Discrete Element Methods, 2002.
- [16] Connor R, Gill MJ, Williams J. A linear complexity contact detection algorithm for multi-body simulations, Proceedings of the 2nd International Conference on Discrete Element Methods 1993;53-64.
- [17] Cooper J.W. "Java Design Patterns", Addison Wesley, 2000.
- [18] Cundall PA. A computer model for simulating progressive large scale movements in block rock systems, Proceedings of the Symposium of International Society of Rock Mechanics 1971;1, paper II-8, Nancy, France.
- [19] Cundall, P. A, and Hart R. D. "Numerical Modelling of Discontinua," Engr. Comp., 1992;9(2):101-113.
- [20] Cundall, P. A, J. Marti, P. J. Beresford, N. C. Last and M. I. Asgian. "Computer Modeling of Jointed Rock Masses," U.S. Army Engineer Waterways Experiment Station, Vicksburg, Mississippi, Tech. Report N-78-4, August, 1978.

References

- [21] Demosthenous M and Manos G.C. Study of the dynamic response of models of ancient columns or colonnades subjected to horizontal base motions, *Structural Dynamics-EURODYN* 1996.
- [22] Feng YT, Owen DRJ. Discrete Element Methods: Numerical Modelling of Discontinua, *Proceedings of the Third International Conference on Discrete Element Methods* 2002;32-41.
- [23] Fenves G. L, McKenna F, Scott M. H, Takahashi Y. “An object- oriented software environment for collaborative network simulation”, *13th World Conference on Earthquake Engineering Conference Proceedings*, Vancouver, Canada, 2004.
- [24] Fletcher B. *A history of architecture on the comparative method for the student, craftsman, and amateur* (1905).
- [25] Forde B. W. R, Russell A. D, Stiemer S. F, “Object-oriented knowledge frameworks”, *Engineering with Computers*, 1989;5(2):79-89.
- [26] Forde B. W. R, Russell A. D, Stiemer S. F., “Object- oriented finite element analysis”, *Computers and Structures*, 1990;34(3):355-374.
- [27] Gamma E., Helm R., Johnson R., Vlissides J., “Design Patterns: Elements of reusable object-oriented software”, Addison Wesley, 1995.
- [28] Hogan S. The many steady state responses of a rigid block under harmonic forcing. *Earthquake Engineering and Structural Dynamics* 1990;19:1057-71.
- [29] Housner GW. The behaviour of inverted pendulum structures during earthquakes, *Bulletin of seismological Society of America* 1963;53:403-417.
- [30] Ishiyama Y. Motions of Rigid Bodies and Criteria for Overturning by Earthquake Excitations. *Earthquake Engineering and Structural Dynamics*, 1982;10:635-650.
- [31] Ishiyama Y. Motions of rigid bodies and criteria for overturning by earthquake excitations. *Earthquake Engineering and Structural Dynamics* 1982;10(5):635-50.

References

- [32] Itasca Consulting Group, Inc. UDEC-Universal Distinct Element Code version 4.0, Theory and Background Manual, Minnesota, USA; 2004.
- [33] Kim, Y.-S., Miura, K., Miura, S., Nishimura, M. Vibration characteristics of rigid body placed on sand ground *Soil Dynamics and Earthquake Engineering*, 2001;21(1):19-37.
- [34] Kimura H. and Iida K. On rocking of rectangular columns (I&II) (in Japanese), *J. seismological soc. Japan*, 1934;6:125-149&165-212.
- [35] Koh A S, Spanos PD, Roesset J. Harmonic rocking of rigid body block on flexible foundation. *Journal of Engineering Mechanics*, ASCE 1986;112(11):1165-80.
- [36] Koh A S, Spanos PD. Analysis of block random rocking. *Soil Dynamics and Earthquake Engineering* 1986;5:178-83.
- [37] Komodromos, P. A simplified updated Lagrangian approach for combining discrete and finite element methods *Computational Mechanics*, 2005;35(4):305-313.
- [38] Komodromos P, Papaloizou L, and Polycarpou P. Simulation of the response of ancient columns under harmonic and earthquake excitations, *Engineering Structures* 2008;30(8):2154-2164
- [39] Komodromos P, Papaloizou L, Polycarpou P and Mavronicola E. Modern Object-Oriented Design of Structural Engineering Software, *Proceedings of The Eleventh International Conference on Civil, Structural and Environmental Engineering Computing*, St. Julians, Malta 2007
- [40] Komodromos P, and Williams J. Utilization of Java and Database Technology in the development of a Combined Discrete and Finite Element Multibody Dynamics Simulator, *Proceedings of the 3rd International Conference on Discrete Element Methods*, Santa Fe, New Mexico, USA, ASCE Geotechnical Special Publication 2002;117:118-124.

References

- [41] Komodromos P.I, Williams J.R. Dynamic simulation of multiple deformable bodies using combined discrete and finite element methods (2004) *Engineering Computations* (Swansea, Wales), 21 (2-4):431-448.
- [42] Konstantinidis D and Makris N. Seismic response analysis of multidrum classical columns. *Earthquake Engineering and Structural Dynamics*, 2005;34:1243-1270.
- [43] De Lorenzis, L., DeJong, M., Ochsendorf, J. Failure of masonry arches under impulse base motion (2007) *Earthquake Engineering and Structural Dynamics*, 36 (14), pp. 2119-2136.
- [44] Lemos JV. Discrete element modelling of masonry structures, *Journal of Architectural Heritage* 2007;1:190-213.
- [45] Liu XL, Lemos JV. Procedure for contact detection in discrete element analysis, *Journal of Advances in Engineering Software* 2001;32:409-415.
- [46] Mackie R. I, "Object-oriented programming of the finite element method", *Intern. Journal of Numerical Methods in Engineering*, 1992;(35):425-436.
- [47] Mackie R. I. "Using objects to handle complexity in finite element software" *Engineering with Computers*, 1997;13(2):99-111.
- [48] Madan A. "Object-Oriented Paradigm in Programming for Computer-Aided Analysis of Structures", *Journal of Computing in Civil Engineering*, 2004;18(3):226-236.
- [49] Makris N, Roussos Y.S. Rocking response of rigid blocks under near-source ground motions *Geotechnique*, 2000;50 (3):243-262.
- [50] Makris N, Zhang J. Rocking response of anchored blocks under pulse-type motions, *Journal of Engineering Mechanics* 2001;127:484-493.
- [51] Manos G.C, Demosthenous M, Kourtides V, Hatzigeorgiou A. Dynamic and earthquake behaviour of models of ancient columns and colonnades with or without

References

- energy absorptions systems, Proceedings of Second Greek National Conference on Earthquake Engineering and Seismology 2001;1:257-276.
- [52] Manos G.C, Kourtides V, Demosthenous M, Tsakmakides E. Experimental and numerical investigation of the sliding behaviour of a set of two rigid blocks subjected to cyclic shear-type loads WIT Transactions on the Built Environment, 2007;95:633-643.
- [53] Mitsopoulou E, Doudoumis I.N and Paschalidis V. Numerical analysis of the dynamic seismic response of multi-block monumental structures. Proceedings of the Eleventh European Conference on Earthquake Engineering, Paris 1998.
- [54] Mitsopoulou E, Papaloizou L, "Evaluation of the response of a stone-masonry building using inelastic analysis procedure", 2nd International conference on Nonsmooth/Nonconvex mechanics with applications in engineering (II. NNMAE), Thessaloniki, Greece 2006.
- [55] Mouzakis H, Psycharis I, Papastamatiou D, Carydis P, Papantonopoulos C, Zambas C. Experimental investigation of the earthquake response of a model of a marble classical column, Earthquake Engineering and Structural Dynamics 2002;31:1681-1698.
- [56] Mustoe, G., Henriksen, M., and Huttelmaier, H. (Editors). Proceedings of the 1st U.S. Conference on Discrete Element Methods, Colorado School of Mines, Golden, CO, 1989.
- [57] Newmark NM. Effects of earthquakes on dams and embankments. Fifth Rankine Lecture. Geotechnique 1965;15:139 –160.
- [58] O'Connor M. Ruaidhri, "A Distributed Discrete Element Modelling Environment - Algorithms, Implementation, and Applications", Ph.D. thesis, Department of Civil and Environmental Engineering, MIT, 1996.

References

- [59] Omori F. Seismic Experiments on the Fracturing and Overturning of Columns. Publications of the Earthquake Investigation Committee in foreign language. 1900;4:69-141.
- [60] Omori F. On the Overturning and Sliding of Columns. Publications of the Earthquake Investigation Committee in foreign language. 1902;12:8-27
- [61] Papastamatiou D, Psycharis I. Seismic response of classical monuments. A numerical perspective developed at the temple of Apollo in Bassae, Greece, Terra Nova 1993;5:591-601.
- [62] Papantonopoulos C, Psycharis I, Papastamatiou D, Lemos J, Mouzakis H. Numerical prediction of the earthquake response of classical columns using the distinct element method, Earthquake Engineering and Structural Dynamics 2002; 31:1699-1717.
- [63] Peña, F., Prieto, F., Lourenço, P.B., Campos Costa, A., Lemos, J.V. On the dynamics of rocking motion of single rigid-block structures Earthquake Engineering and Structural Dynamics, 2007;36(15):2383-2399.
- [64] Peng J, McKenna F, Law K. H. "A modular framework for earthquake engineering analysis and simulations", 13th World Conference on Earthquake Engineering Conference Proceedings, Vancouver, Canada, 2004.
- [65] Pompei A, Scalia A, Sumbatyan MA. Dynamics of Rigid Block due to Horizontal Ground Motion, Journal of Engineering Mechanics 1998;124:713-717.
- [66] Pompei A, Scalia A, Sumbatyan MA. Dynamics of rigid block due to horizontal ground motion. Journal of Engineering Mechanics, ASCE 1998;124(7):713-7.
- [67] Psycharis I.N. Dynamic behaviour of rocking two-block assemblies. Earthquake Engineering & Structural Dynamics 1990;19(4):555-575.
- [68] Psycharis I.N. Applications in the Restoration of Ancient Monuments. Book Chapter 4.4 of Fracture and Failure of Natural Building Stones. Springer Netherlands 2006.

References

- [69] Psycharis I, Jennings P. Rocking of slender rigid bodies allowed to uplift. *Earthquake Engineering and Structural Dynamics* 1983;11:57-76.
- [70] Psycharis I, Lemos J, Papastamatiou D, Zambas C, Papantonopoulos C. Numerical study of the seismic behaviour of a part of the Parthenon Pronaos, *Earthquake Engineering and Structural Dynamics* 2003; 32:2063-2084.
- [71] Psycharis I.N, Papastamatiou D.Y and Alexandris A. P. Parametric investigation of the stability of classical columns under harmonic and earthquake excitations. *Earthquake Engineering and Structural Dynamics* 2000;29:1093-1109.
- [72] Scalia A, Sumbatyan MA. Slide rotation of rigid bodies subjected to a horizontal ground motion. *Earthquake Engineering and Structural Dynamics* 1996;25:1139-49.
- [73] Shenton H, Jones N. Base excitation of rigid bodies. 1: Formulation. *Journal of Engineering Mechanics*, ASCE 1991;117(EM10):2286-306.
- [74] Shenton H, Jones N. Base excitation of rigid bodies. 2: Periodic slide-rock response. *Journal of Engineering Mechanics*, ASCE 1991;117(EM10):2307-28.
- [75] Shenton H. Criteria of initiation of slide, rock, and slide-rock rigid-body modes. *Journal of Engineering Mechanics*, ASCE 1996;122:690-3.
- [76] Shi B, Anooshehpour A, Zeng Y, Brune JN. Rocking of rigid blocks due to harmonic shaking. *Journal of Engineering Mechanics* 1984;110:1627-42.
- [77] Shi G. H. "Discontinuous Deformation Analysis — A New Numerical Model for the Statics and Dynamics of Block Systems," Lawrence Berkeley Laboratory, Report to DOE OWTD, Contract AC03-76SF0098, September 1988; also Ph.D. Thesis, University of California, Berkeley, August, 1989.
- [78] Sinopoli A. Dynamics and impact in a system with unilateral constraints. The relevance of dry friction. *Journal of the Italian Association of Theoretical and Applied Mechanics* 1990;22:210-15.

References

- [79] Spanos PD, Koh AS. Rocking of rigid blocks due to harmonic shaking. *Journal of Engineering Mechanics* 1984;110:1627-42
- [80] Spanos P.D, Roussis P.C, Politis N.P.A. Dynamic analysis of stacked rigid blocks *Soil Dynamics and Earthquake Engineering*, 2001;21(7):559-578.
- [81] Takahashi Y, Fenves G. L, “Software framework for distributed experimental-computational simulation of structural systems”, *Earthquake Engineering and Structural Dynamics*, 2005;35(3):267-291.
- [82] Tso W, Wong C. Steady state rocking response of rigid blocks. Part 1: Analysis. *Earthquake Engineering and Structural Dynamics* 1989;18:89-106.
- [83] Tso W, Wong C. Steady state rocking response of rigid blocks. Part 2: Experiment. *Earthquake Engineering and Structural Dynamics* 1989;18:107-120.
- [84] Wen Y K. Approximate method for nonlinear random vibration. *Journal of Engineering Mechanics Division (ASCE)* 1975;102(EM4):389–401.
- [85] White S., Fisher M., Cattell R., Hamilton G. and Hapner M. (1999) *JDBC API Tutorial and Reference: Universal Data Access for the Java 2 Platform*", 2nd Edition, Addison-Wesley Pub Co.
- [86] Williams, J. and Mustoe, G. (Editors). *Proceedings of the 2nd Int. Conf. on Discrete Element Methods*, Dept. of CEE, Massachusetts Institute of Technology, IESL Publications, 1993
- [87] Williams John "Contact analysis of large numbers of interacting bodies using discrete modal methods for simulating material failure on the microscopic scale ", *International Journal of Computer Aided Engineering*, *Engineering computations*, 1988;5(3).
- [88] Williams, J. R and G. G. W. Mustoe. “Modal Methods for the Analysis of Discrete Systems,” *Computers & Geotechnics*, 1987;4:1-19 .
- [89] Working Model. User’s manual. MSC Software Corporation: San Mateo, CA, 2000.

References

- [90] Younis C, Tadjbakhsh G. Response of sliding rigid structure to base excitation. *Journal of Engineering Mechanics (ASCE)* 1984;110(3):417– 432.
- [91] Yim CS, Lin H. Nonlinear impact and chaotic response of slender rocking objects. *Journal of Engineering Mechanics, ASCE* 1991;117(9):2079-100.
- [92] Yim CS, Chopra A, Penzien J. Rocking response of rigid blocks to earthquakes. *Earthquake Engineering and Structural Dynamics* 1980;8(6):567-87.
- [93] Zhang J, Makris N. Rocking response of free-standing blocks under cycloidal pulses. *Journal of Engineering Mechanics, ASCE* 2001;127(5):473-83.
- [94] Zimmermann T, Dubois-Pèlerin Y, Bomme P. “Object-oriented finite element programming: I: Governing principles”, *Computer Methods in Applied Mechanics and Engineering*, 1992;98(2):291-303.
- [95] Zimmerman T, Bomme P, Eyheramendy D, Vernier L, Commend S. “Aspects of an object-oriented finite element environment”, *Computers and Structures*, 1998;68:1-16.

Index

<u>2</u>		Design Patterns (DPs)	68
2D analysis	80	Discontinuous Deformation Analysis" (DDA)	45
<i>2DEC</i>	39	discrete element codes	47
		distance between the columns	148
		Doric Order	26
<u>3</u>		<u>E</u>	
3D analysis	80	earthquakes	120, 121, 132
3D sensitivity	80	entablature	26
<i>3DEC</i>	39	epistyle mass	152
		epistyles	132
		eps	77
		equations of motion	57
		experimental investigation	38
		experimentally	34
		experiments	103
<u>A</u>		<u>F</u>	
Amathus	24	Factory Design Pattern	70
analytical solutions	100	FDM	81
Animation	77	FEM	39, 81
architrave	26	Flow chart	62
		Fortran	65
		friction	114, 126
		frieze	26, 152
<u>B</u>		<u>G</u>	
Behavioral DP	70, 73	gap elements	81
boundary element methods	81	Graphical-user interface	76
		Greek temples	26
<u>C</u>		<u>H</u>	
C# (Sharp)	68	hard-contact	43
C/C++	74	Housner	34, 85, 89, 179
capital	26		
CDM	58	<u>I</u>	
cella walls	27	input file	78
Central Difference Method	58, 63	Ionic Order	26
coefficient of friction	114		
colliding bodies	46	<u>J</u>	
colonnade systems	132	Java Foundation Classes (JFC)	75
command line input	77	Java Media Framework	74
<i>Composite DP</i>	72		
contact area	53		
contact interaction	46		
Contact stiffnesses	56		
Corinthian Order	26, 27		
<i>creational DP</i>	70		
Cyprus	24, 25, 26		
<u>D</u>			
Damping	56		
deformability	44		
DEM	43		

Index

Java programming language	74	<u>R</u>	
Java Virtual Machine (JVM)	75	rigid bodies	46
Java2D API	74		
JDBC	74		
<u>L</u>			
land slide	82		
<u>M</u>			
marble	27		
Masonry building	81		
masonry structures	80		
Mortar	27		
<u>N</u>			
non-linear formulation	102		
normal plane	53		
number of columns	146		
numbers of drums	115, 138, 144		
<u>O</u>			
Object Oriented Programming OOP	66, 69, 70		
objectives	28		
OpenSees	67		
Orders of Architecture	26		
Output graphs	77		
overturn	142		
<u>P</u>			
pairwise contact detection	50		
PGA	111		
Procedure-Oriented Programming (POP)	65		
<u>R</u>			
<u>S</u>			
Sanctuary of Amathus	25		
Sanctuary of Apollo	24		
self-similar	91		
Shake Table	106		
shape of the individual drums	118		
soft-contact	43		
spatial reasoning	49, 51		
standalone	110, 142		
stone	27		
<i>structural DP</i>	70		
stylobate	26		
<i>Swing</i>	74		
<u>T</u>			
tangential plane	53		
tapered	155		
tapered column	118		
temple	27		
time step	51		
tympanon	152		
type of epistyle	150		
<u>U</u>			
Unified Modeling Language (UML)	71		
upper row	161		
<u>V</u>			
validation	85, 87		
<u>W</u>			
Working Model 2D	40		